Strigolactone signaling through the eye of the mass spectrometer

Alan Walton

PhD Thesis

Promoters:
Prof. Dr. Sofie Goormachtig
Prof. Dr. Kris Gevaert

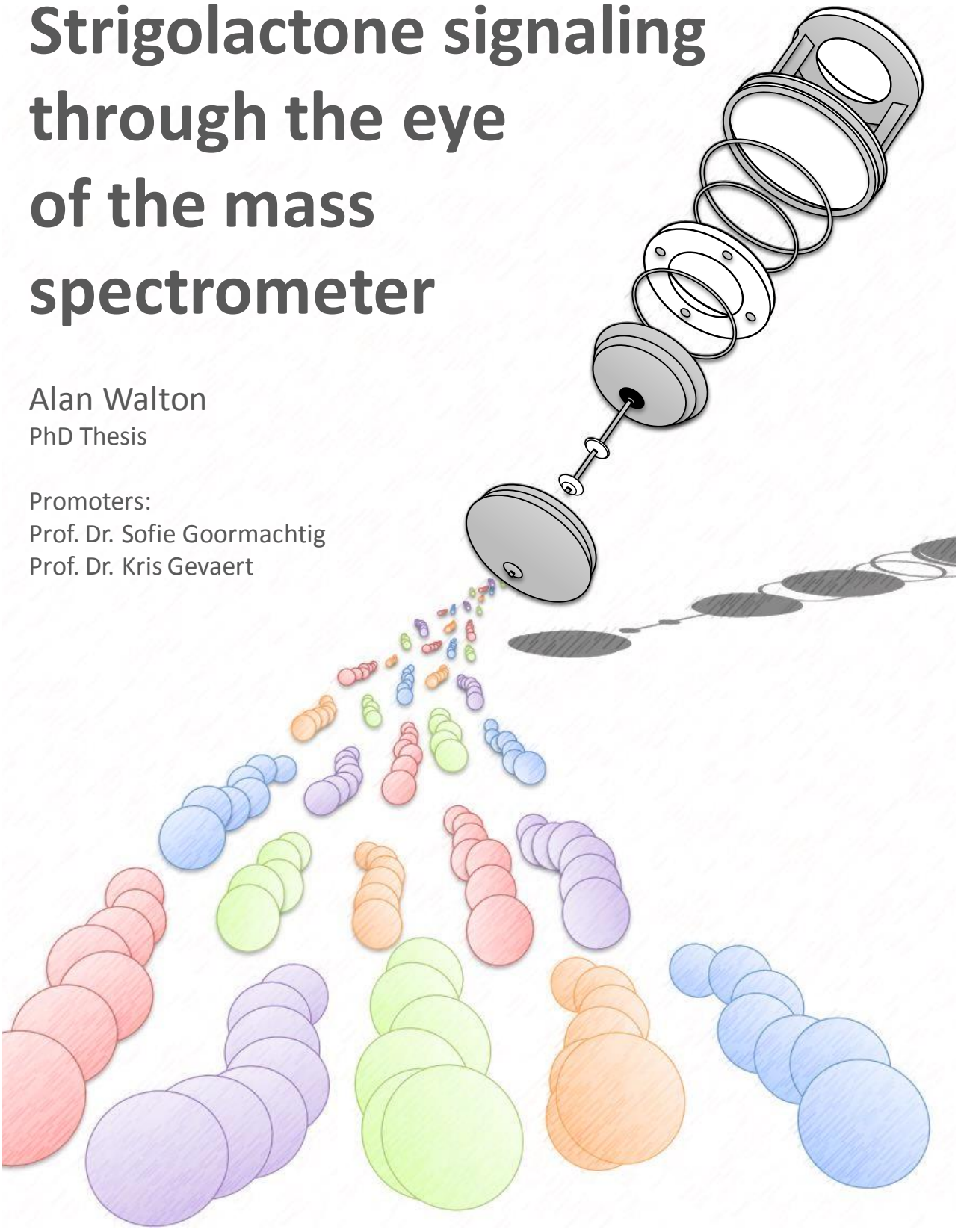

Strigolactone Signaling through the eye of the mass spectrometer

Alan Walton
Promoters: Prof. Dr. Sofie Goormachtig & Prof. Dr. Kris Gevaert

Ghent University
Faculty of Sciences
Department of Plant Biotechnology and Bioinformatics
Department of Plant Systems Biology
VIB Department of Plant Systems Biology

Research funded by VIB International PhD grant
Dissertation submitted un fulfillment of the requirements of the degree of Doctor (PhD) in Sciences: Biochemistry, Biotechnology

Thanks to

After almost 4 years of working in Belgium, the time has come to acknowledge the many different people that have contributed to making this project a success. I'm going to start at the very top of the pyramid, with my PIs and my guiding post-doc as these are without a doubt the people that I made suffer the most! To Sofie (aka. Wendy/Bob), thank you for creating an atmosphere in the lab that makes us all happy to come in in the mornings. The strong ties between the members of the group are the fruit of your great team management and have made these 4 years really enjoyable. I will take with me lots of great memories from numerous team building (with a special place for the canoeing!), Christmas dinners and summer BBQs that you organized for us. I am also enormously grateful for all of the input you have given to my project. I think you described it best when you told me that I'm someone who emits a lot of 'random' energy and your job is to canalize it for me so I can put it to good use. Without your guidance and critical assessment of my work I do not dare to think where I might have ended up. To Kris, I would like to start by thanking you for sharing your enthusiasm for proteomics with me. I really enjoyed gradually discovering this world and it provided me with new and interesting challenges which kept the PhD interesting until the end. We all saw as well the enormous effort that you made to dive into the world of plant research and I would even dare to venture that we have almost converted you into a fully flung Arabidopsis specialist (don't worry, it can be our secret!). Thanks to both you for the countless manuscript corrections and guidance meetings as well as just general support and opportunities that you gave me during my time in your labs. I was looking through my emails the other day and I found at least 10 emails from both of you that were either sent at ridiculously early morning hours or even on the 25th December to help me push my papers through and to solve problems we were encountering in experiments. I know that you guys consider this to be 'normal' but I really think that you are exceptional promoters that really invest a lot of time in the projects of your PhDs and I think this is really reflected in what we managed to achieve at the end of this work.

Next on the list, Miss Elisabeth. In order to properly thank you I would need to write a good chapter or 2! I don't think there is anywhere on this planet another post-doc that invested as much time as you did in helping their PhDs. Thank you for all the corrections that you did on my manuscripts and on my thesis and also thank you for creating opportunities for me to work on exciting projects, like the original COFRADIC

paper. I am also very grateful for all of the soft skills that you taught me over the time that I worked for you. I'm fairly confident that the protocol for persuading mass spec people to run our samples will be transferable and very useful in my future ventures! You also really helped me to integrate when I arrived a helped me get through some more difficult patches when I doubted whether the PhD was really something for me. So to wrap up, I guess the best way that I can thank all 3 of you will be to do you proud on the day itself (so once I'm done writing this I am going straight to lock myself in my house for the next 6 weeks for solid revision!).

Next up is the lab members! I'll start with the plant side first and with my PC neighbor Mister C. Thanks for the fun times in the lab, the conversations, the messing around and the general nice atmosphere. Also I huge thank you for showing me the ropes in Arabidopsis research when I first got to the lab. I wish you great success for the future. Next to Lukas for the great 9 months which we worked together on my project in the beginning and then for the general fun in the lab the years afterwards (especially letting me destroy you systematically in squash…it really helped to keep my self-esteem high). I think that both of you really make a massive effort to integrate foreigners, and at least in my case it really made the whole adventure much more enjoyable. Miss Sylvia, thanks for very delicately helping me find motivation in times where I had lost momentum (although next time maybe not in front of a car full of people ☺). But really, I needed to hear it and it was really fun collaborating with you for the last 1 year. I'm really happy to have met you (and am still waiting for the invitation to come to discover Poland!). Miss Justine, thanks for bringing a bit of crazy frenchness to the lab and listening to me nag about how I would never manage to finish the PhD. Your endless organizing of social event really contributed to making the rhizo lab THE best lab in PSB. To Annick, the lab GPS and queen of cloning, thanks for taking the time to explain gateway cloning, touch down PCR, crazy cloning techniques for difficult genes….and the list goes on! You really helped me to improve my labs skills and without you I think all of our projects would just grind to a halt! To Carolien, thanks for the insight that you gave to my project and the help to get going in the beginning and the friendly chats to distract me when results weren't going the way they should have been. Mister Tom, although I'm not fully happy about the fact that now I'm no longer the squash god of the lab, it was really great working in the same lab and thanks for all the critical insight that you gave that has helped to improve my project. Finally to Tibby, Stein and Sarah, the newest editions to the lab, thanks for all the fun we've had so far and also for bringing a bit of diversity to the lab with some cool talks about new topics (although I still don't understand the rubix cube slide! But I guess I did learn how many different groups of bacteria you can make from 25 strains). Finally, not really a lab member, but for sure important, Mister W!!! So much fun! We really had a great time! Thanks for all the nice moments, whatever happens we have to keep in touch.

Next to the mass spec lab! First the MS gods themselves. To Evy, An, PJ, Jonathan and later Jarne, Delphi and Francis thanks for always being there to rescue our experiments. A special thanks to An and Evy for their impressive patience in the face of my endless list of random mass spec questions! To Giel, Emmy thanks for including me in the team and making my 'adoption' by the second lab much easier (and also

holding my hand whilst I was crying from fear on the plane back from Spain!). PJ thanks for all the crazy fun…I must say though, Odette de La Planche is still wondering why you haven't sent her your PhD diploma and Mathias' insurance company has been trying to contact you for like a year now! It's cool to have you back in the lab. Miss Kim, my office buddy! Thanks for all the fun talks and laugh. It really made working in Rommelaere a lot of fun and you taught me a lot as well.

Several Post-Doc and Professors also contributed greatly to this work through either fruitful scientific discussions or support. From PSB, I would like to thank Ive, Laurens and Alain for providing both data and support to help us get the Ubiquitin COFRADIC paper into TPC. From MBC, a big thank you to Petra and Sven for the interesting scientific discussion that helped us to view our research from a new angle. To Sven, the optimization experiment that you suggested really did help us to get the most of this project and to Petra thanks for reassuring me even after my paper got rejected for the 10th time!

To the guys from squash, Nathan, Jonas, Fabi, Mibon and Phil thanks for helping me discover the sport and also for changing my ideas and providing me with a much needed pressure release every week. To Jonas and Nathan thanks for all fun times out (particularly the one that ended up with me locked in Jonas' house and having to exit through the bathroom window!). Mr. Phil, really I don't think I would have got this far without out you. You've been here from the very beginning (the annoying German guy in the taxi that wouldn't stop talking before the interview) and have helped me to stay motivated throughout the PhD.

To my Family, thanks for supporting me throughout the whole of my studies. To Mum and Dad, having Hugo has really made me become aware of everything that you guys did for us when we were kids and I will be forever grateful for that. Through both the motivation and enthusiasm that you guys gave us and the numerous occasions where you helped us broaden our horizons and general good advice on how to live life, you have helped all me to reach the goals that I set out to achieve. I am glad that Hugo (and unknown) will be able to benefit from this in their lives too. To Greg, Cath and Nick, thanks for all the support and fun times during the hols that really helped me to get my mind off work! I hope to see a lot more of all of you once this is all over.

To my friends, thanks to all of the gang from Chato. Almost 11 years of friendship now, which has been essential over these 4 years! And finally to the Toulouse Trio. Popo and Pierrot, you guys helped me bridge the (enormous) knowledge gap in M2 and gave me you enthusiasm for research. I also promise to substantially increase the frequency of visits as soon as this is done.

Finally, but most importantly, to my Wife Loren for putting up with me through the engineering degree, the master's degree and now the PhD. Thanks for helping me get through all of it and being with me on this journey. I must have done something extremely good in a previous life to merit spending this one with you and little Hugs! Without you I would not be who I am today and I look forward to living the next adventure together with our family!

Examination Committee

Prof. Dr. Tom Beeckman (Chair)

Faculty of Sciences, Department of Plant Systems Biology, Ghent University

Prof. Dr. Sofie Goormachtig (Promotor)

Faculty of Sciences, Department of Plant Systems Biology, Ghent University

Prof. Dr. Kris Gevaert (Promotor)

Faculty of Medicine and Health Sciences, Department of Biochemistry, Ghent University

Dr. Elisabeth Stes

Faculty of Medicine and Health Sciences, Department of Biochemistry, Ghent University

Dr. Laurens Pauwels

Faculty of Sciences, Department of Plant Systems Biology, Ghent University

Prof. Dr. Petra Van Damme

Faculty of Medicine and Health Sciences, Department of Biochemistry, Ghent University

Prof. Dr. Caroline Gutjahr

Faculty of Biology – Genetics, LMU München

Prof. Dr. David Komander

MRC Laboratory of Molecular Biology, Cambridge Biomedical Campus

Contents

Abbreviations

ABA Abscissic acid

AFB auxin binding factor

ANOVA analysis of variance

ARF auxin responsive factor

Aux/IAA auxin/indole-3-acetic acid proteins

AXR auxin resitant

BL Brassinolide

CDK cyclin dependent kinase

CHAPS 3-[(3-cholamidopropyl)dimethylammonio]-1-propanesulfonate

COFRADIC, combined fractional diagonal chromatography

coIP, co-immunoprecipitation

Col-0 Columbia-0

D, DWARF

DAD, DECREASED APICAL DOMINANCE

Dag Days after germination

DNA deoxyribonucleic aicd

DPBA, diphenylboric acid 2-amino ethyl ester

DUB Deubiquitinating enzyme

GA gibberellin

GFP Green Flourscent Protein

GO, gene ontology

GR24 synthetic strigolactone analog

GUS β-glucuronidase

His Histidine

hpt, hours post treatment

HPTLC High Performance Thin Layer Chromatography

HTL, HYPOSENSITIVE TO LIGHT

IAA indole acetic acid

IAA Iodoacetamide

IMAC Immobilized Metal-Affinity Chromatography

iTRAQ Isobaric Tags for Absolute and Relative Quantification

JA-Ile, jasmonoyl-isoleucine

JAZ jasmonate ZIM domain

kb kilobase

kDa kilodalton

LC liquid chromatography

LFQ Label Free quantification

LR, Lateral root

LRD, Lateral root density

LTQ, linear trap quadrupole

MAX, MORE AXILLARY GROWTH

mM Millimolar

MS, Murashige and Skoog

MudPIT Multidimensional Protein Identiication Technology

NAP, nonintrinsic ABC protein

NHS, N-hydroxysuccinimide

PAGE Polyacrylamide Gel Electrophoresis

PCR polymerase chain reaction

PPI Protein-Protein Interaction

PTM Post Translation Modification

qRT-PCR, quantitative reverse-transcription polymerase chain reaction

rac-GR24, racemic strigolactone analog

RNA ribonucleic acid

RP-HPLC Reverse Phase High Performance Liquid Chromatography

RUB Related to Ubiquitin (Plant equivalent of NEDD8)

SCF, Skp, Cullin, F-box

SDS Sodium Dodecyl Sulfate

SILIA, 15N stable isotope labelling in Arabidopsis

SL, Strigolactone

TAP Tandem Affinity Purification

TCEP Tris(2-carboxyethyl)phosphine

TFA Trifluoroacetic acid

TPL Topless

TUBE Tandem Ubiquitin Binding Entity

ULPC, ultra-performance liquid chromatography

USP2cc, the catalytic core domain of the USP2 deubiquitinase

WT, Wild type

Outline and scope

Strigolactones are carotenoid-derived metabolites originally identified to stimulate seed germination of plant parasitic weeds, such as *Striga* sp. and *Orobanche* sp. (Cook et al. 1966). Additionally, these molecules were found to be crucial for the initiation of arbuscular mycorrhization, a plant-fungal symbiosis that facilitates water and nutrient uptake by host plants (Akiyama et al. 2005). More recently, the role of strigolactones as plant hormones controlling various developmental processes, such as germination, photomorphogenesis, and root and shoot architecture, was demonstrated (reviewed in Al-Babili et al. 2015). Although research in the model plants Arabidopsis, rice and pea starts to provide more insight in strigolactone signaling, key pieces are still missing in our understanding of this signaling cascade. A central regulator of strigolactone signaling, the Arabidopsis MAX2 protein, is a nuclear leucine-rich-repeat-containing F-box protein belonging to the same family as the auxin receptor TIR1 and the jasmonate receptor COI1 (Gomez-Roldan et al. 2008). All these proteins are part of SCF-type E3 ubiquitin ligase complexes that target proteins for ubiquitin-dependent proteasomal degradation (Gary et al. 2001, Thines et al. 2007). Upon challenge with auxin or jasmonates, such SCF complexes are formed and through recognition by the F-box proteins, negative regulators are ubiquitinated and degraded by the 26S proteasome, allowing hormone-dependent gene activation. Over the past few years, members of the SMXL family were identified as targets of the F-box protein MAX2 (Jiang et al. 2013; Stanga et al. 2013; Zhou et al. 2013; Kong et al. 2014). However, despite this, information concerning what happens downstream of the degradation of these negative regulators that gives rise to the described phenotypes, is still missing. More specifically, given the circumstances in which they were originally described as being plant hormones, most research has so far focused on the role of strigolactones in shoot branching, leaving our knowledge of their evoked signaling cascade in the below ground part of the plant lagging behind. We therefore decided to focus, when possible, on this hormonal pathway in Arabidopsis roots.

Over the past ten years, mass spectrometry based proteomics methods have gradually been introduced into plant research studies. Thanks to both the vast improvements in both instruments and sample preparation techniques, tailor-made to suit plant material, a new toolbox became available for plant scientists to investigate plant biology on the proteome level.

During this PhD project, we decided to make use of such a proteomics toolbox to make a critical contribution to the understanding of strigolactone responses that underlie various plant functions. We aimed to

identify new players in strigolactone signaling, in particular downstream of MAX2, and to position them in the available strigolactone regulatory network map. In this manner, our main objective was to broaden the current knowledge on strigolactone signaling, pivotal for untangling the various strigolactone-mediated effects in plant development and rhizosphere interactions. To accomplish these objectives, we decided to focus on the use of two main tools:

- Proteome profiling to compare the roots of WT and *max2* seedlings, grown in mock or GR24 (synthetic analog of strigolactone) treated conditions, to identify key players and downstream segments of the strigolactone signaling pathway, and
- PTM scanning through use of a new technology that we developed to allow for comprehensive ubiquitination profiling, at the site level, in plants. This would enable us to identify proteins whose ubiquitination status changes upon GR24 treatment and investigate in detail the importance of the different sites of ubiquitination.

I present my thesis in four parts. In a first part, two of our published reviews are bundled and re-formatted to serve as an introduction and to further clarify the context of my research project. Chapter 1 explains in detail the advances in mass spectrometry-based proteomic tools and the opportunities they have opened for plant scientists studying hormone signaling. This is followed by Chapter 2 that gives a thorough review of strigolactone signaling with a specific focus on what is known so far about this pathway in the roots and the challenges that lie ahead.

In the second part, a first research chapter (Chapter 3) describes the comparative proteome profiling experiments that were carried out to gain insight into the downstream elements of strigolactone signaling pathway in roots. In Chapter 4 we investigate in greater depth some of the new root responses that were uncovered in the previous chapter.

The third part begins with chapter 5, which describes the development and application of our ubiquitin COFRADIC technology in mammalian systems. Chapter 6 then provides a research section in which we describe the implementation of our technology in Arabidopsis cell cultures. Finally, Chapter 7 presents the use of this tool to identify changes in the ubiquitinome upon GR24 treatment and investigates the importance of sites discovered on known targets of the MAX2 proteins.

Finally, in the final part, my thesis is brought to a close by discussing the obtained results and putting them in a broader context. I also give perspectives, both on how our new insights on the biological level can be followed up, as well as on how the techniques developed during this thesis could be of use to plants scientists in the future.

Part I
Introduction

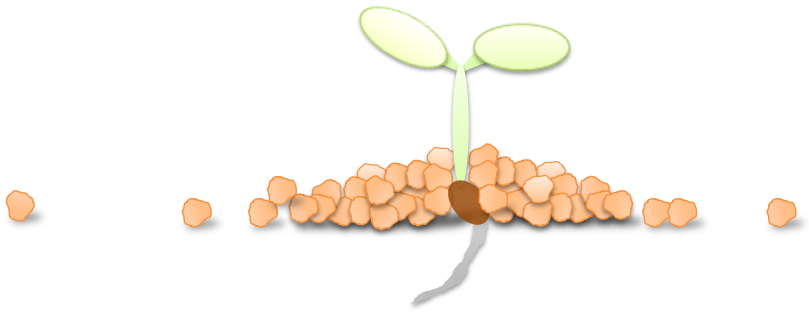

Chapter 1: Plant hormone signalling through the eye of the mass spectrometer

Alan Walton[1,2,3,4,+], Elisabeth Stes[1,2,3,4,+], Ive De Smet[3,4], Sofie Goormachtig[3,4] and Kris Gevaert[1,2,*]

[1]Department of Medical Protein Research, VIB, B-9000 Ghent, Belgium

[2]Department of Biochemistry, Ghent University, B-9000 Ghent, Belgium

[3]Department of Plant Systems Biology, VIB, B-9052 Gent, Belgium

[4]Department of Plant Biotechnology and Bioinformatics, Ghent University, B-9052 Gent, Belgium

Author's contribution: + These authors contributed equally to this work

This chapter is adapted from Walton, Stes et al. 2014 *Proteomics*, 15(5-6), 1113-1126

Abstract

Plant growth and development are regulated by hormones and the associated signalling pathways share several common steps, the first being the detection of the signal by receptor proteins. This typically leads to conformational changes in the receptor, thereby modifying its spectrum of interaction partners. Next, secondary signals are transmitted via rapid post-translational cascades, such as targeted phosphorylation or ubiquitination, resulting in the activation/deactivation, relocalization or degradation of target proteins. These events finally give rise to the signal-dependent read-out, such as changes in gene expression and regulation of protein activity. So far, the majority of studies aimed at unravelling hormone signalling pathways in plants relied on genetic or transcriptomic approaches. During the last decade however, mass spectrometry-driven proteomic methods became increasingly popular tools in plant research as they reveal the specific mechanisms controlled by phytohormones, which for a large part occur at the proteome level. Here, we provide an up-to-date review on the growing body of work in these areas using mass spectrometry-based techniques, with a focus on non-peptide plant hormones.

1. An introduction to plant hormone signalling

Plants dispose of a spectrum of hormones that orchestrate plant growth and development and mediate responses to biotic and abiotic stresses. The different classes of plant hormones known to date consist of small molecules, mostly structurally unrelated, that are active at very low concentrations. In contrast to animals, all plant tissues have the capacity to synthesize hormones. Plant hormones can act locally or can be transported throughout the plant, acting as long-distance signalling molecules. Each class of plant hormones is typically involved in a range of developmental processes and environmental responses, rather than being limited to one physiological event (Santner and Estelle, 2009). Hormones often function as instructive agents, directing plant cell fate towards specific developmental programs. For example, in shoot apical meristems, cytokinins are essential for meristem functioning by keeping stem cells in a proliferative state, while patterning and organ initiation is regulated by auxin, resulting in emerging primordia (Murray et al., 2012).

Most characterized plant hormone signal transduction pathways lead towards changes in gene expression. The majority of those signalling circuits are based on protein ubiquitination and/or phosphorylation cascades. In the ubiquitin-proteasome pathway, proteins that negatively regulate hormonal signalling are targeted for degradation upon (poly)ubiquitination. Ubiquitin is covalently conjugated to proteins by the sequential activity of three enzymes: the ubiquitin-activating enzyme (E1), the ubiquitin-conjugating enzyme (E2) and the ubiquitin protein ligase (E3). In plants, different types of E3 ligases exist (Chen and Hellmann, 2013), of which the SKP1-CULLIN1-F-box (SCF) complex is most commonly described in the plant hormone signalling field. The F-box protein confers the substrate specificity of SCF ubiquitin ligases. The proteasome finally recognizes the ubiquitin-tagged protein and degrades it, enabling signalling of the respective plant hormone (Santner and Estelle, 2010). In the case of auxin, two types of F-box auxin receptors are characterized in Arabidopsis: TRANSPORT INHIBITOR RESISTANT1/AUXIN-BINDING F-BOX PROTEIN (TIR1/AFB) proteins (Calderon-Villalobos et al., 2010) and S-PHASE KINASE-ASSOCIATED PROTEIN 2a (SKP2a) (Jurado et al., 2010). These receptors are localized in the nucleus and, upon auxin binding, directly interact with co-receptor proteins like the AUXIN/INDOLE-3-ACETIC ACID (Aux/IAA) proteins. This interaction results in the degradation of the co-receptors via the ubiquitin-proteasome pathway, thereby relieving repression of transcription factors, such as the AUXIN RESPONSE FACTORs (ARFs), that regulate the expression of auxin-responsive genes (Peer, 2013). A similar mechanism was revealed for jasmonates, phytohormones that are essential for successful defence against biotic stresses, but that also regulate aspects of growth and development (Santino et al., 2013). The bioactive form, jasmonoyl-isoleucine (JA-Ile), is perceived by an F-box protein CORONATINE-INSENSITIVE 1 (COI1) that is part of an ubiquitin E3 ligase complex, which targets transcriptional repressors called JASMONATE ZIM-DOMAIN (JAZ) proteins for degradation in a proteasome-dependent manner. Analogous to the Aux/IAA proteins, JAZ proteins are required for perception of the hormone signal and function as co-receptors (Perez and Goossens, 2013).

The core signalling circuit described above can be fine-tuned by additional regulating PTMs and signalling pathways. For example, the activity of SCF E3 ligases is controlled via their complex assembly, which is guided by the post-translational NEDDylation of cullin RING ligases (Hotton and Callis, 2008). This process is characterized extensively in auxin signalling, where NEDD8 conjugation to CUL1, essential for normal functioning of SCF^{TIR1}, is facilitated by AUXIN RESISTANT 1 (AXR1) (del Pozo et al., 2002) and E1 C-TERMINAL RELATED 1 (ECR1) (Dharmasiri et al., 2003), and antagonized by the COP9 signalosome (CSN) (Stuttmann et al., 2009). Furthermore, it was recently shown that ARF activity is regulated through phosphorylation by BRASSINOSTEROID-INSENSITIVE2 (BIN2) (Cho et al., 2014). This action liberates the ARFs from Aux/IAA repression, increasing their transcriptional activity, and hence constitutes an additional regulatory module in auxin response.

Whereas E3 ligases in auxin and jasmonate responses directly bind hormones, during gibberellin signalling, the F-box protein SLEEPY1 (SLY1) is involved downstream of hormone perception. Gibberellins are a large family of tetracyclic, diterpenoid growth regulators that are primarily associated with promotion of stem growth, but also play pivotal roles in other growth processes including seed development, fruit initiation and the control of flowering time. The gibberellin receptor GIBBERELLIN INSENSITIVE DWARF 1 (GID1), a nuclear α/β-fold hydrolase, binds biologically active gibberellin. Gibberellin-bound GID1 facilitates DELLA proteins, which are negative regulators of the gibberellin response, to be recognized by the SCF^{SLY1} and their subsequent ubiquitination and proteasome-directed degradation, thereby promoting gibberellin-mediated transcription (Daviere and Achard, 2013). Signal perception of strigolactones, a more recently discovered class of phytohormones functioning in rhizosphere communication and plant architecture, occurs via α/β-fold hydrolases assisted by SCF complexes containing the F-box proteins MORE AXILARY GROWTH2 (MAX2) in Arabidopsis and DWARF3 (D3) in rice (Zhou et al., 2013a). High strigolactone levels induce SCF^{D3}-mediated degradation of the Clp ATPase D53, a positive regulator of shoot outgrowth in rice (Jiang et al., 2013; Zhou et al., 2013a). In Arabidopsis, the SMAX1 family, homologous to D53, represents likely candidates for negative regulators of strigolactone signalling, as they suppress aspects of the *max2* phenotype (Stanga et al., 2013).

E3 ligases also directly control the levels of transcription factors during signal transduction of the gaseous hormone ethylene. Ethylene is known as the fruit ripening hormone, but it is also associated with many other developmental processes and responses to biotic and abiotic stresses (Lin et al., 2009). Positive ethylene response regulators ETHYLENE INSENSITIVE2 (EIN2) and EIN3 are quickly degraded under low ethylene conditions through the ubiquitin/proteasome pathway mediated by F-box containing E3 ligases. In the case of EIN2, this is facilitated by its phosphorylation by CONSTITUTIVE TRIPLE RESPONSE1 (CTR1), a Raf-like protein kinase that is positively regulated by the ethylene receptors. Upon ethylene perception, the receptors, two-component protein kinases in the endoplasmic reticulum membrane, become inactive and the CTR1-controlled inhibition of EIN2 is relieved (Merchante et al., 2013).

Signalling of abscisic acid, a sesquiterpene hormone primarily known for its growth inhibiting capacities, was also linked to ubiquitin ligases, more specifically RING E3 ligases that promote abscisic acid responses by regulating the abundance of abscisic acid responsive transcription factors (Stone et al., 2006; Zhang et al., 2005). However, most studies focused on the phosphorylation-dependent aspects of abscisic acid signalling (Nakashima and Yamaguchi-Shinozaki, 2013): the abscisic acid receptors PYRABACTIN RESISTANCE/ PYR-LIKE/ REGULATORY COMPONENT OF ABSCISIC ACID RECEPTOR (PYR/PYL/RCAR) inhibit the activity of a group of protein phosphatase 2C proteins, including ABSCISIC ACID INSENSITIVE 1 (ABI1) and ABI2. These phosphatases are negative regulators of the abscisic acid response through interaction and dephosphorylation of SNF1-related protein kinases 2 (SnRK2s).

Additionally, brassinosteroids and cytokinins mediate signalling mostly via phosphorylation cascades. Brassinosteroids are steroidal plant hormones that are perceived at the plasma membrane to promote plant growth and development and their metabolism changes in response to abiotic and biotic stress. The receptor kinases BRASSINOLIDE INSENSITIVE 1 (BRI1) and its homologs BRI1-LIKE1 (BRL1) and BRL3 are membrane-localized brassinosteroid receptors. Brassinosteroid binding of BRI1 allows association with a second kinase in the plasma membrane, BRI1-ASSOCIATED RECEPTOR KINASE 1 (BAK1), activating the receptor via trans-phosphorylation. Active BRI1 will phosphorylate and activate BRASSINOSTEROID SIGNALING KINASES (BSK1, BSK2, and BSK3), which bind to and activate the protein phosphatase BRI1 SUPPRESSOR1 (BSU1). Via dephosphorylation, BSU1 represses BRASSINOSTEROID INSENSITIVE 2 (BIN2). This action frees transcription factors BRI1 EMS SUPPRESSOR1 (BES1) and BRASSINAZOLE RESISTANT 1 (BRZ1) to induce transcription of brassinosteroid response genes (Vriet et al., 2013).

The phosphorylation cascades during the cytokinin response are similar to the two-component signalling systems used by bacteria. Natural cytokinins are N^6-substituted adenine-based molecules that play a central role in the regulation of cell division (El-Showk et al., 2013). In Arabidopsis four cytokinin receptors are characterized, CYTOKININ-INDEPENDENT1 (CKI1), ARABIDOPSIS HISTIDINE KINASE (AHK) 2, AHK3 and AHK4, localized mostly to the endoplasmic reticulum (Wulfetange et al., 2011). Perception of cytokinin initiates a multiple phosphorelay system starting with autophosphorylation of the receptor followed by the phosphorylation of ARABIDOPSIS HIS PHOSPHOTRANSFER (AHP) proteins. The AHPs translocate to the nucleus were they activate ARABIDOPSIS RESPONSE REGULATOR (ARR) proteins by phosphorylation. Type B ARRs are direct activators of the cytokinin transcriptional response, and induce the transcription of many genes including a family of transcription factor genes, the CYTOKININ RESPONSE FACTORS and the type A ARRs. The activation of the latter constitutes a negative feedback mechanism as they are negative regulators of cytokinin signalling (Hwang et al., 2012).

Finally, hormone signalling pathways can also be controlled through direct protein activation without the intervention of transcription factors. For example, the dynamic and asymmetric localization PIN FORMED proteins (PIN), auxin efflux transporters, which creates directed auxin fluxes and are critical for auxin effects, are directly regulated via phosphorylation. Several kinases were reported to directly

phosphorylate PIN proteins, such as PINOID (PID), WAG1, WAG2 (Dhonukshe et al., 2010; Kleine-Vehn et al., 2009) and, more recently, D6 PROTEIN KINASE (D6PK) (Zourelidou et al., 2014), and thereby shift PIN polar distribution.

2. Plant hormone responses at the protein level

Over the past decade, the growing popularity of proteomics-based protein studies has filled substantial knowledge gaps in the plant hormone signalling field. With rapidly improving instruments and the optimization of proteomic workflows to handle plant extracts, mass spectrometry driven protein profiling has allowed the identification of several response factors in different phytohormone signalling pathways. The results of these proteomics studies have been equally important in fine-tuning the definition of the roles of individual hormones, as well as unravelling cross-talk mechanisms. In this section we review the major proteomics studies focusing on changes in total protein levels that have contributed to a better understanding of the different hormonal pathways in plants (Table 1).

2.1. Gel-based studies

To study the effect of phytohormones on the plant proteome, a popular technique is two-dimensional gel electrophoresis (2-DE). This technique consists in the subsequent separation of proteins through isoelectric focusing and size separation via use of SDS-PAGE in an orthogonal dimension allowing for the resolution of complex protein mixtures (Fig. 1). Proteins displaying an altered abundance on different gels can subsequently be identified via mass spectrometry, after in-gel digestion of the relevant protein spot.

2-DE-based proteomics have contributed to a better understanding of the function of some well-characterized players in plant hormonal pathways. For example, the auxin-dependent gravity response in Arabidopsis roots and the role of PIN2 therein were studied via 2-DE (Tan et al., 2011). Changes in the protein levels in the gravity-insensitive *pin2* mutant and wild-type root tips were monitored upon gravitropic stimuli. This allowed a group of proteins to be identified as responsive to altered gravitropic conditions exclusively in wild-type but not in *pin2* root tips. Validation of these results via protein-GFP fusion studies, pinpointed one of those proteins, ANNEXIN2, as an early response factor to the PIN2- and auxin-mediated gravity signal in the columella cells of the root cap. 2-DE has further served to study the cross-talk of auxin and ethylene in plant tissues. The effects of exogenously applied auxin (indole-3-acetic acid) and ethylene (1-aminocyclopropane-1-carboxylic acid) were investigated in Arabidopsis roots through 2-DE and MALDI-TOF/TOF-MS analysis (Slade et al., 2012). Whereas a moderate number of proteins spots changed upon auxin and ethylene treatment, no overlap in proteins involved in both responses could be identified. The low number of proteins identified, as well as the lack of overlap, can most likely be attributed to the limitations of the 2-DE gels and the mass spectrometers used in this study (Slade et al., 2012). Indeed, it is well known that both

hormones are intimately connected in the control of root development (Muday et al., 2012; Strader et al., 2010).

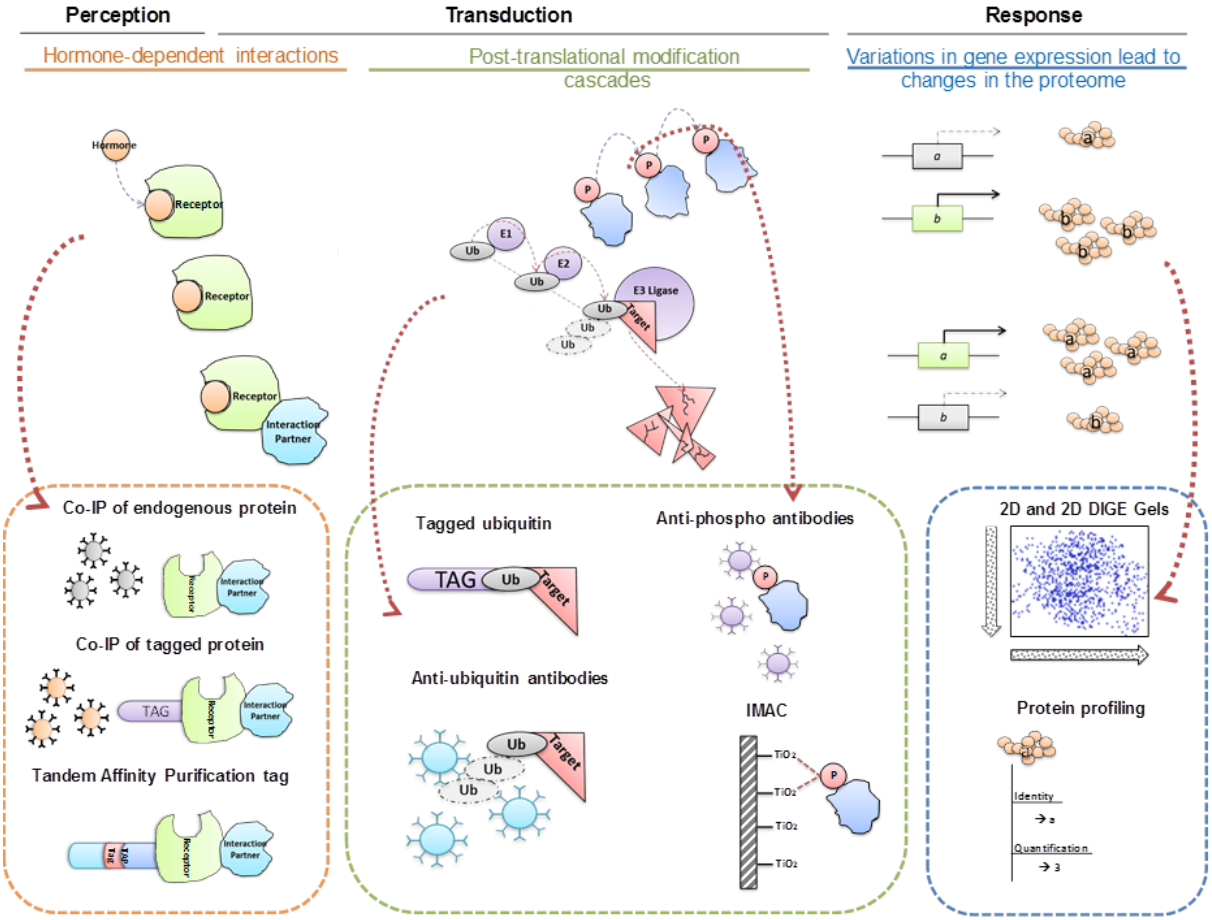

Figure 1: Available proteomics-driven techniques applicable in the investigation of the perception, transduction and responses linked to plant hormone signals.

Organ- and tissue-specificity can be introduced into these studies by sampling from selected parts of the plant and comparing their proteomes. Žd'árská and colleagues studied the effect of cytokinin in Arabidopsis shoots and roots via 2-DE (Zd'arska et al., 2013). The cytokinin 6-benzylaminopurine was shown to up-regulate abscisic acid biosynthesis and response genes in shoots, whilst in roots, this phytohormone up-regulates ethylene biosynthesis proteins. This study helped to establish the fundamental difference in the cytokinin response in above- and below-ground parts of the plants. Furthermore, a differential protein expression analysis in roots of the legume *Medicago truncatula* was performed to assess proteome variation in response to ethylene and inoculation with its symbiont *Sinorhizobium meliloti* (Prayitno et al., 2006). Proteomic differences were compared in wild-type and the ethylene-insensitive *skl* mutant roots, revealing an ethylene-mediated stress response that is likely involved in controlling root nodule numbers.

2-DE has suffered from possible variability, resulting in insufficiently reproducible proteome patterns, making reproducible detection of differences between proteomes challenging. The development of 2-

dimensional difference gel electrophoresis (2D DIGE) greatly improved this aspect (Unlu et al., 1997; Viswanathan et al., 2006), as this technique makes use of different spectrally resolvable fluorescent dyes to label multiple proteome samples prior to 2-DE. During visualization of the proteome in the gel, proteins that differ between samples will be represented as spots with different fluorescence ratios, thereby overcoming the need to compare several individual gels and enabling more accurate quantitation. In the plant hormone field, 2D DIGE was applied in a study of long-term auxin effects on rice root development (Shi et al., 2008). The fluorescent dyes Cy3 and Cy5 were used to simultaneously visualize extracts from the basal part of rice seedlings, where adventitious roots are formed, treated with either synthetic auxins or auxin blockers. This enabled the identification of 9 differentially regulated proteins, and suggested a role for the 76 kDa mitochondrial complex I subunit, myosin heavy chain and EF-1β' in the promotion of lateral root formation by auxin.

The Wang lab made use of 2D DIGE to describe brassinosteroid-regulated protein expression events in rice and Arabidopsis (Deng et al., 2007; Wang et al., 2010). Through comparison of brassinosteroid-insensitive mutants and brassinosteroid-deficient mutants with wild-type samples, substantial numbers of brassinosteroid-regulated proteins could be identified. Further validation of some of these proteins in rice showed that overexpression of *OsGRP1* and *DREPP2* partially suppressed the dwarf phenotype of the brassinosteroid-insensitive Arabidopsis mutant *bri1-5*, pinpointing these proteins as potential regulators of cell expansion. In Arabidopsis, it was demonstrated that brassinosteroids regulate 14-3-3 proteins, signalling proteins that bind specifically to phosphorylated proteins, in line with the previously described phosphorylation-dependent signal transduction of brassinosteroids (Vriet et al., 2013). Furthermore, a 2-D DIGE analysis of both the plasma membrane proteome and the phosphoproteome (Tang et al., 2008a) allowed the identification of early brassinosteroid-response proteins, which were not detected in the previous study on the total proteins (Deng et al., 2007). Additionally, the BSKs were identified as BRI1 substrates, which are phosphorylated upon brassinosteroid activation of BRI1 (Tang et al., 2008b). Hence, this work nicely illustrates the potential of quantitative proteomics approaches, when combined with sample fractionation, to empower the identification of major signaling components of a hormone pathway.

Although gel-based methods for protein profiling remain widely used in plant research, gel-free approaches are rapidly gaining ground. So-called shotgun techniques provide a well-performing alternative to the labour-intensive gel-based techniques, and additionally address some other drawbacks related to 2-DE and 2D DIGE, such as limited capacity to deal with the broad dynamic range of plant proteomes (resulting in a poor representation of low abundant proteins), the inability to study certain classes of proteins like very hydrophobic proteins (e.g., transmembrane proteins), and incompatibility of gel-based techniques with automation.

2.2. Gel-free studies

In a shotgun proteomics workflow, complex protein samples are digested into peptides, which can then be separated via one or a combination of several chromatographic steps. Peptide identification and quantification is accomplished via mass spectrometry.

Similar to gel-to-gel variation when comparing 2D gels, LC-MS runs also suffer from reproducibility issues, and variation between runs can be observed (Liu et al., 2004). In addition, although peptide peak intensity is linearly proportional to peptide abundance, mass spectrometry is not inherently quantitative, because different ionization properties of distinct peptides will lead to major differences in the intensities of their mass spectra (Hale et al., 2000). To facilitate robust relative quantification, wide arrays of stable-isotope containing labels were developed, allowing differentiation of peptides originating from different samples (Bantscheff et al., 2012; Nelson et al., 2014). Samples can either be labelled metabolically, by adding the labels to the growth medium of the organism, or post-metabolically, through chemical or enzymatic modification of proteins or peptides. Through the mass shift that the labels introduce, peptides from different samples can be mixed and run simultaneously on the LC-MS system, enabling relative quantification and resolving the inter-run variability problems. Although metabolic labelling of plants is possible, most efficiently done by growing plants on $^{14}N/^{15}N$-supplemented medium (Kierszniowska et al., 2009; Li et al., 2012), most protein profiling studies concerning plant hormone effects reported so far made use of post-metabolic chemical labels. More specifically, the most popular chemical labels in plant proteomics to date are the commercially available isobaric tags for relative and absolute quantification (iTRAQ), which target α-amines on peptide N-termini and ε-amines on lysines. They are called isobaric as the labelled peptides have identical masses, but can be distinguished after a fragmentation event (i.e., in the MS/MS spectra). The iTRAQ technology was successfully applied in an Arabidopsis cell type-specific study from the Assmann lab to collect data on the role of abscisic acid in guard cell movement. Guard cell protoplasts prepared from wild-type and G protein mutant leaves were treated with abscisic acid, followed by differential proteome analysis. This quantitative proteomics approach resulted in the discovery of several G protein regulated proteins in guard cells (Zhao et al., 2010). Another iTRAQ-based study revealed 36 abscisic acid controlled proteins in rice suspension cells, including some known abscisic acid responsive proteins and providing clues for potential novel ones (Rao et al., 2010). Moreover, Alvarez and colleagues used iTRAQ to compare Arabidopsis root proteomes of wild-type plants with G protein mutants and GTG protein mutants, again upon abscisic acid stimulus, elucidating global effects of this hormone in roots (Alvarez et al., 2011; Alvarez et al., 2013). Finally, the response of Arabidopsis seedlings to the synthetic strigolactone analogue GR24 was explored by iTRAQ (Li et al., 2014). Several GR24-regulated proteins were identified in wild-type and strigolactone biosynthesis mutant *max3−12* backgrounds, shedding new light on the molecular networks that link strigolactones to specific cellular and developmental processes.

Finally, some protein profiling studies of hormonal responses in plants are based on label-free quantitation, relying on computational frameworks and statistics to identify differential peptides. This type of quantitation was used in a time course proteomics study of Arabidopsis plants to determine the auxin-regulated proteome. More than 750 proteins with altered abundances upon auxin treatment were identified in wild-type plants, whereas less than 150 auxin-controlled proteins could be detected in the auxin receptor mutant *tir1-1* (Xing and Xue, 2012). Another label-free proteomics study investigated the crosstalk of brassinosteroids and cytokinin in Arabidopsis organelles (Zhang et al., 2012). Here, samples of plants treated with the respective hormones were enriched for mitochondria and chloroplasts via centrifugation, and the organelle proteomes were evaluated via MudPIT-based proteomics. This approach showed that brassinosteroids mostly down-regulate lipid metabolism, while cytokinins induce sucrose and starch metabolic pathways in the organelles studied. Although both studies brought up interesting candidate proteins involved in hormonal pathways, more power and biological significance can be expected from label-free approaches that incorporate a critical number of biological and technical replicates (Olsen and Mann, 2013). Due to parallel sample processing and MS analysis, label-free studies are particularly susceptible to errors and require replicate samples to designate discriminatory peptides.

2.3. Interacting proteins in plant hormone signalling

Specific hormone-induced protein interactions play essential roles during the hormone signalling cascade, ranging from the early perception stage to the later downstream transduction responses. Interestingly, genetics and the vast improvement of wide-range transcriptomic techniques, such as microarrays and more recently RNA-seq (Wang et al., 2009), allowed the identification of multiple essential players in different phytohormonal signalling pathways. To further dissect the precise roles of these proteins, methods enabling unbiased identification of possible interaction partners became indispensable. Generally, two types of techniques were employed to discover new interaction partners of plant proteins already known as parts of signalling hubs: heterologous expression systems in yeast allowing the screening of plant cDNA libraries to find potential interactors (for example yeast two-hybrid (Y2H)) (Zhang et al., 2010) and MS-based identification of members of protein complexes purified from plant material (affinity purification-mass spectrometry (AP-MS) approaches) (Van Leene et al., 2010). The most widely used MS-based strategies for the elucidation of interaction partners in plants are co-immunoprecipitation (coIP), pull-down assays and tandem affinity purification (TAP) (Fig. 1).

In coIP methods the protein of interest is targeted with an antibody for the isolation of this protein together with its interaction partners from cell or tissue lysates. In theory, coIP is one of the least error-prone techniques, as it does not require tags or overexpression of target proteins. However, this is the case when antibodies raised specifically against the protein of interest are available. Because of the scarce availability of antibodies against plant proteins, coIPs in plants are often executed using antibodies against tagged versions of the protein of interest. To do so, transgenic plants are made expressing the protein fused to an affinity tag,

and hence a generic antibody can be used to target any bait protein of choice. However, this strategy does introduce a possible experimental bias, as it cannot be ruled out that the tag affects the capability of the bait protein to engage in interactions with its normal partners. If a knockout mutant with an aberrant phenotype is available, it is preferred to express the tagged bait protein in this knockout background and check for the rescue of the phenotype, indicating that the fusion protein is able to functionally replace the absent endogenous version.

A coIP approach based on CFP tags was used to provide in-depth insight into brassinosteroid detection (Fig. 2). In a first study, Karlova and colleagues targeted SOMATIC EMBRYOGENESIS RECEPTOR LIKE KINASE (SERK1), a leucine-rich repeat receptor like kinase that is involved in male sporogenesis and embryogenic competence (Karlova et al., 2006). An interaction with BAK1 was detected, a protein known as part of the membrane-bound brassinosteroid receptor complex, possibly functioning as a brassinosteroid co-receptor together with BRI1 (Li et al., 2002; Nam and Li, 2002). Along with this interaction, strong indications arose for the involvement of several other proteins in this complex, such as CDC48, a zinc finger protein and a member of the 14-3-3 family. CoIP experiments of FLAG-tagged proteins were later used to elucidate the early molecular events that regulate brassinosteroid-dependent BRI1/BAK1 association and phosphorylation (Wang et al., 2008).

In addition to coIPs, pull-down experiments can be applied to provide insight into protein-protein interactions involved in plant hormonal signalling. However, this *in vitro* form of affinity purification, where the bait protein needs to be recombinantly produced as a tagged fusion protein and immobilized on an affinity support, is predominantly used to confirm and further dissect physical interactions of proteins, for instance the binding of auxin receptor TIR1 with Aux/IAA proteins (Dharmasiri et al., 2005; Gray et al., 2001; Kepinski and Leyser, 2005)

A common drawback of coIP and pull-down procedures is that they typically produce large sets of proteins, containing a sizable proportion promiscuously interacting proteins. Alongside the tag-specific interactors, other proteins that are generally promiscuous in their interactions, sometimes coined as ‘sticky’ proteins, are often detected in such setups. To address this issue, more stringent protocols that rely on multiple steps for complex purification were developed, with the TAP procedure holding a prominent first place in terms of efficiency and throughput for unravelling protein networks in plants (Braun et al., 2013; Van Leene et al., 2008). This technique relies on the expression of a tandem tagged version of the protein of interest, which allows a two-step purification procedure of the respective protein complex, hence reducing the number of contaminating protein interactors in the final protein list..

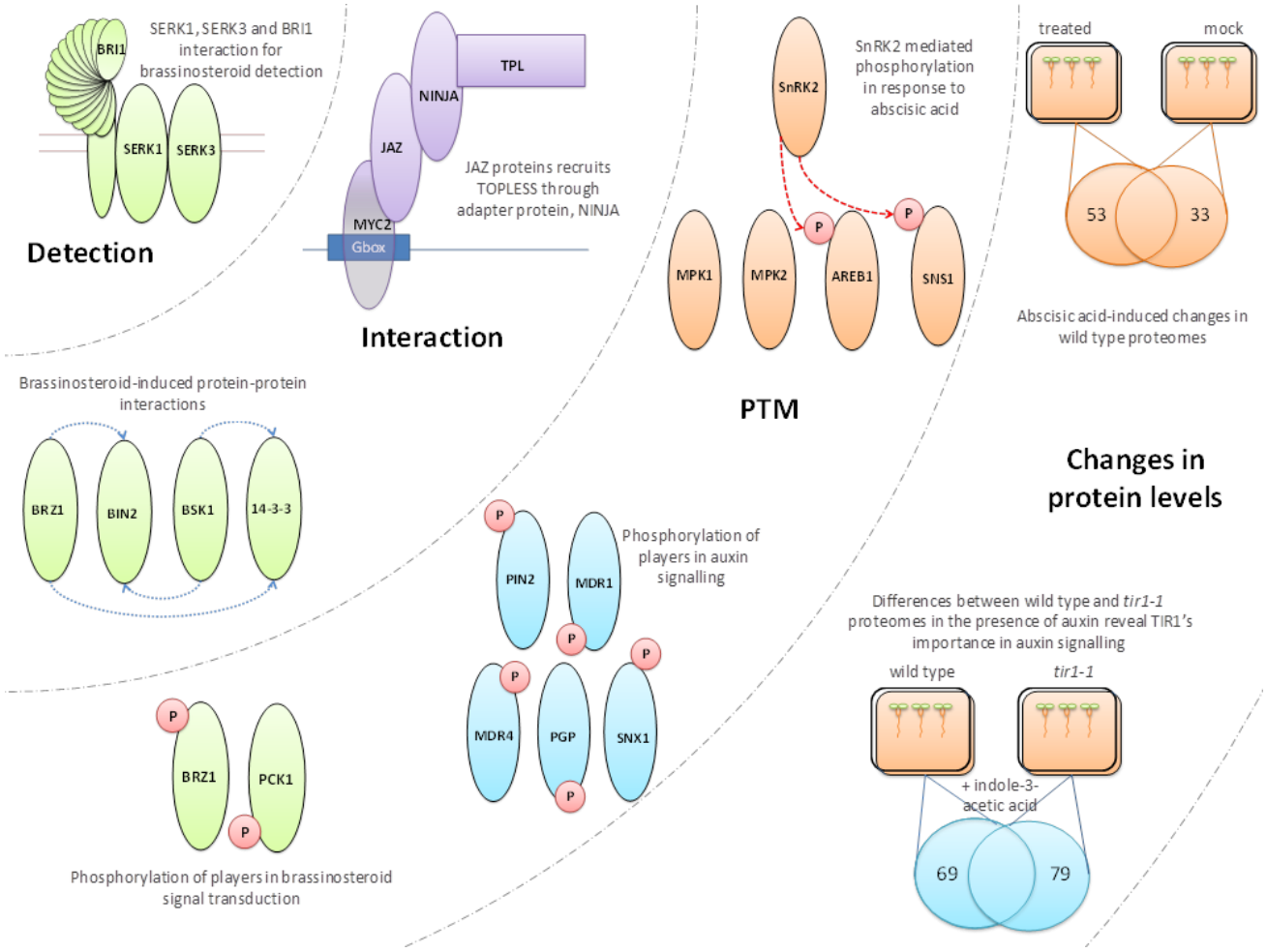

Figure 2: Plant hormone signaling components uncovered through mass spectrometry-based studies. The numbers in the figure refer to the relevant publications.

Since the original TAP experiment in plant cell lysates, the double tag has been greatly improved, from the original double protein A domain linked to a calmodulin-binding peptide, evolving to the latest *GS tag*, consisting of a double protein G domain with a streptavidin-binding peptide (Van Leene et al., 2011). The latter version allowed the discovery of adaptor proteins called NOVEL INTERACTOR OF JAZ (NINJA) important during jasmonate signalling (Pauwels et al., 2010). When undisturbed, JAZ proteins repress the transcription factor MYC2 through binding with the co-repressor TOPLESS (TPL) via NINJA. In the presence of JA-Ile, JAZ proteins are targeted by the SCF^{COI1} complex, resulting in their proteasomal degradation by which MYC2 becomes available to binds to cis-acting elements of jasmonate response genes (Fig. 2). The TAP technology was also applied to identify physical interactors of the brassinosteroid-triggered transcription factor BRASSINAZOLE-RESISTANT 1 (BZR1) (Tang et al., 2011; Wang et al., 2013a). As such, PP2A could be assigned as the long-sought after phosphatase that dephosphorylated BZR1 and

consequently positively regulates brassinosteroid-responsive gene expression (Tang et al., 2011). Functional confirmation experiments show that PP2A binds to the PEST domain of BZR1, and a dominant mutation, *bzr1-1D*, enhances BZR1 binding to PP2A, hereby causing constitutive activation of the brassinosteroid response. Further, TAP purification of the BZR1 complex revealed potential new components of the brassinosteroid signal transduction pathway, in addition to several proteins with known functions during brassinosteroid signalling, like BSK1 and, BIN2 By demonstrating the *in vitro* phosphorylation of BRZ1 through one of the novel candidate proteins, the kinase MITOGEN-ACTIVATED PROTEIN KINASE KINASE 5 (MKK5), another component potentially playing a role in BZR1 regulation was revealed.

Finally, TAP has also been put to use to explore the importance of the dynamics of protein interaction in the leaf development of maize (Nelissen et al. 2015 see **addenda**). This was done through the use of the fairly recently developed label free quantification tool (LFQ) implemented in the MaxQuant software. The use of this tool in combination with affinity enrichment/purification techniques provide now a powerful new technique to identify functionally relevant protein-protein interaction involved in hormonal signalling (Smaczniak et al. 2012).

It is important to note that all of the tools described above that are currently used to investigate protein-protein interactions in plants, are most efficient when dealing with strong and stable interactions. Approaches to identify weak and transient interactions that are already established in the mammalian field, like crosslinking protein interactions (Walzthoeni et al., 2013) and label transfer protein interaction analyses such as BioID (Roux et al., 2013), would certainly benefit the plant hormone signalling field to more comprehensively grasp the plethora of protein-protein interactions that take place.

3. PTM proteomics for elucidating plant hormone signalling

Following plant hormone perception, the signal is transduced via cascades often involving PTMs of key proteins. The most extensively studied plant PTMs via proteomics-driven technologies to date are phosphorylation and ubiquitination, which will be the focus of this section of the review (Fig. 1). Other less investigated modifications such as sumoylation have also been claimed as important for plant hormone signalling (Miura and Hasegawa, 2010; Park et al., 2011), however they will not be discussed here.

3.1. Phosphoproteomics studies in plant hormone signalling

Reversible phosphorylation of plant proteins is an important regulatory mechanism involving protein kinases and phosphatases, capable of respectively phosphorylating and dephosphorylating proteins. This protein modification can affect protein function, subcellular localization, interacting partners and stability in response to hormones. In plants, phosphorylation is generally observed on serines and threonines, and more scarcely on tyrosine residues (Ghelis, 2011; Lin et al., 2014).

An early study combined 2D DIGE with prior phosphoprotein enrichment by gallium-based Immobilized Metal Affinity Chromatography (IMAC) to investigate brassinosteroid signal transduction (Tang et al., 2008a). Six proteins showed brassinosteroid-dependent changes in their phosphorylation status, including BAK1 and BRASSINAZOLE-RESISTANT 1 (BZR1), established players in the brassinosteroid signalling pathway. In addition, *in vivo* phosphorylation sites were identified for two tetratricopeptide repeat proteins and a phosphoenolpyruvate carboxykinase (PCK1). A few years later, Chen *et al*. carried out a phosphoproteomics study of plants treated with abscisic acid, auxin, gibberellic acid, jasmonate or cytokinin, to reveal phosphorylation events that act during different hormonal responses (Chen et al., 2010). Arabidopsis cell cultures were harvested at several time points post treatment and, after protein digestion, TiO_2 tips were used to enrich for phosphopeptides. In total, 152 phosphosites were identified as being affected by at least one of the phytohormones, including new phosphorylation sites in abscisic acid response element binding factors and auxin transporters. Interestingly, the G protein α subunit 1 was found phosphorylated in response to all of the hormones, and thus possibly represents a common phosphorylation hub in hormonal signalling.

The development of more robust approaches for phoshopeptide enrichment (Rappsilber et al., 2007; Zhou et al., 2013b), together with the increase in resolving power and mass accuracy of mass spectrometers, fuelled recent phosphoproteomics studies in the plant field. Enrichment of phosphopeptides with Ti^{4+}-IMAC-affinity matrices, enabled the Menke lab to identify 3,068 phosphopeptides in auxin-treated roots, of which 20 showed a robust and significant up-regulation after auxin treatment as compared to control samples (Zhang et al., 2013). Several known auxin signalling and transport proteins such as ARF2, SUPPRESSOR OF AUXIN RESISTANCE 3 (SAR3), SORTING NEXIN1 (SNX1), PIN2, MULTIDRUG RESISTANCE PROTEIN 1 (MDR1) and MDR4 were shown to be differentially phosphorylated. The study was further validated by functionally analyzing phosphoprotein SNX1, showing that phosphorylation of its serine-16 is instrumental during auxin-induced lateral root development.

With a specific focus on the role of SnRK2 protein kinases in abscisic acid signalling, phosphoproteomic differences were compared in wild-type seedlings and *snrk2.2/2.3/2.6* triple mutants treated with abscisic acid (Wang et al., 2013b). Phosphopeptide enrichment was performed by two partially complementary polymer-based metal ion affinity chromatography techniques, with titanium and zirconium, enabling the identification of 5,386 unique phosphorylated peptides. Label-free quantitation assigned 130 proteins (166 peptides) as differentially phosphorylated in wild-type seedlings in response to exogenous abscisic acid. Moreover, 58 of these proteins were no longer up-regulated in the triple SnRK2 mutant background upon treatment, hence constituting possible SnRK2 substrates. Several known SnRK2.6 substrates as well as proteins involved in nucleotide binding and flowering time regulation were identified. A similar study brought more precision to these results, revealing that SnRK2 promotes abscisic acid induced activation of MITOGEN-ACTIVATED PROTEIN KINASE 1 (MPK1) and MPK2 and mediates phosphorylation of serine-45 of bZIP transcription factor ABSCISIC ACID RESPONSIVE ELEMENT

BINDING PROTEIN (AREB1) (Umezawa et al., 2013). Additionally, a previously unknown protein, SNRK2-SUBSTRATE 1 (SNS1), was characterized as a SnRK2 substrate, playing a repressive role during abscisic acid signalling. In a different approach, phosphoproteins extracted from abscisic acid supplemented Arabidopsis guard cell protoplasts were visualized via far-Western blot analysis with 14-3-3 proteins as tagged bait proteins and subsequently identified via LC-MS/MS (Takahashi et al., 2013). Importantly, this work revealed the significance of a set of bHLH proteins, designated as ABSCISIC ACID-RESPONSIVE KINASE SUBSTRATE 1 (AKS1), AKS2 and AKS3, as transcription factors facilitating stomatal opening.

These large-scale strategies to identify hormone-dependent phosphorylation events in plant proteomes have showed great potential so far in unravelling key steps in different hormonal signalling cascades. It will now be important to further apply these contemporary phosphoproteomics techniques on various hormone pathways and validate the observed differences to unequivocally demonstrate their importance in the different signaling cascades.

3.2. Hormonal signalling can be propagated by ubiquitination of plant proteins

Ubiquitination plays a pivotal role in most plant hormonal signalling circuits. As discussed above, degradation of ubiquitinated proteins through the 26S proteasome enables plants to regulate production, perception or downstream effects of hormones. Profiling studies of the ubiquitinome are still scarcely performed in plants (Kim et al., 2013; Manzano et al., 2008; Saracco et al., 2009; Svozil et al., 2014), and were based on ubiquitin-binding domains or overexpression of tagged variants of ubiquitin. In the future these approaches could, in combination with signalling mutants or hormone treatments, definitely contribute to a better understanding of the different phytohormonal signalling pathways. In addition, novel technologies to enrich ubiquitinated peptides are rapidly emerging which would also be beneficial in plant research, like antibodies raised against the ubiquitin remnant motif, which were proven very efficient to map ubiquitination sites in mammalian proteomes in numerous studies (Kim et al., 2011; Udeshi et al., 2013a; Udeshi et al., 2013b; Wagner et al., 2011; Xu et al., 2010a), and the COFRADIC technique that has been adapted recently to identify ubiquitinated peptides (Stes et al., 2014). Considering the described importance of ubiquitination processes in plant hormonal signalling cascades, these techniques hold great potential to uncover hormone-induced changes in the plant ubiquitinome.

4. Conclusions and future perspectives

In this review we discussed MS-based techniques as useful tools for uncovering the molecular mechanisms of plant hormonal signalling. Improvements of the mass spectrometers and the sample preparation techniques have led to increasingly higher numbers of proteins identified, providing a constantly growing insight into phytohormonal signalling cascades. Proteomics-driven research of hormone-directed

changes in protein abundance, protein-protein interactions and PTMs empowered great leaps in this field, nevertheless, a number of challenges lie ahead.

A deep exploration of complex proteomes and low abundant proteins require contemporary, state-of-the-art proteomics tools. Differential protein expression analyses of hormone signalling mutants together with hormone treatments offered several new insights. As plant hormones regulate diverse responses in a tissue- or cell-specific manner, the material sampled can hugely impact the outcome of a proteomics experiment. In that respect, cell sorting techniques, like fluorescence-activated cell sorting (FACS), could be employed to investigate cell type specific hormonal signalling events, for example by using plants that express fluorophores such as GFP under cell type specific or hormone-responsive promoters as protoplast sources (Petricka et al., 2012). Furthermore, the brassinosteroid work by the Wang lab nicely exemplified how fractionation into subcellular compartments can be instrumental for unravelling hormone signalling cascades (Deng et al., 2007; Tang et al., 2008a; Tang et al., 2008b). The use of isotope-containing labels ensures robust and precise quantitation. In contrast to the prevalent use of SILAC (Stable Isotope Labelling with Amino Acids in Cell Culture) in mammalian proteome research, this method has not yet been widely implemented in the plant field. Despite several efforts to adapt SILAC to plants (Bindschedler et al., 2008; Lewandowska et al., 2013), the auxotrophic nature of plants imposes low uptake and incorporation efficiencies of the supplemented light or heavy amino acids. Leaving a substantial part of the proteins unlabelled, accurate quantification of most proteins is generally not possible. Plants proteins can be efficiently labelled metabolically with ^{15}N stable isotope labelling in Arabidopsis (SILIA). Upon addition of ^{15}N-containing inorganic salts, like $K^{15}NO_3$, to plants, incorporation of more than 98% can be achieved, making ^{15}N labelling the method of choice today in quantitative plant proteomics studies (Ippel et al., 2004). Also, in plant hormone studies a subtle trend towards this labelling method can be noticed, slowly moving away from post-metabolic chemical labelling. The advantage of metabolic labelling is that proteins are labelled while being synthesized, and samples can be mixed directly after protein extraction. This eliminates experimental variability during protein digestion and subsequent sample processing steps, which can give rise to artefacts (Mann, 2006). The above-mentioned phosphoproteomics study of auxin-treated roots nicely illustrates the power of ^{15}N-based metabolic labelling, where in combination with Ti^{4+}-IMAC chromatography more than 3,000 phosphopeptides could be quantified (Zhang et al., 2013).

In the case of protein-protein interactions, techniques currently compatible with plant material are mostly designed for the detection of strong and stable interactions. However, weak and transient interactions also play important roles in hormone responses. Therefore, alternative techniques or adaptations of the existing techniques will certainly create valuable tools to study the whole of the interactions induced upon hormone perception. As for PTMs in hormone transduction cascades, a more generalized use of the available techniques to study phosphorylation and ubiquitination would prove useful in combination with hormone treatments or signalling mutants, followed by the validation of the identified proteins and the modifications

they carry. Additionally, other PTMs, such as oxidation, glycosylation, sumoylation and rubylation/neddylation, represent interesting future study subjects in the plant hormone field.

Finally, we would like to highlight that major breakthroughs have been made when quantitative proteomics results were validated in follow-up functional studies, like the discovery of BSKs (Tang et al., 2008b) and PP2A (Tang et al., 2011) as core components of the brassinosteroid signalling cascade, and of NINJA as an adaptor protein instrumental in regulating the jasmonate response (Pauwels et al., 2010). To transform proteomic data into biological data, confirmation on the gene level of selected candidates and further functional validation are mandatory.

Tables

Table 1: Overview of plant hormone studies using mass spectrometry-based strategies.

Hormone	Study	Sample	Treatment	Labelling techniques	Enrichment techniques	Chromatography and Mass spectrometry	Organism	Reference
Abscisic acid	Changes in guard cell proteomes of wild type and G protein mutant backgrounds after abscisic acid treatment.	Guard cell protoplasts	50 µM abscisic acid (4 h)	iTRAQ Labelling		SCX MALDI-TOF/TOF-MS	Arabidopsis	[52]
	Abundance changes on the protein level in rice post abscisic acid treatment.	Cell cultures	100 µM abscisic acid (0.5, 2, 6 h)	iTRAQ Labelling		SCX LC-MS/MS	Rice	[53]
	Abscisic acid and/or G-protein dependent changes in the root proteome.	Root tissue from 2-week-old seedlings	100 µM abscisic acid (8 h)	iTRAQ Labelling		SCX LC-MS/MS	Arabidopsis	[54]
	Abscisic acid and/or GTG protein dependent changes in the root proteome.	Root tissue from 2-week-old seedlings	100 µM abscisic acid (8 h)	iTRAQ Labelling		SCX LC-MS/MS	Arabidopsis	[55]

	SnRK2-dependent changes in protein phosphorylation status post abscisic acid treatment.	2-week-old seedlings	50 µM abscisic acid (0, 15, 30, 90 min)		Phosphopeptide enrichment with TiO_2	LC-MS/MS	Arabidopsis	[87]
	Search for SnRK2 substrates involved in abscisic acid response.	12-day-old seedlings	50 µM abscisic acid (30 min)		Phosphopeptide enrichment with TiO_2	LC-MS/MS	Arabidopsis	[86]
Auxin	Factors downstream of PIN2 involved in auxin-mediated gravity response.	Root tissue from 4-day-old seedlings	-			2-DE LC-MS/MS	Arabidopsis	[33]
	Comparison of changes in wild-type and *tir1* proteomes in response to auxin.	7-day-old seedlings	1 µM or 1 nM indole-3-acetic acid (6, 12, 24 h)			LC-MS/MS	Arabidopsis	[57]
	Differential phosphorylation of proteins post auxin treatment with a focus on lateral root development.	7-day-old seedlings	Lateral root inducing conditions	^{15}N labeling	Phosphopeptide enrichment with Ti^{4+}-IMAC	LC-MS/MS	Arabidopsis	[85]
	The effects of auxin on proteins involved in root formation.	Basal parts of leaf sheaths 2-week-old rice seedlings	Soil drenching with 2,4-dichlorophenoxyacetic acid			2-D DIGE LC-MS/MS	Rice	[41]

Brassinosteroids	Interaction partners of SERK1.	7-day-old Arabidopsis plants	-	CoIP	(LC) MALDI-TOF/MS	Arabidopsis	[63]
	Phosphorylation, kinase activation, and oligomerization of the BRI1/BAK1 complex in response to brassinosteroids.	11-day-old seedlings	100 nM brassinolide (90 min)	CoIP	LC-MS/MS	Arabidopsis	[66]
	Brassinosteroid signalling events and early response proteins.	4-day-old plants	100 nM brassinolide (2 h)	Phosphopeptide enrichment with Ti^{4+}-IMAC	2D DIGE LC-MS/MS	Arabidopsis	[44]
		Plasma membrane isolated from 7-day-old seedlings	100 nM brassinolide (2 or 24 h)				
	BZR1-interacting partners.	cell cultures	-	TAP	LC-MS/MS	Arabidopsis	[74]
	Identification of brassinosteroid-regulated proteins.	Fully grown plants	-		2-D DIGE LC-MS/MS	Rice	[42]
	BSK Mediate signal transduction from the receptor kinase BRI1 in *Arabidopsis*	Plasma membrane isolate	100 nM brassinolide (2 h)		2-D DIGE LC-MS/MS	Arabidopsis	[45]

Ethylene	Comparison of root proteomes of the *skl* mutant and wild-type plants, in response to ethylene and inoculation with bacterial symbionts.	Root material	1-Aminocyclopropane-1-carboxylic acid (1 and 3 days)		2-DE MALDI-TOF MS/MS	*Medicago truncatula*	[38]
Jasmonates	Study to elucidate interaction partners of JAZ proteins.	Cell cultures	100 µM jasmonic acid	TAP	MALDI-TOF/TOF-MS	Arabidopsis	[73]
Strigolactones	Changes in protein abundance upon strigolactone treatment.	14-day-old seedlings	5 µM GR24 (12 h)	iTRAQ labelling	MudPIT LC-MS/MS	Arabidopsis	[56]
Cytokinins	Tissue and temporal specificity of the proteome response to cytokinin.	Roots and shoots from 6-day-old seedlings	5 µM benzyl adenine (30 min, 2 h)		2-DE LC-MS/MS	Arabidopsis	[37]

Hormonal cross-talk	Crosstalk between auxin and ethylene on the protein level.	6-day-old plants	1 µM amino-cyclopropane acid or 1 µM indole-3-acetic acid (24 h)		2-D DIGE MALDI TOF/TOF/MS	Arabidopsis	[34]
	Brassinosteroid and cytokinin cross-talk.	Organelle-enriched pellet from 4-week-old plant tissue	100 µM zeatin and 0.5 mg/L 24-epibrassinolide (24 h)	organelle enrichment	MudPIT LC-MS/MS	Arabidopsis	[58]
	Changes in the phosphoproteome upon abscisic acid, cytokinin, jasmonate, gibberellin, or auxin application.	Cell cultures	100 µM of abscisic acid, gibberelic acid, indole-3-acetic acid, kinetin and jasmonic acid (1, 3, 6 h)	phosphopeptide enrichment with TiO_2	LC-MS/MS	Arabidopsis	[82]

Chapter 2: The whats, the wheres and the hows of strigolactones in the roots

Cedrick Matthys[1,2,7] • Alan Walton[1,2,3,4,7] • Sylwia Struk[1,2] • Elisabeth Stes[1,2,3,4] • François-Didier Boyer[5,6] • Kris Gevaert[3,4] • Sofie Goormachtig[1,2]

✉ Sofie Goormachtig

sogoo@psb.vib-ugent.be, Tel: +32 9 33 13 910; Fax: +32 9 33 13 809

[1] Department of Plant Systems Biology, VIB, Technologiepark 927, 9052 Gent, Belgium

[2] Department of Plant Biotechnology and Bioinformatics, Ghent University, Technologiepark 927, 9052 Gent, Belgium

[3] Department of Medical Protein Research, VIB, Albert Baertsoenkaai 3, 9000 Gent, Belgium

[4] Department of Biochemistry, Ghent University, Albert Baertsoenkaai 3, 9000 Gent, Belgium

[5] Institut Jean-Pierre Bourgin, Unité Mixte de Recherche 1318, Institut National de la Recherche Agronomique-AgroParisTech, 78026 Versailles Cedex, France

[6] Centre de Recherche de Gif, Institut de Chimie des Substances Naturelles, Unité Propre de Recherche 2301, Centre National de la Recherche Scientifique, 91198 Gif-sur-Yvette, France

Author's contribution: [7] These authors contributed equally to this work.

This chapter is adapted from Matthys, Walton, et al. 2016 *Planta*, 1-11.

Abstract

Strigolactones are a group of secondary metabolites produced in plants that have been assigned multiple roles, of which the most recent is hormonal activity. Over the last decade, these compounds have been shown to regulate various aspects of plant development, such as shoot branching and leaf senescence, but a growing body of literature suggests that these hormones play an equally important role in the root. In this review, we present all known root phenotypes linked to strigolactones. We examine the expression and presence of the main players in the biosynthesis and signaling of these hormones and bring together the available information that allows us to explain how strigolactones act to modulate the root system architecture.

1. Introduction

Strigolactones are a class of terpenoid lactones derived from carotenoids which were originally identified as signals that stimulate seed germination of plant parasitic weeds, such as *Striga* sp. and *Orobanche* sp. (Cook et al. 1966). Additionally, within the rhizosphere, these molecules have been found to enhance the initiation of arbuscular mycorrhization, a plant-fungal symbiosis that facilitates water and nutrient uptake by host plants (Akiyama et al. 2005). More recently, the role of strigolactones as plant hormones controlling various developmental processes was demonstrated.. (Woo et al. 2001; Snowden et al. 2005; Shen et al. 2007, 2012; Gomez-Roldan et al. 2008; Umehara et al. 2008; Tsuchiya et al. 2010; Toh et al. 2012). Strigolactones were initially assigned a role in the repression of shoot branching. Since then they have been implicated in various other aspects of plant development: they have been shown to increase secondary growth leading to thicker stems, accelerate leaf senescence and also play a role in germination. Furthermore, they regulate below ground architecture, reducing the number of lateral roots and increasing root hair length. An overview of the hormonal roles of strigolactones is given in Fig. 1.

To date, over 20 naturally occurring strigolactones have been reported, all of which possess a conserved basic structure made up of a tricyclic lactone linked to a methyl butenolide group via an enol ether bridge (reviewed in Xie et al. 2010). These two parts of the main structure are often referred to as the ABC-ring and the D-ring respectively (Fig 2A). Several studies have attempted to identify the elements within this general structure that are fundamental for the bioactivity of these molecules. The enol-ether bridge has been shown to be important for these compounds to act as hormones controlling various aspects of plant development. Although initially believed to also be essential for their role as germination stimulants for parasitic seeds (Magnus et al. 1992), it has been shown that the carbon–carbon double bond in the enol ether can be replaced by a carbon–nitrogen double bond without a loss of activity (Kondo et al. 2007). Finally, in the case of their role as branching inducers for AM fungi, the truncation of A- and AB-rings from the tricyclic ABC lactone resulted in **a** drastic reduction in hyphal branching activity (Akiyama et al. 2010). In conclusion, different aspects of the structure of these molecules are important for the different roles they are implicated in.

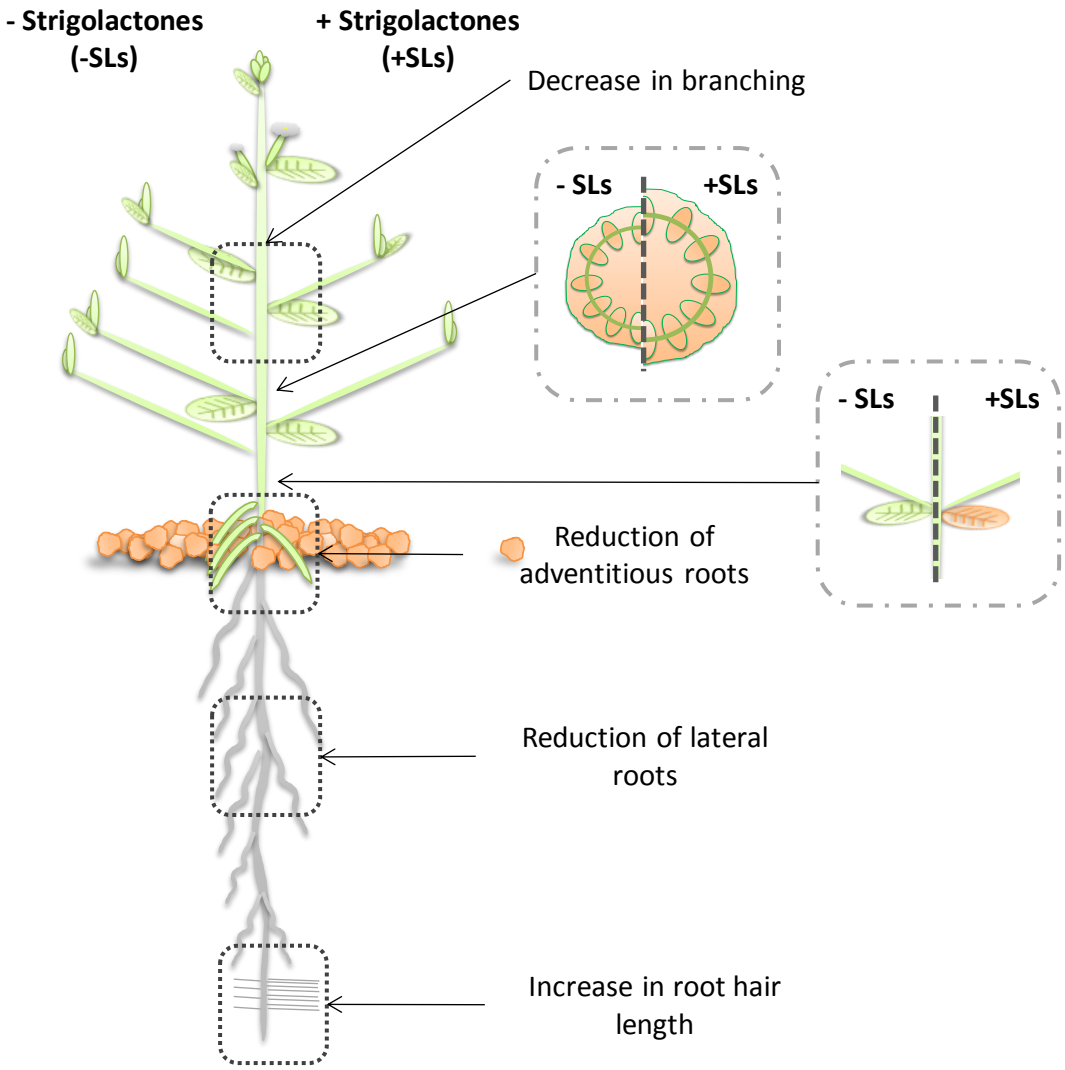

Figure 1: Hormonal Roles of Strigolactones. Strigolactones lead to a reduction in shoot branching, an acceleration of leaf senescence, an increase in secondary thickening, a reduction in the number of adventitious roots and lateral roots and an increase in root hair length. Figure based on Al-Babili and Bouwmeester, 2015.

Multiple research teams contributed to a better understanding of the strigolactone biosynthetic pathway (reviewed in Waldie et al., 2014). The DWARF27 (D27) protein has been shown to be involved in the first step of the biosynthesis pathway in rice and to catalyze the isomerization of 9-trans-β-carotene to 9-cis-β-carotene (Lin et al., 2009). Subsequent cleavage and oxygen integrative steps carried out by the CAROTENOID CLEAVAGE DIOXYGENASE 7 (CCD7)/MORE AXILLARY GROWTH 3 (MAX3) and CCD8/MAX4 in Arabidopsis give rise to the production of the strigolactone intermediate carlactone (Alder et al., 2012), a bioactive molecule that can save several strigolactone mutant phenotypes (Alder et al., 2012). Downstream of carlactone, a cytochrome P450-encoding MAX1 protein might generate bioactive strigolactones (Booker et al., 2005; Kohlen et

al., 2011; Alder et al., 2012) (Fig 2B). It has also been reported that MAX1 can produce molecules with related structures that are derived from carlactones.

Finally, the basic structure of these strigolactones contains various chiral centers and it has been shown that differences in the stereochemistry can also affect the bioactivity of these molecules. Interestingly, *rac*-GR24, the synthetic analog of strigolactones, common used in laboratories around the world, is itself a racemic mixture of 2 enantiomers that are referred to as GR24+ and GR24- (Fig 2C). GR24+ is thought to mimic naturally occurring strigolactones whereas GR24- is believed to mimic karrikins and other butenolide compounds.

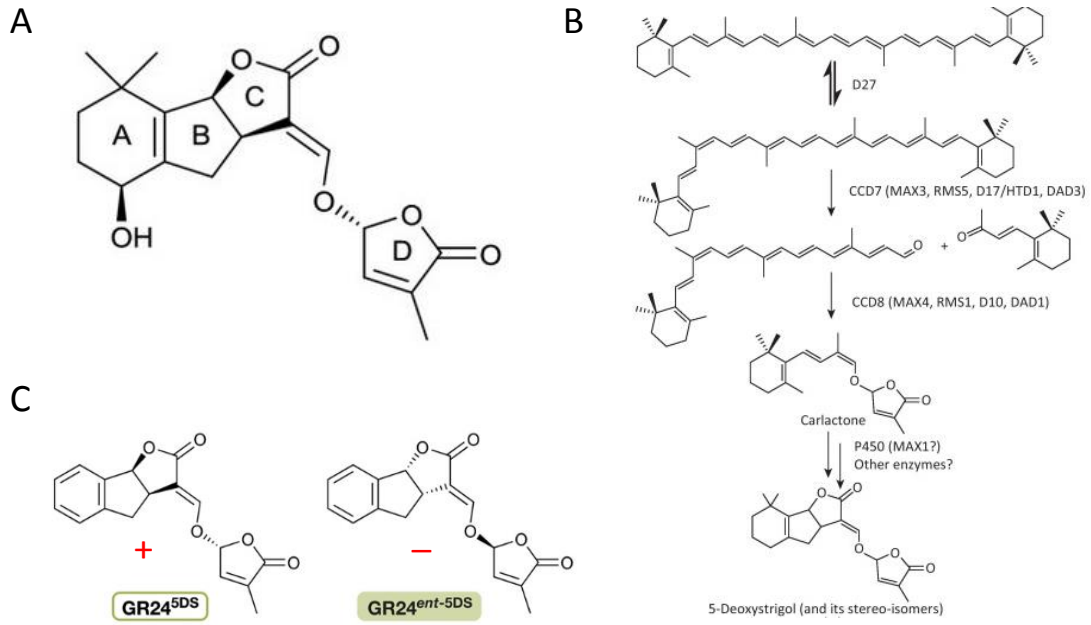

Figure 2: Strigolactone chemistry. (A) Basic A-, B-, C-rings linked via an enol ether bridge to a butenolide D-ring represented on a strigolactone molecule. (B) The strigolactone biosynthesis pathway. (C) The GR24+ (also known as GR24^{5DS}) and the GR24- (also known as GR24$^{ent\text{-}5DS}$) contained within the rac-GR24 racemic mixture. This image is adapted from Scaffidi *et al*. 2014 and Ruyter-Spira *et al*. 2013

The strigolactone signaling pathway is in the process of being unraveled with a central role for the *Arabidopsis thaliana* MORE AXILLARY GROWTH2 *(*MAX2) protein and its orthologs in various plant species (Beveridge et al. 1996; Ishikawa et al. 2005; Stirnberg et al. 2007; Drummond et al. 2011). This MAX2 F-box protein belongs to the same family as the auxin receptor TRANSPORT INHIBITOR RESPONSE1 (TIR1) and the jasmonate receptor CORONATIN INSENSITIVE1 (Dharmasiri et al. 2005; Stirnberg et al. 2007; Sheard et al. 2010). These proteins all display conserved F-box motifs and C-terminal LRRs as well as similar intron-exon positions (Stirnberg et al. 2007). Like TIR1 and COI1, MAX2 is part of a Skp, Cullin, F-box (SCF)-type E3 ligase complex that ubiquitinates proteins, often to target them for proteasomal degradation (Stirnberg et al. 2007;

Vierstra, 2009). TIR1 is localized in the nucleus and can directly interact with proteins like the AUXIN/INDOLE-3-ACETIC ACID (Aux/IAA) proteins upon the detection and binding of auxin, leading to their proteasomal degradation. Aux/IAA proteins bind to transcription factors and repress their activity in collaboration with TOPLESS proteins (Peer, 2013). Their degradation in the presence of auxin therefore results in an increase in expression levels for the auxin responsive genes that these transcription factors control (Figure 3). Similarly, COI1 is an essential nuclear localized player in the signalling pathway of another phytohormone, jasmonates. This F-box protein detects the bioactive forms of jasmonates and targets transcriptional repressors called JASMONATE ZIM-DOMAIN (JAZ) proteins for degradation in a proteasome-dependent manner. In the same way that Aux/IAA proteins repress transcription factors that regulate the expression of auxin responsive genes, JAZ proteins, in collaboration with NINJA, an adaptor that links to TOPLESS proteins, repress the activity of several MYC transcription factors (Perez and Goossens, 2013) (Figure 3). Based on structural similarities, it was suggested that the activity of MAX2 in strigolactone signaling could mimic that of TIR1 for auxin and COI1 for jasmonates.

In *Oryza sativa* (rice) and *Petunia hybrida* (petunia), the MAX2 orthologs were found to interact with the DWARF14 (D14) protein, an α/β hydrolase that is able to bind and hydrolyze strigolactones (Hamiaux et al. 2012; Zhou et al. 2013). D14 is essential for strigolactone signaling and the *d14* mutant shares several traits in common with the *max2* mutant, such as its high shoot branching and aberrant leaf shape. Although similarities can be observed between the TIR1, COI1 and MAX2 F-box proteins, the fact that the D14 alpha-beta hydrolase in necessary for strigolactone signaling represents a major difference between strigolactone signaling and auxin or jasmonate signaling. Indeed, in this respect, parallels can be drawn between strigolactone signaling and gibberlins signaling as the latter, GA INSENSITIVE DWARF1 (GID1), a soluble protein with structural similarity to the hormone-sensitive lipases, is necessary for the detection of the phytohormone. Upon detection of the hormone, GID1 associates with the F-Box protein SLEEPY1 (SLY1) which leads to the targeted degradation of DELLA, releasing the TFs responsible for the transcriptional changes induced by GA to occur (Dill et al., 2004). However, here a clear difference can be seen with strigolactone signaling. For instance, GID1 has no enzymatic activity whereas strigolactones need to be hydrolyzed by D14 to give rise to downstream events in the strigolactone signaling cascade (Figure 3).

Based on studies in rice and *Arabidopsis*, DWARF53 (D53) and members of the SUPPRESSOR OF MAX2 1 LIKE (SMXL) family (consisting of SMAX1 and SMXL2 to SMXL8), respectively were proposed to be D3/MAX2 targets (Jiang et al. 2013; Stanga et al. 2013; Zhou et al. 2013; Kong et al. 2014). The GR24-induced, D3/MAX2- and D14-dependent ubiquitination, and subsequent proteasomal degradation of D53 and SMXL6, SMXL7 and SMXL8, respectively, was demonstrated, bringing us closer to understanding how the MAX2/D14 signaling components give rise to the well-described phenotypes (Wang et al. 2015, Soundappan et al. 2015).

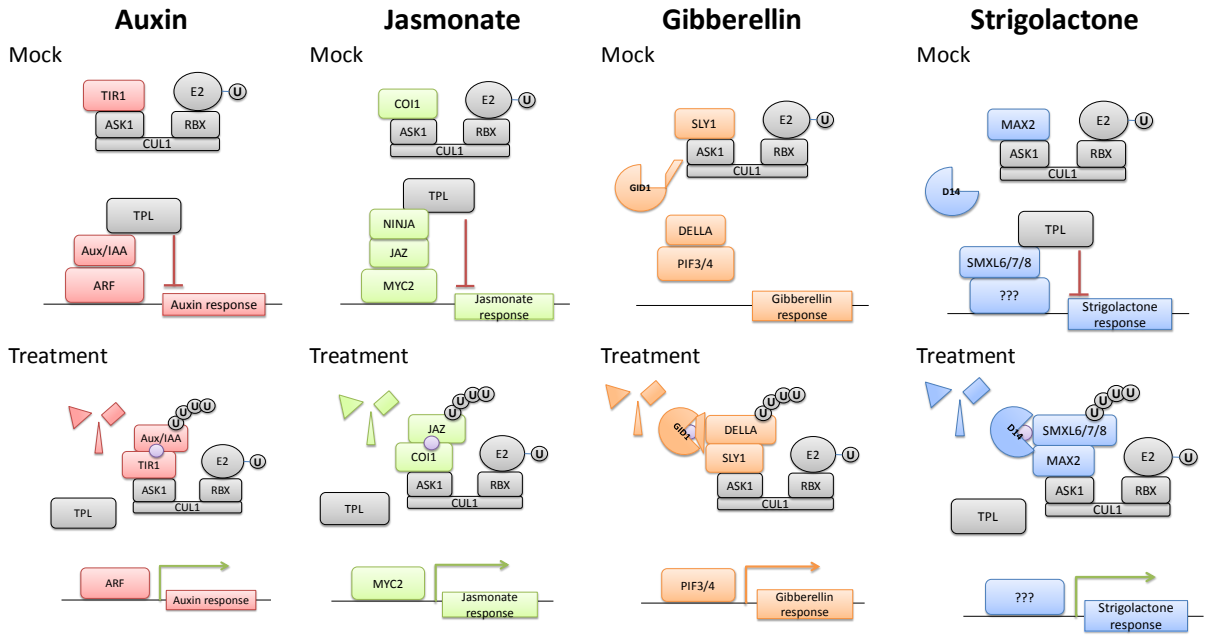

Figure 3: **F-box proteins involved in SCF complexes regulating phytohormonal signaling cascades.** The F-box proteins TIR1, COI1, SLY1 and MAX2 and the substrates of the SCF complexes in which they can be found are shown. Purple circles represent how the phytohormones are bound to the direct protein players in the various cascades.

A higher level of complexity has appeared concerning the strigolactone signaling network as certain of the core components have been shown to also be involved in the signaling of other molecules. For instance, KARRIKIN INSENSITIVE2 (KAI2) in *Arabidopsis*, a protein structurally closely related to D14, is responsible for the detection of karrikins, smoke-derived signals that induce seed germination, a process that also appears to require the MAX2 F-box protein and a member of the SMXL gene family, namely SUPRESSOR OF MAX2 1 (SMAX1) (Nelson et al. 2011; Stanga et al. 2013). Additionally, the commonly used strigolactone analog *rac*-GR24 has been found to trigger also non-strigolactone responses, making the understanding of the strigolactone signaling and the resulting physiological effects even more tangled (Scaffidi et al. 2014). The GR24+ enantiomer in rac-GR24 mimics a natural strigolactone molecule that initiates D14-dependent signaling. However, the unnatural GR24- enantiomer was found to initiate KAI2-specific signaling, rather than a signaling cascade via D14 (Scaffidi et al. 2014). In other words, this enantiomer mimics karrikins and other unknown endogenous compounds that signal via KAI2. Much care should thus be taken when the MAX2-dependent phenotypes resulting from *rac*-GR24 treatment are evaluated, because the outcome might not be strigolactone specific. To further complicate matters, it would appear that, in parasitic plants, some KAI2 orthologs have evolved to recognize strigolactones rather than karrikins (Conn et al. 2015, Tsuchiya et al. 2015).

Much of the initial progress made in unraveling both the biosynthesis and the signaling pathway of strigolactones has initially been based on a set of high shoot branching/tillering mutants identified in multiple species, such as high shoot branching phenotypes of *decreased apical dominance1* (*dad1*) in petunia, *ramosus1* (*rms1*) to *rms5* in *Pisum sativum* (pea), *max1* to *max4* in *Arabidopsis*, and *dwarf* (*d*) and *high tillering dwarf* (*htd*) mutants in rice (Beveridge et al. 1996; Bainbridge et al. 2005; Zou et al. 2006; Stirnberg et al. 2007; Alder et al. 2008; Drummond et al. 2009; Vogel et al. 2010), causing the main focus towards of research, aiming to decipher strigolactone mode of action, to concentrate on the aerial part of the plant. In the meantime, an increasing amount of research is emerging on the effect of strigolactones on the root of various plant species. Here, we review how strigolactones or other molecules that signal through the strigolactone signaling components may give rise to the root phenotypes.

2. What happens in the root?

Although the involvement of strigolactones in shaping the root system architecture has been demonstrated in various species, including *Arabidopsis*, pea, *Medicago truncatula* (barrel medic), rice, and *Solanum lycopersicum* (tomato), most research has been done on *Arabidopsis* (Kapulnik et al. 2011a; Koltai, 2011; Ruyter-Spira et al. 2011; Rasmussen et al. 2012), where a strigolactone effect has been identified on all important aspects of root system architecture such as primary root length, root hair formation, lateral root density (LRD), and adventitious rooting (Fig. 4).

The influence of strigolactones on primary root growth has been reported to be subtle and to depend on the growth conditions and the plant species used. Addition of *rac*-GR24 increased the primary root length of *Arabidopsis*, which is the result from an increase of cortical cells in the primary root meristem, especially when plants are grown in the absence of exogenous sucrose (Ruyter-Spira et al. 2011). This also coincides with an increase in meristem and transition zone size of the primary root (Ruyter-Spira et al. 2011). In agreement, the biosynthetic strigolactone mutants *max1* and *max4* and the signaling mutant *max2* have a shorter primary root than that of the wild type (WT), with a corresponding lower numbers of cortical cells in the primary root meristem, suggesting that endogenous strigolactones control root growth (Ruyter-Spira et al. 2011). However, high concentrations of *rac*-GR24 (> 2.5 µM) lead to a MAX2-independent inhibition of primary root growth, probably due to the toxicity of nonphysiological concentrations (Ruyter-Spira et al. 2011; Shinohara et al 2013).

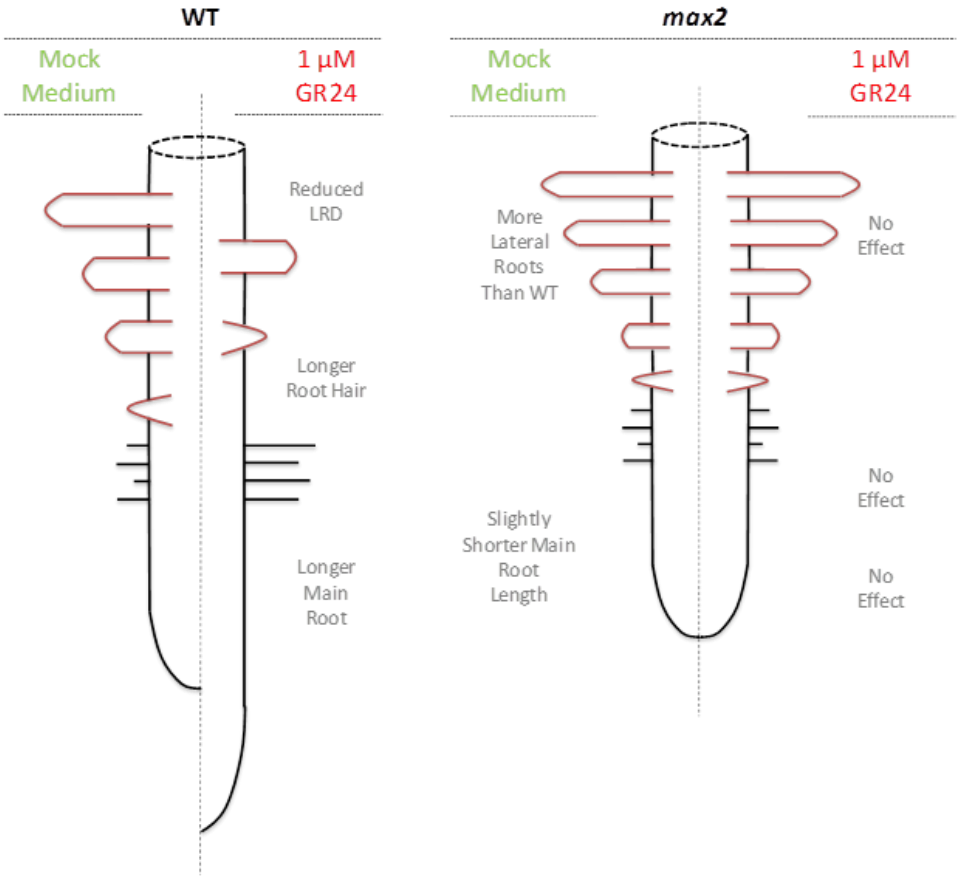

Figure. 4 Known effects of *rac*-GR24 on WT and *max2* mutant *Arabidopis* roots when grown in nutrient rich media

Also in rice, similar effects have been reported, although the seminal root of strigolactone mutants was only shorter than that of the WT under low phosphate and low nitrate conditions, demonstrating that the effect of endogenous strigolactones is influenced by the growth conditions (Sun et al. 2014). Under both normal and nutrient-poor conditions, application of *rac*-GR24 results in an elongation of the primary root of the WT and strigolactone mutants, except for the signaling mutant *d3* (Sun et al. 2014). However, *rac*-GR24 has been reported to have no effect on the seminal root length (Arite et al. 2012) as well as on the primary root length of tomato and *M. truncatula* (Koltai et al. 2010; De Cuyper et al. 2015). For tomato, only a combined treatment with auxin uncovered an effect on the primary root length: the inhibitory effect of auxin on root growth diminishes with the addition of increased concentrations of *rac*-GR24 (Koltai et al. 2010). On the other hand, in *Lotus japonicus* (birdsfoot trefoil) upon silencing of the MAX3 ortholog, a longer rather than a shorter primary root has been reported (Liu et al. 2013). Hence, it is difficult to make general conclusions on the strigolactone influence on the primary root length, probably because of subtle phenotypes, the influence of the growth conditions, or, possibly, because of varying endogenous hormonal backgrounds between different species.

The effect of strigolactones is more pronounced on lateral root (LR) development. In *Arabidopsis*, LR development has been well described as consisting of consecutive developmental

programs (Péret et al. 2009). The process starts with priming of root xylem pole pericycle cells in the root meristem zone, followed by LR initiation through asymmetric cell division of primed pericycle cells, then by a well-controlled pattern of cell division to finally form the dome-shaped LR primordium that pierces through the primary root during LR emergence (Péret et al. 2009). Treatment with *rac*-GR24 has been shown to affect LR initiation or outgrowth in a MAX2 dependent way (Kapulnik et al. 2011a; Ruyter-Spira et al. 2011). More recently, an in depth spatio-temporal analysis using the early LR marker *GATA23* has revealed that the *rac*-GR24 effect on LR development is indeed dual as treatment with GR24 results in both a minor effect on priming (the earliest step in LR development) and a major effect on outgrowth, the latter especially but not exclusively, in the root region closest to the shoot-root junction (Jiang et al. 2015). Accordingly, the lateral root density (LRD) is higher in *max2* than in the WT, indicative of a negative effect of strigolactones on LR development. However, the LR phenotypes of the strigolactone biosynthetic mutants *max3* and *max4* are currently not clear, because the phenotype is the same as that of the WT or, at best, intermediate between that of the WT and that of the *max2* mutant (Kapulnik et al. 2011a; Ruyter-Spira et al. 2011). This observation might indicate that signals other than strigolactones are at play in the regulation of this phenotype, or that some residual strigolactone metabolites are present in the used biosynthesis mutants. Just as for the root length, at increased *rac*-GR24 concentrations, a MAX2-independent decrease of the LRD has been observed that could hint at a toxicity effect when *rac*-GR24 is applied at concentrations higher than 1 µM (Ruyter-Spira et al. 2011). Similar to *Arabidopsis*, the LRD of WT rice is reduced after treatment with various concentrations of *rac*-GR24 (Sun et al. 2014). Comparable to the effect on the primary root length, growth conditions also influence the strigolactone impact, because enhanced auxin levels or signaling as obtained through growth under low phosphate, revert the negative effect of *rac*-GR24 on the LRD into a positive one (Ruyter-Spira et al. 2011). The molecular basis for these observations is still unknown, but could reflect the influence of the auxin landscape on the outcome of strigolactone treatments, as observed during shoot lateral branching (Ruyter-Spira et al. 2011; Shinohara et al. 2013).

Root hair development is an inherent part of root architecture, because root hairs play an essential role in taking up nutrients from the soil (Gilroy and Jones, 2000; López-Bucio et al. 2003). In both *Arabidopsis* and tomato, *rac*-GR24 elongates the root hairs (Kapulnik et al. 2011a; Koltai et al. 2010). However, strigolactone mutants (*max2*, *max3*, and *max4*) do not seem to exhibit shorter root hairs than the WT under control conditions, indicating that this phenotype might not be controlled by endogenous strigolactones (Kapulnik et al. 2011a; Koren et al. 2013; Pandya-Kumar et al. 2014). On the contrary, under phosphate-limiting conditions, the root hair density of the SL-biosynthetic mutant *max4* and signaling mutant *max2* appears to be lower than that of the WT, an effect that can be complemented with a high dose of exogenous *rac*-GR24 (Mayzlish-Gati et al. 2012)

Finally, an effect on root initiation from non-root tissue in *Arabidopsis*, pea (adventitious roots), and rice (crown roots) has been attributed to strigolactones (Arite et al. 2012; Rasmussen et al. 2012). In *Arabidopsis* and pea, both strigolactone biosynthesis and signaling mutants show a higher adventitious rooting capacity than the WT, suggesting that endogenous strigolactones suppress the formation of adventitious roots (Rasmussen et al. 2012). Likewise, application of *rac*-GR24 results in a clear dose-dependent decrease in adventitious roots, but not in the signaling mutants (Rasmussen et al 2012). In dark-grown pea, the SL-biosynthetic mutants, but not the SL-signaling mutants, show a reduced number of adventitious roots instead, pointing to a potential role of SLs, independently of MAX2, in adventitious root formation in the dark (Urquhart et al. 2014). In rice, the crown roots of all strigolactone mutants seem to be shorter than those of the WT and are fewer in number, a phenotype that is rescued by *rac*-GR24 in a concentration-dependent manner for all biosynthesis mutants (Arite et al. 2012; Sun et al. 2014), suggesting that strigolactones regulate crown root development positively in rice, rather than negatively in *Arabidopsis* and pea.

Hence, thus far, of the four root-specific SL-triggered phenotypes that have been observed, two seem directly related to SLs, namely increased primary root length and adventitous rooting. For the effect on root hairs and LRD, more research needs to be done. For the time being, it cannot be excluded that a yet unknown signal, mimicked by *rac*-GR24 and signaling through MAX2, might also be at play.

3. Where does it happen in the root?

3.1. strigolactone biosynthesis and transport

Several decisive initial studies provided the foundations for the strigolactone biosynthesis pathway, mainly in pea (for a review, see Beveridge et al. 2009), but also in *Arabidopsis*, where grafting of WT rootstocks to either the scions of *max1, max3*, or *max4* can rescue the high shoot branching phenotype (Turnbull et al. 2002; Sorefan et al. 2003; Booker et al. 2004). These data underline the importance of the root for (at least a precursor of) strigolactone production, because the root is sufficient to rescue entirely the shoot branching phenotype in these grafting experiments. However, the strigolactones are not exclusively produced in the root, because *max3* and *max4* rootstocks do not lead to an increased shoot branching phenotype in WT scions, a phenotype expected to occur when all strigolactone production would be abolished (Turnbull et al. 2002; Sorefan et al. 2003).

More clues about strigolactone production came from the expression patterns of the biosynthesis genes. The first step in the strigolactone biosynthesis pathway is catalyzed by D27 inside the plastids, being the isomerization of all-*trans*-β-carotene into 9-*cis*-β-carotene (Lin et al. 2009; Waters et al. 2012). Although the grafting experiments hinted at the roots as important sites for strigolactone production, the relative expression of this biosynthesis gene was lower in the roots than

in the above ground tissue (Lin et al. 2009). Additionally, the *d27* mutant root stock, similar to that of the *max3* and *max4* mutants, does not increase the shoot branching of grafted WT scions, suggesting that the D27 activity in the shoot is sufficient to inhibit shoot branching (Waters et al. 2012). Hence, these data indicate that the root is not the main site for the first committed step in the strigolactone biosynthesis pathway. Still, by means of mRNA *in situ* hybridization in rice, *D27* was shown within the root tissue to be specifically expressed in the LRs and in the vascular tissue of the crown roots (Lin et al. 2009). However, an overview of the expression pattern along the primary root is currently missing in the literature.

The expression pattern of the *MAX3* and *MAX4* genes coding for carotenoid cleavage dioxygenase also points to a general production of strigolactones in several tissues, nonetheless with a main production site in the root. Detailed analysis of p*MAX4*:*GUS Arabidopsis* lines showed that, although a weak expression can be detected in the hypocotyl, the petioles and -to a certain extent- in the nodal tissue, the vast majority of staining is in the primary root tip as early as the first day post germination and in the tips of emerged LRs (Sorefan et al. 2003; Bainbridge et al. 2005). Additionally, detailed comparative analysis of *MAX3* expression in multiple tissues hints at a predominant expression in the roots, although relatively high levels are also detected in siliques, the primary inflorescence stem, and to a lesser extent in secondary inflorescence stems and petioles (Booker et al. 2004).

Finally, the *MAX1* gene, coding for a cytochrome P450 enzyme, involved in the last documented step(s) of the formation of a bioactive SL, has been shown to be expressed all over the plant, more particularly within the vascular tissue (Booker et al. 2005). In the root, the expression starts in the developing vascular tissue above the differentiation zone of the root tip, a pattern that does not overlap with the *MAX4* expression within the root tip (Booker et al. 2005). The nonoverlapping expression patterns are in agreement with the demonstrated mobile nature of carlactone, a known intermediate in strigolactone biosynthesis, which is the end product of MAX4 and the substrate of MAX1 (Booker et al. 2005; Scaffidi et al. 2013; Seto et al. 2014). However, the general *MAX1* expression suggests that strigolactones can be produced everywhere in the plant, thus also in the root.

Altogether, these data imply that strigolactones are not exclusively produced in the root, but more generally within the vascular tissue of many organs, but long-distance transport from the root toward the shoot has been considered as well. In agreement, mass spectrometry revealed that strigolactones occur in the xylem sap of *Arabidopsis* and tomato (Kohlen et al. 2011). Valuable information regarding cell-to-cell transport was obtained from research in petunia that identified an ATP-binding cassette transporter, designated PLEIOTROPIC DRUG RESISTANCE1 (PDR1) as a key strigolactone transporter (Kretzschmar et al. 2012). This transporter was shown to be localized asymmetrically in root cells, with different expression patterns depending on the cell type involved (Sasse et al. 2015). In root hypodermal cells, PDR1 is localized on the apical membrane, hinting at an

active strigolactone transport mechanism toward the shoot, whereas in the hypodermal passage cells, which are specific sites in which arbuscular mycorrhizal fungi can penetrate the host, the expression is confined to the outer-lateral membrane, indicative for active transport outward into the rhizosphere.

3.2. Strigolactone Signaling

Both known strigolactone signaling genes *MAX2* and *D14* are expressed in the vascular tissue of several plant organs. MAX2 is mainly localized in the nucleus and distributed in the cells associated with vascular tissues throughout the plant (Shen et al. 2007; Stirnberg et al 2007). Also in the root, *MAX2* expression occurs in vascular, pericycle, and endodermal cells, with decreasing expression levels toward the root base (Stirnberg et al. 2007). In *Arabidopsis*, the expression pattern of the *D14* largely ties in with that of *MAX2*. However, inside the root, *D14* expression is absent in the meristematic zone of the root tip, but appears in the root differentiation and elongation zones, whereafter it progressively gets restricted to the phloem cells (Chevalier et al. 2014). So, both in the root tip and in older part of the root vascular bundle, the expression patterns of *MAX2* and *D14* do seemingly not overlap. Nevertheless, because a translational *D14:GUS* fusion has an enlarged expression pattern compared to a transcriptional fusion, with an accompanying high expression level in the root tip, the D14 protein should be present where *MAX2* is expressed (Chevalier et al. 2014). The subcellular localization of D14 has been found to be both cytoplasmic and nuclear in all investigated tissue types (Chevalier et al. 2014).

This general expression pattern suggests that strigolactone signaling mediated by MAX2 and D14 can happen throughout the plant, although generally restricted to the vascular tissue of the various organs. In the root, it is noteworthy that the signaling components are not always expressed in the specific zones where strigolactones play a role, such as in the trichoblasts, *i.e.* the epidermal cells from where root hair cells develop (Stirnberg et al. 2007; Koren et al. 2013; Chevalier et al. 2014). Additionally, re-establishment of the *MAX2* expression specifically in the endodermis via expression through the endodermis-specific *SCARECROW* (*SCR*) promoter could rescue the root hair, LRD, and primary root length phenotypes in the *max2* mutant (Koren et al. 2013). As such, a non-cell-autonomous action of the strigolactone signaling complex in the root is very likely, because of the possible mobility of the D14 protein (Chevalier et al. 2014; Thieme et al. 2015). Nevertheless, the non-cell autonomous theory of strigolactone signaling should be studied in further detail. Alternatively, mobile secondary messengers, other than SLs, might be generated that move to the action site.

Finally, the expression profiles for the genes encoding 4 SMXL proteins, responsible for coordinating strigolactone signaling downstream of MAX2, were published (Wang et al. 2015, Soundappan et al. 2015). Through use of promoter GUS-GFP reporter lines, root-based expression of

SMAX1,6,7 and *8* was shown to occur in the vascular tissue of the main root and also, specifically for *SMAX1*, in the root cap (Soundappan et al. 2015).

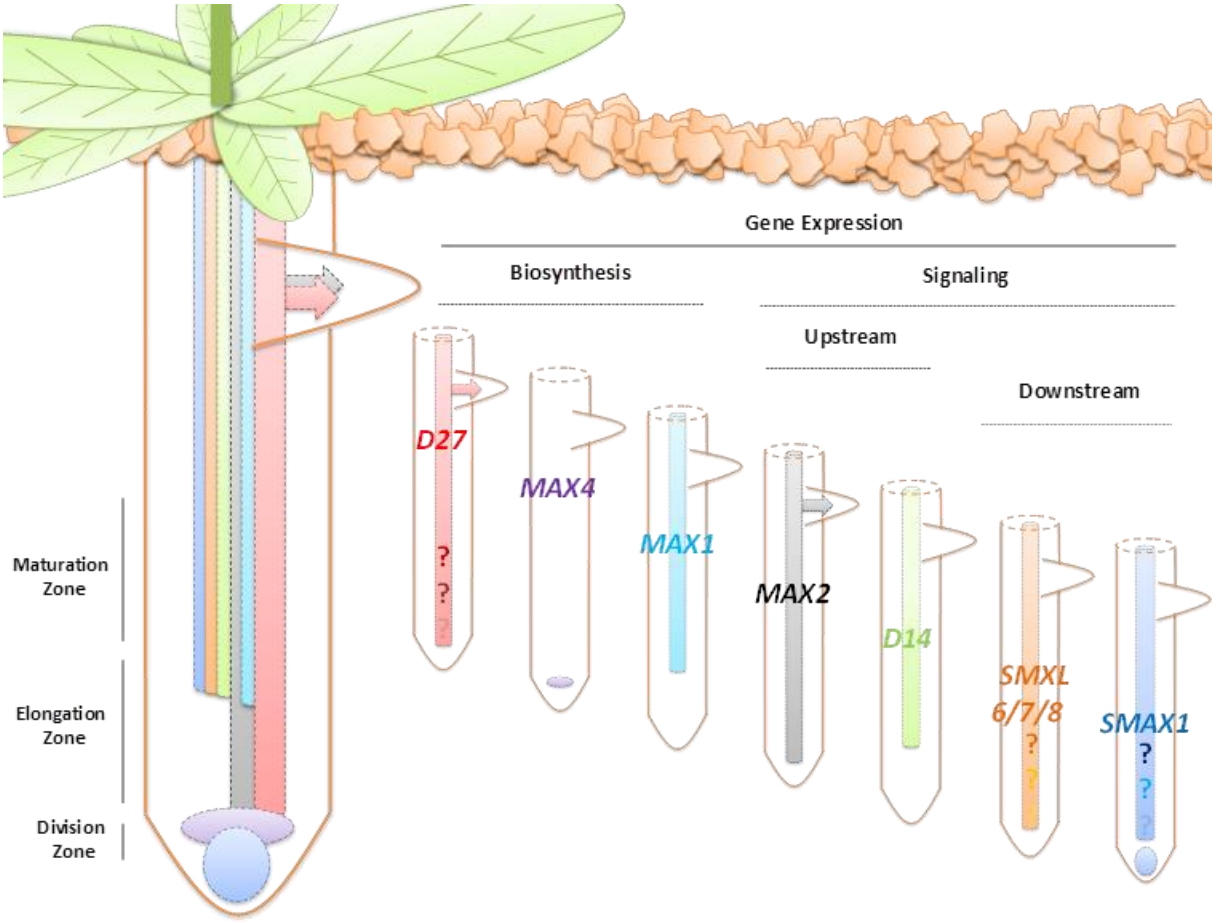

Figure. 5 *Arabidopsis* gene expression in the roots for the main strigolactone biosynthesis genes (*D27, MAX4,* and *MAX1)* and the upstream (*MAX2* and *D14)* and downstream *(SMXL6 SMXL7 SMXL8* and *SMAX1)* signaling components. *MAX4* is only expressed in the root tip, whereas *MAX1* is expressed in the vasculature until the differentiation root zone. *MAX2* is expressed in the root vasculature until the root tip, not completely overlapping with the *D14* expression pattern, because *D14* expression is absent in the root tip, but the D14 protein is present in the root tip (data not included in the figure). * As no data for *D27* are available in *Arabidopsis*, the current profile is deduced from information available in rice, and because of lack of spatial information on the *D27* expression along the primary root, assumptions on the extent of the expression pattern were made, indicated by '???'.

The available information concerning the tissue-specific localization of the main players in the strigolactone network is summarized Fig. 5. The expression data of all genes are based on studies carried out in *Arabidopsis*, with the exception of *D27* that was deduced from work in rice, because no spatial expression data are available in *Arabidopsis*. MAX3 has been omitted, because, to our knowledge, no detailed spatial expression analyses have been carried out for this gene.

3.3. How does it happen in the roots?

Phytohormones are known to interact with each other to regulate specific phenotypes. A large body of research has revealed that, just as for other organs, the action of strigolactones in the root often takes place in concert with other phytohormones. The best studied case is the tight crosstalk between strigolactones and auxin for the action of strigolactones on shoot branching (Crawford et al. 2010; Domagalska and Leyser, 2011; Shinohara et al. 2013). For instance, exogenous auxin can directly affect the key strigolactone biosynthesis genes, inducing the expression of both *MAX3* and *MAX4* (Foo et al. 2005; Hayward et al. 2009). Inversely, *rac*-GR24 leads to a significant decrease in expression of *INDOLE-3-ACETIC ACID INDUCIBLE 1* (*IAA1*), an auxin-responsive gene for which the mutant is known to be insenstivie to auxin with regard to the usual inhibition of root and hypocotyl elongation and stimulation of LR growth upon treatment (Park et al. 2002; Yang et al. 2004; Mashiguchi et al. 2009). Additionally, in the root tip, prolonged treatments with *rac*-GR24 resulted in a down-regulation of the auxin efflux carriers PIN-FORMED1 (PIN1), PIN3, and PIN7 (Ruyter-Spira et al. 2011). However, in-depth research on *PIN1* expression revealed that, in contrast to strigolactones that induce the endocytosis of PIN1 proteins from the plasma membrane in shoots, roots are not responsive to short strigolactone treatments, both regarding total PIN1 protein levels and subcellular localization (Shinohara et al. 2013). This observation could indicate that the crosstalk between strigolactones and auxin might be differently regulated in the shoot and in the root, or that some root responses might be the indirect result of PIN1-affecting strigolactones in the shoot (Shinohara et al. 2013).

The effect of *rac*-GR24 on the LRD of *Arabidopsis* is influenced by the auxin status of the plant (Ruyter-Spira et al. 2011). At low auxin concentrations, the addition of *rac*-GR24 leads to a decreased LRD, whereas at high auxin concentration this treatment causes an increased LRD (Ruyter-Spira et al. 2011). To explain this phenomenom, *rac*-GR24 might cause auxin levels to sink below an optimum for LR development, through a reduction in auxin flow via modified PIN recycling at the membrane in the xylem parenchyma cells, leading to a decreased LRD. However, at high auxin concentrations, the *rac*-GR24-triggered reduction in the auxin flow would cause the total auxin content to move closer to the given optimum, thereby giving rise to an increased LRD (Ruyter-Spira et al. 2011; Shinohara et al. 2013). Nevertheless, more research will be required to fully understand these observations.

Cytokinins (CKs) are also known to play an important role in the regulation of root architecture e.g. by inhibiting LR development by impinging on PIN auxin transporters (reviewed in Vanstraelen and Benková 2012). Cytokinin signaling through the ARABIDOPSIS HISTIDINE KINASE 3 (AHK3)/ARABIDOPSIS RESPONSE REGULATOR 1 (ARR)1/ARR12/ cytokinin signaling module interacts with the *rac*-GR24 mediated inhibition of LR development (Jiang et al. 2015). Mutants in this module show insensitivity to *rac*-GR24 concerning the reduction in LRD and

this insensitivity was shown to be the result of an altered auxin landscape in these mutants (Jiang et al. 2015). This cytokinin module probably acts through the SHORT HYPOCOTYL 2 (SHY2) auxin signaling pathway to interact with strigolactone signaling during lateral root development (Koren et al. 2013; Jiang et al. 2015).

The crosstalk between auxin and strigolactone signaling in root hair elongation is less clear, although both hormones activate elongation of root hairs. An independent way of action would be expected, because auxin treatment enhances the root hair responses to *rac*-GR24 and the *max2* mutant remains responsive to auxin in its root hair phenotype (Kapulnik et al. 2011b), but some crosstalk might occur. Indeed, the auxin receptor mutant, *tir1* was less responsive to *rac*-GR24 (Kapulnik et al. 2011b). Recently, a link between strigolactones and auxin transport has been established that controls root hair elongation, because *rac*-GR24 increases the PIN2 abundance at the epidermal plasma membrane during root hair elongation, suggesting that *rac*-GR24 affects PIN2 endocytosis and endosomal trafficking via actin dynamics in a MAX2-dependent manner (Pandya-Kumar et al. 2014). Besides the auxin-strigolactone link, a role for ethylene in the SL-induced root hair elongation has been elucidated (Kapulnik et al. 2011b). strigolactones appear not to be necessary for the root hair response to ethylene, but both the ethylene signaling mutants *ethylene insensitive2* (*ein2*) and *ethylene response1* (*etr1*) are less responsive to *rac*-GR24 in their root hair phenotype, indicating that ethylene is epistatic to strigolactones for this phenotype. Furthermore, the *rac*-GR24 effect could be abolished by blocking ethylene biosynthesis, indicating that ethylene is required for the impact of *rac*-GR24 on root hair elongation (Kapulnik et al. 2011b).

The effect of *rac*-GR24 on adventitious rooting in *Arabidopsis* has been studied as well by the interaction between strigolactones and auxin and has been found to act mainly independently in the regulation of this process (Rasmussen et al. 2013). Moreover, a possible interaction between cytokinins and strigolactones was investigated and ruled out, because strigolactone mutants are responsive to cytokinins and cytokinin mutants to *rac*-GR24 for the adventitious rooting phenotype (Rasmussen et al. 2013).

The previous experiments allow for insight into the strigolactone effects at the physiological level however in these studies, insight on the molecular level of how this is happening is scarce. The next challenge in understanding strigolactone signaling in roots is to bridge the gap between the hormonal crosstalk network and MAX2 targets. As MAX2 acts in an SCF complex to degrade specific strigolactone targets, a considerable research effort was directed toward uncovering these elusive targets, whose degradation might explain some of the SL-induced MAX2-dependent phenotypes. Recently, the elevated lateral root density observed in the *max2* mutant was shown to be rescued in the *max2,smxl6,smxl7,smxl8* quadruple mutant indicating that signaling through these SMXL proteins controls the effects on lateral root development (Soundappan et al., 2015). It would now be interesting

to assess the response of this quadruple mutant for other known GR24 response such as root hair elongation or effect on primary root length.

Additionally, whereas the involvement of MAX2 in the different root responses is well established, the role of the strigolactone receptor D14 has not been investigated for root length, LR development, root hair elongation, or adventitious root phenotype. This research is all the more relevant when recent findings are taken into account, namely that the commonly used racemic GR24 mixture is apparently not specific to SLs, but can mimic other naturally occurring signaling compounds as well, such as karrikins and unknown endogenous ones, that are perceived through the D14 homolog KAI2 (Guo et al. 2013). To solve this problem, it would be useful to investigate first whether any of the known root phenotypes are either specific to a given *rac*-GR24 enantiomer or a given receptor protein. As indicated above, the *smxl6smxl/smxl8* mutant can rescue the naturally increased LRD of the *max2* mutant (Soundappan et al. 2015). Hence, although not tested yet, these data would predict that D14 is involved in the strigolactone effect on the LRD.

4. Concluding remarks

Thanks to contributions made in several new studies, we progressively gain more insights into the intricate strigolactone signaling networks in the roots. The importance of strigolactones in shaping the root architecture is clear from the various phenotypes that have been identified across multiple species. Detailed information is now available describing the elaborate crosstalk between strigolactones and other plant hormones. Furthermore, it is becoming clear that this new hormone acts in concert with at least auxin, cytokinin, and ethylene for several of the known root phenotypes. Two main challenges remain to be tackled to fully unravel the role of strigolactones in the root. The first task will be to bridge the gap between the MAX2 F-BOX targets and the known root phenotypes (i.e. unraveling the pathway downstream of the SMXLs) and the second will be to investigate the possibility of other compounds than strigolactones that could also be at play in some of the described *max2* phenotypes.

Part II

Identifying key players in the strigolactone signaling pathway in the root of Arabidopsis

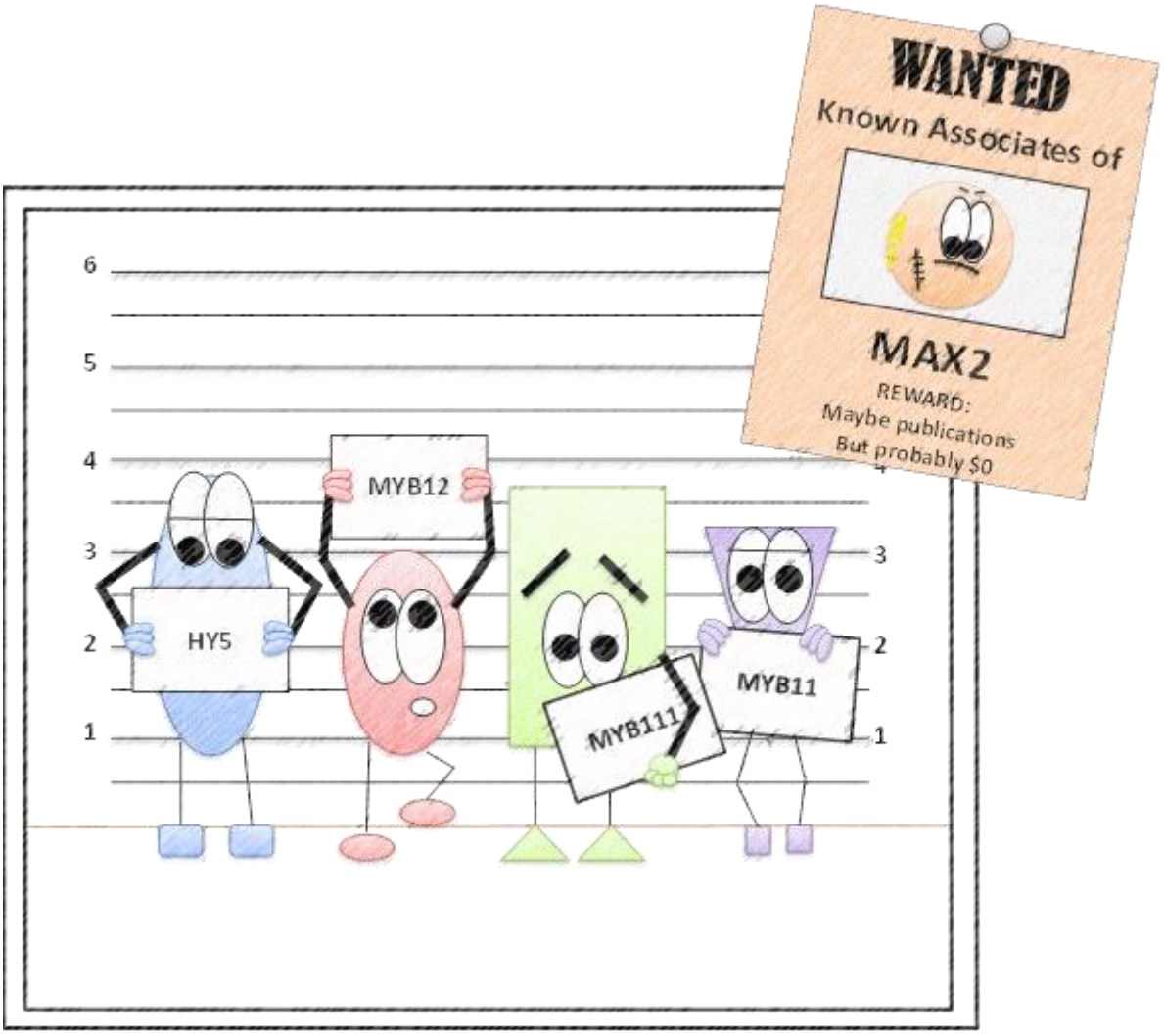

Chapter 3: The response of the root proteome to the synthetic strigolactone GR24 in Arabidopsis*[S]

Alan Walton‡¶§||[**], Elisabeth Stes‡¶§||, Geert Goeminne‡¶, Lukas Braem‡¶, Marnik Vuylsteke✧, Cedrick Matthys‡¶, Carolien De Cuyper‡¶, An Staes§||, Jonathan Vandenbussche§||, François-Didier Boyer‡‡¶¶§§, Ruben Vanholme‡¶, Justine Fromentin‡¶|||||#, Wout Boerjan‡¶, Kris Gevaert§||**[a], and Sofie Goormachtig‡¶**[a]**

From the ‡Department of Plant Systems Biology, VIB, 9052 Ghent, Belgium; ¶Department of Plant Biotechnology and Bioinformatics, Ghent University, 9052 Ghent, Belgium; §Medical Biotechnology Center, VIB, 9000 Ghent, Belgium; ||Department of Biochemistry, Ghent University, 9000 Ghent, Belgium; ✧Gnomixx, 9000 Ghent, Belgium; ‡‡Institut National de la Recherche Agronomique, Institut Jean-Pierre Bourgin, Unité Mixte de Recherche 1318, Equipe de Recherche Labellisée Centre National de la Recherche Scientifique 3559, Saclay Plant Sciences, 78026 Versailles, France; ¶¶AgroParisTech, Institut Jean-Pierre Bourgin, Unité Mixte de Recherche 1318, Equipe de Recherche Labellisée Centre National de la Recherche Scientifique 3559, Saclay Plant Sciences, 78026 Versailles, France; §§Centre de Recherche de Gif, Institut de Chimie des Substances Naturelles, Unité Propre de Recherche 2301, Centre National de la Recherche Scientifique, 91198 Gif-sur-Yvette, France, ||||Laboratoire des Interactions Plantes-Microorganismes, Unité Mixte de Recherche 441, Institut National de la Recherche Agronomique, 31326 Castanet-Tolosan, France; and #Laboratoire des Interactions Plantes-Microorganismes, Unité Mixte de Recherche 2594, Centre National de la Recherche Scientifique, 31326 Castanet-Tolosan, France

Author contributions: A.W., E.S., K.G., and S.G. designed research; A.W., E.S., G.G., L.B., M.V., C.M., C.D.C., A.S., J.V., F.-D.B., and J.F. performed research; A.W., E.S., G.G., and R.V. analyzed data; A.W., E.S., K.G., and S.G. wrote the paper.

Abstract

Strigolactones are plant metabolites that act as phytohormones and rhizosphere signals. Whereas most research on unraveling the action mechanisms of strigolactones is focused on plant shoots, we investigated proteome adaptation during strigolactone signaling in the roots of *Arabidopsis thaliana*. Through large-scale, time-resolved, and quantitative proteomics, the impact of the strigolactone analog *rac*-GR24 was elucidated on the root proteome of the wild type and the signaling mutant *more axillary growth 2 (max2)*. Our study revealed a clear MAX2-dependent *rac*-GR24 response: an increase in abundance of enzymes involved in flavonol biosynthesis, which was reduced in the *max2-1* mutant. Mass spectrometry-driven metabolite profiling and thin-layer chromatography experiments demonstrated that these changes in protein expression lead to the accumulation of specific flavonols. Moreover, quantitative RT-PCR revealed that the flavonol-related protein expression profile was caused by *rac*-GR24--induced changes in transcript levels of the corresponding genes. This induction of flavonol production was shown to be activated by the two pure enantiomers that together make up *rac*-GR24. Finally, our data provide much needed clues concerning the multiple roles played by MAX2 in the roots and a comprehensive view of the *rac*-GR24--induced response in the root proteome.

1. Introduction

Root development is pivotal for plant survival, providing anchorage, ensuring water and nutrient uptake, and allowing the plant to engage in beneficial interactions with soil microorganisms. Root growth is modulated in response to numerous abiotic and biotic environmental cues, which are interpreted and transduced by hormonal pathways. Besides the well-known regulators of root development, such as auxin and cytokinin, a group of carotenoid-derived terpenoid lactones, coined strigolactones, have recently been described to play a role in the regulation of root architecture. The influence of strigolactones on the lateral root density (LRD), adventitious root formation, and induction of root hair elongation has been demonstrated, but the molecular networks ruling these belowground effects are still not well understood (1-7).

Multiple research teams have contributed to a better understanding of the strigolactone biosynthesis pathway, early signaling processes, and transport mechanisms (8-14). Early signaling occurs mainly through the action of an α/β-hydrolase D14/DECREASED APICAL DOMINANCE2 (DAD2) that interacts with an F-box protein, MORE AXILLARY GROWTH2 (MAX2) (15). MAX2 together with an additional α/β-hydrolase and a D14 paralog, KARRIKIN INSENSITIVE2 (KAI2), also mediates the response to smoke-derived karrikins (16) as well as to certain strigolactone analogs (17, 18). The capacity of both the D14 and KAI2 proteins to recognize strigolactone analogs is reported to be stereospecific (18). MAX2 is part of a Skp, Cullin, F-box-containing (SCF^{MAX2}) complex (19, 20), which, in response to the hormone, gives rise tothe ubiquitination of specific targets leading to their proteasomal degradation. Several groups contributed to the identification various memebrs of the SMXL family which have shown to be the targets of this SCF complex (21-25). .

Despite its long history as a rhizosphere signaling molecule, the main body of research concerning strigolactones' role as hormones has, up until now, mainly focused on its effect in shaping the above ground architecture of the plant. This can be explained by the fact that the initial discovery of the hormone action of strigolactones was based on a set of high shoot branching or high tillering mutants in various plant species, (19, 26-29). However, an increasing number of studies demonstrate a role for this hormone in regulating root development, several of which even hint towards a complex signaling pathway (1, 3, 4, 7).

Initially, supported by the co-localization of the signaling components in the nucleus, strigolactone signaling has been suggested to function through the induction of transcriptional changes. However, despite the availability of several transcriptome datasets (30-33), strigolactone-regulated transcription factors and strigolactone-responsive genes are rare, of which *BRANCHED1* (*BRC1*) is one of the best known in *Arabidopsis* (34). On the whole, only a few differentially expressed genes, often with low differences in expression levels, were identified upon *rac*-GR24 treatment, a synthetic strigolactone analog (31-34). Of last, several studies have emerged that support strigolactone signaling occurring to a large extent at the protein level (29, 35, 36), as illustrated by the

direct effect of strigolactones on PIN-FORMED1 (PIN1) recycling at the plasma membrane in xylem parenchyma cells that results in modified auxin flows in the stem and, finally, altered shoot branching (35, 37).

Here we executed a proteome-wide study to gain a broader insight into the intricate strigolactone signaling network in the roots. To this end, we adopted a mass spectrometry-driven, quantitative proteomics approach to compare the profiles of the *max2-1* mutant and wild-type (WT) *Arabidopsis* roots in response to *rac*-GR24. This procedure, in concert with an unbiased metabolite profiling experiment, revealed that MAX2-dependent and *rac*-GR24--induced changes in protein abundance give rise to specific changes in the root metabolome. We used this knowledge to further dissect the link between signaling pathways stimulated by *rac*-GR24 and flavonol accumulation in the root.

2. Results

2.1. Proteome Profiling Reveals Differences Between WT and max2-1 Roots upon rac-GR24 Treatment

To gain insight into the *rac*-GR24--induced signaling pathway and the role of MAX2 in the roots, we used *max2-1* and WT *Arabidopsis* (accession Columbia-0) roots to study differences in protein abundance by means of a time-resolved, quantitative proteomics approach. Five-day-old plants were transferred to control (mock) medium or medium containing 1 µM of a *rac*-GR24 mixture for either 9 or 24 h. This experiment was conducted in four biological replicates (Fig. 1).

A reference pool was created by mixing half of each digested proteome extract and labeling the resulting peptide pool with $^{13}C_3$-propionate tags. The peptides of the individual samples were labeled with $^{12}C_3$-propionate. After each individual sample had been mixed with an equal amount of the reference pool, the peptides were prefractionated by RP-HPLC to reduce the sample complexity prior to LC-MS/MS analysis (Fig. 1). This set-up enabled the identification of proteins of which the abundances depended on MAX2, the *rac*-GR24 treatment, or both.

In total, 4,260 proteins were identified and quantified. To increase the stringency of our analysis, we kept only proteins with valid quantification values in at least two of the four biological replicates for every condition tested. As a result, a subset of 1,968 proteins was retained and subsequently a linear mixed model was fitted to the log-transformed data to assess the genotype {WT and *max2-1*} and treatment {mock, SL} main effects and the genotype.treatment interaction on protein abundance.

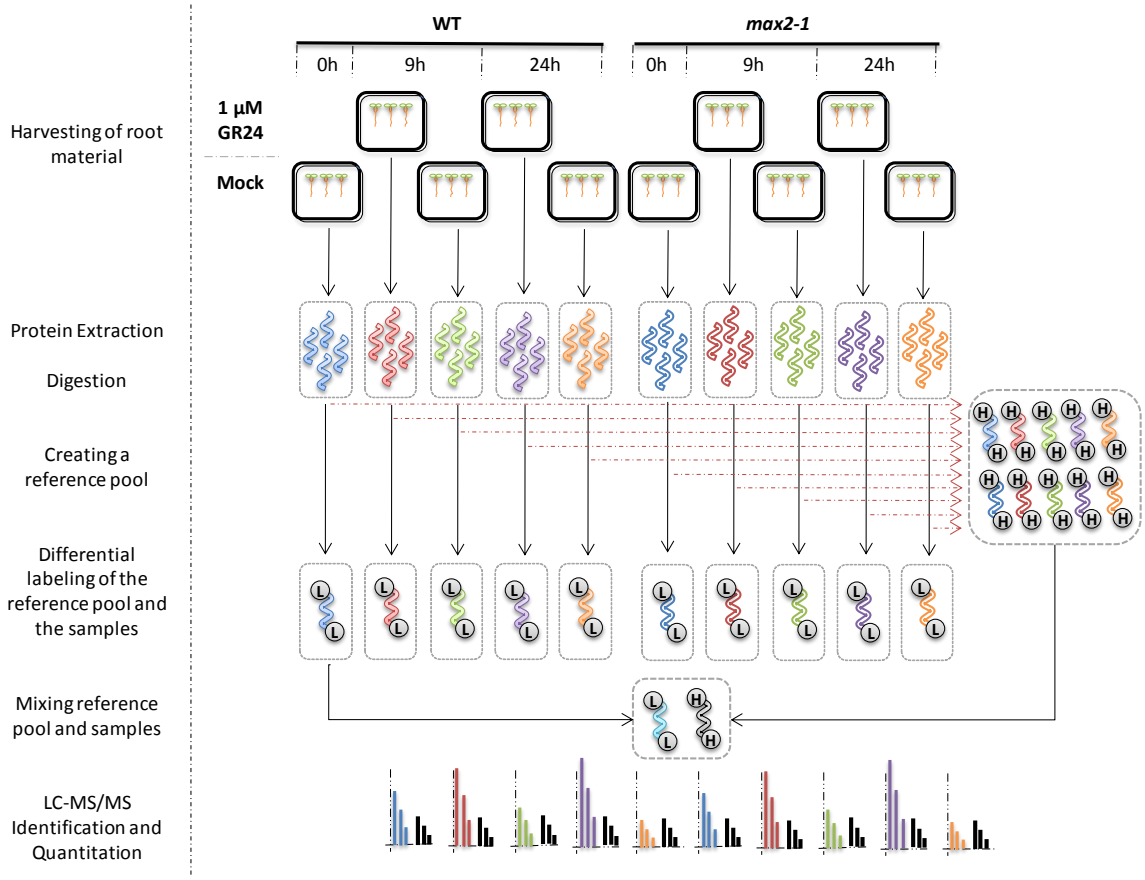

Fig. 1. Experimental set-up for protein profiling experiment. WT and *max2-1* plants were grown for 5 days before transfer to media containing 1 µM *rac*-GR24 (GR24) or the acetone carrier (mock). Root tissue was harvested at 0h, 9 h and 24 h post treatment (hpt) for samples treated with only acetone and 9 h and 24 h post treatment for samples treated with GR24. Protein extraction, endoproteinase-LysC digestion, and peptide labeling were done as described (see Experimental Procedures). To produce a reference labeling pool, half of each sample was mixed together. The individual samples were mixed with equal amounts of the reference pool. Samples were fractionated by RP-HPLC and pooled into 20 fractions that were analyzed by LC-MS/MS. Spectra were subsequently searched and analyzed with MaxQuant and Perseus. Quantified proteins were filtered and only those that had valid values for at least three of the four biological repeats of each sample were retained for final analysis.

Figure 2 shows all proteins for which at least one of the terms (genotype, treatment, or their interaction) was significant with $p < 0.01$ (red dots). All ratio values for these proteins are given in Supplementary Table 1. In total, 33 proteins at *p*-value <0.01 differed significantly in abundance after *rac*-GR24 treatment, whereas 117 (*p-value* <0.01) were differentially abundant when the root proteomes of *max2-1* and WT plants were compared (Fig. 2). Finally, the interaction between treatment and genotype had a statistically significant effect on the abundance of 9 (p <0.01) proteins (Fig. 2). Ratios of all proteins as well as p-values (when the proteins were included in the statistical analysis), are given in Supplementary Table 2.

Fig. 2. Differential molecular responses in *max2-1* and WT roots either mock grown or treated with *rac*-GR24.

Heat map showing average log2 values of protein ratios of four biological repeats (z-scored for graphical representation). Levels are shown for WT and *max2-1* plants grown under mock conditions (0 h, 9 h and 24 h) or after treatment (9 h, 24 h) in the presence of 1 µM *rac*-GR24. The columns labeled G, T, and T*G indicate whether the protein abundance was detected as statistically significantly different between genotypes, treatment, and interaction of both factors, respectively. Only the proteins that are significantly different with a *p* value <0.01 (red dots) in at least one of the terms are presented.

Upon examination, 4 out of the 9 proteins that have a significant interaction term (genotype.treatment) have been shown to be involved in different steps of flavonoid biosynthesis. For 3 of these proteins, phenyl ammonia-lyase (PAL1), CFI family protein and flavanone 3'-hydroxylase (F3'H), their abundance rises upon *rac*-GR24 only in the WT, suggesting that a functional MAX2 protein is necessary for this change to occur (Fig. 3).

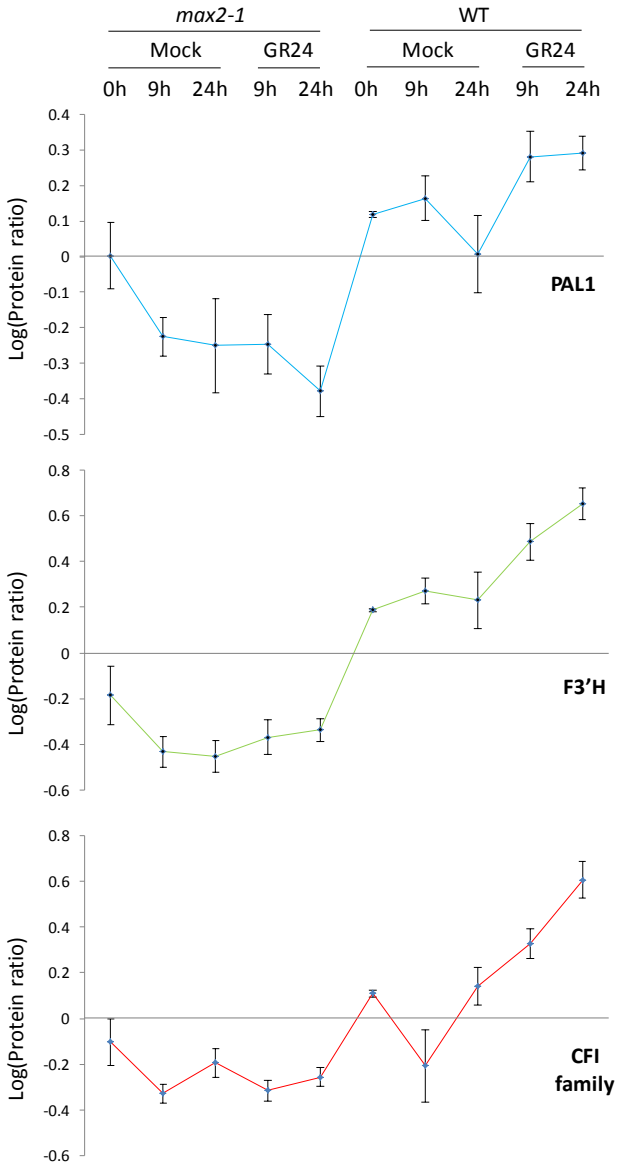

Fig. 3. Protein abundance profile of flavonol biosynthesis related proteins. Protein ratios for flavonol biosynthesis-related proteins (PAL2, CFI family protein and F3'H) in WT and *max2-1* backgrounds under mock conditions and after *rac*-GR24 treatment.

More broadly, multiple proteins involved in the flavonoid metabolism are significant for the genotype term, including PAL2, and enzymes more specifically involved in flavonoid biosynthesis and transport, such as flavonol synthase 1 (FLS1), flavanone 3-hydroxylase (F3H), chalcone synthase (CHS), UDP-glucosyl transferase 78D2 (UGT78D2), cinnamate-4-hydroxylase (AtC4H), and the nonintrinsic ABC protein 9 (AtNAP9). These proteins were more abundant in WT than in *max2-1* roots. Taken together, these results suggest that in the absence of a functional MAX2, a large set of the enzymes responsible for flavonol biosynthesis are less present and that at least for part of these enzymes, their abundance increases in a MAX2 dependent manner upon GR24 treatment. An overview of the flavonol biosynthesis pathway is given in Supp. Fig. 1.

2.2. Transcript Analysis Reveals a MAX2-Dependent rac-GR24-Induced Regulation of Genes Coding for Flavonoid Biosynthesis Enzymes

With a detected enrichment for proteins involved in phenylpropanoid and, more specifically, flavonoid synthesis, we wanted to investigate whether these changes between genotype and/or upon *rac*-GR24 treatment were regulated at the transcript level.

WT and *max2-1* roots grown in the presence or absence of *rac*-GR24 were used to study the gene expression of markers for phenylpropanoid and flavonol biosynthesis, such as enzymes catalyzing early steps of the phenylpropanoid pathway (*PAL1* and *PAL2*) and proteins more specifically involved in flavonol biosynthesis (*CHS*, *UGT78D2*, and *F'3H*) via qRT-PCR analysis. For all genes tested, no differences in expression levels were detected when untreated WT and *max2-1* samples were compared (Fig. 4). In contrast, the transcript levels of all tested genes increased statistically significantly (*t*-test with $p < 0.05$) upon *rac*-GR24 treatment in WT background, a response that was completely abolished in the *max2-1* mutant. These results indicate that the flavonoid biosynthesis pathway is transcriptionally activated by *rac*-GR24 treatment in a MAX2-dependent manner.

2.3. Secondary Metabolite Profiling Pinpoints Specific Flavonols to Accumulate upon rac-GR24 Treatment in a MAX2-Dependent Manner

As *rac*-GR24 treatment and MAX2 function appeared to regulate enzymes involved in flavonoid biosynthesis and, more broadly, phenylpropanoid biosynthesis, at the transcript and protein levels, metabolite profiling experiments were conducted. In a first experiment, methanol extracts from the roots of WT plants grown on mock or *rac*-GR24-containing medium were compared and, in a second experiment, metabolite profiles of untreated root tissues of WT and *max2-1* plants were evaluated (Fig. 5*A*). Methanol extracts were analyzed via Ultra-HPLC-MS (for details, see Experimental Procedures).

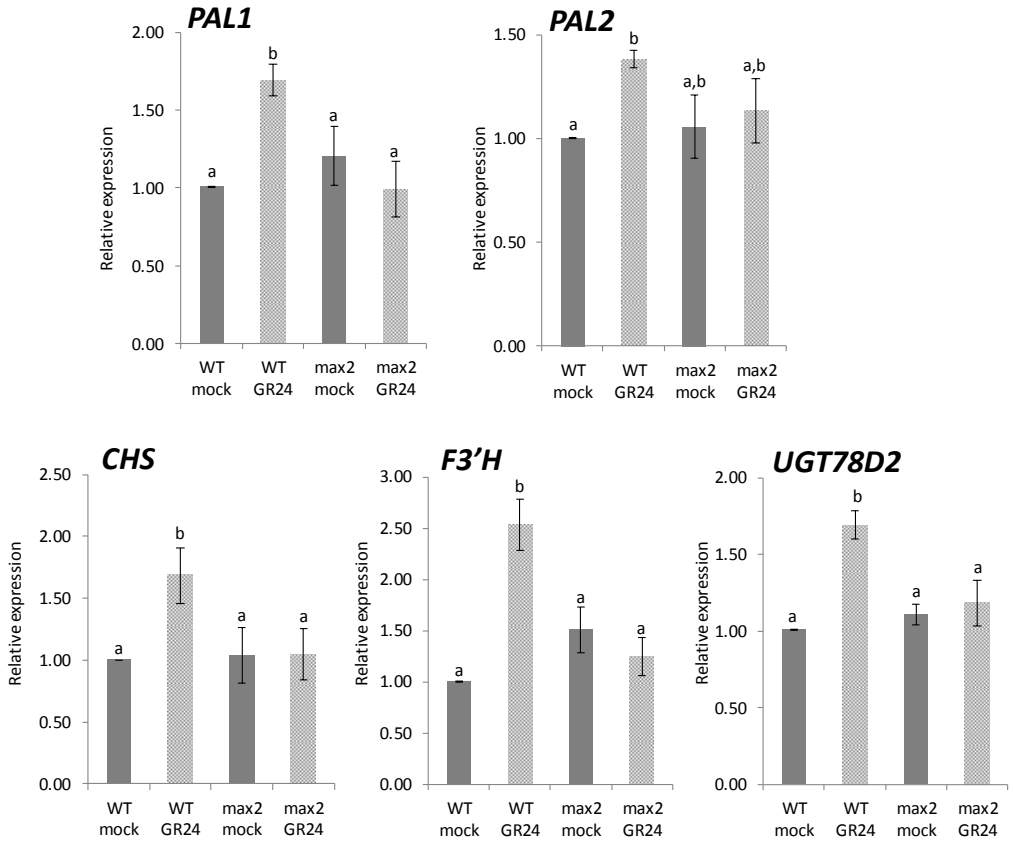

Fig. 4. MAX2-dependent *rac*-GR24-induced transcriptional regulation of marker genes for phenylpropanoid and flavonol biosynthesis. Relative transcript levels for two phenylpropanoid biosynthesis genes (*PAL1* and *PAL2*) and three flavonol biosynthesis genes (*CHS, F'3H,* and *UGT78D2)* in WT and *max2-1* backgrounds under mock conditions and after 24 h of *rac*-GR24 treatment.

In total, 1,121 compound ions were detected in experiment 1 (Fig. 5*A*). Prior to univariate analysis, two filters were applied to increase the stringency. An intensity threshold of 500 spectrum counts in at least one group and an average peak width threshold of minimum 0.05 min in at least one group were applied, resulting in 474 remaining compound ions. By Student's *t*-test analysis and multiple testing corrections, 93 and 48 compound ions were found to be significantly more and less abundant, respectively, in WT upon *rac*-GR24 treatment (Fig. 5*A*). A principal component analysis (Fig. 5*B*) was carried out and showed a separation between two groups, indicating that plants grown on mock-treated medium or on *rac*-GR24-supplemented medium had different phenolic profiles.

In the second experiment, 1,512 compound ions were detected. With the same filters as in experiment 1, 701 compound ions remained for univariate analysis. The *t*-test analysis indicated that 134 and 167 compound ions were significantly more and less abundant, respectively, in *max2-1*

mutants. The second principal component analysis (Fig. 5*B*) showed difference in the phenolic profiles of *max2-1* and WT roots grown under mock conditions.

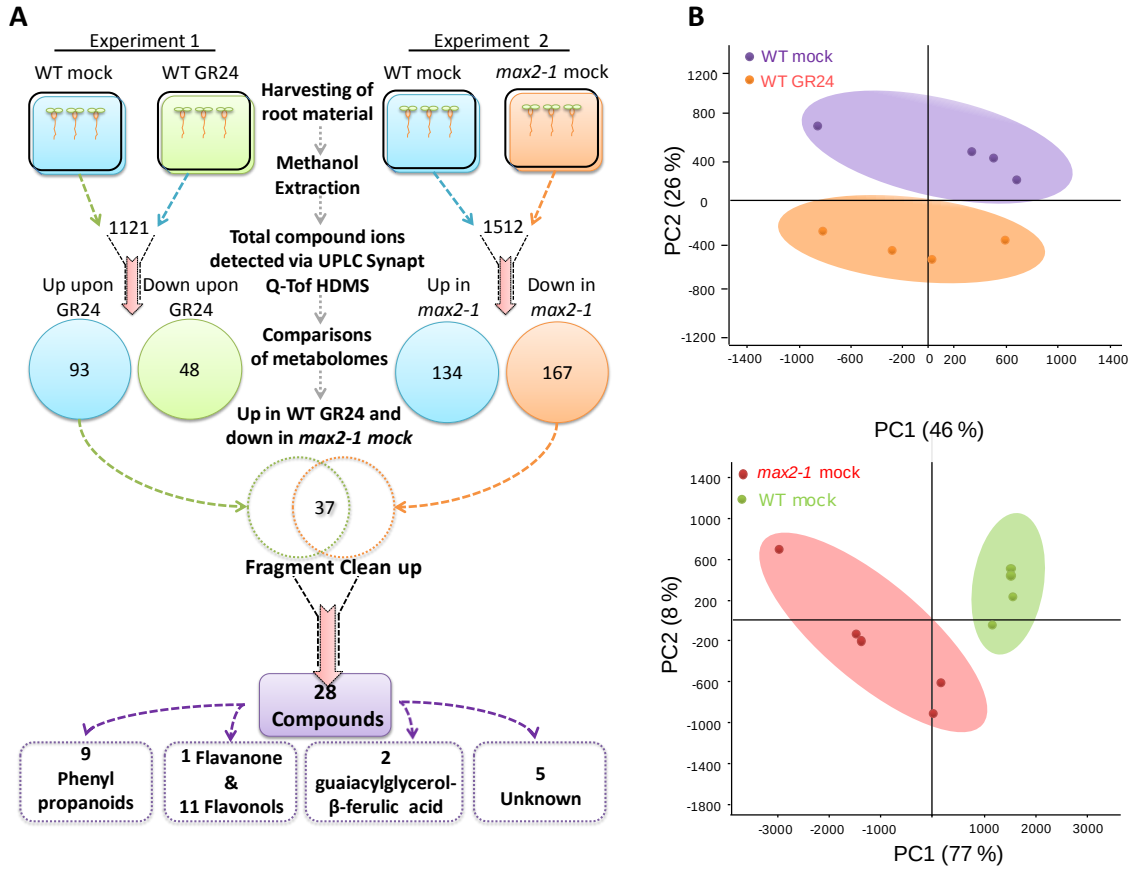

Fig. 5. Metabolite profiling of *max2-1* and WT roots with and without *rac*-GR24 treatment. (*A*) Outline of the strategy. Two separate metabolomics experiments were done. In the first, WT plants were grown on *rac*-GR24-containing medium or mock-treated medium for 5 days for comparison. In the second experiment, metabolites from WT roots were compared with those from *max2-1* roots after 5 days of growth. In total, 2,633 compounds were identified. After an abundance filter, 37 compounds were found to be upregulated upon *rac*-GR24 treatment and downregulated in *max2-1* compared to WT. Clean-up of fragments reduced this number to 28 compounds, of which 5 were unknown, 9 were lignin precursors, 2 were guaiacylglycerol-β-ferulic acid ethers, and 12 were flavanones or flavonols. (*B*) Principal component analysis plot showing difference when WT and *max2-1* samples and mock and *rac*-GR24--treated samples are compared.

After manual fragment ion clean-up and assessment of numbers and types of compound ions that displayed a MAX2-dependent and *rac*-GR24--induced profile, 28 compounds were retained from the two combined experiments (Supplemental Table 3) that could be structurally characterized based on MS/MS fragmentation (Fig. 5*A*). Nine compounds could be classified as phenylpropanoids, such as several glycosyl derivates of *p*-coumaric acid, caffeic acid, and ferulic acid, two as guaiacylglycerol-β-ferulic acid ethers, 11 as flavonols, and one was assigned as flavanone naringenin (Supplemental Table 3; Fig. 5*A*). Regarding the flavonols, derivates from each of the three main flavonol families, kaempferol, quercetin, and isorhamnetin, accumulated in WT roots upon *rac*-GR24 treatment and

were less abundant in *max2-1* mutants than in WT plants (Supplemental Table 3). These phenolic profiling results indicate that *rac*-GR24 treatment gives rise to a MAX2-mediated flavonol accumulation in *Arabidopis* roots, in line with the abundance profiles of the biosynthesis enzymes and the transcript profiles of the corresponding genes.

2.4. A New Flavonol Readout to Dissect Strigolactone Signaling

To confirm the MAX2-dependent *rac*-GR24 metabolic response in roots, we separated methanol extracts on HPTLC, followed by flavonol-specific DPBA staining and UV/VIS spectrophotometry.

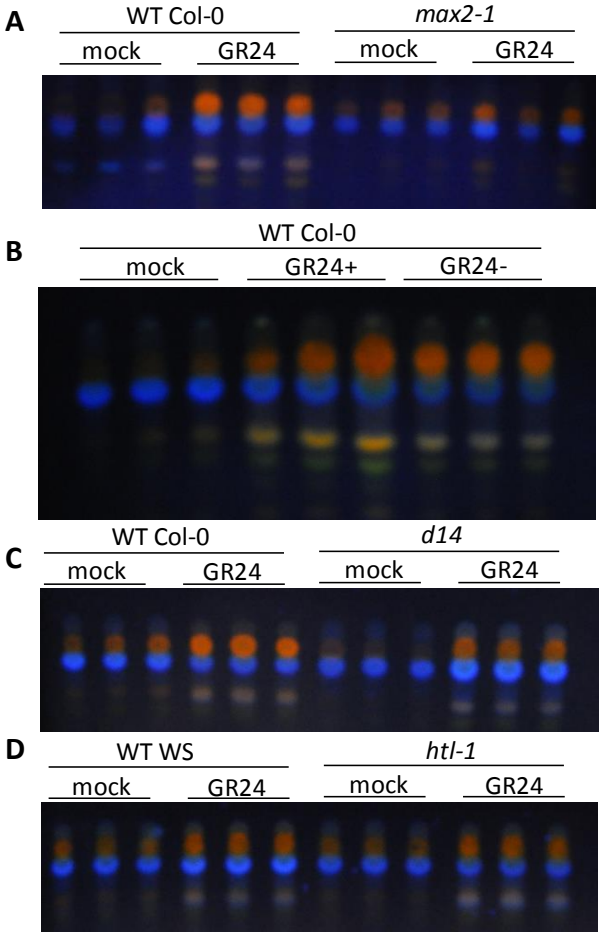

Fig. 6. Visualization of flavonol induction on HPTLC plates. (*A*) HPTLC plate with DPBA-stained methanol extracts from WT and *max2-1* roots treated with *rac*-GR24 or not. (*B*) HPTLC plate with DPBA-stained methanol extracts from a mock-treated WT root and grown either with 1 µM GR24+ or 1 µM GR24-. (*C*) HPTLC plate with DPBA-stained methanol extracts from a mock-treated WT root and *d14* mutant roots grown either with 1 µM GR24+ or 1 µM GR24-. (*D*) HPTLC plate with DPBA-stained methanol extracts from a mock-treated WT (accession Wassilewskija [WS]) root and a *htl-1* mutant root grown either with 1 µM GR24+ or 1 µM GR24-.

Firstly, to independently confirm the large-scale metabolome analysis, new methanol extracts were prepared from roots of WT and *max2-1* plants grown with or without *rac*-GR24. *Rac*-GR24 treatment of WT roots resulted in the accumulation of compounds stained mainly orange and blue, corresponding to quercetin and kaempferol derivates, respectively (Fig. 6*A*). Furthermore, this *rac*-GR24-triggered flavonol accumulation was abolished in the *max2-1* mutant background (Fig. 6*A*), confirming the UHPLC-MS data that revealed an increase in flavonol production upon *rac*-GR24 treatment in roots.

The applied *rac*-GR24 consisted of two enantiomers, $GR24^{5DS}$ (GR24+) and $GR24^{ent\text{-}5DS}$ (GR24-), thought to mimic naturally occurring strigolactones and potentially karrikins or other unknown compounds, respectively (18). Next, the specificity of the observed flavonoid response to one of the two enantiomers was evaluated. Flavonols accumulated after treatment with both 1 µM GR24+ or 1 µM GR24– in roots of 5-day-old plants (Fig. 6*B*). Additionally, the roles were examined of the two receptor proteins D14 and HTL/KAI2 that can mediate the response to *rac*-GR24 (17) in the observed strigolactone response. The *d14* mutant still accumulated flavonols in response to *rac*-GR24 (Fig. 6*C*) as did the *htl-1/kai2* mutant, available in the *Arabidopsis* Wassilewskija (Ws) accession and responding similarly as the Ws control (Fig. 6*D*). Taken together, these results show that the uncovered flavonol response is common to both *rac*-GR24-containing enantiomers and can be induced both through D14 and/or KAI2.

3. Discussion

With the present study, we shed more light on the processes that are at play downstream of the *rac*-GR24 perception and underline the multiplicity of roles played by MAX2 in the roots of *Arabidopsis*. A protein profiling approach led to the identification of 4,260 proteins in the root proteome in four biological replicates. By means of a linear mixed model analysis of variance a total of 147 proteins displayed a statistically significant difference in abundance (p value < 0.01), either when *max2-1* and WT root proteomes were compared, upon *rac*-GR24 treatment, or due to the interaction of both genotype and treatment.

Interestingly, our dataset of significantly regulated proteins presented a clear enrichment for phenylpropanoid/flavonoid metabolism-related proteins, which we further explored via transcriptional and metabolome analyses. For several of the genes encoding these enzymes, qRT-PCR data revealed a MAX2-dependent increase in transcript levels upon *rac*-GR24 treatment. Accordingly, metabolome analysis confirmed the *rac*-GR24-induced accumulation of flavonols requiring a functional MAX2. As flavonol compounds are known to be stress responsive in some cases (43), it is imperative to underline the MAX2-dependent character of this response, hinting at a specific response to *rac*-GR24 and ruling out the possibility that merely a general stress response is observed. On the metabolite level, 11 flavonols, one direct flavonol precursor, naringenin and, more broadly, 9 phenylpropanoids displayed

a MAX2-dependent increase in response to the *rac*-GR24 treatment, supporting a clear link between strigolactones and flavonols in the root. Previously, a *rac*-GR24--triggered induction of *CHS* expression, comparable to the one described here, had been observed in whole seedlings (44), implying that flavonol might accumulate in different plant tissues. Accordingly, a transcriptome analysis has revealed that flavonol biosynthesis genes are induced at lower levels in *max2-1* than in WT upon drought stress in leaves (31). Moreover, flavonol production has been shown to be misregulated in the strigolactone biosynthesis mutant *max1* in the shoot (45). However, because mutants affected in flavonol biosynthesis have no enhanced shoot branching phenotype, flavonols probably do not play a main role in strigolactone-controlled shoot branching (46). As flavonol accumulation and aspects of the root architecture have been linked (47-49), the next challenge will be to examine the role of flavonols in *rac*-GR24-affected processes in the root.

We have translated the connection between strigolactones and flavonols in the root into a cost-effective and user-friendly HPTLC tool that allowed us to acquire more insight into the *rac*-GR24 signaling pathways. Recently, the use of *rac*-GR24 as a generic strigolactone analog has been questioned, because *rac*-GR24 is actually a mixture of two enantiomers. Whereas GR24+ mimics natural strigolactones and is perceived via D14, GR24- is active via the KAI2 receptor and represents a non-canonical strigolactone analog. Importantly, both enantiomers have been shown to signal via MAX2. In this context, some strigolactone-related phenotypes have been linked to specific stereo-isoforms of *rac*-GR24 or specific receptors, although these observations were not absolute (18). On the one hand, shoot branching is elicited by GR24+ via D14 signaling, whereas on the other hand, GR24- and KAI2 affect hypocotyl elongation and aberrant cotyledon morphology (18, 25). Therefore, we tested whether the flavonol response was specific to an enantiomer receptor pair. The application of the specific enantiomers revealed that both GR24+ and GR24- could increase the flavonol production. In addition, both the *d14* and *kai2* signaling mutants were examined for their capacity to transduce the *rac*-GR24 and give rise to the flavonol read out. In agreement with the enantiomer experiment, the flavonol induction was maintained in both mutants. Together, these results imply that the *rac*-GR24--induced and MAX2-controlled flavonol production is not stereo-selective and, hence, can occur upon activation of either D14 or KAI2. This observation suggests that, at least in the roots, a crosstalk of D14 and KAI2 pathways exists and raises the question whether other known root phenotypes can also be instigated by both receptors. It would now be interesting to build on this result and to investigate whether these are the only receptors at play, for instance by testing whether the *kai2d14 double* is displays any flavonol read out in response to GR24.

Besides flavonols, our data indicate that also other secondary metabolites could contribute to strigolactone-mediated effects in *Arabidopsis* roots. Several antioxidant phenylpropanoids, sharing *p*-coumaric acid as a precursor, accumulate with the same strigolactone-related abundance profiles as flavonols. From the proteomics results, we can infer that this effect might be caused by a change in

production of CINNAMATE 4-HYDROXYLASE (C4H), the enzyme producing *p*-coumaric acid from cinnamic acid. Moreover, two hexosylated G(8-O-4)ferulic acid compounds were found to accumulate similarly as the flavonols. The *in planta* function of these neolignan-like compounds is unknown, but we can postulate that their accumulation is the consequence of an increase in (hexosylated) ferulic acid.

Previously, a comparable proteome analysis in the context of strigolactone signaling had been conducted (36). Only a limited overlap could be observed with our data (10% on the protein level), potentially arising from technical differences. We used a 5-fold lower concentration of *rac*-GR24 and sampled roots in contrast to whole plants. Nevertheless, a more attractive explanation is also plausible: we used the signaling mutant *max2-1* instead of the biosynthesis mutant *max3*. Thus, the previous approach focused on proteome changes upon signaling of natural strigolactones (36), whereas our work spans an enlarged signaling network, uncovering all downstream effects of MAX2. In this context, it is important to note that the role of MAX2 is broader than strigolactone signaling alone and also to encompass signal transduction of unknown molecules (18, 50). Although not yet biochemically characterized, additional MAX2 activity elicitors are expected to exist based on genetic studies, as illustrated by the increase of LRD in the *max2-1* mutant, which is not phenocopied in the *max3* and *max4* mutants, despite their inability to synthesize strigolactones (1, 2).

Additionally, we detected a set of proteins that responded to *rac*-GR24, both in the *max2-1* background and in the WT control, possibly pointing toward the existence of a MAX2-independent response to strigolactones. In agreement, MAX2-independent responses in root growth and development to *rac*-GR24 were reported (2, 35).

In conclusion, the large set of proteins shown to be regulated by the MAX2 function provides a comprehensive resource that can serve as a foundation for studies aiming to further elucidate the roles of MAX2 in roots. Finally, the link between strigolactones and flavonols will allow the dissection of the molecular networks that act between strigolactone signaling and the induction of transcriptional changes.

4. Material and Methods

Plant Material

Seeds of *Arabidopsis thaliana* (L.) Heyhn. (accession Columbia-0) plants were surface sterilized with consecutive treatments of 70% (v/v) ethanol with 0.05% (w/v) sodium dodecyl sulfate (SDS), and then washed with 95% (v/v) ethanol. For material destined to proteomics experiments or RNA preparation, seeds were sown on nylon meshes (20 µm) placed on half-strength Murashige and Skoog (MS) medium containing 1% (w/v) sucrose. Fifty plants were sown per plate in two rows of 25. Seeds were stratified for 2 days at 4°C, where after they were grown for 5 days, before being transferred to mock-treated medium or medium containing 1 µM *rac*-GR24. Finally, for high-performance thin-layer

chromatography (HPTLC) analysis, seeds were stratified for 2 days at 4°C, where after they were grown for 5 days either on mock or *rac*-GR24--containing medium before methanol extraction. All seeds were grown in 21°C in permanent light conditions.

The *rac*-GR24 that was used for the proteome and the metabolite profiling contained both the $GR24^{5DS}$ (GR24+) and $GR24^{ent\text{-}5DS}$ (GR24-) enantiomers (18). In experiments designed to test the effect of the stereochemistry on the flavonol response, purified enantiomers, GR24+ and GR24-, were applied separately.

Time-Resolved Quantitative Proteomics

The roots of 5-day-old *Arabidopsis* WT and *max2-1* plants were transferred to MS medium containing 1% (w/v) sucrose and either 1 µM *rac*-GR24 or 100 µL of the acetone carrier, harvested, and snap-frozen in liquid nitrogen at given time points. Tissues were thawed in 1.5 mL extraction buffer (1% [w/v] CHAPS, 0.5% [w/v] sodium deoxycholate, 0.1% [w/v] SDS, 5 mM EDTA, 10% [v/v] glycerol in phosphate buffered saline, pH 7.5) and a protease inhibitor mixture was added according to the manufacturer's instructions (Roche).

Lysates were incubated for 30 min on ice before centrifugation at 16,000×*g* for 20 min at 4˚C to remove any debris. Samples were desalted over a NAP-10 column (GE-Heathcare) with 1 mL of 20 mM triethylammonium bicarbonate buffer. Protein concentrations were measured with the Bradford DC assay (Bio-Rad) to keep 400 µg of protein material for the following steps. Samples were digested with endoproteinase Lys-C (Sigma-Aldrich) and incubated overnight at 37°C with gentle agitation.

Because of the reference pool design, samples were divided into two equal parts. One half of each sample was pooled together to produce a reference sample and the other half was maintained to represent the sample itself. The samples were labeled differentially: the reference pool with heavy $^{13}C_3$-propionate and the individual samples with light $^{12}C_3$-propionate as described (38). Labeling was followed by addition of with 40 mM glycine to quench of *N*-hydroxysuccinimide esters, followed by 80 mM hydroxylamine (NH_2OH) to revert O-propionylation of Ser (S), Thr (T), and Tyr (Y). Individual samples were mixed in a one-to-one ratio with the reference pool (checked on a single shot pre-run on a XL linear trap quadrupole [LTQ] Orbitrap [Thermo Fisher Scientific]).

RP-HPLC Fractionation of Peptide Mixtures

Peptides were separated on a 2.1 mm internal diameter (I.D.)×150 mm column (Zorbax®, 300 SB-C18 Narrowbore, Agilent Technologies) preceded by a C8 pre-column. An 140-min gradient was

used with HPLC solvent A, consisting of 10 mM ammonium acetate (pH 5.5) in HPLC grade 98/2 (v/v) water/acetonitrile and solvent B composed of 10 mM ammonium acetate (pH 5.5) in HPLC grade 30/70 (v/v) water/acetonitrile to fractionate in one-minute-wide fractions and finally pooled into 20 fractions for liquid chromatography-tandem mass spectrometry (LC-MS/MS) analysis. Thirty minutes before the samples were injected for reverse-phase (RP)-HPLC, a methionine oxidation step was carried out by adding to a final concentration of 0.5% (v/v) H_2O_2. Tris(2-carboxyethyl)phosphine was added to a final concentration of 2 mM to reduce S-S bridges just before the injection. Samples were vacuum-dried and resuspended in 20 µL of solvent A' (2% [v/v] acetonitrile with 0.1% [v/v] trifluoroacetic acid). The obtained peptide mixtures were introduced into the Ultimate 3000 RSLC nano LC-MS/MS system (Dionex) connected in-line to a hybrid LTQ Orbitrap Velos (Thermo Fisher Scientific). The sample mixture was loaded on an in-house--made trapping column (100 µm I.D.×20 mm, 5-µm C18 Reprosil-HD beads [Dr. Maisch]). After back-flushing from the trapping column, the sample was loaded on an in-house--made analytical reverse-phase column (75 µm I.D.×150 mm, 5-µm C18 Reprosil-HD beads [Dr. Maisch]). Of the peptide mixture, 6 µL was loaded with solvent A' and separated with a linear gradient from 2% (v/v) solvent A" (0.1% [v/v] formic acid) to 50% (v/v) solvent B" (0.1% [v/v] formic acid and 80% [v/v] acetonitrile) at a flow rate of 300 nL/min followed by a wash with 100% solvent B".

LC-MS/MS Analysis and Peptide Identification

The mass spectrometer was operated in data-dependent mode, automatically switching between MS and MS/MS acquisition for the 10 most abundant peaks in a given MS spectrum. In the LTQ-Orbitrap Velos (Thermo Fischer Scientific), full-scan MS spectra were acquired at a target value of 1E6 with a resolution of 60,000. The 10 most intense ions were isolated for fragmentation in the linear ion trap, with a dynamic exclusion of 20 s. Peptides were fragmented after filling the ion trap at a target value of 1E4 ion counts. The MS/MS spectra were searched with the MAXQUANT software (version 1.4.0.3) (39, 40) against The Arabidopsis Information Resource (TAIR10_pep_20101214 containing 27,416 protein-coding genes) database, with a precursor mass tolerance set at 10 ppm for the first search (used for nonlinear mass recalibration) and at 4.5 ppm for the main search. Methionine oxidation was searched as fixed modification, whereas variable modifications were set for pyroglutamate formation of amino-terminal glutamine and acetylation of the protein N-terminus. Mass tolerance on peptide precursor ions was fixed at 10 ppm and on fragment ions at 0.5 Da. The peptide charge was set to 2+,3+. The instrument was put on electrospray ionization-TRAP. EndoLysC was the selected protease, with one missed cleavage allowed; cleavage was accepted as well when lysine was followed by proline. Only peptides were withheld that ranked first and scored above the 99% confidence threshold score. $^{13}C_3$-propionate and $^{12}C_3$-propionate were used as heavy and light labels,

respectively, with specificity for lysines and peptide N-termini. The feature “matching between runs” was activated. The false discovery rate (FDR) for peptide and protein was set to 1% and the minimum peptide length was set to 7. All mass spectrometry proteomics data have been deposited to the ProteomeXchange Consortium via the PRIDE partner repository with the PRIDE accession PXD003879.

Statistical Analysis of the Shotgun Proteomics Data

We first applied a stringent filter to the dataset, keeping only protein for which at least 2 valid values were available from the 4 biological repeats for every condition tested. The remaining 1,968 proteins were analyzed by fitting a linear mixed model of the following form:

$Y_{ijkl} = \mu + \beta_i + g_j + m_k + t_l + gm_{jk} + gt_{jl} + mt_{kl} + gmt_{jkl} + \varepsilon_{ijkl}$,

partitioning the variation in protein abundances (Y_{ijkl}) into fixed genotype effects (WT and *max2*; represented by g_i), treatment effects (mock and SL; represented by m_k), time effects (0 h, 9 h and 24 h for mock, 9 h and 24 h for SL; represented by t_l) and all interaction effects, and random block effects, referring to the biological replicates. The genotype.treatment interaction effect is the one of highest importance because it assesses whether the difference in response between the two genotypes is affected by the treatment (averaged over the time series). Random block effects in the model were assumed to be independent and normally distributed with means zero and variance σ^2. The linear mixed model was fitted by the residual maximum likelihood (REML) approach as implemented in Genstat v17 (For details see Payne, R.W. (2013) Genstat Release 17 Reference Manual, Part 3: Procedure library PL24. Oxford: VSN International, Hemel Hempstead, UK). Significance of the fixed main and interaction effects was assessed by an *F*-test.

The distributions of the p-values for the treatment effect, the genotype effect and the genotype.treatment effect were assessed. Only in the case of the genotype effect we have estimated the FDR to correct for multiple hypotheses testing seeing the large number of proteins significant for this term.

Metabolite Profiling: LC-MS Conditions

For the LC-MS analysis, an Acquity Ultra-Performance Liquid Chromatography (UPLC) system was used connected to a Synapt Q-TOF high-definition MS system (Waters). Chromatographic separation was done by injecting a 15-µL aliquot on an Acquity BEH C18 column (2.1 mm I.D.×150 mm, 1.7 µm beads, Waters) with a gradient elution. Mobile phases consisted of water containing 1% (v/v) acetonitrile and 0.1% (v/v) formic acid (A) and acetonitrile containing 1% (v/v) water and 0.1% (v/v) formic acid (B). All solvents used were ULC/MS grade (Biosolve). Water was

produced by a DirectQ-UV water purification system (Millipore). The column temperature was maintained at 40°C and the autosampler temperature at 10°C. A flow rate of 350 µL/min was applied during the gradient elution starting at time 0 min 5% (B), 30 min 50% (B), and 33 min 100% (B). The eluant was directed to the mass spectrometer equipped with an electrospray ionization source and lock spray interface for accurate mass measurements. MS source parameters were: capillary voltage 2.5 kV, sampling cone 37 V, extraction cone 3.5 V, source temperature 120°C, desolvation temperature 400°C, cone gas flow 50 L/h, desolvation gas 550 L/h. The collision energy for trap and transfer cells was set at 4 V and 3 V, respectively. For data acquisition, the dynamic range enhancement mode was activated. Full-scan data were recorded in negative centroid V-mode with a mass range between *m/z* 100-1000 and a scan speed of 0.2 s/scan by means of the MASSLYNX software (Waters). Leu-enkephalin (400 pg/µL solubilized in water/acetonitrile [1:1, v/v] acidified with 0.1% [v/v] formic acid) was used for the lock mass calibration by scanning every 10 s with a scan time of 0.5 s; three scans were averaged. For MS/MS purposes, the same settings were applied, except that the trap collision energy was ramped from 10 V to 45 V.

For the LC-MS data processing, the PROGENESIS QI software v 2.0 (Nonlinear Dynamics) was used to align all chromatograms and to analyze statistically the ArcSinh-transformed compound intensities (normalized to dry weight) through principal component analysis and analysis of variance (*p* value threshold = 0.01). Descriptive statistics were calculated by EZinfo extension (v 3.0) (Umetrics) on Pareto-scaled compound intensities.

RNA Extraction and Quantitative (q)RT-PCR

Roots from WT and *max2-1* plants were harvested and snap-frozen in liquid nitrogen 24 hours post treatment (hpt). Cell walls were disrupted by 3-mm metal beads in 2 mL Eppendorf tubes with a mixer mill 400 (Retsch) for 2 min at 20 Hz. RNA was extracted and purified with the RNeasy mini kit (Qiagen). Genomic DNA was removed by DNase treatment and the samples were purified by ammonium acetate (2.5 M final concentration) precipitation. Concentrations were measured with a ND-1000 Spectrophotometer (Nanodrop). The iScript cDNA synthesis kit (Bio-rad) was used to reverse transcribe RNA. qRT-PCR primers were designed with the Quant Prime website software. SYBR Green detection was used during qRT-PCR run on a Light Cycler 480 (Roche). Reactions were done in triplicate in a 384-multiwell plate, in a total volume of 5 µL and cDNA fraction of 10%. Cycle threshold values were obtained and analyzed with the 2-ΔΔCT method (41). The values from four biological repeats and three technical repeats were normalized against those of *ACTIN2* (*ACT2*, AT3G18780) that was used as an internal standard. Normalized values were analyzed according to the published model (42) with the mixed model procedure of SAS Enterprise.

HPTLC Diphenylboric Acid 2-Amino Ethyl Ester (DPBA) Staining

For the HPLTC analysis of roots, methanol extracts from four biological repeats were prepared from 5-day-old *Arabidopsis* plants grown on 1% (v/v) MS medium containing either 1 µM *rac*-GR24 or 100 µL of the acetone carrier. Roots were harvested. After a methanol extraction, samples were dried with a concentrator 5301 (Eppendorf). The dried samples were resuspended in 20 µL of an 80% (v/v) methanol solution. The concentrated extract was analyzed by HPTLC. Of the mixture, 2 µL was spotted onto a 20 cm×10 cm silica-60 HPTLC glass plate (Merck) and placed in a glass tank with a paper wick of 18 cm by 9 cm (Whatman) and a mobile polar phase consisting of ethyl acetate, dichloromethane, acetic acid, formic acid, and water in a 100:25:10:10:11 ratio, respectively. After addition of the mobile phase, the glass tank was sealed with silicon grease and gels were run for 25 min. Gels were stained by spraying a methanol solution containing 1% (v/v) DPBA. Plates were placed into an HB-1000 Hybridizer (Fisher Scientific) at 100°C for 10 min, where after the plates were sprayed with a 5% (v/v) methanol solution containing 4000-polyethylene glycol to stabilize the DPBA compound. Plates were observed after UV excitation at 350 nm. Pictures were taken with a D90 camera (Nikon).

				Experiment 1					**Experiment 2**				
				WT mock		**WT *rac*-GR24**			**WT**		***max2-1***		
#	**Compound?**	***m/z***	**Retention time (min)**	**Mean**	**(sd)**	**Mean**	**(sd)**	**Fold change**	**Mean**	**(sd)**	**Mean**	**(sd)**	**% reduction**
Phenylpropanoids													
1	*p*-Coumaroyl hexose	325.09	4.58	12210	-1680	26776	-1482	2.19	25411	-4079	5495	-593	78
2	*p*-Coumaroyl hexose	325.09	5.13	12172	-1497	24825	-870	2.04	27933	-4926	5827	-513	79
4	Dihydro-*p*-coumaric acid + hexose	327.107	3.97	278	-165	586	-55	2.11	1362	-157	1086	-151	20
3	Caffeoyl hexose	341.092	3.39	5963	-664	12761	-589	2.14	12170	-1474	4468	-331	63
5	Caffeic acid 3/4-*O*-hexoside	341.089	5.53	429	-36	570	-104	1.33	2027	-209	1662	-52	18
6	Caffeoyl hexose 3/4-*O*-hexoside	503.142	2.14	514	-73	1141	-84	2.22	813	-191	62	-81	92
7	Ferulic acid 4-*O*-hexoside	355.102	3.81	285	-67	575	-47	2.01	960	-4	708	-102	26
8	Feruloyl hexose	355.101	5.47	1766	-188	6058	-387	3.43	16965	-2603	7974	-593	53
9	Feruloyl hexose	355.103	5.87	269	-160	1342	-199	5	1284	-284	306	-116	76
Guaiacylglycerol-β-ferulic acid ether													
10	G(8-*O*-4)ferulic acid + hexose	551.176	6.47	12585	-1867	20545	-1629	1.63	38815	-3102	29786	-3951	23
11	G(8-*O*-4)ferulic acid + hexose	551.177	6.74	2800	-370	4271	-598	1.53	6249	-500	5253	-495	16
Flavanone													

12	Naringenin	271.06	10.79	784	-92	1083	-36	1.38	1368	-206	942	-116	31
Flavonol glycosides													
13	Quercetin glucoside	463.097	8.92	17084	-2416	32191	-4422	1.88	56786	-6729	30390	-4102	46
14	Quercetin diglucoside	625.142	4.62	7800	-887	11182	-300	1.43	21412	-2869	10631	-919	50
15	Quercetin glucoside rhamnoside	609.146	8.54	7968	-1648	20472	-3165	2.57	20178	-4433	8620	-377	57
16	Quercetin malonylglucoside rhamnoside	695.15	7.84	431	-311	968	-116	2.24	1961	-556	662	-185	66
17	Quercetin diglucoside rhamnoside	771.203	6.47	4149	-336	5223	-298	1.26	8932	-748	5459	-385	39
18	Kaempferol glucoside	447.093	10.32	5445	-641	9241	-1763	1.7	5796	-890	3884	-1073	33
19	Kaempferol glucoside rhamnoside	593.152	9.9	1254	-96	3925	-860	3.13	3666	-683	2258	-120	38
20	Kaempferol diglucoside + quercetin glucoside rhamnoside*	609.147	5.59	6314	-739	9101	-396	1.44	17050	-2275	11275	-445	34
21	Isorhamnetin glucoside	477.103	10.73	8215	-992	13876	-2040	1.69	27520	-2671	13133	-551	52
22	Isorhamnetin glucoside rhamnoside	623.163	8.62	74684	-6500	92489	-2630	1.24	124033	-13793	79015	-8495	36
23	Isorhamnetin diglucoside	639.158	5.95	2062	-352	2666	-310	1.29	6419	-731	3520	-143	45
Uunknowns													
24	Unknown	386.938	0.96	980	-161	1733	-329	1.77	4022	-116	3038	-426	24
25	Unknown	300.07	2.02	3518	-318	4525	-689	1.29	9758	-1487	7648	-398	22
26	Unknown	514.165	5.78	169	-267	1125	-294	6.64	5990	-1733	3150	-508	47
27	Unknown	664.22	8.01	328	-193	698	-228	2.13	4683	-331	3290	-411	30
28	Unknown	519.188	10.81	148	-95	512	-147	3.47	1060	-198	816	-36	23

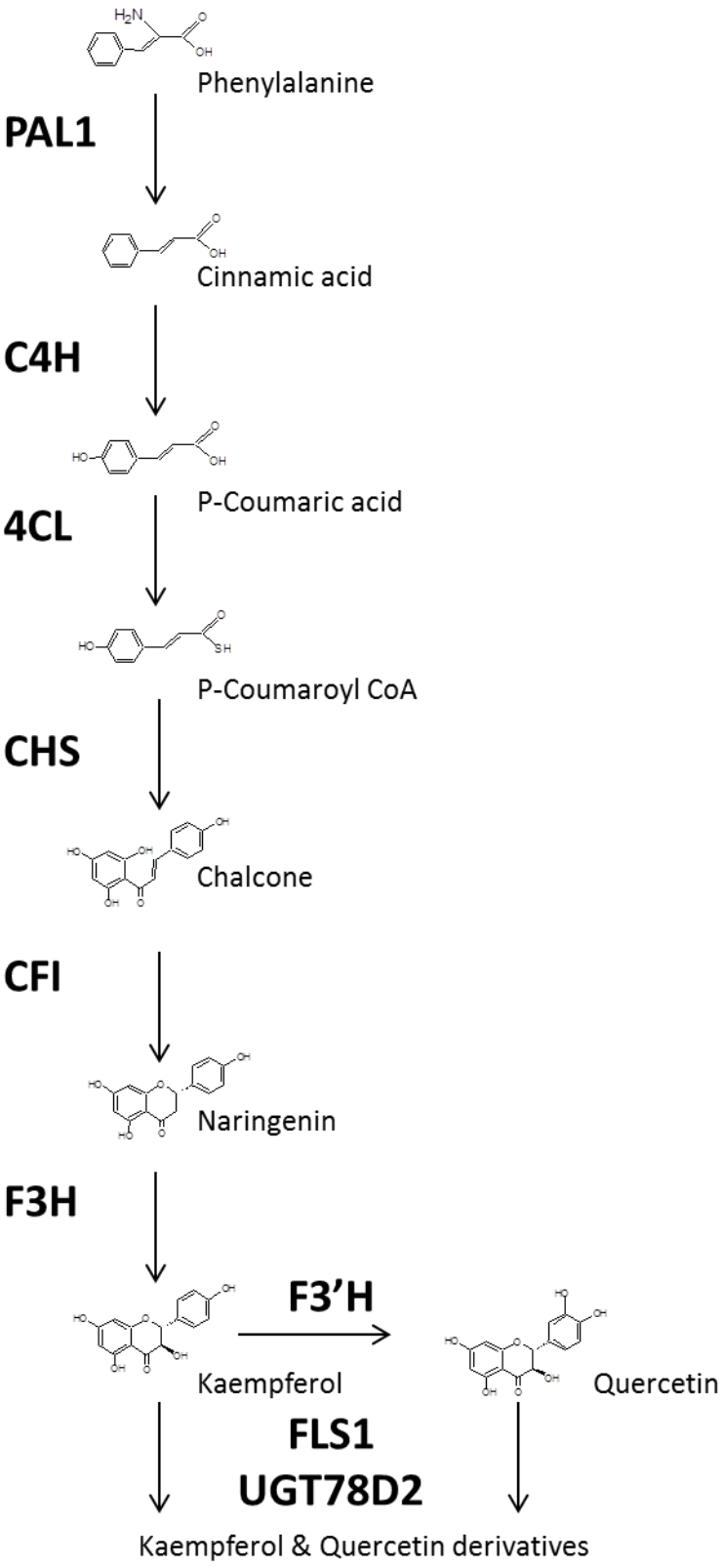

Supplementary Figure 1. Flavonol biosynthesis in Arabidopsis.

Chapter 4: HY5 triggers a network of transcriptional responses to GR24 in Arabidopsis roots, in part by recruiting MYB12

Alan Walton[a,b,c,d], Elisabeth Stes[a,b,c,d], Stan Van Praet[a,b], Nick Vangheluwe[a,b], Lukas Braem[a,b,c,d], Kris Gevaert[c,d] and Sofie Goormachtig[a,b,1]

[a]Department of Plant Systems Biology, VIB, 9052 Ghent, Belgium

[b]Department of Plant Biotechnology and Bioinformatics, Ghent University, 9052 Ghent, Belgium

[c]Medical Biotechnology Center, VIB, 9000 Ghent, Belgium

[d]Department of Biochemistry, Ghent University, 9000 Ghent, Belgium

Running title: A HY5 mediated response to GR24 in the roots of Arabidopsis

Footnotes

[1]Address correspondence to sofie.goormachtig@psb.vib-ugent.be

Author's contribution: Alan Walton was the main researcher involved in the work displayed in this chapter.

Abstract

Almost a decade after the discovery of a hormonal role for strigolactones (SLs) in various aspects of plant development many of the early steps in the strigolactone signaling cascade have been identified. However, players involved in the steps further downstream remain to a large extent elusive. Although strigolactone signaling has been shown to act on the PIN1 protein localization in a transcriptionally independent way to control shoot branching, evidences also exist for the involvement of transcriptional changes during strigolactone signal transduction. Here, we identify two main players involved in the transcriptional cascade activated by the synthetic strigolactone GR24 in the root. We demonstrate an important role for the Arabidopsis transcription factor ELONGATED HYPOTCOTYL 5 (HY5), by showing for the first time that the *hy5-215* mutant is unresponsive GR24 with regard to several of the known responses in the root, such as root hair elongation, reduction of lateral root density and increased flavonol production. We further uncovered a role for the transcription factor *MYB12* in specifically coordinating the GR24-dependent flavonol readout downstream of HY5.

Research contributions**:** Alan Walton carried out all of the research in this chapter
This manuscript is in preparation for submission.

1. Introduction

HY5 is a b-ZIP transcription factor that is essential for the light responses during seedling growth. The Arabidopsis *hy5* mutant shows an array of light response-defective phenotypes, such as reduced greening and exaggerated hypocotyl growth in the light (Koornneef et al. 1980). The mechanisms by which HY5 mediates light responses are mainly controlled by CONSTITUTIVE PHOTOMORPHOGENIC 1 (COP1)-mediated proteasomal degradation of HY5 that occurs only in the dark (Hardtke et al., 2000; Osterlund et al., 2000a; Osterlund et al., 2000b). COP1 is an E3 ligase present in the nucleus in the dark, which is excluded from this compartment in the light, possibly through the action of members of the phytochrome and cryptochrome families of light receptors (Lian et al., 2011; Liu et al., 2011; Yang et al., 2001; Yang et al., 2000). Although *hy5* was initially identified in a screen for impaired light-induced elongation of the hypocotyl, a *hy5* null allele was also found in a screen with altered root morphology (Cluis et al., 2004; Oyama et al., 1997). In particular, HY5 has been shown to play a specific role in mediating the emergence of lateral roots, which depends on shoot derived auxin (Cluis et al., 2004). In the wild-type (WT), there is no outgrowth of the initiated lateral root primordia at 10 days after germination (DAG) for seedlings that are decapitated at 4 DAG. However, *hy5* mutant seedlings that have undergone the same treatment display multiple emerged lateral roots (Cluis et al., 2004). This effect has been correlated with the lower level of transcripts from auxin repressor genes such as *SLR* and *IAA6*.

Strigolactones (SLs), carotenoid-derived compounds, act as plant hormones involved in various plant developmental pathways and as important rhizosphere molecules, inducing parasitic plant germination. Application of the synthetic strigolactone GR24 is known to rescue the defects of the strigolactone biosynthesis mutants, such as the shoot branching phenotype of the MORE AXILLARY BRANCHING 3 and 4 mutants (*max3*, *max4)*. Moreover, this strigolactone analog can give rise to an inhibition of hypocotyl growth in the light and affects multiple aspects of root development. In particular, GR24 leads to an increase in root hair length and a MAX2-dependent reduction in lateral root density (LRD) when grown in nutrient rich conditions (Kapulnik et al., 2011; Kapulnik and Koltai, 2014; Koltai, 2011; Rasmussen et al., 2012; Ruyter-Spira et al., 2011). With respect to the latter, this effect is shown to be auxin dependent to the extent that the effect of GR24 treatment is opposite in high or low auxin backgrounds (on LRD for instance) (Ruyter-Spira et al., 2011). A recent paper shows that the impact on LRD 10 DAG is largely due to an effect on lateral root emergence rather than priming or lateral root initiation (Jiang et al., 2016). Finally, strigolactones are also proposed to act as secondary messengers for light perception (Tsuchiya et al., 2010). This was based on the observation that a screen for chemical compounds that induce light responses in Arabidopsis identified cotylimides, compounds that potentially induce strigolactone biosynthesis (Tsuchiya et al., 2010).

HY5 is hypothesized to play a role in strigolactone signaling in the hypocotyl, because *hy5* and *max2* strigolactone signaling mutants share a long hypocotyl phenotype and, similar to the HY5-dependent reaction to light, the response to GR24 is seen mainly in photomorphogenic growth with no reported effect on skotomorphogenic growth (Tsuchiya et al., 2010). Just as the *max2* mutant, *hy5* was shown to not mimic the WT in its GR24-enhanced inhibition of hypocotyl growth in the light (Tsuchiya et al., 2010). It was therefore suggested that GR24 enhanced photomorphogenic growth in the hypocotyl by leading to the stabilization of the HY5 protein. Indeed, high doses of GR24 could induce migration of COP1 outside the nucleus resulting in the stabilization of HY5 (Toh et al., 2014; Tsuchiya et al., 2010). However, the role of MAX2 in this process seemed minor as this phenotype was MAX2 independent and because *hy5 max2* double mutant hypocotyl phenotypes were additive (Waters and Smith, 2013). However, a later study showed that GR24, when used in physiologically relevant concentrations (i.e. below 10 µM), enhances HY5 transcript levels and stabilizes the HY5 protein in a MAX2-dependent manner in the light, and that the latter effect is not observable in the dark (Jia et al. 2014) due to COP1 nuclear localization which continuously causes HY5 degradation (Hardtke et al., 2000; Osterlund et al., 2000a; Osterlund et al., 2000b). In summary, it seems that inside the hypocotyl, GR24 causes a transcriptional induction of *HY5* in a MAX2 dependent manner, while it causes COP1 migration outside the nucleus independently of MAX2.

The role of HY5 signaling is until now mainly investigated in the hypocotyl, although it is known that both MAX2 and HY5 are important for proper root development and that both affect root architecture by impinging on auxin transport or signaling (Cluis et al. 2004; Jiang et al. 2016). Moreover, in a recent study investigating the effect of GR24 treatment on the Arabidopsis root proteome, we reported an increase in flavonols (**Chapter 3**) via induction of the accumulation of flavonol biosynthesis genes that are known to be HY5 dependent (Lee et al., 2007).

This increasing number of parallels between HY5 and strigolactone in regulating root architecture led us to investigate the role of this protein in GR24 root based signaling. We found that the *hy5* mutant does not show several of the described GR24 effects on root development and that the flavonol readout is entirely abolished in the absence of this transcription factor. Furthermore, we also identified a new transcription factor, MYB12, which is transcriptionally activated by HY5, to be specifically responsible for the GR24-dependent flavonol readout. Moreover, based on GR24 induced root phenotypes and expression analysis, we showed that at least one gene responds to GR24 in a HY5-dependent manner, but independently of MYB12. Further, the MYB12 coordinated flavonol response to GR24 treatment was found not to be responsible for the GR24-dependent root development. Finally, we hypothesize that HY5 plays a much broader role than that of MYB12 in the control of GR24 responses in the root.

2. Results

2.1. Over one third of the genes encoding proteins that differentially accumulated in the max2 mutant are transcriptionally regulated by HY5

In our previous work, we compared the root proteomes of *max2* and WT plants (**Chapter 3**). The levels of 120 proteins were shown to be significantly different (P-value ≤ 0.05) when comparing WT with *max2-1* roots. Within this selection, proteins involved in flavonol synthesis were enriched more than 10-fold (**Chapter 3**). Interestingly, qPCR analysis demonstrated that transcripts for several of these enzymes were upregulated upon GR24 treatment. The effect of GR24 on one of these genes, chalcone synthase (*CHS)*, was described previously (Waters and Smith, 2013). A particularity of this gene, in comparison to other GR24 reporters, such as *KUF1*, *DLK2* and *IAA1*, is that its response to GR24 is dependent upon both MAX2 and the transcription factor HY5 (Waters and Smith, 2013). On the whole, 34% of the promoters of the genes coding for the subset of 120 proteins are predicted to be targeted by HY5, representing a more than 2-fold enrichment for HY5 regulated genes. This result suggests that HY5 could play a role in mediating GR24 signaling in the root.

2.2. The hy5 mutant does not displays GR24-induced responses in the root

GR24 treatment reduces both the total number of emerged lateral roots and LRD (Ruyter-Spira et al. 2011). To investigate whether HY5 plays a role in strigolactone signaling in the root, we tested the *hy5-215* mutant for various known GR24 root responses. Both *hy5-215* and WT plants were grown for 9 days in either mock (acetone carrier) or treated conditions (1 µM GR24), and the number of emerged lateral roots and LRD was counted. Whereas the WT seedlings displayed a significant (p-value≤0.01) 34% drop in the total number of emerged lateral roots and a significant 26% decrease in LRD, the *hy5* mutant showed no difference in the total number of emerged lateral roots and only a minor difference in its LRD (7%) which was not found to be statistically significant (p-value<0.01) (Figures 1A and 1B). GR24 is reported to give rise to a MAX2-dependent increase in root hair length (Kapulnik et al., 2011). Here, we could confirm these findings, as WT plants grown in the presence of GR24 showed a 2-fold increase in root hair length that was not seen in *max2*. The root hair lengths of *hy5* seedlings were mildly, but significantly shorter in mock conditions when compared to WT, however, their elongation was not significantly affected by GR24 (Figure 1C). Finally, we have recently shown that the Arabidopsis root responds to GR24 through a MAX2-dependent increase in flavonol production (**Chapter 3**). DPBA *in planta* staining was used to specifically visualize flavonol production in *hy5* and WT seedlings grown in the presence or absence of GR24. The WT roots showed an increase in flavonol production as expected, however this response was abolished in the *hy5* mutant (Figure 1D).

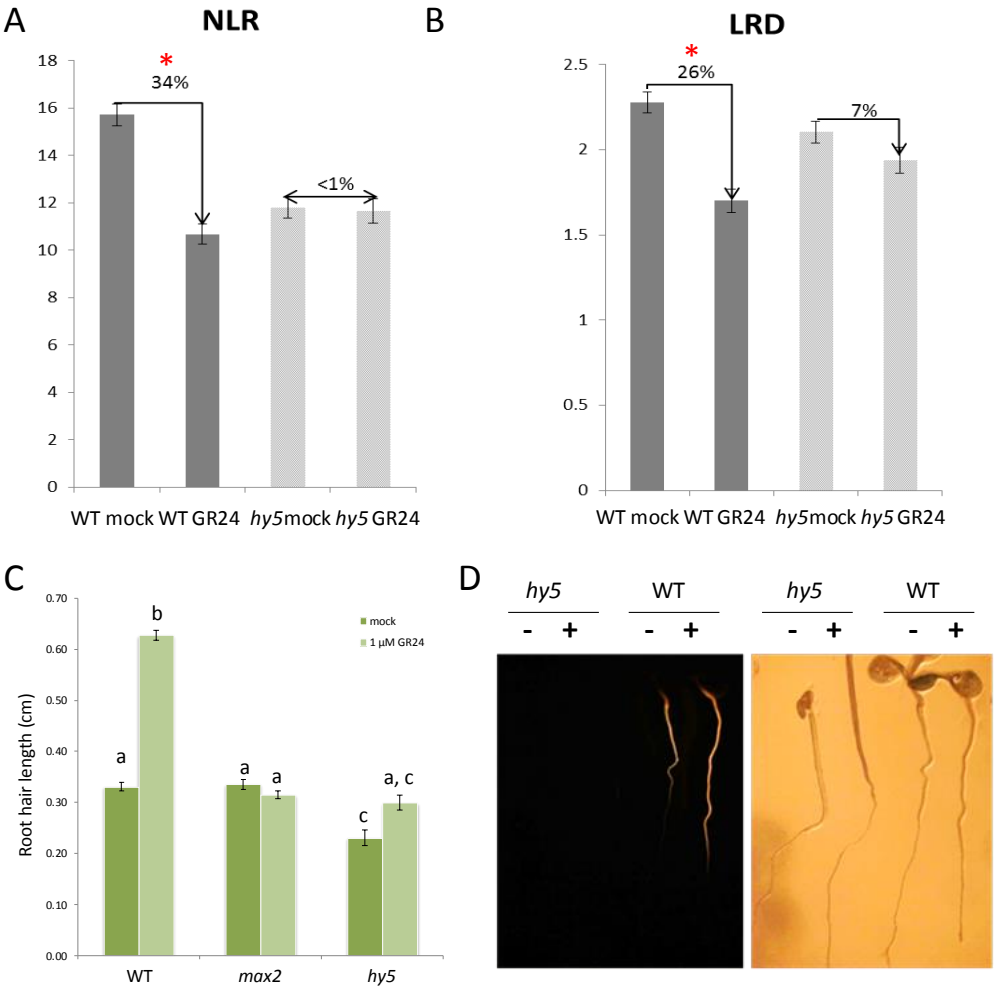

Figure 1: **Effect of GR24 on the *hy5* mutant.** (A) The number of emerged lateral roots (NLR) and the (B) lateral root density (LRD) in 9-day-old WT and *hy5* seedlings grown on 0.5 MS media with 1% sucrose and in the presence of the acetone carrier (mock) or 1 µM GR24 (GR24). (C) The root hair length of WT, *max2* and *hy5* 5-day-old plants grown on 0.5 MS media with 1% sucrose and in the presence of the acetone carrier (mock) or 1 µM GR24 (GR24). (D) *In planta* DPBA staining of 5-day-old WT and *hy5* plants grown on 0.5 MS media with 1% sucrose and in the presence of the acetone carrier (mock) or 1 µM GR24 (GR24) under UV excitation (left) or in normal light (right). Data presented are means ± SE of three biological repeats. Letters (a,b,c) or * indicate statistically significant different means (P<0.01), according to ANOVA mixed-model statistical analyses.

Also, in mock conditions, a lower overall flavonol staining was observed in *hy5* mutant compared to the WT plants. Taken together, these results show that the *hy5* mutant is insensitive to GR24 for several of the known GR24-induced root phenotypes. This suggests a role for HY5 in the signaling cascade during the root response to GR24 that affects LRD, root hair length and flavonol production.

2.3. MYB12 coordinates flavonol accumulation in response to GR24

Flavonol production is one of the processes controlled by HY5 (Li et al. 2007). Three transcription factors, MYB11, MYB12 and MYB111, which are themselves transcriptionally regulated by HY5, have been shown to coordinate the expression of the flavonol biosynthesis enzymes downstream of HY5 (Stracke et al., 2010). Hence, in a next step, we tested the contribution of these three transcription factors in the GR24-induced flavonol response.

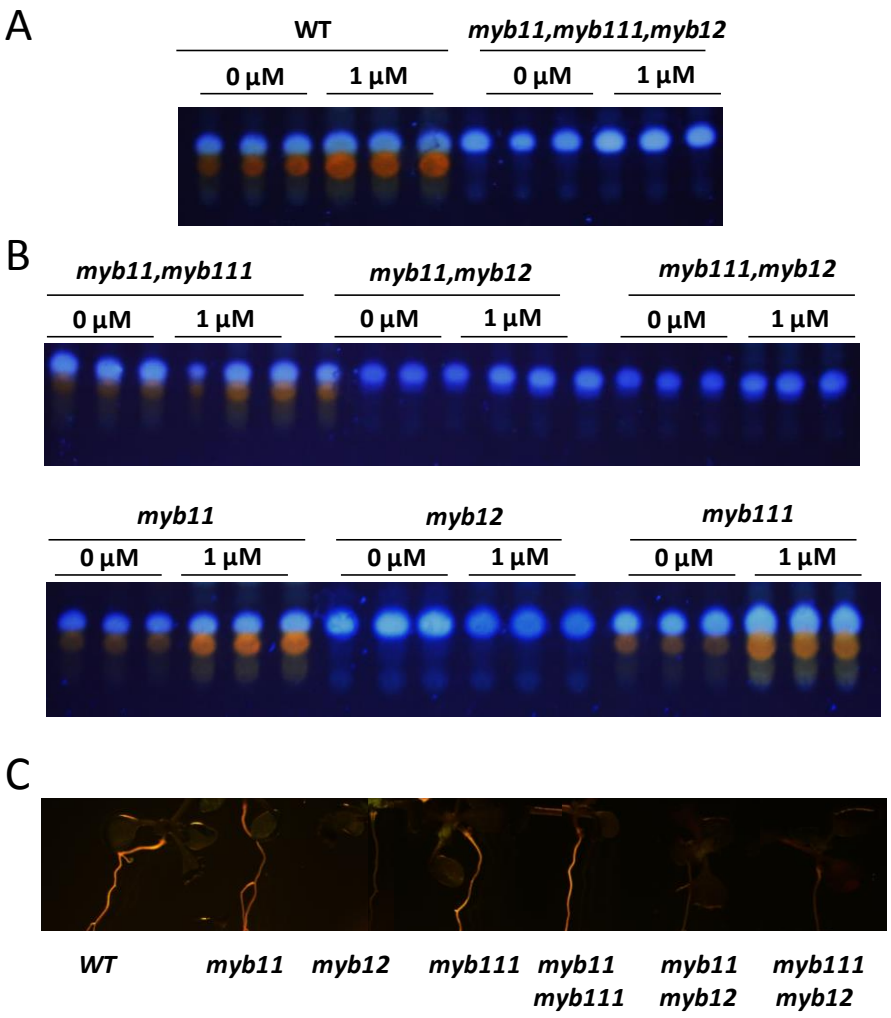

Figure 2: The root response of *myb* mutants to GR24. (A) HPTLC analysis of DPBA stained methanol extracts from WT and *myb11,myb111,myb12* triple mutant seedlings, grown with or without 1 µM GR24. (B) HPTLC analysis of DPBA stained methanol extracts from WT, single and double mutants for *myb11, myb12* and *myb111* seedlings, grown with or without 1 µM GR24. (C) *In planta* DPBA staining of WT, single and double mutants for *myb11, myb12* and *myb111.*

To assess whether these transcription factors play a role in the HY5-mediated increase in flavonol production upon GR24 treatment, a DPBA stained HPTLC of methanol extracts from WT

and the *myb11,myb111,myb12* triple mutant was prepared (Figure 2A). After 5 days of growth on medium containing 1 µM GR24, WT plants displayed a significant increase in flavonol levels, whereas no response was detected in the triple mutant. This suggested that one or several of these transcription factors was responsible for the GR24-induced increase in flavonol production. To further isolate the transcription factor responsible for this effect, the experiment was repeated using double and single mutants (Figure 2B). As shown in Figure 2B, only in the *myb12* mutants GR24 treatment did not cause flavonol accumulation while the *myb11* and *myb111* mutants responded just like WT. A lower basal level of flavonols was also observed in the *myb12* mutant and other mutants containing the *myb12* allele grown in mock conditions, while this was not the case for the mutants with a functional *MYB12* allele (Figure 2C). These results show conclusively that *MYB12* is necessary for the GR24 induced flavonol response.

To investigate whether these changes in flavonol response were due to changes in transcriptional regulation of flavonol genes, the expression level of the flavonol biosynthesis gene *CHS* was tested in the *myb12* mutant background. cDNA was prepared from WT and *myb12* mutant seedlings grown for 5 days on non-supplemented media before being moved for 24 h on mock (acetone carrier) or 1 µM GR24 containing media, and levels of the *CHS* transcript were measured.

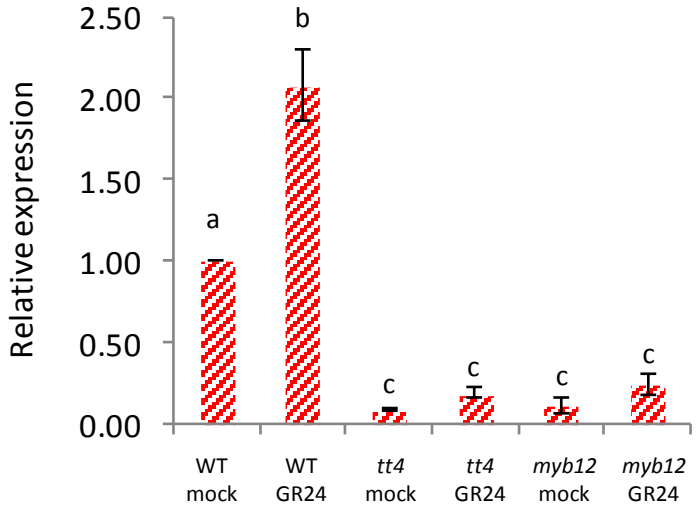

Figure 3: Response of *CHS* to GR24 treatment in various mutant backgrounds. *CHS* transcript levels were analyzed through RT-qPCR from 5-day-old WT and *hy5* plants grown in the presence of the acetone carrier (mock) or 1 µM GR24 (GR24) for 24 h. The *tt4* mutant is a tDNA insertion mutan for *CHS* and is shown here as a negative control. Letters (a,b,c) indicate statistically significant different means (P<0.01), according to ANOVA mixed-model statistical analyses.

The 2-fold increase in *CHS* levels upon GR24 treatment was abolished in the *myb12* mutant and the *CHS* transcript levels were much lower in *myb12* roots when compared to the WT (Figure 3). The expression levels of *CHS* are given as a control in the *tt4-4* mutant (tDNA insertion mutan for CHS). Hence, taken together, these result show that MYB12 is an essential player in the GR24 induced flavonol root read-out.

2.4. MYB12 action is subordinate to that of HY5 during flavonol accumulation

Having shown the need for both HY5 and MYB12 in the flavonol root response to GR24, we verified the relative position of these two transcription factors in relation to the activation of the flavonol biosynthesis genes. Since HY5 is known to control the expression of *MYB12*, we hypothesized that HY5 gives rise to *MYB12* expression upon GR24 treatment, which in turn would then give rise to the increase in flavonol biosynthesis gene expression. To investigate this possibility, changes in expression of *MYB12* upon GR24 treatment were examined. cDNA was prepared from plants grown as described above. Levels of *MYB12* transcripts increase nearly 2-fold in the WT upon 24 h treatment with 1 μM GR24 when compared to mock grown seedlings (Figure 4A). This result was confirmed through the use of two separate prom*MYB12::GUS* lines. When grown for 5 days on either mock or in GR24, a higher intensity in GUS staining was observed throughout the roots of GR24 treated seedlings (Figure 4B). This induction is completely abolished in the *max2-1* mutant roots at all concentrations of GR24 tested.

We also collected material from seedlings treated with 2 and 5 μM GR24 to test whether the *MYB12* response was dose dependent (Figure 4A).

MYB12 was induced significantly upon all treatment in the WT but not in the *max2* mutant. The difference in gene induction in the WT between different concentrations of GR24 tested was however not significant. These results show that *MYB12* is induced upon GR24 in a MAX2-dependent manner. Moreover, little or no dose response is involved and this response remains MAX2-dependent up to and including 5 μM treatment (Figure 4A).

Finally, to assess whether this MAX2-dependent increase in *MYB12* expression is also dependent upon HY5, the effect of GR24 on *MYB12* expression levels in the *hy5* background was examined. As anticipated, the GR24 induced increase in *MYB12* gene expression did not occur in the *hy5* mutant, and basal levels of *MYB12* were also lower in this background (Figure 4C).

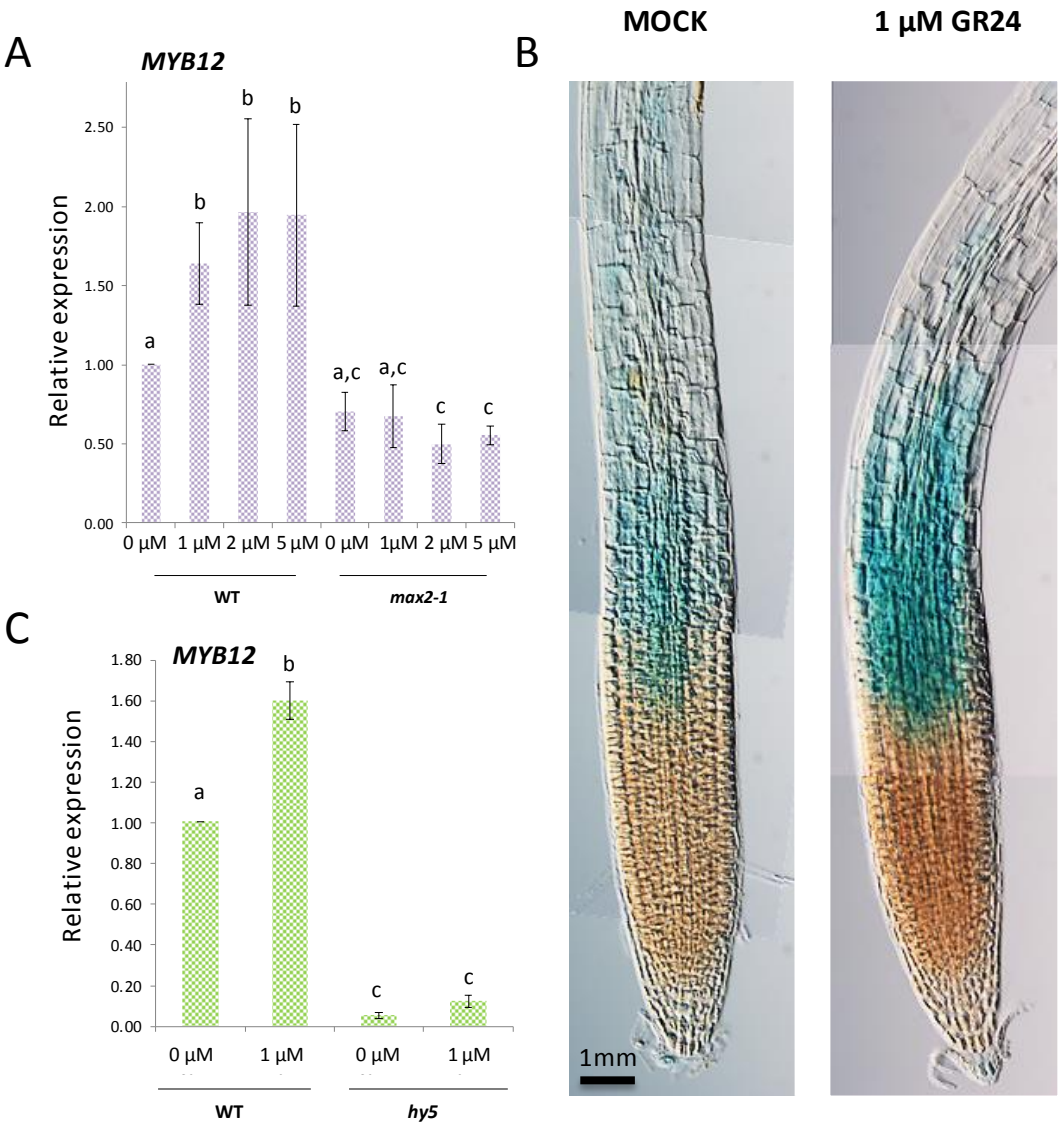

Figure 4: Analysis of the *MYB12* response to GR24. (A) *MYB12* transcript levels were analyzed through RT-qPCR from 5-day-old WT and *max2* plants grown on 0.5 MS media with 1% sucrose and in the presence of 0, 1, 2 or 5 µM GR24 for 24 h. (B) GUS staining of promMYB12::GUS lines grown on 0.5 MS media with 1% sucrose and in the presence of 0 or 1 µM GR24 for 24 h. (C) *MYB12* transcript levels were analyzed through RT-qPCR from 5-day-old WT and *hy5* plants grown on 0.5 MS media with 1% sucrose and in the presence of 0 or 1 µM GR24 for 24 h. Letters (a,b,c) indicate statistically significant different means (P<0.01), according to ANOVA mixed-model statistical analyses.

Taken together, these results suggest that MYB12 coordinates part of the HY5 mediated response to GR24 downstream of MAX2 in roots.

2.5. The *myb12* mutant does not phenocopy the *hy5* mutant's morphological defects in root architecture

MYB12 appears to coordinate at least part of the HY5 mediated response to GR24 in roots. As the *myb12* mutant shares the aberrant flavonol response to GR24 with *hy5*, we investigated if MYB12

was necessary for any of the other GR24 root responses that *hy5* showed resistance to. WT and *myb12* knockout plants were grown for 9 days and LRD was measured (Figure 5A). Both the WT and the *myb12* knockout showed a reduced LRD upon GR24 treatment. Furthermore, the *myb12* knockout also showed a significant increase in root hair length upon GR24 treatment similar to that observed in the WT (Figure 5B).

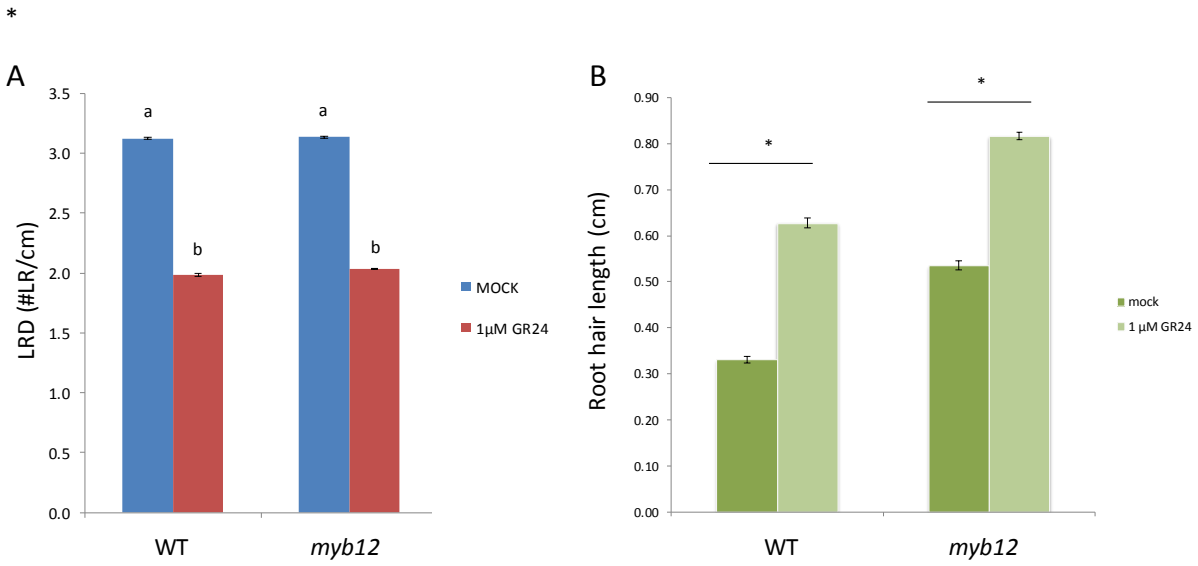

Figure 5: Root responses of WT and *myb12* plants to GR24. (A) The lateral root density of 9-day-old WT and *myb12* seedlings grown on 0.5 MS media with 1% sucrose and in the presence of the acetone carrier (mock) or 1 µM GR24. (B) The root hair length of WT and *myb12* 5-day-old plants grown on 0.5 MS media with 1% sucrose and in the presence of the acetone carrier (mock) or 1 µM GR24. Letters (a,b,c) or * indicate statistically significant different means (P<0.01), according to ANOVA mixed-model statistical analyses.

In conclusion, these results suggest that the absence of a functional MYB12 does not lead to the resistance to GR24 as was observed for the *hy5* mutant roots, and the action of MYB12 probably only accounts for a small part of the action range of HY5.

2.6. HY5 exerts an action broader than that orchestrated by MYB12

Because *myb12* mutants still respond to GR24 in their root hair and LRD phenotypes, while *hy5* mutants do not, the action of HY5 seems to be broader than that of MYB12 in controlling GR24 responses. To further confirm this, we checked the dataset of 120 significantly different proteins in *max2* and WT roots (**Chapter 3**) for genes that respond to GR24 in a HY5-dependent but MYB12-independent manner. cDNA was prepared from the roots of *hy5* and WT seedlings. We have so far identified one gene, *KIN2*, that fulfills these criteria (Figure 6).

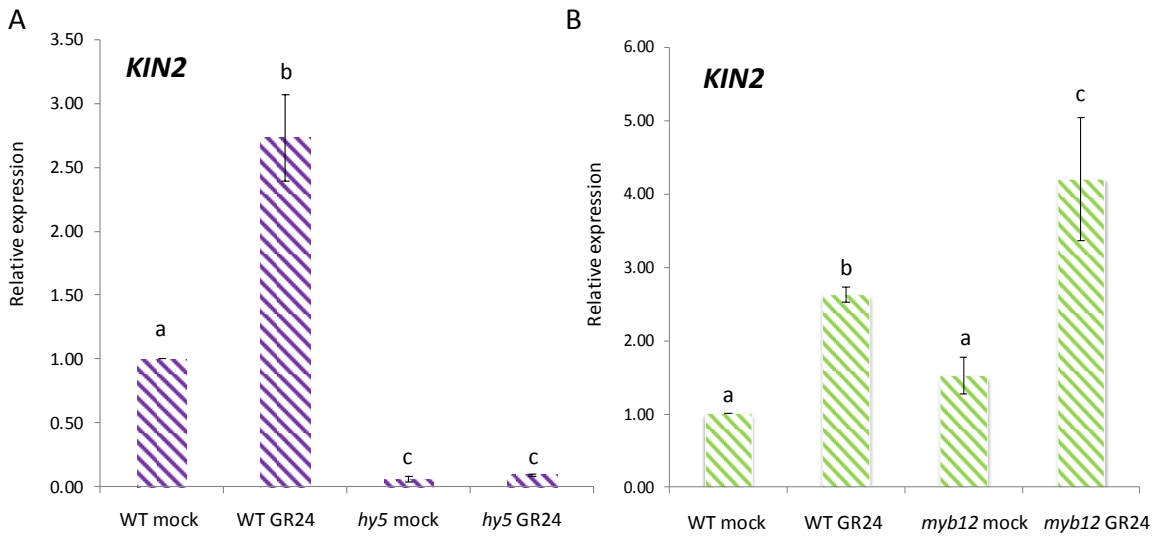

Figure 6: Change in expression levels of *KIN2* in different mutants. (A) qPCR analysis of the *KIN2* gene in WT (Col-0) and *hy5-215* seedlings treated for 24 h with 1 µM GR24 or the acetone carrier. (B) qPCR analysis of the *KIN2* gene in WT (Col-0) and *myb12* seedlings treated for 24 h with 1 µM GR24 or the acetone carrier. Letters (a,b,c) or * indicate statistically significant different means (P<0.01), according to ANOVA mixed-model statistical analyses.

This result corroborates the hypothesis that HY5 coordinates a GR24 induced response in the roots by regulating a transcriptional network, which is in part MYB12-dependent.

3. Discussion

The role of HY5 in GR24 responses is so far only investigated in the hypocotyl and in seeds (Toh et al., 2012; Tsuchiya et al., 2010; Waters and Smith, 2013). In a proteome analysis of WT and *max2* roots, we found a more than two-fold enrichment of HY5-regulated gene products in the WT root proteome when compared to the *max2* background (**Chapter 3**). Together with similarities between the root phenotypes of *max2* and *hy5* mutants, this provided indications that HY5 might play a role in the GR24 root response. We therefore set out to investigate the role of this transcription factor in GR24-induced signaling in Arabidopsis roots. Root phenotyping assays demonstrated that the *hy5* mutant displayed several of the resistances to GR24 treatment that can be observed in the *max2* mutant. More specifically, we could show that treatment with GR24 of *hy5* mutants does not give rise to the decrease in LRD and the elongation of root hairs observed in WT roots.

Also in **Chapter 3**, we observed that GR24 treatment causes a transcriptional induction of flavonol biosynthesis genes, which results in the accumulation of the corresponding proteins and finally in an accumulation of particular flavonols. Interestingly, the *hy5* mutant was insensitive for the GR24-dependent flavonol read-out. Further, we observed that *CHS*, encoding the enzyme executing the first dedicating step in flavonoid biosynthesis, is transcriptionally upregulated in the root by GR24 (**Chapter 3**). *CHS* has been described as a GR24 responsive gene dependent on HY5 in the hypocotyl,

again illustrating the importance of HY5 in the response to this compound (Nelson et al., 2010; Waters and Smith, 2013). However, because *CHS* was the only one from 5 tested marker genes for which the GR24-dependent expression profile was modulated by HY5, the authors argued that, for the most part, HY5 did not play a role in strigolactone and MAX2 dependent processes. However, here we show that the GR24-dependent accumulation of flavonols is preceded by the transcriptional activation of *CHS*, which itself is dependent of that of the transcription factor *MYB12*. Importantly, HY5 controls the action of MYB12-mediated signaling by increasing the expression levels of the *MYB12* gene itself. Gene expression analysis in the *max2* mutants showed that this regulation is also dependent upon MAX2. We have shown that *CHS* is actually part of a group of GR24 responsive genes whose expression is all regulated by MYB12, providing conclusive evidence that *CHS* is far from being the only HY5 and MAX2-dependent gene in the GR24 response.

In summary, HY5 and MYB12 are the first transcription factors to be reported controlling GR24-dependent responses in the root, coordinating the flavonol response. However, MYB12 is not the only transcription factor acting downstream of HY5, because we also have identified a GR24-induced gene, *KIN2*, from which the expression pattern is dependent on MAX2 and HY5, but independent on MYB12. Hence, it will be interesting in the future to also reveal other transcription factors controlling GR24-dependent responses. An in-depth transcriptome study including the analysis of GR24 responses in WT, *max2* and *hy5* roots, will certainly help to seek for candidates.

It has recently been shown that the GR24 effect on LRD is mainly due to inhibition of lateral root emergence, rather than an effect on lateral root priming of initiation. Moreover, several studies have shown that this effect of GR24 is dependent on the auxin landscape and on the shoot-to-root auxin transport (Jiang et al. 2015, Ruyter-Spira 2011). After the initial observation of aberrant root phenotypes in *hy5* mutants (Oyama et al., 1997), it was also shown that this transcription factor is responsible for mediating the effect of shoot-derived auxin on lateral root emergence (Cluis et al. 2004). Therefore, the *hy5* phenotype described in the present work correlates with previous studies. Furthermore, the observation that *myb12* does not share the resistance to the GR24 effect on LRD with *hy5* suggests that the members of the MYB12-independent part of the HY5-triggered network could be responsible for this phenotype. Hence, this further supports that it would therefore be of great interest to identify the genes that make up this part of the network and to study potential candidates that might be responsible for the LRD phenotype.

Although the *hy5* mutant appears to fill a large part of the phenotypic space of the root responses to GR24, it is likely that other factors downstream of MAX2 and the SMXL proteins are also at play. Several lines of evidence lead us to this conclusion. First, despite the reported naturally occurring higher LRD, in our hands, the *hy5-215* mutant does not display the increased LRD of the *max2* mutant when grown in mock conditions. This difference would seem to indicate that other

factors probably also function downstream of MAX2 and the SMXL proteins to account for the entire *max2* phenotype. Second, the fact that, although largely insensitive, *hy5* suffers a modest reduction in LRD could corroborate this theory. Thirdly, at the proteome level still a part of the GR24-regulated root proteome has not been linked with HY5 so far.

With this work we have contributed to closing the gap between the known GR24-induced root phenotypes and the upstream signaling which is being rapidly unraveled. The next step will be to see how the degradation of SMXL proteins leads to HY5 action.

4. Material and methods

Plant Material

Seeds of *Arabidopsis thaliana* (L.) Heyhn. (accession Columbia-0) plants were surface sterilized with consecutive treatments of 70% (v/v) ethanol with 0.05% (w/v) sodium dodecyl sulfate (SDS), and then washed with 95% (v/v) ethanol. For material destined to proteomics experiments or RNA preparation, seeds were sown on nylon meshes (20 µm) placed on half-strength Murashige and Skoog (MS) medium containing 1% (w/v) sucrose. Fifty plants were sown per plate in two rows of 25. Seeds were stratified for 2 days at 4°C, where after they were grown for 5 days, before being transferred to mock-treated medium or medium containing 1 µM *rac*-GR24. Finally, for high-performance thin-layer chromatography (HPTLC) analysis, seeds were stratified for 2 days at 4°C, where after they were grown for 5 days either on mock or *rac*-GR24-containing medium before methanol extraction.

The *rac*-GR24 that was used for the proteome and the metabolite profiling contained both the $GR24^{5DS}$ (GR24+) and $GR24^{ent\text{-}5DS}$ (GR24-) enantiomers (Scaffidi et al. 2014). In experiments designed to test the effect of the stereochemistry on the flavonol response, purified enantiomers, GR24+ and GR24-, were applied separately.

RNA Extraction and Quantitative (q)RT-PCR

Roots from WT and *max2-1* plants were harvested and snap-frozen in liquid nitrogen 24 h post treatment (hpt). Cell walls were disrupted by 3-mm metal beads in 2 mL Eppendorf tubes with a mixer mill 400 (Retsch) for 2 min at 20 Hz. RNA was extracted and purified with the RNeasy mini kit (Qiagen). Genomic DNA was removed by DNase treatment and the samples were purified by ammonium acetate (2.5 M final concentration) precipitation. Concentrations were measured with a ND-1000 Spectrophotometer (Nanodrop). The iScript cDNA synthesis kit (Bio-rad) was used to reverse transcribe RNA. qRT-PCR primers were designed with the Quant Prime website software. SYBR Green detection was used during qRT-PCR run on a Light Cycler 480 (Roche). Reactions were

done in triplicate in a 384-multiwell plate, in a total volume of 5 µL and a cDNA fraction of 10%. Cycle threshold values were obtained and analyzed with the 2-ΔΔCT method (41). The values from four biological repeats and three technical repeats were normalized against those of *ACTIN2* (*ACT2*, AT3G18780) that was used as an internal standard. Normalized values were analyzed according to the published model (Rasmussen et al, 2012) with the mixed model procedure of SAS Enterprise.

HPTLC Diphenylboric Acid 2-Amino Ethyl Ester (DPBA) Staining

For the HPLTC analysis of roots, methanol extracts from four biological repeats were prepared from 5-day-old *Arabidopsis* plants grown on 1% (v/v) MS medium containing either 1 µM *rac*-GR24 or 100 µL of the acetone carrier. Roots were harvested. After a methanol extraction, samples were dried with a concentrator 5301 (Eppendorf). The dried samples were re-suspended in 20 µL of an 80% (v/v) methanol solution. The concentrated extract was analyzed by HPTLC. Of the mixture, 2 µL was spotted onto a 20 cm×10 cm silica-60 HPTLC glass plate (Merck) and placed in a glass tank with a paper wick of 18 cm by 9 cm (Whatman) and a mobile polar phase consisting of ethyl acetate, dichloromethane, acetic acid, formic acid, and water in a 100:25:10:10:11 ratio, respectively. After addition of the mobile phase, the glass tank was sealed with silicon grease and gels were run for 25 min. Gels were stained by spraying a methanol solution containing 1% (v/v) DPBA. Plates were placed into an HB-1000 Hybridizer (Fisher Scientific) at 100°C for 10 min, after which the plates were sprayed with a 5% (v/v) methanol solution containing 4000-polyethylene glycol to stabilize the DPBA compound. Plates were observed after UV excitation at 350 nm. Pictures were taken with a D90 camera (Nikon).

Root phenotpyes

The lateral root phenotype of nine-day-old seedlings was analyzed by measuring the main root length and counting all visible lateral roots under Leica S4E light microscope (Leica Microsystems, Wetzlar, Germany). After the roots were counted, the plates were scanned and the main root length was measured using ImageJ software and a digitizer tablet (Walcom). Lateral root densities (LRD) were calculated by dividing the number of lateral roots by the corresponding primary root length.
The means of the biological repeats were subjected to a statistical analysis of two-way ANOVA, followed by the post-hoc Tukey–Kramer test with SAS enterprise 9.4. For the statistical analyses of the root hair length a general linear model was used as the data followed a normal distribution. While for the statistical analyses on the lateral root density a generalized linear model was performed as the data followed a poison distribution, because of the discrete data of the number of laterals (i.e. counting data).

PART III

A new tool for dissecting the strigolactone pathway

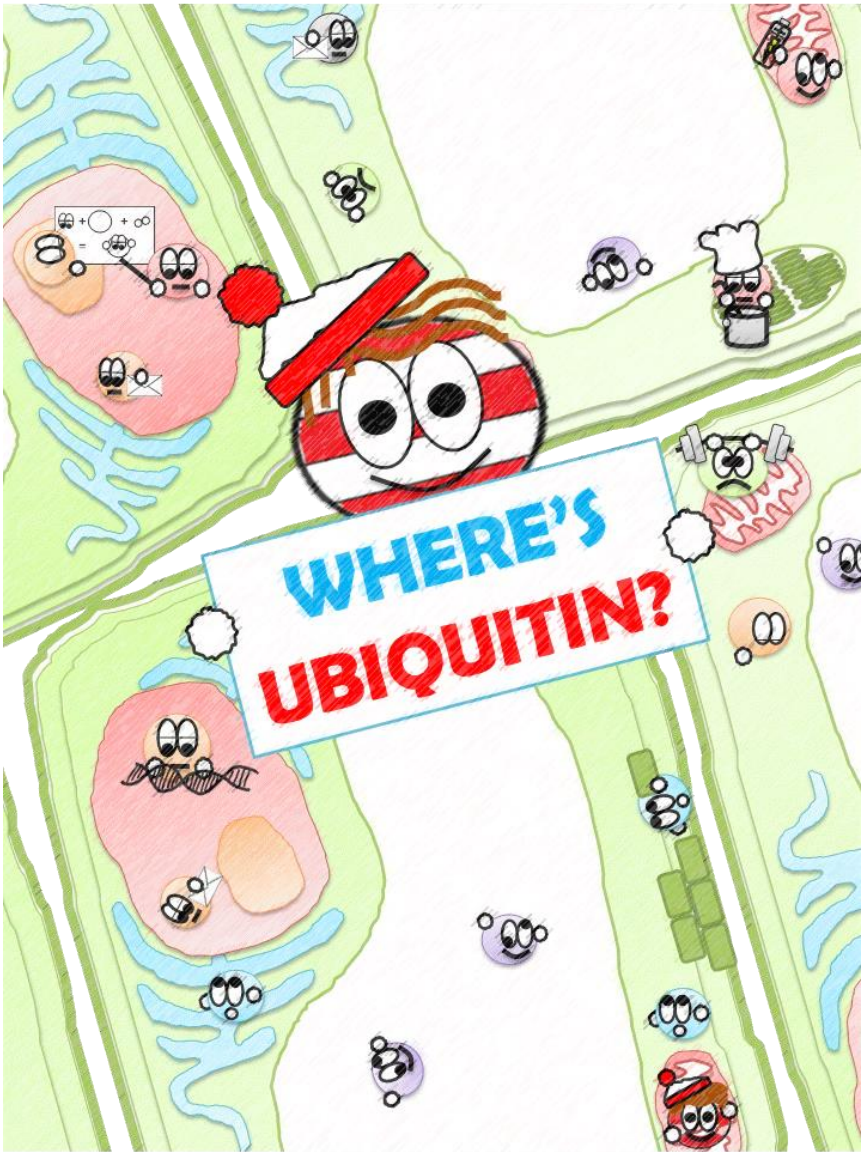

*Note concerning Part III:

At the time the research presented in the following section was carried out, the targets of the MAX2 protein were still unknown. However, despite the knowledge that these targets should be differentially ubiquitinated upon GR24 treatment, the tools available in plants to carry out a differential ubiquitin profiling experiment were not available. Our primary aim therefore was to develop the necessary technology for ubiquitination site profiling and to implement this technology in plants. We then moved on to test if this technology could detect the differential ubiquitination of the SMXL proteins when comparing plant tissue grown in the presence or absence of GR24.

Chapter 5: A COFRADIC protocol to study protein ubiquitination

Elisabeth Stes[1,2,$], Mathias Laga[1,2,$], Alan Walton[1,2,3,4,$], Noortje Samyn[1,2], Evy Timmerman[1,2], Ive De Smet[3,4], Sofie Goormachtig[3,4] and Kris Gevaert[1,2,*]

[1]Department of Medical Protein Research, VIB, B-9000 Ghent, Belgium

[2]Department of Biochemistry, Ghent University, B-9000 Ghent, Belgium

[3]Department of Plant Systems Biology, VIB, B-9052 Gent, Belgium

[4]Department of Plant Biotechnology and Bioinformatics, Ghent University, B-9052 Gent, Belgium

[$]These authors contributed equally to this work.

[*]To whom correspondence should be addressed: Department of Medical Protein Research and Biochemistry, VIB and Faculty of Medicine and Health Sciences, Ghent University, A. Baertsoenkaai 3, B-9000 Ghent, Belgium. Tel.: 32-92649274; Fax: 32-92649496; E-mail: kris.gevaert@vib-ugent.be.

* Research contributions**:** Preliminary experiments were carried out by M. Laga. M. Laga. And E. Stes designed the Ubiquitin COFRADIC pipeline. Alan Walton carried out the Ubiquitin COFRADIC and control experiments and anlayzed the data from this research in this chapter

This manuscript is an adaptation of a publication in JPR March 2014

Abstract

Here, we apply the COmbined FRActional DIagonal Chromatography (COFRADIC) technology to enrich for ubiquitinated peptides and identify sites of ubiquitination by mass spectrometry. Our technology bypasses the need to overexpress tagged variants of ubiquitin and the use of sequence-biased antibodies recognizing ubiquitin remnants. In brief, all protein primary amino groups are blocked by chemical acetylation after which ubiquitin chains are proteolytically and specifically removed by the catalytic core domain of the USP2 deubiquitinase (USP2cc). As USP2cc cleaves the isopeptidyl bond between the ubiquitin C-terminus and the ε-amino group of the ubiquitinated lysine, this enzyme re-introduces primary ε-amino groups in proteins. These amino groups are then chemically modified with a handle that allows specific isolation of ubiquitinated peptides during subsequent COFRADIC chromatographic runs. This method led to the identification of over 7,500 endogenous ubiquitination sites in more than 3,300 different proteins in a native human Jurkat cell lysate.

1. **Introduction**

Ubiquitin is a small protein of 76 amino acids that can be conjugated to substrate proteins in a process called ubiquitination. This protein modification can occur co- or post-translationally and is essential for the regulation of various protein functions (Vierstra, 2012), but it is most intensely studied in the ubiquitin proteasome system, where ubiquitin-tagging of proteins directs them to proteasomal degradation routes (Clague and Urbe, 2010). Protein ubiquitination is catalyzed by an enzymatic cascade involving three different enzymes (E1 ubiquitin activating enzymes, E2 ubiquitin-conjugating enzymes and E3 ubiquitin ligases) and by which an isopeptidyl bond between the carboxyl terminus of ubiquitin and the Ɛ-amino group of a lysine in the substrate is formed. In more rare cases, the N-terminal protein amine (Ciechanover and Ben-Saadon, 2004) and cysteine, threonine and serine residues can be modified (Cadwell and Coscoy, 2005; Kravtsova-Ivantsiv and Ciechanover, 2012). Ubiquitination is reversible through the action of deubiquitination enzymes, DUBs, which can cleave off ubiquitin moieties from substrates (Nijman et al., 2005).

Proteome-wide profiling of ubiquitination sites remains challenging, amongst others due to difficulties in enriching for ubiquitinated proteins and peptides that are typically present in substoichiometric amounts. Nonetheless, a number of such studies were published and these typically use overexpressed tagged ubiquitin (Danielsen et al., 2011; Peng et al., 2003) or antibodies against ubiquitin or its remnant created by trypsin digestion; the Lys-Ɛ-Gly-Gly motif (Kim et al., 2011; Mertins et al., 2013; Udeshi et al., 2013a; Udeshi et al., 2013b; Wagner et al., 2011; Xu et al., 2010a). Overexpression of epitope-tagged ubiquitin can create artifacts (Hjerpe and Rodriguez, 2008; Shi et al., 2011) and hamper the formation of linear ubiquitin chains (Stieglitz et al., 2012), and although di-glycine remnant directed antibodies were used for identifying thousands of putative ubiquitination sites, different antibodies appear to recognize somewhat different epitopes, leading to specificity differences (Sylvestersen et al., 2013; Wagner et al., 2012). In addition, neddylation and ISGylation also produce a di-Gly tag upon trypsinization, and although these types of ubiquitin-like modifiers are less prevalent, this leads to a small fraction of falsely identified ubiquitinated sites (Kim et al., 2011).

To overcome these problems, we developed and validated a COFRADIC technology (Gevaert et al., 2002) to map *in vivo* ubiquitinated sites without the need for prior enrichment of ubiquitinated proteins or peptides. COFRADIC is a non-gel proteomics technique that reduces the complexity of peptide mixtures by enriching for peptides of interest by repeated liquid chromatographic peptide separations intermitted by a specific peptide modification (Ghesquiere et al., 2011; Staes et al., 2011).

2. Results and discussion

The COFRADIC technology comprises three successive steps: (1) RP-HPLC fractionation of peptides, (2) a chemical or enzymatic modification step that targets a subset of peptides in each peptide fraction, and (3) a series of identical chromatographic separations of the modified peptide fractions aimed at separating specific peptides. The second step results in a change of chromatographic retention so that peptides of interest separate out of the bulk of non-modified peptides in the last series of chromatographic separations (Gevaert et al., 2007).

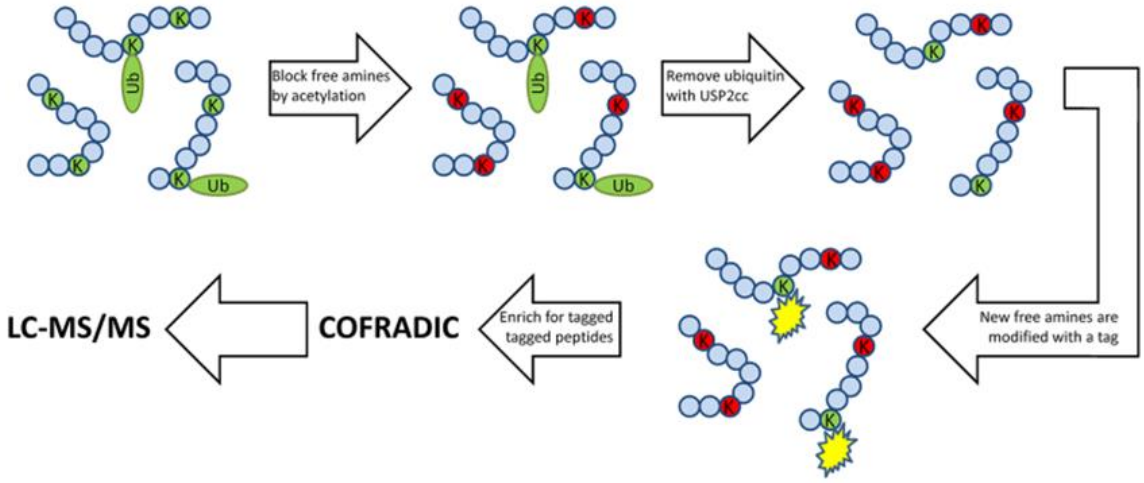

Figure 1: Principle of the method. All primary amino groups are first blocked by acetylation after which ubiquitin is enzymatically removed using USP2cc. As USP2cc cleaves the bond between the C-terminus of ubiquitin and the ε-amino group of the ubiquitinated lysine, it frees the lysine ε-amino group. These are then chemically modified with a Boc-Gly-handle in order to specifically tag the previously ubiquitinated peptides. After tryptic digestion, the peptides are separated by RP-HPLC and 1 min fractions are collected in the 20 to 80 min elution interval. Fractions are pooled (for example, the three fractions highlighted in red), treated for 20 min with 10% TFA, and separated a second time under identical conditions. Peptides undergoing a hydrophilic shift due to Boc-group removal are collected in an interval of 13 min prior to the elution (the interval between -17 and -4 min) of the initial fraction, followed by LC-MS/MS analysis.

Here, we implemented a COFRADIC–based sorting protocol for ubiquitinated peptides. The rationale of the method is shown in Fig. 1 and explained as follows. To allow for a reaction that specifically alters ubiquitinated peptides in between peptide separations, we reasoned that the ubiquitinated amino acids needed to be modified first. Here, after blocking the primary protein amino groups (i.e., primary protein N-termini and ε-amino groups on lysines) by an N-acylation reaction with an N-hydroxysuccinimide (NHS) ester of acetate, and after remaining NHS-acetate is removed by desalting, ubiquitin is cleaved off by the catalytic core domain of the linkage-nonspecific USP2 deubiquitinase (USP2cc). Next, an N-tert-butoxycarbonyl (Boc)-glycine group is introduced onto the hence-released ε-amino groups of the de-ubiquitinated lysines by using Boc-glycine NHS ester (Boc-Gly-OSu). Boc groups are widely used as protective agents during solid-phase peptide synthesis

(Chandrudu et al., 2013), and can be easily removed under acidic conditions, such as by using trifluoroacetic acid (TFA). Following desalting, protease incubation and RP-HPLC fractionation of the resulting peptide mixture, TFA treatment of Boc-Gly-linked peptides will thus cause a hydrophilic shift when the peptides are re-separated in another series of chromatographic runs (Fig. 1). Subsequently, these peptides are collected for further LC-MS/MS analysis.

2.1. Acetylated ubiquitin is recognized and removed by USP2cc

Several steps of the COFRADIC protocol needed to be optimized. Of importance is that USP2cc must still recognize acetylated ubiquitin chains and cleave these efficiently from proteins.

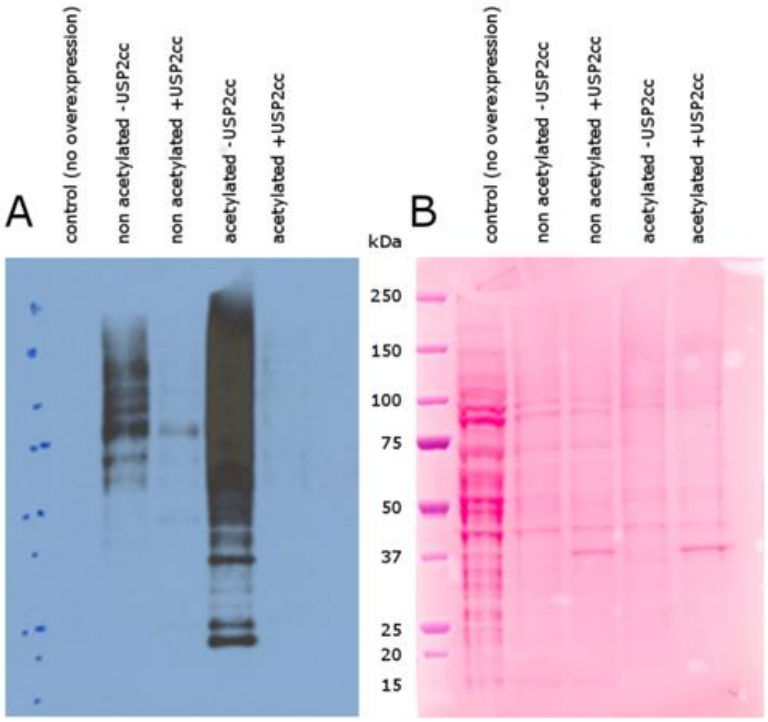

Figure 2: USP2cc efficiently hydrolyses ubiquitin from N-acetylated proteins. Western blot developed with anti-HA antibodies (*A*) and Ponceau S staining of blotted proteins (*B*) of non-acetylated and N-acetylated Jurkat proteins, treated or not with USP2cc. Clearly, this enzyme removes ubiquitin as efficient from the lysines of non-acetylated as well as from N-acetylated proteins.

We therefore first tested the activity of USP2cc on an acetylated proteome of HEKT293 cells overexpressing HA-tagged ubiquitin. Following overnight incubation at 37°C with USP2cc, proteome samples were separated by SDS-PAGE and Western blots were probed with anti-HA antibodies. This showed that N-acetylated and ubiquitinated proteins are as efficient substrates of USP2cc as compared to the native ubiquitinated proteome (Fig. 2). Note that the Western blot profiles of the acetylated and non-acetylated proteins are different, both in terms of the overall pattern and the intensities of the recognized bands, which might be due to the increase in a protein's molecular weight and/or less

efficient SDS binding upon N-acetylation, and higher affinity epitopes created by N-acetylation, respectively.

2.2. Using TFA for Boc group removal as a sorting tool for the COFRADIC based isolation of Boc-Gly-modified peptides

We then optimized the hydrophilic shift evoked by the sorting step, i.e., the TFA-based hydrolysis of the Boc group, on a synthetic peptide, Ac.AEVDYKNR.OH of which the Ɛ-amino group of the internal lysine residue was acylated following a reaction with Boc-Gly-OSu.

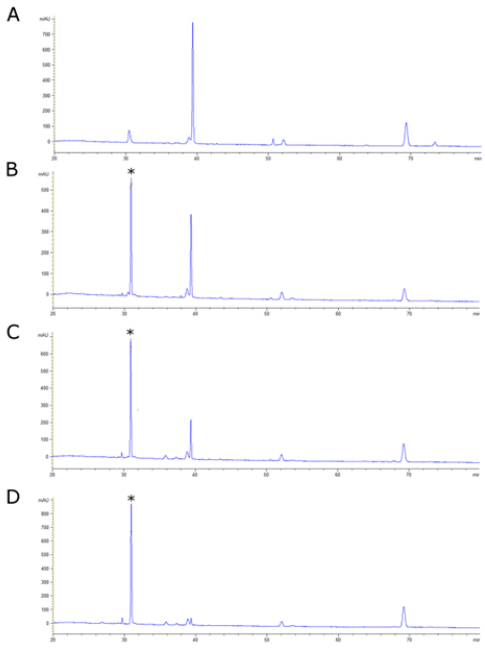

Figure 3: Optimization of the column retention shift with the synthetic peptide Ac.AEVDYKNR.OH. *A*, The lysine in peptide Ac.AEVDYKNR.OH was acylated with Boc-Gly-OSu and next separated on a reverse-phase column (UV absorbance at 214 nm is shown). After 20 min incubation with (*B*) 5% TFA; (*C*) 10% TFA; and (*D*) 20% TFA, the peptide undergoes a hydrophilic shift of about 9 min. The shifted peaks representing peptides that lost the Boc-group are indicated with *. *mAU*, milliabsorbance units.

Upon loss of the Boc group, the peptide elutes earlier because of a decrease in hydrophobicity and hence shifts out of the original interval. While 5% and 10% TFA resulted in a part of the peptide undergoing a hydrophilic shift (Fig. 3B and 3C), treatment with 20% TFA for 20 min was needed to ensure a complete removal of the Boc group (Fig. 3D).

2.3. The ubiquitinome of human Jurkat cells

We then applied our methodology on human Jurkat T cells, not treated with any proteasome inhibitor whatsoever, to screen for endogenous ubiquitinated lysines. Starting with about 4 mg of protein material, we generated 878,064 MS/MS spectra, of which 67,765 or 7.7% were identified by MaxQuant. Overall, this resulted in the identification of 17,299 unique peptides and 4,994 unique

proteins. In total, 7,504 of the peptides carried a Lys-Ɛ-Gly modification, thus originating from proteins that were ubiquitinated *in vivo*, while non-Lys-Ɛ-Gly peptides made up 57% of the total number of all identified peptides. The Lys-Ɛ-Gly peptides could be assigned to 3,338 different proteins (for a complete list of the identified ubiquitinated peptides and proteins see Supplemental Table S1).

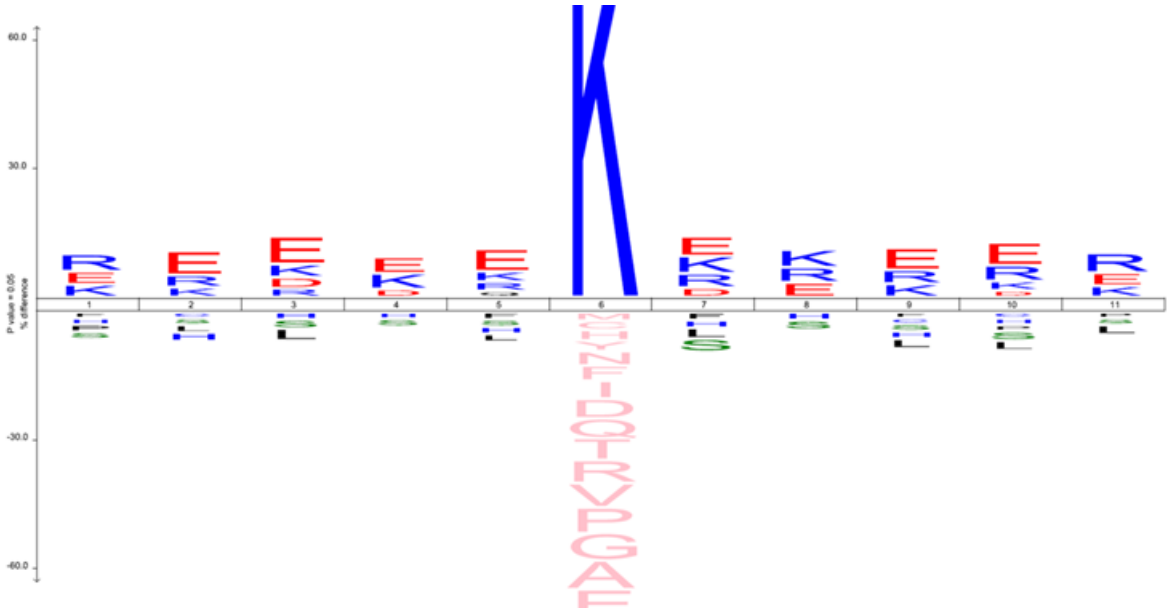

Figure 4: Sequence analysis of ubiquitin sites. The amino acid frequencies at every site of the 7,517 unique Lys-Ɛ-Gly peptides identified in this study are plotted. Only residues that are statistically over-represented (*upper part* of the iceLogo) or under-represented (*lower part* of the iceLogo) at a 95% confidence level are depicted.

We further aligned the general amino acid conservation of the ubiquitin site environments with the modified lysine residue as anchor point and the resulting iceLogo (Colaert et al., 2009) is shown in Figure 4. In accordance with previous reports (Carrano and Bennett, 2013; Sylvestersen et al., 2013; Xu et al., 2010a), no clear sequence motif for ubiquitination could be discerned. However, we noticed a subtle preference for acidic amino acids, surrounding the ubiquitinated lysines, which was also noted in the large-scale ubiquitination study by Kim and colleagues (Kim et al., 2011). In addition to the lysine ubiquitination, some proteins can undergo N-terminal ubiquitin conjugation (Ciechanover and Ben-Saadon, 2004). In contrast to the antibodies raised against ubiquitin remnants specifically on lysine residues, our COFRADIC method allows mapping these sites, and we found 9 protein N-termini carrying a Gly modification (Supplemental Table S2).

Finally, we repeated the COFRADIC experiment as described above, however omitting the USP2cc treatment of the proteins. This control test allowed us to check the extent of protein acetylation during the first step of the protocol, and to examine the specificity of the method. The acetylation occurred on 95 % of the lysines, indicating the chemical modification needed to firstly block the free amino groups is almost complete. However, the small number of unmodified lysine residues can result in incorrect ubiquitination site identifications. Indeed, 502 Lys-Ɛ-Gly peptides

could be identified in this experimental set-up, demonstrating an acceptable false positive value of 6.7 % on the peptide level.

3. Conclusions

One of the challenges for proteomics is the detection of protein modifications. Although protein modifications are generally thought to play important cellular roles, most of them are only present in small numbers. To detect such low levels of modified proteins or peptides, a sample often needs to be selectively enriched for these. The COFRADIC technology here described provides an unbiased and effective strategy to enrich for ubiquitinated peptides and precisely map the modified site. It identified 7,504 ubiquitinated lysines on 3,338 proteins and 9 ubiquitinated protein N-termini from human Jurkat T-lymphocytes, thus establishing a large dataset of endogenous protein ubiquitination sites. We achieved an enrichment of ubiquitinated peptides of 43%, which is higher than or comparable to the degree of enrichment reported in studies using overexpressed HA-ubiquitin (Danielsen et al., 2011) and the antibodies against ubiquitin remnants (Udeshi et al., 2013a), respectively.

This method requires no overexpression or tags, hence avoiding lengthy cloning procedures and, more importantly, it thus allows the investigation of endogenous levels of protein ubiquitination. In this context, we opted not to use proteasome inhibitors in this work. Although proteasome inhibitors, like MG-132, are reported to increase the numbers of potentially detected ubiquitin sites up to four-fold (Carrano and Bennett, 2013) and are hence used in most analyses of the ubiquitin-modified proteome (Kim et al., 2011; Sarraf et al., 2013; Udeshi et al., 2012; Udeshi et al., 2013b; Wagner et al., 2011), they are known to cause proteotoxic stress in living cells (Carrano and Bennett, 2013; Kim et al., 2011).

Moreover, in contrast to enrichment strategies using antibodies against diGly (Sylvestersen et al., 2013; Wagner et al., 2012), our technology is not biased toward a particular sequence surrounding the ubiquitinated lysine as we select for ubiquitin sites based on recognition and cleavage by USP2cc. This catalytic core domain of the deubiquitinating enzyme USP2 strips ubiquitin moieties from all ubiquitin-conjugated proteins, including linear or branched chains (Kim et al., 2011; Renatus et al., 2006; Ryu et al., 2006). The lack of a strong enrichment for any particular sequence motif within our data further suggests that no clear consensus sequence for lysine ubiquitination exists. This might also be explained by the fact that, rather than a linear consensus motif such as in the case of SUMOylation, ubiquitination site determination may depend more on properties, such as protein disorder, structure, accessibility.

It is of note that our COFRADIC method is also suited for quantitative ubiquitination studies as it can easily be combined with stable isotopic labeling. Furthermore, the greatest flexibility of this technique lies in use of the USP2cc enzyme. By replacing this linkage-nonspecific deubiquitinase by an enzyme specific for ubiquitin-like modifiers or for a certain linkage-type of ubiquitin, the peptides

of interest can be isolated. For example, it is appealing to consider incorporating deSUMOylases (Shin et al., 2012) in the COFRADIC procedure to enrich for SUMOylated peptides, or, alternatively, linkage-specific deubiquitinases (Mevissen et al., 2013) to target specific linkage types of ubiquitin. To our knowledge, techniques to study specifically these types of protein modifications are rare, paving the way for new varieties of the presented COFRADIC protocol.

4. Material and Methods

USP2cc modification of N-acetylated proteins

HEKT293 cells (5 x 10^6 cells) overexpressing HA-tagged ubiquitin (Plasmid 18712 encoding HA-tagged Ubiquitin (Gene ID: 7314) from Addgene, Cambridge, MA, USA) were lysed with a lysis buffer containing 50 mM phosphate buffer (pH 8), 150 mM NaCl, 1 mM DTT and 8 M urea to prevent endogenous deubiquitinase (DUB) activity. The sample was then diluted two-fold with 50 mM phosphate buffer (pH 8) to reduce the urea concentration to 4 M, protein concentration was measured, and proteins were acetylated with NHS-acetate (final concentration of 40 mM) for 2 h at 30°C. The remaining non-reacted NHS-esters were quenched by the addition of glycine (final concentration of 80 mM), and after desalting over a Pierce desalting column (Thermo Scientific, Waltham, MA, USA) the sample was treated with USP2cc (Enzo Life Sciences, Antwerp, Belgium) in an enzyme-to-substrate ratio of 1:100 (w:w). Following overnight incubation at 37°C, the samples were separated using 4−12% SDS-PAGE precast gels (Biorad, Hercules, CA, USA) at 150 V and Western blots were probed with anti-HA antibodies (rat monoclonal antibody 11867423001; Roche, Basel, Switzerland).

Evaluation of the differences in chromatographic properties using a synthetic peptide

The peptide Ac.AEVDYKNR.OH was in-house synthesized by Fmoc (*N*-(9-fluorenyl)methoxycarbonyl) chemistry on a 433A peptide synthesizer (Applied Biosystems, Framingham, MA, USA). The Ɛ-amino group of the lysine residue was acylated via reaction with an NHS ester of N-tert-butoxycarbonyl (Boc)-glycine (Boc-Gly-OSu; Sigma-Aldrich, Missouri, USA), which was added in a 150-fold molar excess over the peptide to ensure complete modification. Such acylated peptides were then treated with different concentrations of TFA for 20 min, and removal of the Boc group was monitored following RP-HPLC separation (Staes et al., 2011) of 1 nmol of peptide. This was done via injection onto a capillary RP-HPLC column (2.1 mm internal diameter (I.D.) × 150 mm (length) 300SB-C18 column, Zorbax (Agilent, Waldbronn, Germany)) using an Agilent 1100 Series HPLC system. A linear gradient from 100% HPLC solvent A (10 mM ammonium acetate in water/acetonitrile, 98/2 (v/v)) to 100% solvent B (10 mM ammonium acetate in water/acetonitrile, 30/70 (v/v)) was applied over 100 min, at a flow rate of 80 µl /min.

Enrichment of ubiquitinated peptides from a Jurkat cell lysate by COFRADIC

Human Jurkat T cells (30 x 10^6 cells) were lysed with cell lysis buffer containing 50 mM sodium phosphate buffer (pH 8), 100 mM NaCl, 0.8 % (wt/vol) CHAPS and the appropriate amount of the complete protease inhibitor mixture (Roche, Basel, Switzerland). Guanidinium hydrochloride (f.c. of 4M) was added to a total of 4 mg of protein material. Alkylation of cysteines was carried out by adding a combination of tris(carboxyethyl)phosphine (TCEP, Pierce, Rockford, IL) and iodoacetamide (Sigma-Aldrich) to final concentrations of 15 mM and 30 mM respectively, and reaction was allowed for 15 min at 30°C. Samples were desalted on a PD-10 column (GE Healthcare, Uppsala, Sweden) and eluted with 2 M guanidinium hydrochloride in 50 mM sodium phosphate buffer (pH 8). Next, the sample was N-acetylated and then de-ubiquitinated overnight with USP2cc as described above. Subsequently, samples were incubated in 40 mM Boc-Gly-OSu for 2 h at 30°C. The reaction was stopped by adding glycine (final concentration of 80 mM) and possible O-acylation was reversed by hydroxylamine treatment for 20 minutes (final concentration of 320 mM). Next, the sample was purified over a PD-10 column (GE Healthcare, Uppsala, Sweden) and eluted in 10 mM ammonium bicarbonate buffer, pH 7.6. Prior to digestion, the protein concentration was measured using the Bio-Rad Protein Assay. The protein mixture was overnight digested at 37°C with trypsin (sequencing-grade modified trypsin, Promega, Madison, WI, USA) at an enzyme-to-substrate ratio of 1:50 (w:w). The resulting peptide mixture was vacuum-dried and re-dissolved in 100 µl 10 mM ammonium acetate (pH 5.5) in 2% acetonitrile, followed by oxidation by H_2O_2 at a final concentration of 0.5% (v/v) to uniformly convert methionine into its sulfoxide derivatives (Staes et al., 2008). The peptides were fractionated a first time by RP-HPLC with a linear water/acetonitrile gradient in 10 mM ammonium acetate as described previously (Staes et al., 2011). Fractions of 1 min were collected from 20 to 80 min after sample injection, and fractions eluting 20 min apart were pooled and vacuum-dried. Subsequently, the Boc group was removed by incubating peptides in 50 µl 10% TFA for 20 min, after which the samples were vacuum-dried and re-dissolved in 10 mM ammonium acetate pH 5.5. Next, these 20 samples were re-separated on the same RP column using the same gradient as during the first peptide separation. Peptides that lost a Boc group were collected in 6 fractions during an interval ranging from 4 to 17 min before the collection interval of each initial peptide fraction. This resulted in 18 collected fractions per secondary run and 360 fractions in total.

LC-MS/MS analysis and peptide identification

To reduce LC-MS/MS analysis time, peptide fractions eluting 15 min apart were pooled, dried and re-dissolved in 15 µl of 2% acetonitrile with 0.1% TFA. In total, 60 samples were analyzed via LC−MS/MS on an Ultimate 3000 RSLC nano LC (Thermo Fisher Scientific, Bremen, Germany) in-line connected to a Q Exactive mass spectrometer (Thermo Fisher Scientific, Bremen, Germany). The sample mixture was first loaded on a trapping column (made in-house, 100 µm internal diameter (I.D.) × 20 mm, 5 µm beads C18 Reprosil-HD, Dr. Maisch, Ammerbuch-Entringen, Germany). After

flushing from the trapping column, the sample was loaded on an analytical column (made in-house, 75 µm I.D. × 150 mm, 3 µm beads C18 Reprosil-HD, Dr. Maisch). Peptides were loaded with loading solvent (0.1% TFA in water) and separated with a linear gradient from 98% solvent A' (0.1% formic acid in water) to 55% solvent B′ (0.1% formic acid in water/acetonitrile, 20/80 (v/v)) in 30 min at a flow rate of 300 nL/min. This is followed by a 5 min wash reaching 99% solvent B'.

The mass spectrometer was operated in data-dependent, positive ionization mode, automatically switching between MS and MS/MS acquisition for the 10 most abundant peaks in a given MS spectrum.

The source voltage was 3.4 kV, and the capillary temperature was 275°C. One MS1 scan (m/z 400−2,000, AGC target 3×10^6 ions, maximum ion injection time 80 ms) acquired at a resolution of 70,000 (at 200 m/z) was followed by up to 10 tandem MS scans (resolution 17,500 at 200 m/z) of the most intense ions fulfilling predefined selection criteria (AGC target 5×10^4 ions , maximum ion injection time 60 ms, isolation window 2 Da, fixed first mass 140 m/z, spectrum data type: centroid, underfill ratio 2%, intensity threshold $1.7xE^4$, exclusion of unassigned, 1, 5-8, >8 charged precursors, peptide match preferred, exclude isotopes on, dynamic exclusion time 20 s). The HCD collision energy was set to 25% Normalized Collision Energy and the polydimethylcyclosiloxane background ion at 445.120025 Da was used for internal calibration (lock mass).

MS/MS spectra were searched against the Swiss-Prot database (taxonomy *Homo sapiens*; 20,264 entries; version of March 2014) with the MaxQuant software(Cox and Mann, 2008; Cox et al., 2011) (version 1.4.0.3), with a precursor mass tolerance set to 20 ppm for the first search (used for nonlinear mass re-calibration) and set to 4.5 ppm for the main search. ArgC was selected as enzyme setting as cleavage after lysine residues is obstructed by acylation of their side chains. Cleavages between arginine-proline residues and up to one missed cleavage were allowed. Methionine oxidation and carbamidomethylation of cysteines were searched as fixed modifications, whereas N-terminal protein acetylation, lysine acetylation, N-terminal pyro-glutamate, Lys-Ɛ-Gly, and Gly on protein N-termini were set as variable modifications. The false discovery rate for peptide, protein and site identification was set to 1%, and the minimum peptide length was set to 7. The minimum score threshold for both modified and unmodified peptides was set to 40.

The total list of identified peptides is available through the ProteomeXchange Consortium via the PRIDE partner repository (http://proteomecentral.proteomexchange.org; dataset identifier PXD000934) (Vizcaino et al., 2009).

Chapter 6: It's time for some "site"-seeing: novel tools to monitor the ubiquitin landscape in Arabidopsis thaliana

Alan Walton,[a,b,c,d,1] Elisabeth Stes,[a,b,c,d,1] Nicolas Cybulski,[a,b] Michiel Van Bel, [a,b] Sabrina Iñigo,[a,b] Astrid Nagels Durand,[a,b] Evy Timmerman,[c,d] Jefri Heyman,[a,b] Laurens Pauwels,[a,b] Lieven De Veylder,[a,b] Alain Goossens,[a,b] Ive De Smet,[a,b] Frederik Coppens,[a,b] Sofie Goormachtig[a,b,2] and Kris Gevaert,[c,d,2,3]

[a]Department of Plant Systems Biology, VIB, 9052 Ghent, Belgium

[b]Department of Plant Biotechnology and Bioinformatics, Ghent University, 9052 Ghent, Belgium

[c]Department of Medical Protein Research, VIB, 9000 Ghent, Belgium

[d]Department of Biochemistry, Ghent University, 9000 Ghent, Belgium

Running title: Ubiquitination profiling in *Arabidopsis*

Footnotes

[1]These authors contributed equally to this work.

[2]These authors contributed equally to this work.

[3]Address correspondence to kris.gevaert@vib-ugent.be

The author responsible for distribution of materials integral to the findings presented in this article in accordance with the policy described in the Instructions for Authors (www.plantcell.org) is: Kris Gevaert (kris.gevaert@vib-ugent.be).

*Research contributions**:** Alan Walton and Elisabeth Stes carried out all of the research in this chapter

This chapter is a modified version of a publication from TPC January 2016

Abstract

In the postgenomic era, it has become increasingly apparent that the one gene – one function model is not sufficiently broad to fully understand the molecular mechanisms at play within a cell. Numerous levels of complexity, such as protein-protein interactions and posttranslational modifications, were shown to be essential in determining the role, localization, and activity of a protein. A frequently studied modification is ubiquitination, the covalent binding of the small protein modifier ubiquitin to a target protein. Its importance in various aspects of plant cellular biology was already underlined by genetic research, but the need to validate ubiquitination of target proteins and to understand the mode of action has led to a call for biochemical studies. Multiple reports provide useful insights into the plant 'ubiquitinome', but most of these studies are carried out at the protein level without comprehensive site identification. Here, we implemented a new technology, ubiquitin combined fractional diagonal chromatography (COFRADIC), for proteome-wide ubiquitination site mapping on *Arabidopsis thaliana* cell cultures. We identified 3,009 sites on 1,607 proteins, thereby greatly increasing the number of known ubiquitination sites in this model plant. Finally, we have designed The Ubiquitination Site tool that provides access to the obtained ubiquitination sites, not only to consult the ubiquitination status of a given protein, but also to conduct intricate experiments aiming to study the roles of specific ubiquitination events. Together with the antibodies recognizing the ubiquitin remnant motif, ubiquitin COFRADIC represents a powerful tool to resolve the ubiquitination maps of numerous cellular processes in plants.

1. The importance of ubiquitin in plants

By affecting activity, structure, complex formation, and subcellular localization of targeted proteins, posttranslational modifications (PTMs) dynamically regulate various cellular processes in plants (Guo et al., 2013; Barneche et al., 2014; Seo and Mas, 2014; Banfield, 2015; Furniss and Spoel, 2015; Polyn et al., 2015). An important PTM, not only in plants, but in all eukaryotes, is the conjugation of the small (~8.5 kDa), highly conserved, and abundant protein ubiquitin to substrates. Ubiquitination most often occurs via the formation of an isopeptidyl bond between the flexible C-terminus of ubiquitin and the ε-amino group of lysine residues of a substrate (Heride et al., 2014). Besides regulation of protein catabolism through targeted degradation by the ubiquitin proteasome system (UPS), ubiquitination can also alter protein activity, localization, and interactions (Hua and Vierstra, 2011). As ubiquitin can form linear or branched chains by means of linkage of ubiquitin moieties to its own N-terminus or internal lysine residues, respectively, a large diversity in ubiquitination types exists, each thought to affect protein fate in a specific manner (Komander and Rape, 2012).

In view of the importance of this PTM in plants, more than 1,500 *Arabidopsis thaliana* genes are predicted to encode components of E3 ligases, proteins responsible for the transfer of ubiquitin to specific targets (Hua and Vierstra., 2011). More specifically, close to 900 F-Box-type E3 ligases are annotated in the *Arabidopsis* genome, which is 10-fold more than in the human genome (Hua et al., 2011). The role of protein ubiquitination by E3 ligases in plants is illustrated by numerous studies, mostly at the single protein level, revealing that this PTM acts in the plant's response to drought stress, temperature tolerance, and coordination of responses to phytohormones, such as auxin, brassinosteroids, and jasmonates (Cui et al., 2012; Cuéllar Pérez and Goossens, 2013; Guseman et al., 2015). E3 ligases are shown to be essential regulators in plant immunity and many microbes even seem to have evolved a way to sabotage the host UPS (Marino et al., 2012). Whereas a growing body of research supports the importance of ubiquitination in plants, a full grasp of the significance and the variety of roles played by this PTM can only be reached via comprehensive mapping of the ubiquitinome.

2. The state of the art of ubiquitin profiling

2.1. Trapping ubiquitinated proteins in plants

Various strategies were developed to gain a proteome-wide insight into ubiquitination processes in plants. Pioneering studies relied on single step purification approaches based on affinity matrices, such as ubiquitin-associated domains, ubiquitin interaction motifs, and monoclonal anti-ubiquitin antibodies, to enrich for ubiquitin conjugates at the protein level (Maor et al., 2007; Manzano

et al., 2008, Igawa et al., 2009). In the most successful case, almost 300 potentially ubiquitinated proteins could be identified in *Arabidopsis* (Maor et al., 2007). Although these studies represented a major leap for the field at the time, the non-denaturing conditions used were cause for concern. A large number of false positives is potentially generated as it is difficult to distinguish between ubiquitinated proteins and aspecific proteins, such as co-purified interaction partners and proteins that aspecifically bound the affinity matrix (Fig. 1).

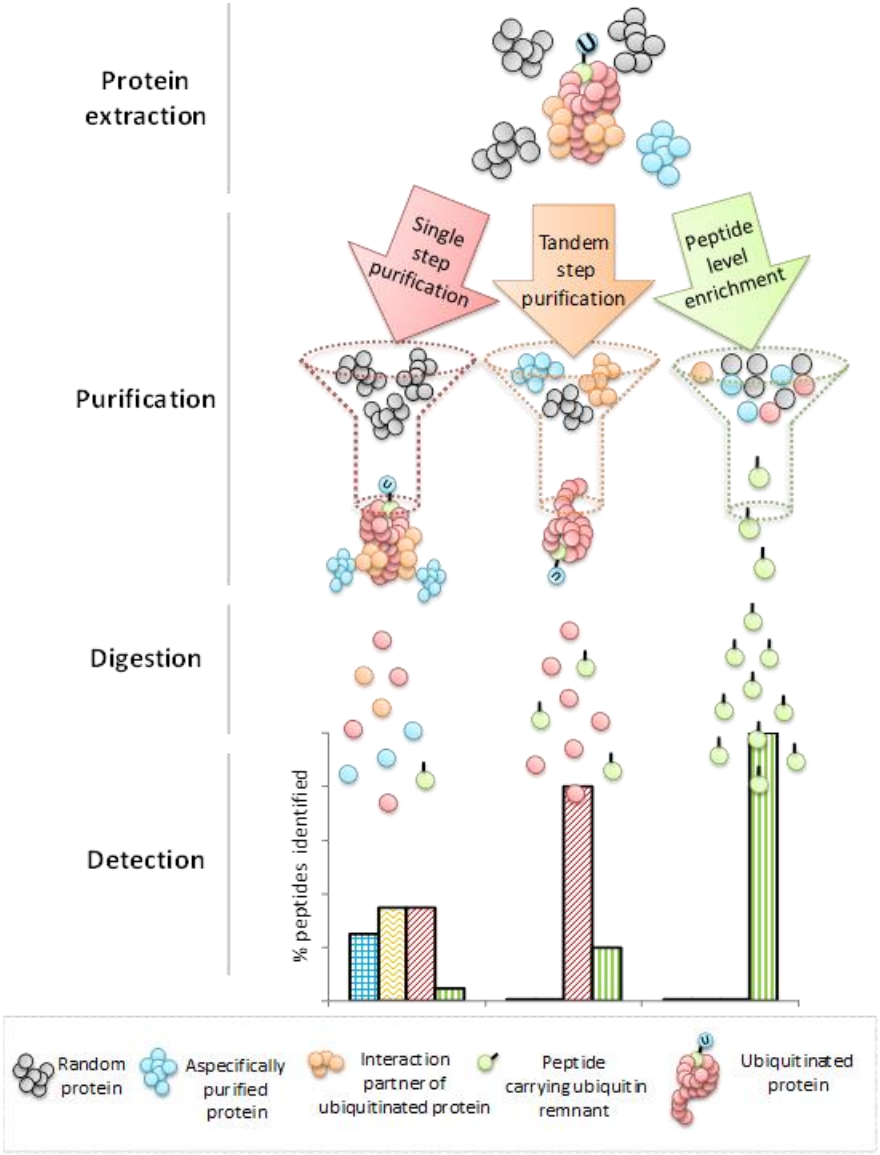

Figure 1. Theoretical comparison of the peptides identified via different techniques for ubiquitin profiling in plants. Comparison between single-step purification, TAP approaches, and techniques based on enrichment at the peptide level. The peptide types that will eventually be injected into the mass spectrometer for detection are illustrated.

To reduce this experimental bias, Saracco and colleagues (2009) created an *Arabidopsis* line that over-expresses a His-tagged variant of ubiquitin, which was combined with a newly developed tandem affinity purification (TAP) protocol. The initial enrichment step of ubiquitin conjugates based

on the ubiquitin-binding region from human HHR23A (USU) could now be followed by nickel-chelate affinity chromatography under strong denaturing conditions, hereby reducing the background. As a result, 90 possible ubiquitinated proteins were identified. Due to the extra level of stringency associated with this improved experimental setup, the reduced number of identified proteins is largely compensated for by the increased reliability due to the reduced number of false positives. More recently, the same transgenic line was used in a more sensitive two-step affinity approach, by means of tandem ubiquitin-binding entities (TUBEs) as affinity matrices during the first purification step (Kim et al., 2013). The timely transfer of the TUBE technology, previously established in the mammalian research field, to plant protocols allowed the identification of 950 proteins (Vierstra, 2014). Addition of the proteasomal inhibitor MG132 revealed that the ubiquitination state of more than half of the identified ubiquitinated proteins increased upon treatment, pointing toward the probable proteasomal degradation of these ubiquitination targets. In another TAP approach, *Arabidopsis* leaves were exposed to the more specific proteasomal inhibitor syringolin (Svozil et al., 2014), hereby bypassing the broad range of action attributed to MG132 that does not solely target the 26S proteasome (Gu et al., 2010).

2.2. Are We Being Short-'Sited'?

The most reliable manner to discern proteins that are truly ubiquitinated from false positives is by identification of the exact ubiquitination site on the target protein, which, additionally, provides opportunities to investigate its functionality. For instance, site-directed mutagenesis of the respective lysine residues can reveal the role of a given ubiquitination event. Table 1 summarizes the results of studies in plants, in which ubiquitination sites had been examined for specific proteins.

With affinity-based methods, in which the enrichment occurs at the protein level, it is not straightforward to reach a comprehensive proteome-wide view of the exact ubiquitination sites. Nevertheless, it is possible to identify a relatively low number of such sites by searching spectra for the typical K-ε-GG motif that remains upon tryptic cleavage of ubiquitinated proteins. Maor and colleagues (2007) identified 85 of these diglycine footprints on 56 proteins, representing the earliest report on precise protein ubiquitination sites in plants. Subsequently, by means of similar approaches, more exact sites have been identified in *Arabidopsis* (summarized in Table 1). The modest number of identified ubiquitination sites so far is due to the low stoichiometry of the site-modified peptides in relation to all other, unmodified peptides, resulting from digestion of the ubiquitinated proteins. Indeed, one of the main limiting factors in all mass spectrometry-based experiments aiming to profile PTMs is the time needed by the instrument to detect modified peptides in complex mixtures. Even in the case of a very successful purification that retains only ubiquitinated proteins, the largest part of the resulting peptides supplied to the instrument will be unmodified. These peptides will monopolize the instrument's acquisition time, leaving little chance for the identification of the more interesting, but

less abundant, ubiquitination site-carrying peptides. To achieve the goal of comprehensive site mapping, it is imperative to operate at the peptide level by specific enrichment for ubiquitinated peptides and not simply ubiquitin conjugates (Fig. 1).

In the biomedical field, this golden standard has been facilitated by the development of antibodies against the ubiquitin remnant motif K-ε-GG, enabling the specific enrichment of ubiquitination site-carrying peptides. Since then, the number of reported ubiquitination sites has skyrocketed and, nowadays, it is no longer rare to identify >10,000 sites in human cell lines (Kim et al., 2011; Wagner et al., 2011; Udeshi et al 2013). This result is in stark contrast to the total number of approximately 200 sites described in *Arabidopsis*, leaving a gap that needs to be filled in the plant science field (Maor et al., 2007; Manzano et al., 2008; Saracco et al., 2009; Kim et al., 2013) (Table1).

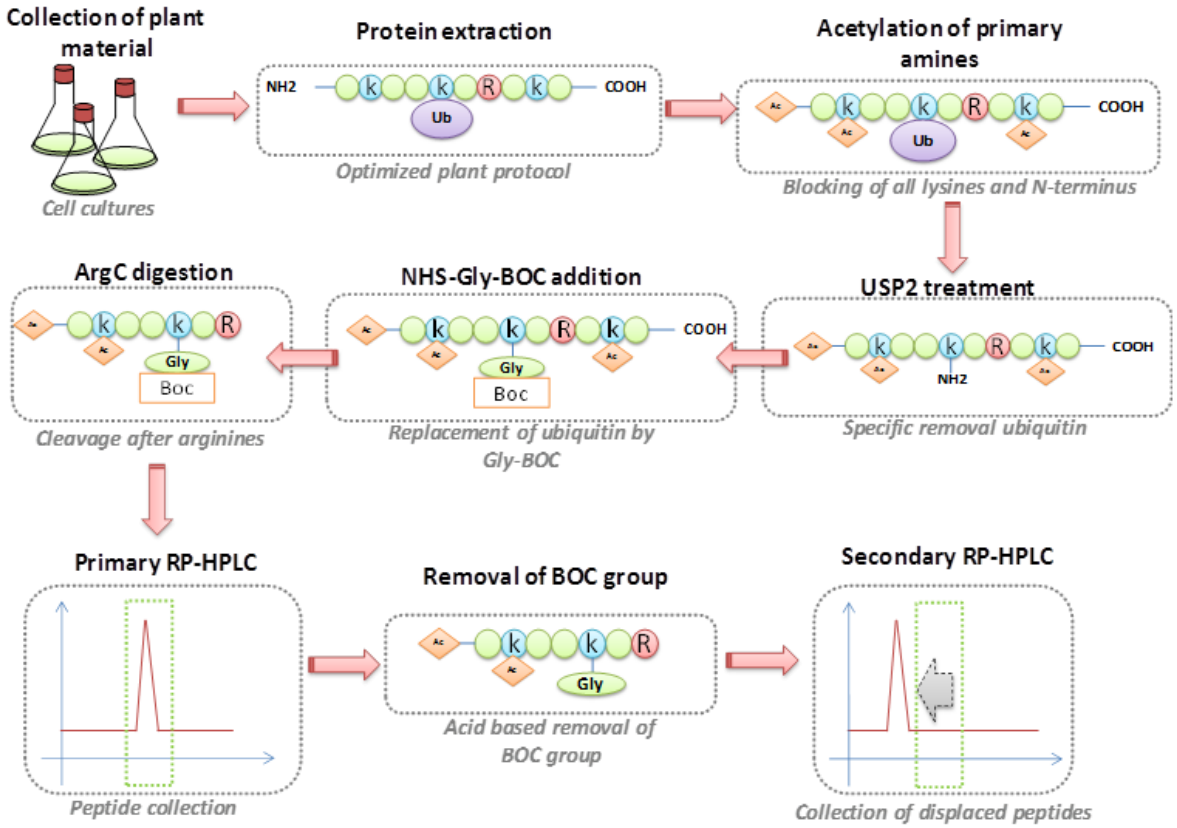

Figure 2. The ubiquitin COFRADIC pipeline.

During ubiquitin COFRADIC, the primary amines of extracted proteins are first chemically acetylated. USP2cc is then used to specifically cleave off the (now acetylated) ubiquitin, revealing a free primary amine on the previously ubiquitinated lysine. A glycine linked to a hydrophobic *tert*-butyloxycarbonyl (BOC) group is linked to this primary amine, followed by a trypsin digest. After a first RP-HPLC run, the peptides are collected and pooled into 20 fractions that are treated with TFA to cleave off the BOC group, after which secondary RP-HPLC runs are conducted. All peaks with a hydrophilic shift are collected and identified by mass spectrometry. This scheme only presents ubiquitination sites on lysines, but the same applies for N-terminally linked ubiquitin.

As a complementary alternative to the K-ε-GG antibodies, the ubiquitin combined fractional diagonal chromatography (COFRADIC) method allows the identification of exact ubiquitination sites, also through enrichment at the peptide level. This technique has been applied to human cell lysates, reporting over 7,000 unique sites (Stes et al., 2014). An overview of this methodology is provided in Figure 2. In short, the protocol starts by blocking all primary amines (lysines and N-termini) via chemical acetylation, followed by incubation with a deubiquitinase (DUB), an enzyme that specifically cleaves ubiquitin from target proteins, thereby freeing primary amines on previously modified residues. To these free primary amines, a chemical handle is attached, which is subsequently used to isolate these peptides via two consecutive reverse-phase—high-performance liquid chromatography (RP-HPLC) runs (Fig. 2).

3. Moving forward: ubiquitination site mapping in plants

3.1. K-ε-GG Antibodies

Since the availability of the K-ε-GG antibodies, two groups have successfully applied them in plants. First, in rice (*Oryza sativa*) leaf tissue, 861 ubiquitination sites were identified on 464 proteins (Xie et al., 2015). Although the commonly accepted 10,000-site benchmark in human cells was not reached, the compatibility of the K-ε-GG antibodies with plant material was proven for the first time. This pioneer study was closely followed by the identification of 1,500 ubiquitination sites in African rice (*Oryza glaberrima*) within a comparative setup (Li et al., 2015). This differential analysis led to the discovery of the role of the Thermo-tolerance 1 protein in heat stress tolerance.

3.2. Ubiquitin COFRADIC

The successful transfer of the TUBE technology and the K-ε-GG antibodies to the plant research field motivated us to apply the ubiquitin COFRADIC technology in *Arabidopsis*. Here, several points of the protocol (Stes et al., 2014) were adapted both to improve the technology and to make it compatible for plants. A more stringent protein extraction protocol, based on a methanol/chloroform precipitation step, allowed us to greatly increase the overall protein yield and also to more rapidly impede endogenous DUB activity.

In respect to compatibility issues, one of our main concerns was the use of the commercially available catalytic core domain of a human DUB, USP2cc, that is used to cleave the isopeptidyl bond between the ubiquitin C-terminus and the ε-amino group of the ubiquitinated residue. The USP2 activity is well documented (Renatus et al, 2006; Shahnawaz et al, 2007; Soboleva and Baker, 2004). Given that UPS2cc specifically recognizes the last five amino acids of ubiquitin (Renatus et al, 2006) and that they are conserved between human and plant ubiquitin (Fig. 3A), we anticipated that USP2cc would be functional on plant proteins.

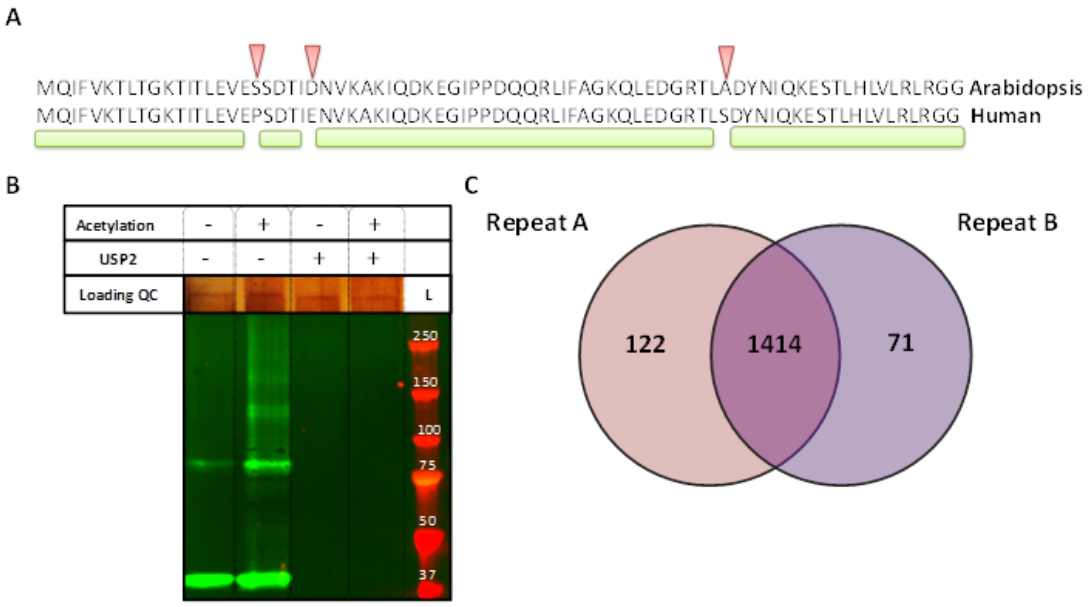

Figure 3. The ubiquitin COFRADIC in plants.

(A) Alignment of the Arabidopsis and human ubiquitin amino acid sequences. Arrowheads indicate mismatches between the two sequences and the green line marks the portions of shared amino acid sequence.

(B) Western blot analysis to test the efficiency of USP2cc to cleave ubiquitin from either acetylated or non-acetylated Arabidopsis proteins. Extracts derived from 35S:HIS6UBQ10 plants were not acetylated (-) or acetylated (+), and subsequently incubated with (+) or without ( ) UPS2cc. Ubiquitinated proteins were detected with the anti-HIS antibodies. Loading quality control (QC) is given by silver staining. L, protein size ladder.

(C) Venn diagram displaying protein overlaps for which at least one ubiquitination site was detected in two replicates of the ubiquitin COFRADIC in Arabidopsis cell cultures.

Moreover, as the first step of the COFRADIC protocol entails a protein N-acetylation step, the USP2cc activity on acetylated plant proteins had to be evaluated as well. To this end, we used protein extracts of seedlings that overexpress *UBIQUITIN 10* (*UBQ10*) that is N-terminally tagged with hexahistidine. Western blot analysis revealed that protein-conjugated ubiquitin, visualized by the anti-hexahistidine antibody, in both the non-acetylated and acetylated protein extracts disappeared after USP2cc treatment (Fig. 3B). This result demonstrated that USP2cc was active on *Arabidopsis* protein extracts, independently of protein acetylation and could, therefore, be used within the COFRADIC approach on *Arabidopsis* proteins.

The COFRADIC experiment was done in two biological replicates, identifying 2,277 and 1,762 ubiquitination sites on 1,536 and 1,485 proteins in the first and second experiment, respectively. In total, 3,009 unique ubiquitination sites were identified and mapped to 1,607 proteins (Supplemental Table 1).

Table 1. Previously reported ubiquitination sites in *Arabidopsis*

Protein	Ubiquitination Sites	Site Identification Technique	Reference
H2B	K143	K-ε-GG footprint via LC-MS/MS	Zhang et al. (2007)
H2B	K143	K-ε-GG footprint via LC-MS/MS	Sridhar et al. (2007)
WRNIP1	Multiple sites	K-ε-GG footprint via LC-MS/MS	Bish and Myers (2007)
IRT1	K146, K171	Site-directed mutagenesis K→R	Kerkeb et al. (2008)
H2A	K121	Site-directed mutagenesis K→R	Bratzel et al. (2010)
CRY2	K541, K554	Site-directed mutagenesis K→R	Zuo et al. (2012)
PIN2	Six sites in hydrophobic loop	Site-directed mutagenesis K→R	Leitner et al. (2012)
COI1	K297	K-ε-GG footprint via LC-MS/MS and site-directed mutagenesis K→A	Yan et al. (2013)
PCNA	K164	Site-directed mutagenesis K→R	Strzalka et al. (2013)
ABI5	K344	Site-directed mutagenesis K→A	Liu and Stone (2013)
SINAL7	K23, K124	Site-directed mutagenesis K→A	Peralta et al. (2013)
GL3	K535, K536	Site-directed mutagenesis K→R	Patra et al. (2013)
EGL3	K493, K495	Site-directed mutagenesis K→R	Patra et al. (2013)
BOR1	K590	Site-directed mutagenesis K→A	Kasai et al. (2014)
PHOT1	K526	K-ε-GG footprint via LC-MS/MS	Deng et al. (2014)
BRI1	K866	Site-directed mutagenesis K→R	Martins et al. (2015)
OLE1-4	Two sites in C terminus	K-ε-GG footprint via LC-MS/MS	Deruyffelaere et al. (2015)
JAZ12	K169	K-ε-GG footprint via LC-MS/MS	Pauwels et al. (2015)
Number of proteins with sites	**Number of reported sites**		
56	85	K-ε-GG footprint via LC-MS/MS	Maor et al. (2007)
15	13	K-ε-GG footprint via LC-MS/MS	Saracco et al. (2009)
109	120	K-ε-GG footprint via LC-MS/MS	Kim et al. (2013)
1,607	3,009	Lys-Gly label via LC-MS/MS	This work

* Three studies that profiled ubiquitinated proteins on a proteome-wide level (Manzano et al., 2008, Igawa et al., 2009, Svozil et al., 2014) were not included because no actual sites had been reported.

Between both biological replicates, an overlap of 87% (Fig. 3C) and 35% was found at the protein and site levels, respectively. Noteworthy, this large number of sites was obtained without proteasomal blockers prior to protein extraction, therefore, most probably providing an unbiased snapshot of the ubiquitinome at endogenous levels in *Arabidopsis* cell cultures.

Several ubiquitination sites were found on various transcription factors belonging to different families, such as the TEOSINTE BRANCHED1/CYCLOIDEA/PROLIFERATING CELL NUCLEAR ANTIGEN FACTOR (TCP), basic Leucine Zipper Domain (bZIP), MYB, WRKY, and basic helix-loop-helix (bHLH) families. For example, we identified ubiquitination sites on TCP8 and

TCP22, class I members of the TCP family regulating cell proliferation and growth (Martin-Trillo and Cubas, 2010), and on the AUXIN RESPONSE FACTOR19 (ARF19), ARF2, ETHYLENE RESPONSIVE TRANSCRIPTION FACTOR113 (ERF113), ERF115, ABSCISIC ACID RESPONSIVE ELEMENTS-BINDING PROTEIN 3 (DPBF3) and ABSCISIC ACID RESPONSIVE ELEMENTS-BINDING FACTOR2 (ABF2), transcription factors involved in auxin, ethylene, brassinosteroids and abscisic acid signal transduction cascades, respectively (Supplemental Table 2). Regulation of cell proliferation and hormonal signaling pathways has been linked extensively to UPS components, with F-box-containing E3 ubiquitin ligases playing central roles (Chapman and Estelle, 2009; Liu and Stone, 2011). Interestingly, ubiquitination sites on enzymes involved in hormone biosynthesis were found as well, such as 12-OXOPHYTODIENOATE REDUCTASE1 (OPR1) and 3-KETO-ACYL-CoA THIOLASE1 (KAT1), two of the three enzymes needed to convert 12-oxo phytodienoic acid into jasmonic acid in the peroxisome (Wasternack et al., 2013).

Ubiquitination sites were also detected on many UPS components, including E1, E2, and many E3 enzymes as well as 26S proteome subunits and deubiquitinating enzymes (Supplemental Table 2). Finally, an ubiquitination site on ubiquitin itself was identified. Of the seven internal lysines, ubiquitination was found only on K48, a branched ubiquitination type known to give rise to proteasomal degradation. The lack of the other linkage types might be due to their relatively reduced stoichiometry (Kim et al., 2013) and to the ArgC-type digestion used, generating relatively larger peptides that, on average, are more difficult to detect than tryptic peptides.

4. GRXS17 as a Proof-of-Concept Protein

An ubiquitination site was detected on a redox enzyme, GLUTAREDOXIN S17 (GRXS17), involved in auxin responses (Cheng et al., 2011). GRXS17 is the *Arabidopsis* ortholog of the human monothiol glutathioredoxin PKCθ-interacting protein (PICOT)/GLRX3, a putative nucleocytoplasmic protein regulating hormone and redox signaling in *Arabidopsis* (Cheng et al., 2011). Although not shown in plants until now, an ubiquitination site in the human GLRX3 has been identified via antibody-based capture of K-ε-GG--containing peptides. To confirm ubiquitination of the plant GRXS17 protein detected with the COFRADIC technique, we applied a technique commonly used in the plant ubiquitin research field. An affinity purification done on *35S:HIS6UBQ10* plants revealed, in agreement with the COFRADIC results, the ubiquitination of GRXS17 in three independent biological replicates. In light of the K48 ubiquitin linkages found in the COFRADIC experiment, possible ubiquitin-mediated proteasomal GRXS17 degradation was tested by recombinant production of a V5-HIS6-tagged protein and incubation with total protein extract derived from wild-type seedlings. The epitope-tagged GRXS17 was degraded over time in seedling extracts, unless the proteasome inhibitor MG132 was added (Fig. 4A). Similarly, the level of epitope-tagged GRXS17 from protein extracts of *35S:GRXS17:3xHA* seedlings decreased over time, an event that could also be prevented by treatment

with MG132 (Fig. 4B). Taken together, our data suggest that the GRXS17 is ubiquitinated and that its ubiquitination leads to proteasomal degradation.

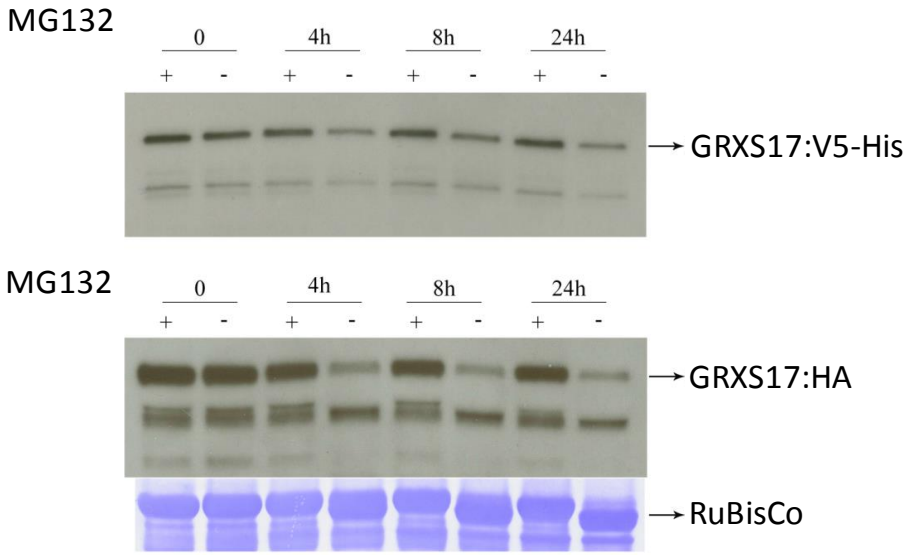

Figure 4. Degradation of GRXS17 by the 26S proteasome.

(A) Cell-free degradation assay. Recombinant protein GRXS17:V5-HIS was incubated with total protein extract prepared from wild-type *Arabidopsis* seedlings in the presence or absence of MG132 for the indicated time.

(B) Total proteins extracted from *35S:GRXS17:HA* seedlings and incubated in the presence or absence of MG132. Samples were harvested at the indicated times. Coomassie Blue-stained ribulose-1,5-bisphosphate carboxylase/oxygenase (RuBisCo) was used as loading control. Proteins were detected with anti-V5 (1/2000) or anti-HA (1/1000) antibodies with their respective horseradish peroxidase (HRP)-conjugated secondary antibody.

5. Sharing is caring

To make our *Arabidopsis* ubiquitination map available to the plant community, we constructed The Ubiquitination Site (http://bioinformatics.psb.ugent.be/webtools/ubiquitin_viewer/), an online database that consolidates the identified ubiquitination sites and serves as a searchable knowledge base. The website with all its functions (Fig. 5) provides the user with a query box in which one or multiple Arabidopsis Genome Initiative locus identifiers can be entered. Ubiquitination sites on corresponding proteins are returned with information concerning the respective splice variant, the modified sequence, the sequence window, as well as the position of the site within the protein. Information on the MaxQuant score and delta score are provided as well. The site is linked to PLAZA (http://plaza.psb.ugent.be/), allowing the user to gain access to more ample information on the protein(s) in question.

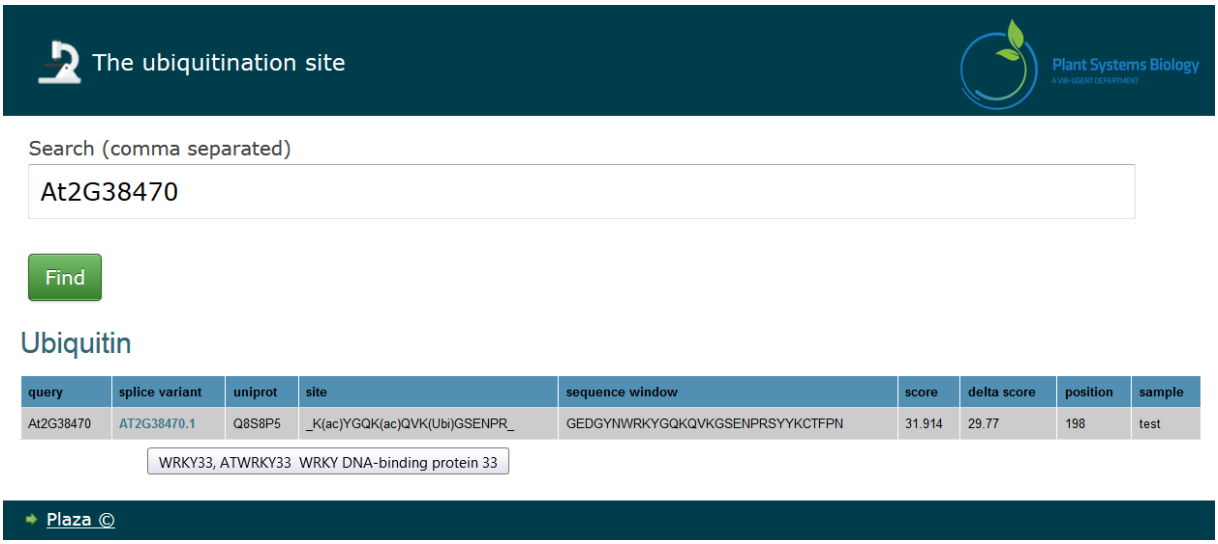

Supplemental Figure 5. The Ubiquitination Site website page.

In a query box, one or multiple AT numbers can be entered, returning the ubiquitination sites on corresponding proteins and information concerning the splice variant, modified sequence, sequence window, and the site position within the protein. The MaxQuant score and delta score are provided as well. Through its link to PLAZA, access can be gained to ample information concerning the protein(s) in question.

6. Outlook

6.1. We are ready for "site"-seeing in plants

With the K-ε-GG antibody-based method and now also the ubiquitin COFRADIC established in plants, two complementary techniques are available for the plant science community to investigate protein ubiquitination at the site level. On the biochemical level, several differences should be considered between both methodologies. For instance, as USP2cc recognizes the last five amino acids of ubiquitin and no other ubiquitin-like proteins harbor this sequence at their C-termini, this DUB is ubiquitin-specific in plants. This is not the case for the K-ε-GG antibodies since the epitope it recognizes is also generated upon tryptic cleavage of other small protein modifiers, such as RUB (Vierstra, 2012). Currently, it is difficult to assess to which extent this ambiguity is problematic, because the degree of rubbylation in plants is unknown, but its functionality has been suggested to supersede that of neddylation, its mammalian PTM counterpart (Hakenjos et al., 2011; Mergner and Schwechheimer, 2014; Mergner et al., 2015).

Different techniques lead to different insights into ubiquitin linkage types. Often, linear or branched ubiquitin chains are formed by conjugating additional ubiquitin moieties to the N-terminus or a lysine residue of the initial ubiquitin. These chains are reported to lead to different fates for the target protein. For example, K48-linked chains commonly trigger degradation by the 26S proteasome and chains linked via K63 play a role in DNA repair (Pickart and Fushman 2004). Hence, the

identification of specific linkage types on the target protein can serve as an important hint for the function of a particular ubiquitination event. Using a TAP approach, Kim and colleagues (2013) could identify several ubiquitination sites on ubiquitin itself, thereby revealing the types of ubiquitin branches present in the sample, together with their relative abundance (Kim et al., 2013). However, in our dataset, only K48 linker chains were retrieved, possibly due to a biochemistry-associated bias. Digestion of acetylated ubiquitin by trypsin (i.e. ArgC digestion type) will generate peptides probably too long or too short to have ideal properties for their identification via mass spectrometry. Although not analyzed in plant ubiquitination studies, the K-ε-GG antibodies should, in principle, not be confronted with this problem and could, therefore, provide a deeper insight into this aspect of ubiquitin biology.

6.2. Ubiquitination beyond lysine residues

Another difference between the antibody-based method and the ubiquitin COFRADIC approach is the manner in which the sites are targeted for enrichment. As the antibodies are raised against the K-ε-GG footprint, exclusively lysine ubiquitination is identified. In contrast, USP2cc recognizes ubiquitin on the target protein, independently of the affected residue, thereby rendering the identification of ubiquitination on other residues theoretically possible. Taking this into account, we searched the spectra for proof of alternative ubiquitination types. One possibility was the ubiquitination on protein N-termini that, so far, has only been described in non-plant species (Bloom et al., 2003; Ciechanover and Ben-Saadon, 2004; Scaglione et al., 2013; Stes et al., 2014; Vittal et al., 2015). We identified 16 proteins (Table 2) that carry ubiquitin on the utmost N-terminal amino acid, including BRASSINAZOLE RESISTANT 1 (BZR1), a key transcription factor involved in control of brassinosteroid-responsive genes (He et al., 2002; Wang et al., 2002). BZR1 is reported to be regulated via various posttranslational regulations, including ubiquitination (Gampala et al., 2007; Wang et al., 2013). Moreover, N-terminal ubiquitination was detected on two ubiquitin-conjugating enzyme variants (UEVs), i.e., proteins related to ubiquitin-conjugating (E2) enzymes, but lacking a catalytic cysteine. UEVs act in a heterodimeric complex together with the UBIQUITIN CONJUGATING ENZYME E2 35 (UBC35) or UBC36 to trigger K63-mediated ubiquitination (Tatham et al 2013). Remarkably, the human Ubc13-UEV1 complex was shown to mediate K63 ubiquitination of one of its target proteins, namely SUMO, only when it is N-terminally ubiquitinated by the E2 ligase Ube2w (Tatham et al 2013). Based on our data, it is tempting to speculate that UEV proteins are themselves regulated by N-terminal ubiquitination. This hypothesis is further supported by the ability of human Ube2w to mediate ubiquitin conjugation to its own N-terminus (Tatham et al., 2013). Together, these results illustrate the power of the ubiquitin COFRADIC as a less biased technique for identification of different ubiquitination types. Nevertheless, for the time being, the protocol allows only detection of ubiquitin sites on lysines and N-terminal residues, due to the currently applied N-acylation steps.

Table 2. N-terminally ubiquitinated proteins present in our dataset

AGI code	Description	Modified peptide sequence
AT1G09330	Golgi apparatus membrane protein ECH	_(Ub)MDPNNQIQAPVENYANPR_
AT1G11240	Uncharacterized protein	_(Ub)TGGIHNEEAGSIATPTSAR_
AT1G68185	Ubiquitin-related protein	_(Ub)GGEGEDLEPLFDYR_
AT1G75080	BRASSINAZOLE-RESISTANT1 (BIN2 SUBSTRATE 2)	_(Ub)TSDGATSTSAAAAAAAAAAAR_
AT1G36310	*S*-adenosyl-L-methionine-dependent methyltransferases superfamily protein	_(Ub)MIIDVIR_
AT2G25830	YebC-related	_(Ub)MASHCSMR_
AT2G17200	Ubiquitin domain-containing protein DSK2b	_(Ub)GGEGDSSQPQSGEGEAVAVNIR_
AT2G36060	Ubiquitin-conjugating enzyme E2 variant 1C (Protein MMS ZWEI HOMOLOG 3)	_(Ub)TIGSGSSVVVPR_
AT3G52560	Ubiquitin-conjugating enzyme E2 variant 1D (Protein MMS ZWEI HOMOLOG 4)	_(Ub)MDDGDDIYMR_
AT3G07230	Wound-responsive-related protein	_(Ub)MIYDVNSGIFR_
AT3G12640	RNA binding (RRM/RBD/RNP motifs) family protein	_(Ub)GSADLVDDR_
AT5G22120	Putative uncharacterized protein	_(Ub)MENTRPNEEEGR_
AT5G27700	40S ribosomal protein S21e	_(Ub)MQNEEGQVTEIYIPR_
AT5G03660	Putative uncharacterized protein	_(Ub)MQPTETSQPAPSDQGR_
AT5G12240	Uncharacterized protein	_(Ub)MDDQEFR_
ATMG00980	Ribosomal protein S12, mitochondrial	_(Ub)PTFNQIIR_

6.3. To be or not to be ubiquitinated

Despite the improved reliability through the use of TAP methods, the estimation of false positive identifications (i.e. the false discovery rate (FDR) intrinsic to the experimental procedure) is currently missing from most plant ubiquitination profiling literature. To reach the standards of the mammalian PTM field, we recommend reporting the FDR in plant ubiquitinome studies, so that the reader can objectively assess the reliability of the methodology and the produced data. In the COFRADIC approach, false positives could arise during the chemical N-acetylation step carried out to block all free amine groups: a low acetylation efficiency could potentially leave free lysines and protein N-termini that later would be falsely detected as ubiquitination sites. Therefore to test the acetylation efficiency, we set up a control experiment in *Arabidopsis* cell cultures, during which the complete COFRADIC protocol was followed, but without the USP2cc step. As a result, only five ubiquitin sites were found, demonstrating the very high N-acetylation efficiency and an FDR < 0.01% confirming our initial results. As such, the previously reported FDR of 6.7% in Jurkat cells is outperformed (Stes et al., 2014), probably due to the newly introduced chloroform/methanol

precipitation step early in the sample preparation process. This may have lead to an increase in the efficiency of amine blocking, thereby resulting in a lower FDR overall.

6.4. Ubiquitination hot spots?

Protein ubiquitination often appears not to be restricted to one lysine residue, but rather to occur in a specific protein region that might be considered as an "ubiquitination hotspot". Hence, multiple lysine-to-arginine mutations need to be considered when the ubiquitination status of a particular protein is studied (Bish and Myers, 2007; Leitner et al., 2012). The "ubiquitination hotspot" hypothesis is supported by our observation that on the protein sequences with more than one detected ubiquitin conjugation site, 33% of these sites could be found within a sequence window of 10 amino acids from each other. Additionally, this observation is also reflected in the high overlap between the two COFRADIC experiments at the protein level (87%), in contrast to the lower overlap at the site level (35%). To fully understand the relative importance of exact sites compared to that of hotspots, a comprehensive mapping of the ubiquitinome in *Arabidopsis* will be necessary. With this issue in mind, it should be underlined that exact site determination remains, until now, the most reliable way of identifying a protein as being ubiquitinated.

7. Conclusion

In contrast to the previous proteome-wide studies that offered insight into the *Arabidopsis* ubiquitinome on the protein level, two novel technologies are now available that enable ubiquitination mapping at the site level: the K-ε-GG antibodies and the ubiquitin COFRADIC. Both approaches greatly increase the ubiquitination profiling resolution in plants, moving toward comprehensive ubiquitin site mapping in a quantitative manner. With a large body of plant research currently focusing on E3 ligases (Ni et al., 2014; Song et al., 2014; Kinoshita et al., 2015), both technologies provide suitable solutions for the identification of their targets by the differential analysis of wild-type and mutant plants. An enhanced knowledge of their substrates will certainly lead to significant advances in the understanding of the biochemical mechanisms and cellular processes governed by protein ubiquitination.

Material and Methods

Ubiquitin COFRADIC

Arabidopsis thaliana (L.) Heynh. (accession Columbia-0) cell suspension cultures (PSB-D) were maintained as described previously (Van Leene et al., 2007) and grown in two biological replicates. After 3 weeks of growth under continuous light, 3 g of fresh weight material was harvested, flash-frozen in liquid nitrogen, and manually ground into a fine powder with pestle and mortar. The material was resuspended in 10 mL of homogenization buffer, containing 290 mM sucrose, 50 mM sodium phosphate buffer (pH 8), and 25 mM EDTA in milliQ water, vigorously agitated for resuspension, and five times sonicated on ice with a 1-cm probe for 10 s to disrupt cell walls. Samples were centrifuged at 4°C for 15 min at 1,500×g to remove debris. Supernatants were collected and a methanol/chloroform precipitation was carried out by addition of 3:1:4 parts of methanol, chloroform, and water. Samples were centrifuged for 10 min at 5,000×g (room temperature). The upper (aqueous) phase was removed and four parts of methanol were added onto the interface and bottom phase remaining in each tube to give rise to a precipitation.

Pellets were washed 3 times with acetone and resuspended in 4 M guanidinium hydrochloride in 50 mM sodium phosphate buffer (pH 8). Ubiquitin COFRADIC was carried out as described previously (Stes et al., 2014). To reduce the liquid chromatography-tandem mass spectrometry (LC−MS/MS) analysis time, peptide fractions eluting 15 min apart were pooled, dried, and redissolved in 15 μL of 2% (v/v) acetonitrile with 0.1% (v/v) trifluoroacetic acid (TFA). In total, 60 samples were analyzed via LC−MS/MS on an Ultimate 3000 RSLC nano LC (Thermo Fisher Scientific) in-line connected to a Q Exactive mass spectrometer (Thermo Fisher Scientific). Settings and machine configurations were as described (Stes et al., 2014). MS/MS spectra were searched with the MAXQUANT Andromeda search engine against The Arabidopsis Information Resource (TAIR10_pep_20101214 containing 27,416 protein-coding genes) database with the MAXQUANT software (version 1.4.0.3); the precursor mass tolerance was set to 20 ppm for the first search (used for nonlinear mass recalibration) and to 4.5 ppm for the main search. ArgC was selected as enzyme setting, because cleavage after lysine residues was obstructed by acylation of their side chains. Cleavages between arginine and proline residues and up to one missed cleavage were allowed. Methionine oxidation and carbamidomethylation of cysteines were searched as fixed modifications, whereas N-terminal protein acetylation, lysine acetylation, N-terminal pyroglutamate, Lys-ε-Gly, and Gly on protein N-termini were set as variable modifications. The FDR for peptide, protein, and site identification was set to 1% and the minimum peptide length to 7. The minimum score threshold for both modified and unmodified peptides was set to 30. All mass spectrometry proteomics data have been deposited to the ProteomeXchange Consortium via the PRIDE partner repository with the PRIDE accession PXD002297.

Generation of HIS6-tagged UBQ10 *Arabidopsis* plants

The UBQ10 genomic open reading frame (ORF) was cloned in two consecutive polymerase chain reaction (PCR) steps. Due to the number of multiple UBQ-encoding genes in *Arabidopsis*, the 5'-TCTGATTTACAGATGCAGATCTTTG-3' forward and 5'-GAAACATTGAACTTCTTAAGCATAAC-3' reverse primers used for the first amplification step included parts of the 5'- and 3'-untranslated regions (UTRs), respectively, to convey specificity to the UBQ10 ORF. A second PCR with the gene-specific 5'-ATGCAGATCTTTGTTAAGACTCTC-3' forward and 5'-TTAAGCATAACAGAGACGAGATTTA-3' reverse primers was used to eliminate the flanking 5'- and 3'-UTR sequences. The UBQ10 ORF was recombined after the HBH TAP-tag42 and inserted into the pKNTAP destination vector, generating an N-terminally tagged UBQ, under control of the constitutive cauliflower mosaic virus 35S promoter by means of the Gateway recombination (Invitrogen). *Arabidopsis* plants were stably transformed with the *Agrobacterium tumefaciens*-mediated floral dip method. Plants were selected by kanamycin resistance.

USP2cc Activity Assay

Plant proteins from cell cultures were extracted as for the affinity enrichment protocol described above. For samples destined for acetylation, NHS-acetate was added to samples in two consecutive steps to reach a final concentration of 40 mM followed by a 2-h incubation at 30°C. Subsequently, 80 mM of glycine was added to quench the residual NHS-acetate. For samples destined for USP2cc treatment, the enzyme was added in a 1/100 (w/w) ratio and samples were incubated overnight at 37°C. For Western blotting, an anti-HIS antibody (RGS-HIS; Qiagen) was used as primary antibody, followed by an anti-mouse fluorophore secondary antibody (800 nm) (LI-COR) and visualized on an Odyssey infrared imaging system (LI-COR). Due to interference of protein acetylation with the antibody activity, a classical loading control could not be used. To overcome this problem, equal loading was assessed with a Silver Stain Kit (Pierce), according to the manufacturer's instructions.

Cell-Free GRXS17 Degradation Assay

Total protein extracts were prepared by resuspending ground tissue (10-day-old wild-type *Arabidopsis* seedlings grown under continuous light at 21ºC) in cold extraction buffer (25 mM Tris-HCl, pH 7.5, 10 mM NaCl, 10 mM $MgCl_2$, 4 mM phenylmethanesulfonyl fluoride, 5 mM dithiothreitol, and 10 mM adenosine triphosphate) at a ratio of 1 g tissue/mL extraction buffer and

centrifuged twice at 12,000×*g* for 15 min. To test the GRXS17 stability, 50 µM MG132 (Boston Biochem) or 1% (v/v) dimethyl sulfoxide as a control was added to the total protein extract. Each reaction was incubated at room temperature and samples were harvested at the indicated time points. To stop the reaction, SDS sample buffer was added, followed by boiling for 10 min before SDS-PAGE. When necessary, 500 ng of *Escherichia coli* recombinant protein GRXS17:V5-HIS was added to the total protein extract just before the incubation at room temperature.

Construction of the Ubiquitination Site Web site

The Web interface was built with Cake PHP (version 2.6.1) and mysql as back-end. The PLAZA platform43 was used as reference for the various possible names and identifiers associated with genes and loci. By means of the PLAZA platform, we could assert that searching for non-canonical identifiers could still occur, of which the results are reported by a JavaScript Object Notation (JSON)-based application programming interface (API).

Supplemental Table 1. Identified ubiquitination sites on transcription factors and UPS members

Type	Entry	AGI code	Description	Modified peptide sequence
Transcription factors				
bZIP				
		AT1G43700	Transcription factor VIP1 (Basic leucine zipper 51) (AtbZIP51)	_GTSELNTENK(Ubi)HLKMR_ _LAELALLDPK(Ubi)R_
		AT3G17609	Transcription factor HY5-like protein HYH (bZip transcription factor AtbZip64)	_KK(Ubi)VYVSDLESR_
		AT5G11260	Transcription factor HY5 (Protein LONG HYPOCOTYL 5)	_VPEFGGEAVGK(Ubi)ETSGR_ _TPAEK(Ubi)ENK(Ubi)R_
MYB				
		AT1G72650	Myb family transcription factor TRFL6	_DSVEK(Ubi)SASR_ _LSEK(Ubi)SEVR_
WRKY				
		AT2G04880	WRKY transcription factor 1 (Transcription factor ZAP1)	_E(Ubi)VMEDGYNWR_ _KK(Ubi)GGNIELSPVER_ _SDVFTAVSKEK(Ubi)TSGSSVQTLR_
		AT4G26640	WRKY20	_KYGQK(Ubi)VVR_
		AT4G22070	WRKY31	_NSSQDHLLAQESK(Ubi)AEGR_
		AT4G30935	WRKY32	_DEEK(Ubi)SLGADMEDLHDETVR_ _ETLGK(Ubi)DQVQGVR_ _K(Ubi)TSFSPR_
		AT2G38470	WRKY33	_KYGQKQVK(Ubi)GSENPR_
		AT3G01970	WRKY45	_LTEFHGVDNSAQPTTSSEEK(Ubi)PR_

	AT5G49520	WRKY48	_SDTINTQTNEENK(Ubi)K_
bHLH			
	AT4G36930	Transcription factor SPATULA (SPT) (Basic helix-loop-helix protein 24)	_AAEVHNLSEK(Ubi)R_
	AT4G02590	Transcription factor UNE12 (Basic helix-loop-helix protein 59, bHLH 59)	_ALQELVPTVNK(Ubi)TDR_
TCP			
	AT1G58100	TCP8	_STPPEDSTLATTSSTATATTTK(Ubi)R_ _SVDLSK(Ubi)ENDDR_
	AT1G72010	TCP22	_EDYFK(ac)EPSSAAEPSESSQK(Ubi)AS
Linked to hormones			
ABA			
	AT1G45249	Abscisic acid responsive elements-binding factor 2 ABF2	_KSGTVEK(Ubi)VVER_
	AT3G56850	ABSCISIC ACID-INSENSITIVE 5-like protein 2 DPBF3 (ABA-responsive element-binding protein 3)	_VASGEVVEK(Ubi)TVER_
Auxin			
	AT1G19220	Auxin response factor 19 ARF19 (Auxin-responsive protein IAA22)	_TYTKVQK(Ubi)R_
	AT5G62000	Auxin response factor 2 ARF2 (ARF1-binding protein, ARF1-BP)	_ASSEVSMK(Ubi)GNR_
Ethylene			
	AT5G13330	Ethylene-responsive transcription factor ERF113	_DPKK(Ubi)AAR_ _EEEEK(Ubi)NYGYNYYNYPR_
Brassinosteroids			
	AT5G07310	Ethylene-responsive transcription factor ERF115	_ANSGNYGK(Ubi)R_
Ubiquitin conjugation			
E1			
	AT5G06460	Ubiquitin-activating enzyme E1 2 UBA2	_LEDVNSK(Ubi)LLR_
E2			
	AT5G50870	Ubiquitin-conjugating enzyme E2 27 UBC27 (Ubiquitin carrier protein 27)	_VCPK(Ubi)SDNLTR_
	AT1G70660	Ubiquitin-conjugating enzyme E2 variant 1B UEV1B (Ubc enzyme variant 1B)	_GSEEEK(Ubi)VVVPR_
	AT2G36060	Ubiquitin-conjugating enzyme E2 variant 1C UEV1C (Ubc enzyme variant 1C)	_GEK(Ubi)GIGDGTVSYGMDDGDDIYM _K(Ubi)LVQPPEGTFF_
E3			
UBOX			
	AT1G01680	U-box domain-containing protein 54 PUB54	_KETIEK(Ubi)SKSNESDEDPR_ _KETIEK(Ubi)SKSNESDEDPR_
	AT5G05230	U-box domain-containing protein 62 PUB62	_VGEQDPK(Ubi)TR_

ASK			
	AT2G45950	SKP1-like protein 20 ASK20	_IIEGK(Ubi)NPEEIR_ _LK(Ubi)NVEVEEHVDER_
	AT3G61415	SKP1-like protein 21 ASK21	_IIEGK(Ubi)TPEEIR_
	AT1G20140	SKP1-like protein 4 ASK4	_GK(Ubi)TPEQMR_
F-box			
	AT2G16365	F-box protein	_K(Ubi)NESSAETNTLEMDR_ _LQSLESSK(Ubi)DTQEDGPR_
	At1g47765	Putative F-box protein	_FELK(Ubi)EIADDQAR_
	AT4G39756	Putative F-box/kelch-repeat protein	_DIK(Ubi)GLATLNR_
26S			
	AT5G43010	26S protease regulatory subunit 10B homolog A RPT4A	_K(Ubi)IEIPLPNEQSR_ _SKVDKEK(Ubi)LTSGTR_
	AT3G05530	26S protease regulatory subunit 6A homolog A RPT5A	_K(Ubi)IEFPHPTEEAR_
	AT1G53750	26S protease regulatory subunit 7 homolog A RPT1A	_DIEDEIRDEK(Ubi)NPR_
	AT5G64760	26S proteasome non-ATPase regulatory subunit 12 homolog B RPN5B	_LLNEEK(Ubi)QMR_
	AT4G29040	26S proteasome regulatory subunit 4 homolog A RPT2A	_LKPQEEK(Ubi)AEEDR_
Deubiquitinating enzymes			
	AT3G11910	Ubiquitin carboxyl-terminal hydrolase 13 UBP13	_AEEIPEEEK(Ubi)NIGPNDR_
	AT1G51710	Ubiquitin carboxyl-terminal hydrolase 6 UBP6	_KK(Ubi)LEAPR_
	AT4G17510	Ubiquitin carboxyl-terminal hydrolase UCH3	_ATASESSSSK(Ubi)R_

Chapter 7: Work in progress: ubiquitin COFRADIC detects differential ubiquitination of Arabidopsis proteins upon GR24 treatment

Alan Walton[a,b,c,d], Elisabeth Stes[a,b,c,d], Carolien De Cuyper[a,b], Kris Gevaert[c,d] and Sofie Goormachtig[a,b]

[a]Department of Plant Systems Biology, VIB, 9052 Ghent, Belgium

[b]Department of Plant Biotechnology and Bioinformatics, Ghent University, 9052 Ghent, Belgium

[c]Medical Biotechnology Center, VIB, 9000 Ghent, Belgium

[d]Department of Biochemistry, Ghent University, 9000 Ghent, Belgium

*Research contributions**:** Alan Walton carried out all research in this chapter, with the exception of the initial qPCR of *BRC1* that was performed by Carolien De Cuyper.

Abstract

We here assess the potential of ubiquitin COFRADIC to become a tool for the identification of proteins targeted by E3 ligases in plants. In our study, we apply this technique on proteins from Arabidopsis cell cultures grown in the presence or absence of the synthetic strigolactone analog, GR24, known to induce the ubiquitination of members of the SMXL family. We mapped a total of 9,215 sites on 4,908 proteins and identified Lys750 as a ubiquitin receptor site on SMXL6, a known target of the strigolactone signaling F-Box protein MAX2, as being ubiquitinated upon GR24 treatment. Despite this proof of concept, it is clear that in the current setup, the overall experimental variability represents a major obstacle that must be overcome. Several adaptations to the protocol that could resolve some of the problems encountered are discussed.

1. Introduction

Ubiquitination is a fundamental protein modification involved in multiple aspects of cell biology (Banfield, 2015; Devoto et al., 2003; Dreher and Callis, 2007; Furniss and Spoel, 2015; Komander and Rape, 2012; Moon et al., 2004; Sadanandom et al., 2012; Seo and Mas, 2014; Sullivan et al., 2003; Vierstra, 2009; Zeng et al., 2006). In plants, one of the most studied roles for this post-translational modification (PTM) is its function in hormone signaling (Chapman and Estelle, 2009; Gagne et al., 2004; Guseman et al., 2015; Martins et al., 2015; Perez and Goossens, 2013; Stirnberg et al., 2007). Indeed, several of the main hormonal signaling pathways in plants are built around a common model that includes an E3 ligase, responsible for targeting specific proteins for ubiquitin-mediated degradation upon the detection of the signaling molecule. For example, the phytohormone auxin gives rise to a transcriptional response, which is mediated by Auxin Response Factors (ARF) activators that induce the expression of the response genes. In low auxin conditions, these transcription factors (TFs) are bound by AUXIN/INDOLE-3-ACETIC ACID (Aux/IAA) proteins that actively repress their activity and therefore lead to low expression levels of auxin responsive genes (Chapman and Estelle, 2009; Guilfoyle and Hagen, 2007; Leyser, 2006). The ARF activators are released from this repression via the action of the TIR1 F-Box protein that specifically targets the Aux/IAA proteins for ubiquitin-mediated proteasomal degradation (Chapman and Estelle, 2009; Leyser, 2006). Similarly, in jasmonate signaling, members of the JASMONATE-ZIM-DOMAIN PROTEIN (JAZ) protein family bind MYC and possibly other TFs that are responsible for coordinating the response to this hormone. The JAZ proteins also repress the activity of MYC2 and this is accomplished through the recruitment of TOPLESS via the NINJA connector protein (Pauwels et al., 2010). Here, CORONATINE INSENSITIVE 1 (COI1), an F-Box protein, is responsible for the targeted degradation of the JAZ repressor proteins (Thines et al., 2007), thereby giving rise to the MYC2-mediated response to this hormone. In the gibberellin (GA) pathway, the F-Box protein SLEEPY1 (SLY1) leads to the targeted degradation of DELLA proteins upon detection of the hormone by its receptor GA INSENSITIVE DWARF1 (GID1), which releases the TFs responsible for the transcriptional changes induced by GA to occur (Dill et al., 2004). These examples clearly underline the importance of ubiquitination in main signaling networks that impinge on various aspects of plant growth and the capacity to adapt to environmental cues. The 1,500 *Arabidopsis thaliana* genes that are predicted to encode components of E3 ligases, and more specifically, the close to 900 annotated F-Box-type E3 ligases, also bear witness to the importance of this PTM in plants (Hua and Vierstra, 2011). This impressive number of E3 ligases, which represent a 10-fold increase when compared to humans (Hua et al., 2011), could theoretically give rise to an equally large number of target proteins. However, with a lack of effective tools adapted to ubiquitin profiling in plants, the identification of these target proteins has thus far remained tricky.

We recently developed the ubiquitin COFRADIC technology to enrich for ubiquitinated peptides (Stes et al., 2014) (see **Chapters 5** and **6**). In a human cell line, this allowed us to identify over 7,000 unique ubiquitination sites, which is within reach of the number of sites that were reported upon the use of anti-diglycine antibodies in the mammalian field (Udeshi et al., 2013a; Udeshi et al., 2013b; Kim et al., 2011; Wagner et al., 2011). Although the latter led to a significant stride forward in ubiquitination research, the application of these antibodies in the plant field has only reached about one-tenth of the yield now considered the gold standard in mammalian research (Li et al., 2015; Xie et al., 2015; Walton et al., 2016a). We recently succeeded in transferring the ubiquitin COFRADIC technology to plants and used it to profile the ubiquitinome of an *Arabidopsis thaliana* cell culture, which allowed us to identify 3,009 sites (Walton et al., 2016a).

Currently, in plants, ubiquitin COFRADIC thus seems to yield the highest number of ubiquitination sites (Walton et al., 2016b see **addenda**). However, it was thus far only applied in profiling experiments, meaning that it remains to be tested in a differential setup aimed to directly identify substrates of E3 ligases. We hypothesized that the value of this technology would increase if it could be used in a comparative study, for example comparing hormone and mock treatments, or comparing WT and E3-ligases KO mutants. As proof-of concept, the phytohormone strigolactone was selected. Similar to auxin, jasmonate and gibberellins, strigolactone signaling has been shown to rely on the action of an F-box protein, MORE AXILLARY BRANCHES2 (MAX2), to target specific proteins for proteasomal degradation. During the two year development period of the technology, large leaps forward were made in the strigolactone research field. For example, the SUPPRESOR OF MAX2-LIKE (SMXL) proteins were identified, a protein family that is shown to be targeted by MAX2 and is responsible for most of the phenotypes observed in the *max2* mutant (Jiang et al., 2013; Kong et al., 2014; Soundappan et al., 2015; Stanga et al., 2013; Wang et al., 2015; Zhou et al., 2013). However, as of yet the exact ubiquitination sites on these particular proteins remain elusive. To assess whether the COFRADIC technology could serve for the identification of the targets of specific F-box E3 ligases and to gain insight into the ubiquitination-related events occurring during strigolactone signaling, we here carried out a comparative study on proteome extracts from cell cultures grown in the presence or absence of GR24, a synthetic analog of SLs.

2. Results

2.1. The strigolactone signalling cascade is functional in cell cultures

As strigolactones were not yet studied in cell cultures, it was first necessary to verify that strigolactone signaling is fully functional in cell cultures. To assess this, cDNA was extracted from cell cultures at 0, 1, 5, 10 and 15 hours after GR24 treatment. The expression levels of the known SL-responsive gene *BRC1* (Braun et al., 2012) were analyzed by RT-qPCR (Figure 1). In cell cultures

treated with GR24, the expression levels of *BRC1* rose over the course of the treatment, reaching a tenfold increase within already 5 hours. This was not the case for the expression of this gene in the mock treated cultures. Taken together, these results suggest that the strigolactone signaling pathway is operational in cell cultures.

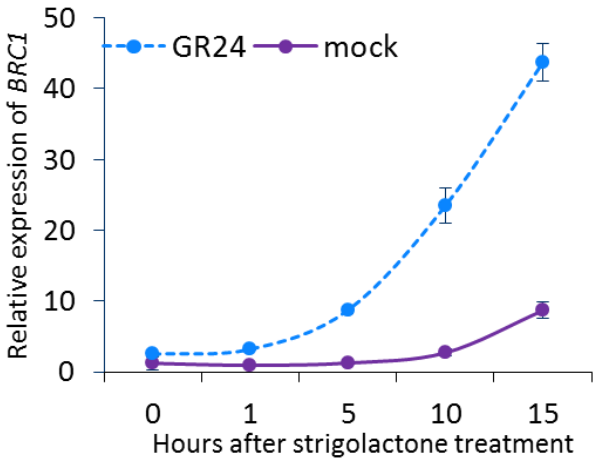

Figure 1: *BRC1* expression in cell cultures. The expression of the *BRC1* gene was assessed by RT-qPCR for responsiveness to treatment with 1 µM GR24 (light blue) and in mock conditions (purple).

2.2. The ubiquitination profile of cell cultures grown in the presence or absence of GR24

To identify proteins that were differentially ubiquitinated upon GR24 treatment, the ubiquitin COFRADIC protocol was carried out on cell cultures grown in the presence or absence of GR24. Cultures were started from PSB-D cultures and grown for 2 weeks with a photoperiod of 16hrs light - 8 hrs. The *BRC1* response is rather downstream in the strigolactone signaling cascade when compared with the strigolactone induced ubiquitination of MAX2 targets. As changes in *BCR1* expression were detected as early as 5 hours post GR24 treatment, we suggested shorter treatment duration when sampling for the ubiquitin COFRADIC experiment. Cell cultures were treated with either 1 µM of GR24 or the acetone carrier for 1 hour, following which proteins were extracted and precipitated using a chloroform/methanol precipitation protocol (Rose et al., 2004). 4 mg of the resulting protein pellets then underwent the ubiquitin COFRADIC protocol as described in Walton *et al*. 2016b to enrich for peptides that carry lysines subject to ubiquitination.

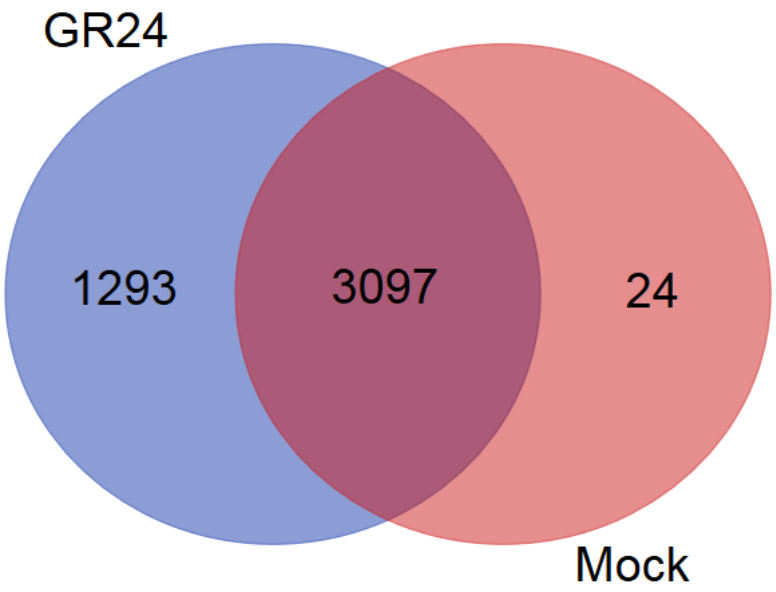

Figure 2: Overlap of ubiquitinated proteins between mock and GR24 treated samples. Ubiquitin COFRADIC was carried out of protein samples from cell cultures grown in the presence or absence of 1 µM GR24. The Venn diagram shows the overlap on the protein level between the two samples.

We generated 878,064 MS/MS spectra, of which 67,765 or 7.7% were identified by MaxQuant. Overall, this resulted in the identification of 16,805 unique peptides and 5,724 unique proteins. In total, 9,866 of the peptides carried a Lys-Ɛ-Gly modification, thus originating from proteins that were ubiquitinated *in vivo*, while non-Lys-Ɛ-Gly peptides made up 59% of the total number of all identified peptides. The Lys-Ɛ-Gly peptides could be assigned to 4,414 different proteins (for a complete list of the identified ubiquitinated peptides and proteins see Supplemental Table S1). Of the 9,866 Lys-Ɛ-Gly peptides, 57% were found in both the mock sample and the treated sample (N.B. in this experiment only one biological repeat was used for each condition). On the protein level this corresponded to a total of 4,414 proteins groups carrying at least one site of ubiquitination (Figure 2). When comparing the samples on the protein level, a larger overlap of 70% (3,097 protein groups) was observed. Despite this, 30% of the proteins differed between the mock and treated and, notably, the total number of identifications was significantly higher upon GR24 treatment as only 24 proteins were found to be uniquely ubiquitinated in the mock sample. There remains therefore considerable variability between samples. For all sites please refer to supplementary dataset 1.

2.3. Lys750 on the SMXL6 protein is ubiquitinated upon GR24 treatment

The datasets of ubiquitinated proteins were searched for members of the SMXL family, known to be ubiquitinated upon GR24 treatment. SMXL6 was identified and, as expected, only in the GR24-treated sample. SMXL 6, 7 and 8 have been shown to be ubiquitinated in response to strigolactones

and the *smxl6smxl7smxl8max2* quadruple mutant rescues the *max2* high shoot branching phenotype. The *BRC1* gene is also known to influence shoot branching (Braun et al. 2012). The fact that we identify an ubiquitination site on SMXL6 in the presence of GR24 is therefore in line with the response of *BRC1* in cell cultures. Only one ubiquitinated lysine, Lys750, was found in SMXL6 and, though in close proximity, this site is not within the 6 amino acids that have previously been shown to render this protein resistant to degradation (Figure 3). Upon alignment (Kalign (Lassmann and Sonnhammer, 2005)), the receptor lysine was shown to be conserved in SMXL7 and SMXL8 but is substituted for an arginine in SMAX1 (Figure 3).

```
SMXL6     MPTPVTTARECLTEEAARALDDAVVVARRRSHAQTTSLHAVSALLAMPSSILREVCVSRA
SMXL7     MPTPVTTARQCLTEETARALDDAVSVARRRSHAQTTSLHAVSGLLTMPSSILREVCISRA
SMXL8     MPTAVNVAKQCLTAEASYALEEAVNVARRRGHSQTTSLHAISALLSLPTSVLRDACAR--
SMAX1     MRAGLSTIQQTLTPEAATVLNQSIAEAARRNHGQTTPLHVAATLLASPAGFLRRACIR--

SMXL6     ARSVPYSSRLQFRALELCVGVSLDRLPSSKSPAT---EEDPPVSNSLMAAIKRSQANQRR
SMXL7     AHNTPYSSRLQFRALELCVGVSLDRLPSSKSTPTTTVEEDPPVSNSLMAAIKRSQATQRR
SMXL8     VRNSAYSPRLQFKALDLCLSVSLDRIQSGHQLGS---DDSPPVSNSLMAAIKRSQAHQRR
SMAX1     -SHPNSSHPLQCRALELCFSVALERLPTATTTP----GNDPPISNALMAALKRAQAHQRR

SMXL6     -HPESYHL-QQIHASNNGGGGCQTTVLKVELKYFILSILDDPIVNRVFGEAGFRSSEIKL
SMXL7     -HPETYHL-HQIHGNNNTE---TTSVLKVELKYFILSILDDPIVSRVFGEAGFRSTDIKL
SMXL8     -LPENFRIYQEMSQSQNQN---SLSCVKVELRQLILSILDDPVVSRVFGEAGFRSSELKL
SMAX1     GCPEQQQQ--------------PLLAVKVELEQLIISILDDPSVSRVMREASFSSPAVKA

SMXL6     DVLH-----------PPVT-QLSSRF-SRGRCPPL----FLCNL---PNSDPNR---EFP
SMXL7     DVLH-----------PPVTSQFSSRFTSRSRIPPL----FLCNL---PESDSGRVRFGFP
SMXL8     SIIR-----------PV---PHLLRY---SSQQPL----FLCNLTGNPEPNPVRWGFTVP
SMAX1     TIEQSLNNSVTPTPIPSVS-SVGLNF-RPGGGGPMTRNSYLNPR---LQQNASSVQSGVS

SMXL6     ---FSGSSGFDENSRRIGEVLGRKDKKNPLLIGNCANE-ALKTFTDSINSGKLG--FLQM
SMXL7     ---FGD---LDENCRRIGEVLARKDKKNPLLVGVCGVE-ALKTFTDSINRGKFG--FLPL
SMXL8     SLNFNG----DLDYRRISAVFTKDKGRNPLLVGVSAYG-VLTSYLNSLEKNQTDGMILPT
SMAX1     ---------KNDDVERVMDILGRAKKKNPVLVGDSEPGRVIREILKKIEVGEVG----NL

SMXL6     DISGLSLISIEKEISEILA---DGSKNEEEIRMKVDDLGRTVEQSGSKSGIVLNLGELKV
SMXL7     EISGLSVVSI--KISEVLV---DGSR----IDIKFDDLGRL------KSGMVLNLGELKV
SMXL8     KLHGLTAVNIGSEISDQISVKFDKTY----TDTRFHDLGKL-AEQGSGPGLLLHYGDLRV
SMAX1     AVKNSKVVSLE-EISSDKALRIKELDGL--LQTRLKNSDPI-----GGGGVILDLGDLKW

SMXL6     LTSE--ANAALEIL--------VSKLSDLLKHESKQLSFIGCVSSNETYTKLIDRFPTIE
SMXL7     LASDVFSVDVIEKF--------VLKLADLLKLHREKLWFIGSVSSNETYLKLIERFPTID
SMXL8     FTNGEGNVPAANYI--------VNRISELLRRHGRRVWLIGATTSNEVYEKMMRRFPNVE
SMAX1     LVEQPSSTQPPATVAVEIGRTAVVELRRLLEKFEGRLWFIGTATC-ETYLRCQVYHPSVE

SMXL6     KDWDLHVLPITASTKPSTQGVYP--KSSLMGSFVPFGGFFSST-SNFRVPLSSTVNQTLS
SMXL7     KDWNLHLLPITSS----SQGLYP--KSSLMGSFVPFGGFFSST-SDFRIPSSSSMNQTLP
SMXL8     KDWDLQLLTITS-----LKPCLPHNKSSLIGSFVPFGGFFSTTPSELKLPFSG-------
SMAX1     TDWDLQAVSVAAK-AP-ASGVFPR-LANNLESFTPLKSFVPAN-------------RTLK
```

```
SMXL6     RCHLCNEKYLQEVAAVLKAGSSLSLADKCSEK-LAPWLRAIETKEDKGITGSSKALDDAN
SMXL7     RCHLCNEKYEQEVTAFAKSGSMID--DQCSEK-LPSWLRNVEHEHEKGNLGKVK--DDPN
SMXL8     --------FKTEIT-----GPVSSISDQTQST-LPPWLQMTTRT------------DLNQ
SMAX1     CCPQCLQSYERELAEIDSVSSPEVKSEVAQPKQLPQWLLKAK--------------PVDR

SMXL6     TSASQTAALQKKWDNIC-QSIHHTPAFPKLGFQSVSPQFPVQ------TEKSVRTPTSYL
SMXL7     VLASRIPALQKKWDDIC-QRIHQTPAFPKLSFQPVRPQFPLQLGSSSQTKMSLGSPTEKI
SMXL8     KSSAKVVQTKEGLESVCGNKFTSSASASTCSAKSVTTDLNLRV-----SSVTTGSGLKKH
SMAX1     LPQAKIEEVQKKWNDAC-VRLHPSFHNKNERIVPIPVPITLTTSPYS-PNMLLRQPLQPK

SMXL6     ETPKL-----------LNPP--------ISKPKPMEDLTASVTNRTVSLPLSCVTTDFGL
SMXL7     VCTRTSESFQGMVALPQNPPHQPGLSVKISKPKHTEDLSSSTTNS----PLSFVTTDLGL
SMXL8     LDSKD----------------------FSQPQSVSS----------------------
SMAX1     LQPNR--ELRE-----------------RVHLKPMSPLVAEQAKKKSP-PGSPVQTDLVL

SMXL6     GVIYASKNQESKTT-----REK---------------PMLVTLNSSLEHTYQKDFKSLRE
SMXL7     GTIYASKNQEPSTPVSVERRDF---------------EVIKEKQLLSASRYCKDFKSLRE
SMXL8     ---YSFDNPRDLNA-------------------------------------ESFKIIYR
SMAX1     GRAEDSEKAGDVQV-----RDFLGCISSESVQNNNNISVLQKENLGNSLDI-DLFKKLLK

SMXL6     ILSRKVAWQTEAVNAISQIICGCKTDSTRRNQ----ASGIWLALLGPDKVGKKKVAMTLS
SMXL7     LLSRKVGFQNEAVNAISEIVCGYRDESRRRNNHVATTSNVWLALLGPDKAGKKKVALALA
SMXL8     RLTDMVSGQDEAARVISCALSQPPKSVTRRD--------VWLNLVGPDTVGKRRMSLVLA
SMAX1     GMTEKVWWQNDAAAAVAATVSQCKLGNGKRRG-VLSKGDVWLLFSGPDRVGKRKMVSALS

SMXL6     EVFFGGKVNYICVDFGAEHCSLDD-----KFRGKTVVDYVTGELSRKPHSVVLLENVEKA
SMXL7     EVFCGGQDNFICVDFKSQD-SLDD-----RFRGKTVVDYIAGEVARRADSVVFIENVEKA
SMXL8     EIVYQSEHRFMAVDLGAAEQGMGGCDDPMRLRGKTMVDHIFEVMCRNPFCVVFLENIEKA
SMAX1     SLVYGTNP--IMIQLGSRQDAGDG-NS--SFRGKTALDKIAETVKRSPFSVILLEDIDEA

SMXL6     EFPDQMRLSEAVSTGKIRDLHGRVISMKNVIVVVT-SGIAKDNATDHVIKPVKFPEEQV-
SMXL7     EFPDQIRLSEAMRTGKLRDSHGREISMKNVIVVATISGSDKASDCHVLEEPVKYSEERV-
SMXL8     DEKLQMSLSKAIETGKFMDSHGREVGIGNTIFVMT-------SSSQGSATTTSYSEEKL-
SMAX1     DMLVRGSIKQAMDRGRIRDSHGREISLGNVIFVMT-------ASWHFAGTKTSFLDNEAK

SMXL6     ---LSARSWKLQIKLGDATK-------F---GVNKRK-------YELETAQ----RAVKV
SMXL7     ---LNAKNWTLQIKLADTSN-------VNKNGPNKRR-------QEEAETEVTELRALKS
SMXL8     ---LRVKGRQVEIRIETVSSLPMVRSVYGPTSVNKRKLMGLGNLQETKDTVESVKRLNRT
SMAX1     LRDLASESWRLRLCMRE--------------KFGKRR----ASWLCSDEERLTKPKKEHG

SMXL6     QRSYLDLNLPVNE-------TEFSPDHE---AEDRDAW------------FDEFIEKVDG
SMXL7     QRSFLDLNLPVDE-------IEANEDEAYTMSENTEAW------------LEDFVEQVDG
SMXL8     TNGVLDLNLPAQE-------TEIEEKYHC--EENSNVW------------LMNLKNHKRL
SMAX1     SGLSFDLNQAADTDDGSHNTSDLTTDN----DQDEQGFSGKLSLQCVPFAFHDMVSRVDD

SMXL6     -KVTFKPVDFDELAKNIQEKIGSHFERCFGSETHLELDKEVILQILAA-SWSSLSSGEEE
SMXL7     -KVTFKLIDFDELAKNIKRNILSLFHLSFGPETHLEIENDVILKILAALRWSS------D
SMXL8     IEVPFKPFDFEGLAEKIKKSVKENFDKCVRSDCLLEVDPKIIERLLAA-VYFS------D
SMAX1     -AVAFRAVDFAAVRRRITETLSERFETIIGESLSVEVEEEALQRILSG-VWLG-------
```

```
SMXL6     GRTIVDQWMQTVLARSFAEAKQKYGSNPM---LGVKLVASSSGLA----SGVE-LPAKVD
SMXL7     EEKTFDQWLQTVLAPSFAKARQKCVPAAP---FSVKLVASRESPAEEETTGIQQFPARVE
SMXL8     SRKDIKELLENIMSPVFLRIKERYEITTS---CVVKLVGRDLDIF---------LEDQMD
SMAX1     -QTELEEWIEKAIVPVLSQLKARVSSSGTYGDCTVARLELDEDSG-ERNAGDL-LPTTIT


SMXL6     VIW----
SMXL7     VI-----
SMXL8     LFFVKSQ
SMAX1     LAV----
```

Figure 3: Sequence alignment of SMAX1, SMXL6,7 and 8. The original deletion box is highlighted in cyan in the SMXL6 protein sequence and the Lys750, found to be ubiquitinated is shown in green.

3. Discussion

We carried out a differential analysis comparing Arabidopsis cell cultures untreated and treated for 1 hour with GR24. Strigolactones have been shown to give rise to the ubiquitination of members of the SMXL protein family leading to their subsequent degradation by the 26S proteasome (Jiang et al., 2013; Kong et al., 2014; Soundappan et al., 2015; Stanga et al., 2013; Wang et al., 2015; Zhou et al., 2013). By applying our ubiquitin COFRADIC protocol, we detected one of the members of this family, SMXL6, as being ubiquitinated upon GR24 treatment.

In fact, we identified Lys750 on SMXL6 as being ubiquitinated upon GR24 treatment. Although recently this protein has been shown to be degraded upon GR24 treatment in Arabidopsis, no specific ubiquitination sites have been reported. Interestingly, although within close proximity, this site of ubiquitination is not contained within the amino acid sequence that, upon deletion, rendered the protein resistant to degradation. Upon alignment of SMXL6/7/8 and SMAX1, Lys750 from SMXL6 was shown to be conserved in SMXL7 and SMXL8, but substituted by an arginine in SMAX1. This is in line with the fact that SMXL6, 7 and 8 are common targets of the $SCF^{MAX2D14}$ complex, whereas SMAX1 is targeted by the $SCF^{MAX2KAI2}$. In this respect, a recent study has suggested that degrons, which are ultimately responsible for the targeted degradation of the substrates of E3 ligases, are tripartite (Guharoy et al., 2016). A first linear sequence, termed the primary degron, is necessary for recognition by the E3 ligases. The secondary degron is the ubiquitinated lysine itself and the tertiary degron is a disordered segment that provides an initiation site for the protein to be unfolded and fed into the 26S proteasome. Our results would therefore suggest that Lys750 might act as the secondary degron, whilst the amino acid stretch in the previously described deletion could be at least part of the primary degron. In future studies, it would be interesting to test the importance of the SMXL6 ubiquitination site here identified, possibly through K→R site directed mutagenesis.

In the current setup, we found that when comparing samples, whether it be comparing two biological repeats of material grown in the same conditions as in **Chapter 6** or in different conditions as here, an overlap of 87% and 70% of ubiquitinated proteins was observed respectively. In the latter, the 30% difference between samples constitutes an obstacle that would need to be overcome before this technique could be used in the discovery phase of a project aiming to identify targets of E3 ligases. To resolve this issue, we could move towards an experimental design with at least 3 biological repeats, to help reduce the variability between conditions and also render the technology compatible with a quantitative analysis. A direct quantitative approach would allow for the identification of peptides that are differentially ubiquitinated, not based on mere presence or absence, but rather on the variation of their abundance over multiple samples. This type or analysis would render a 'rankable' and more refined list of potential candidates that could be the focus of further validation.

We further suggest that the ubiquitin COFRADIC technique can be adapted in at least two ways to provide a quantitative analysis. First, it would be conceivable to incorporate a post-metabolic labeling step directly in the ubiquitin COFRADIC protocol. This could be accomplished by replacing the glycine-BOC group, used to mark the site of ubiquitination on the peptide, with a BOC group linked to a larger amino acid, such as alanine. By introducing stable heavy isotopes (e.g. deuterium and carbon-13) into this amino acid, different variants of the label could be produced. After the Ala-BOC group modification, it should be possible to combine the proteome samples together, perform the trypsin digestion and then run the diagonal chromatography steps, as well as the mass spectrometry analysis together. The alanine variants could subsequently be used to distinguish the origin of each peptide and ultimately to produce relative quantification values for these peptides in the different samples. This would allow carrying out a differential analysis followed by a statistical analysis of the relative quantification values, thereby selecting a more precise list of potential candidates.

A second way to adapt the technology would be through the use of label-free quantification. This again should, in theory, allow for the statistical analysis of the LFQ values for the ubiquitinated peptides detected in different conditions over various repeats and thereby also lead to a more accurate list of candidate proteins for follow-up studies. One foreseeable drawback however, would be that the precision of LFQ is reported to decline when dealing with highly fractionated samples (Jürgen Cox, personal communication). In our COFRADIC protocol, each biological sample ultimately is analyzed as 60 fractions on the mass spectrometer, and therefore, the technology in the current format is not well suited to the use of LFQ. Fractionation in our protocol comes from the peptide enrichment steps which involve rather lengthy chromatography steps. However, the biochemistry prior to these steps is also compatible with other enrichment procedures, such as the addition of an affinity handle like biotin, replacing the Gly-BOC group as previously described (Hendriks et al., 2015), which could circumvent the need for fractionation.

Although part of the variability between samples can be accounted for by the arguments stated above, the snapshot effect alone does not explain the large increase in ubiquitinated proteins found in the GR24 treated sample. In theory, aside from the SMXLs (Soundappan et al. 2015, Wang et al. 2015), one would not expect a large number of differentially ubiquitinated proteins. Therefore we hypothesize that this difference may arise from the number of fractions necessary to analyze one sample in our current setup. A large number of fractions will gradually compromise the quality of the separation on the HPLC column causing the overall sensitivity of the LC-MS analysis progressively to drop, and with it the number of identifications. This could explain the difference between the number of ubiquitinated proteins identified in the mock sample and those in the GR24 treated sample. This also points to a need to miniaturize the COFRADIC protocol or to the integration of a stable isotope label, as this would allow us to combine the samples early on, thereby reducing the number of runs through multiplexing and also minimizing experimental variability between samples.

In summary, we have shown that the COFRADIC technology holds good potential for becoming a tool that could be used to identify targets of E3 ligases in plants. In order to reach this goal, further optimization of the protocol seems necessary to reduce experimental variance between samples, thus to shorten the list of potential candidates. There are several manners in which this can be accomplished, including the integration of a stable isotope labeling step in the COFRADIC protocol and/or reduction of the degree of fractionation, which could also allow for the use of label-free quantification.

4. Material & Methods

Plant Material

Arabidopsis thaliana (L.) Heynh. (accession Columbia-0) cell suspension cultures (PSB-D) were maintained as described previously (Van Leene et al., 2007). After 3 weeks of growth under continuous light, samples were treated with either 1 μM GR24 or the acetone carrier as a control.

Protein extraction

3 g of fresh weight material was harvested, flash-frozen in liquid nitrogen, and manually ground into a fine powder with a pestle and mortar. The material was re-suspended in 10 mL of homogenization buffer, containing 290 mM sucrose, 50 mM sodium phosphate buffer (pH 8), and 25 mM EDTA in milliQ water, vigorously agitated for resuspension, and five times sonicated on ice with a 1-cm probe for 10 s to disrupt cell walls. Samples were centrifuged at 4°C for 15 min at 1,500×g to remove debris. Supernatants were collected and a methanol/chloroform precipitation was carried out by addition of 3:1:4 parts of methanol, chloroform and water respectively. Samples were centrifuged for 10 min at

5,000×g (room temperature). The upper (aqueous) phase was removed and four parts of methanol were added onto the interface and bottom phase remaining in each tube to give rise to a precipitation.

Ubiquitin COFRADIC

Pellets were washed 3 times with acetone and re-suspended in 4 M guanidinium hydrochloride in 50 mM sodium phosphate buffer (pH 8). Ubiquitin COFRADIC was carried out as described previously (Stes et al., 2014). To reduce the liquid chromatography-tandem mass spectrometry (LC−MS/MS) analysis time, peptide fractions eluting 15 min apart were pooled, dried and re-dissolved in 15 µL of 2% (v/v) acetonitrile with 0.1% (v/v) trifluoroacetic acid (TFA). In total, 60 samples were analyzed via LC-MS/MS on an Ultimate 3000 RSLC nano LC (Thermo Fisher Scientific) in-line connected to a Q Exactive mass spectrometer (Thermo Fisher Scientific). Settings and machine configurations were as described (Stes et al., 2014). MS/MS spectra were searched with the MAXQUANT Andromeda search engine against The Arabidopsis Information Resource (TAIR10_pep_20101214 containing 27,416 protein-coding genes) database with the MAXQUANT software (version 1.4.0.3); the precursor mass tolerance was set to 20 ppm for the first search (used for nonlinear mass recalibration) and to 4.5 ppm for the main search. ArgC was selected as enzyme setting, because cleavage after lysine residues was obstructed by acylation of their side chains. Cleavages between arginine and proline residues and up to one missed cleavage were allowed. Methionine oxidation and carbamidomethylation of cysteines were searched as fixed modifications, whereas N-terminal protein acetylation, lysine acetylation, N-terminal pyroglutamate and Lys-ε-Gly were set as variable modifications. The false discovery rate for peptide, protein and site identification was set to 1% and the minimum peptide length to 7. The minimum score threshold for both modified and unmodified peptides was set to 30.

PART IV

Discussion and Perspectives

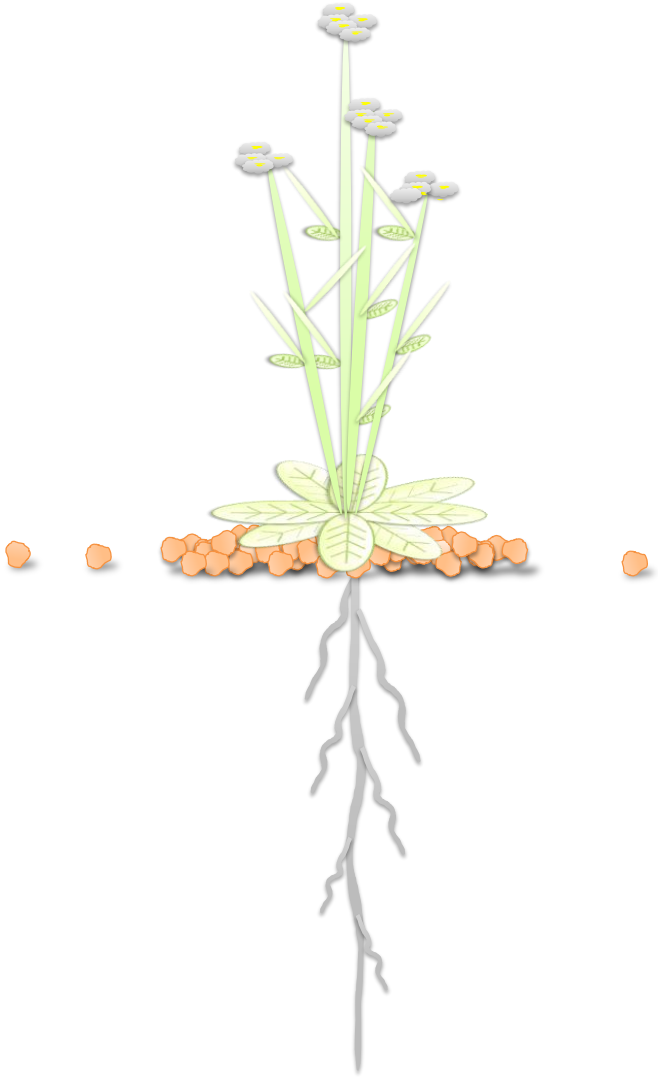

Discussion

Plants rely on integrated hormonal signaling networks to control their development and to adapt to environmental cues. Unraveling these signaling cascades is an ongoing challenge as at least ten different phytohormones have now been described. These small and structurally unrelated molecules give rise to various responses in plants by activating specific signaling cascades that generally all share several critical steps including, detection by a receptor protein, changes in protein interaction partners of key players often including the receptor itself and ultimately the primary signal is translated into a secondary signal, involving post-translational modification (PTM) of a targeted subset of proteins (Santner and Estelle, 2009). Both phosphorylation (Kline et al., 2010; K et al., 2014; Nguyen et al., 2015) and ubiquitination (Kelley and Estelle, 2012; Santner and Estelle, 2010) are frequently observed to either give rise to changes in activity of target proteins or to induce their targeted proteasomal degradation. Finally, the change in protein fate, orchestrated by these PTMs, leads to broader downstream responses, such as transcriptional changes, that will eventually lead to the observed phenotypic role of the given hormone. In order to fully understand the signaling cascade of a given hormone, all of these players and modifications must first be characterized.

Most of the early steps in plant hormone signaling described to date occur on the protein level. Therefore tools that allow the direct investigation of changes in protein interaction partners, abundance and PTM status are most suited to provide information directly concerning the key players of these signaling cascades. In this respect, recent advances in both instruments and sample preparation methods have led mass spectrometry-driven proteomics tools to become the method of choice (see **Chapter 1** for review). Indeed over the last decade, multiple studies revealed great insights into the various levels of the plant hormonal signaling cascades through the use of these tools. For instance, both tandem affinity purification (TAP) and green fluorescent protein trapping (GFP-trapping) have proved very useful tools in studying hormone induced changes in protein-protein interactions (Karlova et al., 2006; Li et al., 2002; Nam and Li, 2002; Wang et al., 2008; Dharmasiri et al., 2005; Gray et al., 2001; Kepinski and Leyser, 2005; Pauwels et al., 2010; Tang et al., 2011; Wang et al., 2013a). Also

PTM scanning is rapidly gaining ground in the plant field. Phospho-enrichment protocols are being systematically carried out with ever improving coverage (Engelsberger and Schulze, 2012; K et al., 2014; Nguyen et al., 2015), and recent advances in ubiquitin profiling have rendered the study of this PTM in plants feasible (Li et al. 2015; Walton, Stes et al. 2016; Xie et al. 2015). Finally, protein profiling has made leaps, both with the staggering increase in sensitivity of instruments and also with the gradual move from 2 DE and 2 DIGE gels towards gel free setups. In sum, there is now a readily available set of mass spectrometry-based tools allowing the plant community to study hormonal signaling cascades at its heart: the proteome (Alvarez et al., 2011; Alvarez et al., 2013; Li et al. 2014; Xing and Xue, 2012; Zhang et al., 2012). During my PhD, we aimed to make use of these newly available techniques to dissect the signaling pathway of recently described phytohormones, strigolactones.

Strigolactones are secondary metabolites derived from carotenoids. They were originally described as germination signals for parasitic plants (Cook et al. 1966) before being shown to play a crucial role in the early steps of establishing the symbiotic interaction between the producing host and arbuscular mycorrhizal fungi (AM fungi) (Akiyama et al. 2005). Most recently these compounds have been shown to also play a role as a hormone, regulating shoot branching, root system architecture, photomorphogenic growth, leaf senescence and, to a certain extent, seed germination (Reviewed in (Al-Babili and Bouwmeester, 2015).

Much of the biosynthesis process of these compounds is now known, with the consecutive actions of DWARF27 (D27), CAROTENOID CLEAVAGE DIOXYGENASE 7 (CCD7)/MORE AXILLARY GROWTH 3 (MAX3),CCD8/MAX4 and finally the cytochrome P450-encoding MAX1 generating bioactive strigolactones (Booker et al., 2005; Kohlen et al., 2011; Alder et al., 2012). Furthermore, the perception and early steps in the signaling cascade have been extensively studied. Early on, the Arabidopsis MAX2, an F-box protein, was shown to be a central player in strigolactone signaling. MAX2 forms a (SKP1)-Cullin-F-box complex, SCF^{MAX2}, with, SKP1 (S-phase kinase-associated protein 1) and CULLIN1 (CUL1) and giving rise to the targeted ubiquitination and subsequent proteasomal degradation of specific protein substrates upon detection of strigolactones (Stirnberg et al. 2007). This action relies on the activity of at least one, and possibly both, of the α/β-hydrolase proteins DWARF14 (D14) and KARRIKIN INSENSITIVE2 (KAI2) (Nelson et al. 2011, Scaffidi et al. 2014). Both receptors have been shown to give rise to the detection of specific enantiomers of the commonly used racemic mixture of the synthetic strigolactone analog GR24 (Scaffidi et al. 2014). Upon detection of GR24, these receptor proteins interact with the SCF^{MAX2} complex allowing the SCF to specifically ubiquitinate members of the SUPRESSOR OF MAX2-LIKE (SMXL) family. The choice of which member of this family that is to be degraded is determined both by the stereoisomer of GR24 and the receptor protein (Stanga et al. 2013; Scaffidi et al. 2014;

Soundappan et al. 2015; Wang et al. 2015). Detection of enantiomer GR24- by KAI2 gives rise to the targeted degradation of SMAX1, a protein that is responsible for the long hypocotyl and aberrant germination phenotypes of the *max2* mutant (Stanga et al. 2013; Scaffidi et al. 2014; Soundappan et al. 2015). On the other hand, detection of GR24+ by D14 gives rise to the targeted degradation of the SMXL6/7/8, proteins responsible for the high shoot branching and high lateral root density phenotypes of the *max2* mutant (Scaffidi et al. 2014; Soundappan et al. 2015; Wang et al. 2015).

Less information is available concerning the later steps of the strigolactone signaling cascade, and it is still not entirely clear whether this hormone gives rise to the observed phenotypes via modulating gene expression (Van Ha et al. 2014; López-Ráez et al. 2008; Mayzlish-Gati et al. 2010; Braun et al. 2012), operating at the protein level (Li et al. 2014; Pandya-Kumar et al. 2014; Shinohara et al. 2013) or whether it acts in both ways. For instance, in the case of shoot branching process, strigolactones dampen the auxin transport by affecting the PIN-FORMED1 (PIN1) recycling at the membrane in xylem parenchyma cells, resulting in modified auxin flows in the stem (Crawford et al., 2010; Shinohara et al., 2013). Furthermore, this response is direct, without the requirement of de novo protein synthesis (Shinohara et al., 2013). In contrast, MAX2 and D14 are localized in the nucleus, indicating that transcriptional changes might be required for strigolactone action (Braun et al., 2012; Dun et al., 2012) and several strigolactone responsive genes have been described. Finally, the members of the SMXL family, which are likely the only targets of the SCF^{MAX2}, contain EAR domains, which have been shown, through yeast-2-hybrid experiments, to allow them to interact with TOPLESS proteins (Soundappan et al. 2015; Wang et al. 2015). This is in line with the idea of a transcriptional regulation downstream of the SMXL proteins, analogous to that which has been described for several other plant hormonal signaling cascades.

In sum, there remains a discrepancy concerning the issue of how strigolactones give rise to the observed phenotypes and little has been done to investigate changes occurring directly at the proteome level. One study initially used isobaric tags for relative and absolute quantitation (iTRAQ) in a quantitative mass spectrometry workflow to reveal difference between the proteomes of the biosynthesis mutant *max3* and the wild-type (WT) plants, supplemented with GR24 or not (Li et al., 2014). Another proteomic analysis gained evidence on the implication of phosphorylation in strigolactone signaling through the use of phosphospecific antibodies in rice seedlings, giving some insight into the complex negative regulatory mechanism involved in this signaling pathway (Chen et al., 2014). However, their contribution to the strigolactone field remains modest and, to date, their results have not been built on by follow up studies. In order to provide necessary proteome information to the strigolactone community, we decided to investigate GR24-triggered signaling in the roots of *Arabidopsis thaliana*. We opted for studying the roots, because most studies so far have focused on the hypocotyl and the shoots, due to the history of the discovery of this hormone, and

information concerning what is happening in the below ground part of the plant is more scarce (see **Chapter 2** for review).

A large-scale shotgun proteomics experiment was carried out in our lab, in which root proteomes of WT and *max2-1* seedlings grown in mock conditions or treated with 1 μM of *rac*-GR24 for 9 hours (h) or 24h post treatment were compared. A gel free approach was used in combination with a post-metabolic labeling technique to quantitatively compare the different root proteomes. Statistical analysis allowed us to identify that over 100 proteins showed shift in abundance upon treatment, over 200 when comparing genotype and 30 a joined effect of both the genotype and the treatment (**Chapter 3**). Among the proteins with significant shifts in their abundance when comparing genotypes and in some cases also upon GR24 treatment, an enrichment for flavonol biosynthesis enzymes was revealed. This rise in protein abundance revealed to be largely caused by an increase in gene expression and this occurred in a MAX2-dependent manner. We were also able to observe that the rise in the abundance of flavonol biosynthesis enzymes led to an increase in the products of the reactions they catalyze, both through non-biased metabolite profiling and finally through the cheaper and simpler technique of diphenylboric acid-2-aminoethyl (DPBA)-stained high performance thin layer chromatography (HPTLC) plates.

Ultimately this study provided not only new strigolactone responsive genes, but also a new root phenotype: the accumulation of flavonols upon GR24 treatment. This phenotype was not dependent of the stereochemistry of the GR24 inducer, as it was activated by either GR24+ or GR24-. In line with that result, both the KAI2 and D14 receptors were required for this effect suggesting a response to GR24 that involves both receptor proteins. Although this goes against the generally accepted hypothesis that the KAI2-mediated and D14-meditated signaling pathways, aside from their shared collaboration with MAX2, are independent, it does fall in line with several other pieces of evidence that suggest that this separation might not be as clear cut as previously suggested. Indeed, it has already been shown that to abolish the GR24-induced upregulation of the *CHS* gene in the hypocotyl, both D14 and KAI2 need to be rendered inactive (Waters et al. 2013 supplementary). Also, although not yet published, we have shown that to mimic the *max2* insensitivity to GR24 for the effect on the lateral root density, the double mutant *kai2 d14* is required. In sum, it is likely that, while for the most part these receptor proteins work separately, there seems to be at least some overlap in their downstream signaling in the hypocotyl and the root.

When comparing the *max2-1* root proteome with the WT, over 30% of the promoters of the genes encoding for the differential proteins were shown to be controlled by the transcription factor LONG HYPOCOTYL 5 (HY5) (Lee et al. 2007). The implication of HY5 in strigolactone signaling has been extensively studied in the hypocotyl, due to the early discovery that the *hy5* mutant, just like the *max2* mutant, did not show the GR24-enhanced inhibition of hypocotyl growth in the light that can

be observed in the WT (Tsuchiya et al. 2010). However, although there seems to be a consensus that HY5 plays at least a minor role in strigolactone signaling, where exactly this protein fits in the cascade is still a matter of debate. For example, there is no agreement on whether the action of this protein in strigolactone signaling is MAX2-dependent (Tsuchiya et al. 2010; Waters et al. 2013; Jia et al. 2013).

In any case, the high percentage of promoters controlled by HY5 found amongst the proteins differentially regulated between *max2* and WT seedlings led us to investigate a possible role for HY5 in the root response to GR24 (**Chapter 4**). We found that the *hy5* mutant shared several of the *max2* mutant's resistance phenotypes to GR24, such as the lack of variation in the lateral root density (LRD) upon treatment and the lack of root hair elongation. We also tested the newly discovered flavonol root read-out and showed that the *hy5* mutant also did not respond to GR24. This is in line with the previously reported control of the flavonol biosynthesis genes by HY5 (Lee et al. 2007; (Stracke et al., 2010). Downstream of HY5, the MYB12 transcription factor (TF) is recruited to exert the effect on the expression of the flavonol biosynthesis genes (Stracke et al. 2010). On closer inspection, the *myb12* knock-out did however not share the *hy5* mutant's resistance to GR24 treatment in its lateral root density or root hair phenotypes. This lack of overlap suggests that, although necessary to coordinate the flavonol response to GR24 downstream of HY5, it is unlikely that MYB12 is required for the entire HY5-mediated response. In line with this, we were able to identify at least one gene, *KIN2*, which is induced by GR24 in a HY5-dependent manner but does not require the action of MYB12.

To date, a consensus has still not been reached concerning whether the role of HY5 in GR24 signaling is MAX2-dependent. In our work, the part of the HY5 response that is mediated by MYB12, was shown to be MAX2-dependent and remains so for concentrations of GR24 varying from 1 to 5 μM. In turn, the expression of the biosynthesis genes that MYB12 controls, such as *CHS*, behave in the same manner. Previous work states that the GR24 effect on HY5 was independent of the action of MAX2 in the hypocotyl (Waters et al. 2013). The authors base this conclusion mainly on the observation that *max2hy5* double mutant's hypocotyl length is superior to that of the two single mutants and that *CHS* is the only HY5 and MAX2 dependent gene in its response to GR24 tested in this article. They therefore conclude that the *CHS* profile is an exception to the rule, and is probably the only gene to require both HY5 and MAX2 to modulate its response to the hormone. Our work is therefore at odds with this conclusion, as we have identified a large subset of strigolactone responsive genes whose induction depends both on MAX2 and HY5. On the other hand, our results are in line with work that later demonstrated that at physiologically relevant concentrations (i.e. less than 10 μM), the MAX2 regulated hypocotyl response to light is HY5-dependent (Jia. et al. 2013). Finally, to date, none of the other numerous phenotypes that GR24 is known to induce have been shown to be MAX2-independent. Therefore the Ockham's razor principle would dictate that it is most likely that the role of HY5 in strigolactone signaling is, for at least a large part, MAX2-dependent, and that observations that

indicate the contrary are likely due to the use of concentration of GR24 that exceed physiological relevance.

Finally, although our work has provided evidence that allows us to affirm that at least part of the response downstream of MAX2 is coordinated by HY5, it is difficult to completely rule out that other factors are also at play. Despite the multiple similarities between the phenotypes of *max2* and *hy5*, their overlap is not perfect. For instance, in our hands, *hy5* does not display a higher lateral root density that can be observed with the *max2* mutant when grown in mock conditions. We therefore assume that other players are also involved in coordinating the response downstream of MAX2. Also, it is likely that MAX2 is not the only protein that can influence HY5 stability. Indeed, it is known that the stability of this TF is dependent on a series of endogenous and exogenous cues (Hardtke et al. 2000; (Vandenbussche et al., 2007); Osterlund 2000; (Yu et al., 2013). Therefore, although MAX2 seems to be necessary for the entire HY5-mediated response to GR24, we hypothesize that other changes, such as hormonal backgrounds or light conditions can also affect the outcome of GR24 treatment on HY5. This hypothesis, when extrapolated to the hypocotyl, would also accommodate the possibility of an increased hypocotyl length in the *hy5max2* compared to the single mutants.

In sum, we propose a model in which GR24 signaling in the roots of Arabidopsis involves an intricate transcription network, which is triggered by the HY5 protein. The detection of GR24 gives rise to an increased stability of the HY5 protein, gradually leading to a rise in this TF abundance (Jia et al. 2013). Increased levels of HY5 in the nucleus lead to the induction of HY5 controlled genes. It would appear that HY5 controls a network of genes that eventually induces the well-described phenotypic response to GR24, such as reduced LRD, elongated root hairs and accumulation of flavonols. We have shown that HY5 delegates the regulation of at least the subset of genes coding for flavonol biosynthesis enzymes, to the TF MYB12. Therefore, after upstream signaling mediated by the MAX2 proteins and possibly either or both KAI2 and D14, an increase in HY5 stability triggers a transcriptional network of responsive genes, part of which are dependent on the action of MYB12. In this model, other factors can also influence HY5 stability (**Figure 1**).

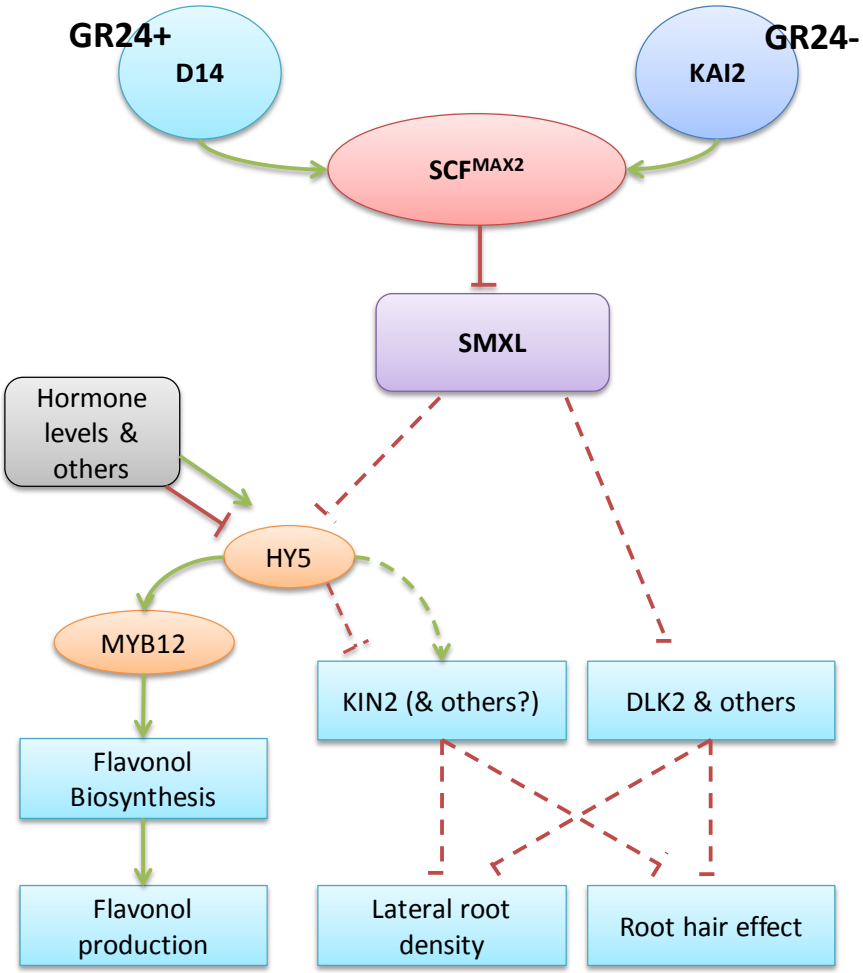

Figure 1: Model of MAX2-mediated signaling in the root: HY5 controled network of transcriptional changes in response to GR24 in the root of Arabidopsis thaliana downstream of MAX2, leading to the previously described and newly identified phenotypes such as the increase in flavonols. The solid lines represent either previously published data or data that is provided in this thesis. Dotted lines respresent possible links between the different signaling components.

Our work thus contributes to the ongoing discussion concerning whether the action of this hormone leads to transcriptional changes or not, by showing that at least part of the root response relies on an intricate transcriptional response. To corroborate our hypothesis, it will now be important to identify genes, like *KIN2*, that are involved in the MYB12-independent part of the HY5 response to GR24, as this part of the HY5-mediated response appears to be responsible for the morphological changes in the root in response to this compound. One way of proceeding here would be to use *KIN2* as a proxy of these genes and investigate the effect of GR24 on candidates that are known to be coexpressed with this gene. Another possibility would be to perform RNAseq to compare the transcriptomes of *max2*, *hy5* and WT in the presence and absence of GR24 treatment.

Another challenge that still has to be met will be to understand how the degradation of SMXL proteins by the SCF^{MAX2} leads to an increase in HY5 stability. To resolve this, it will first be necessary to identify which of the SMXL proteins are involved in the root response to GR24. A recent

publication reported that SMXL6, 7 and 8 are responsible for the higher LRD observed in *max2,* making them promising candidates (Soundappan et al. 2015). However, this study also reports that the long hypocotyl phenotype observed in *max2* is due to the incapacity of the SCF^{MAX2} in collaboration with KAI2 to degrade SMAX1 (Soundappan et al. 2015). This is likely the case for the phenotype of *max2* grown in red light in mock media, however, it has been shown that only the double mutant *kai2 d14* is completely insensitive to GR24 in its hypocotyl response in the light (scaffidi et al. 2014). This suggest that, at least in the hypocotyl, the degradation of not only SMAX1 but also probably SMXL6, 7 and 8 is necessary to give rise to the full GR24 response. We have shown here that to fully compromise the flavonol root response to GR24, both KAI2 and D14 need to be abolished (**Chapter 3**). We have also found that only the *kai2d14* double mutant displays the same insensitivity to GR24 in its LRD (personal communication Sylwia Struk). Taken together, these two elements suggest that, as in the case of the hypocotyl, not only the expected SMXL6, 7 and 8 but also SMAX1 are probably all involved in coordinating the root response to GR24. Also, even with the SMXL proteins identified, it is still not clear how the degradation of any of these proteins could lead to an increase in HY5 stability. The EAR domain in combination with what is known concerning analogous hormone signaling cascades in plants, suggest that in mock conditions the SMXL proteins help to repress expression of specific genes, probably in collaboration with a transcription factor(Pauwels et al., 2010; Szemenyei et al., 2008). It would therefore be interesting to see if the increase in HY5 protein levels as observed by Jia and his team, is actually due to the induction of *HY5* itself. In this case, GR24 would not necessary act on the stability of HY5, but rather simply increase the number of copies of this protein via transcriptional means.

From a broader perspective, more information could be gathered about the SMXL family's targeted degradation by the SCF^{MAX2} complex. Indeed, although their identification as targets represents in itself a large step forward, only a small amount of information is available on how these proteins are recognized and which domains on these proteins are necessary for this process to occur.

Despite the early discovery that MAX2 was part of an SCF complex (Stirnberg et al. 2007) and potentially gave rise to the targeted degradation of specific target proteins, the SMXL family members were not uncovered using proteomic tools (Jiang et al., 2013; Kong et al., 2014; Stanga et al., 2013; Zhou et al., 2013). This is mainly due to the fact that the tools available at the time to study the plant ubiquitinome were limited (Maor et al., 2007; Manzano et al., 2008; Saracco et al., 2009; Kim et al., 2013). More generally, several studies had attempted to profile ubiquitination events in plants through either single step or tandem affinity purification of ubiquitin itself (Maor et al., 2007; Manzano et al., 2008; Saracco et al., 2009). Although these studies provided some insight into the plant ubiquitinome, they all had several draw backs. For instance, for the one step purification protocol, it is difficult to assess to what extent the identified proteins can be considered as truly

ubiquitinated, because such purification techniques are prone to false positive identification. This can be explained by the co-purification of sticky proteins, interaction partners and various other contaminants (see **Chapter 6** for review). The multi-step purification methods overcame this problem, however they still provided very little information concerning the precise sites of ubiquitination (Saracco et al., 2009; Kim et al., 2013; Svozil et al., 2014). In mammalian systems, the anti-diglycine antibodies provided a solution to this problem and have become a landmark technology for ubiquitination site-identification (Kim et al., 2011; Wagner et al., 2011; Udeshi et al 2013). These antibodies are used to enrich peptides that carry the diglycine remnant that is generated upon tryptic cleavage of ubiquitined proteins. However, in plants, these antibodies have so far only provided only limited insight into the ubiquitinome of rice, when compared to the 10,000 site golden standard that is often seen in biomedical research (Li et al. 2015; Walton, Stes et al. 2016; Xie et al. 2015). Furthermore, to date their use has not been reported in Arabidopsis. This leaves the plant ubiquitin field to lag behind, and creates a need for studies that focus on profiling the ubiquitinome.

In an attempt to fill this gap, the ubiquitin COFRADIC technology was developed in our lab (**Chapter 5**) to purify ubiquitinated peptides. In human cell lines, this technology allowed to identify over 7000 ubiquitination sites on over 3000 proteins (Stes, Laga, Walton et al. 2014). Although the ubiquitin COFRADIC technology did not reach the 10 000 site bench mark set by the antibody technology in similar biological material, it did provide some new interesting biological insight. For instance, due to the fact that USP2 removes all ubiquitin, and not just lysine bound ubiquitin, we were able to also identify N-terminal ubiquitination on 9 proteins. In mammals, N-terminal ubiquitination has been reported in single protein studies, however, to our knowledge, this is the first profiling technology that also allows for its identification.

In a next step, the method was transferred to plants (**Chapter 6**). After several optimization experiments we opted for the use of a methanol/chloroform precipitation-based extraction method and also the choice of cell cultures for input material. Cell cultures were chosen because they provide a good protein yield, are the most space economically friendly system, and also allows for trigger-based experiments. The latter enables the comparison of multiple ubiquitinomes from cells subjected to various stimuli. The successful implementation of this technology allowed for the identification of over 3009 ubiquitination sites on over 1607 proteins in *Arabidopsis thaliana*. This first study provided the largest number of sites in any plants species and increased more than 10-fold the number of ubiquitination sites known in this model species. It is also to date the technology that shows simultaneously the highest number of ubiquitination sites and ubiquitinated proteins (**Figure 2**). Furthermore, we were also able to reveal the existence of N-terminal ubiquitination in Arabidopsis for the first time.

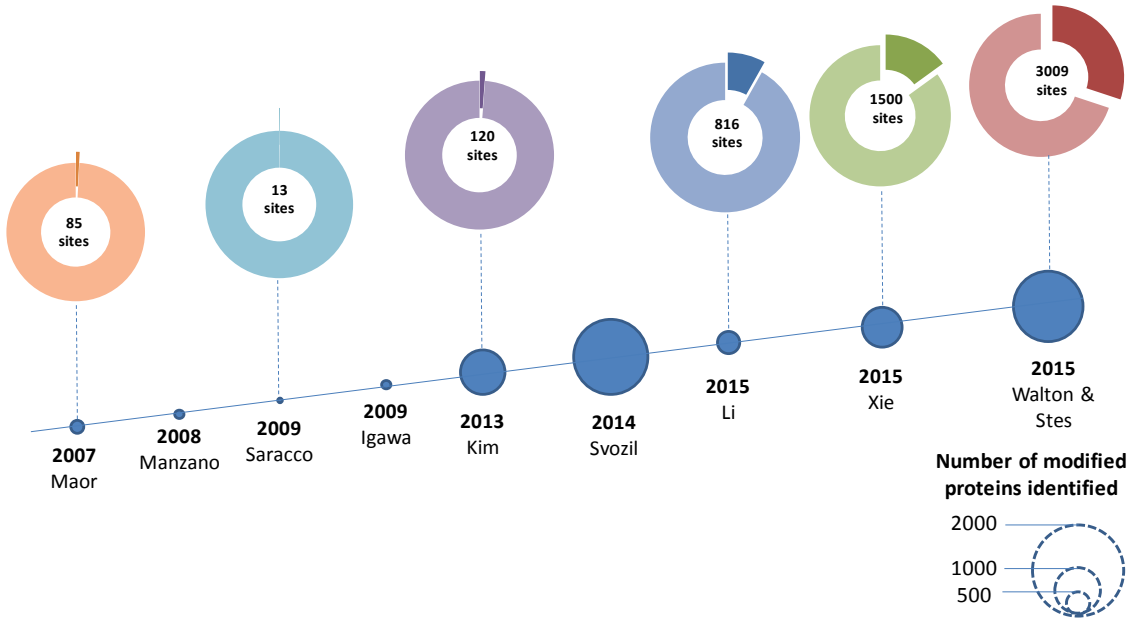

Figure 2: Performance of different ubiquitin profiling techniques in plants. All ubiquitin profiling studies that have been carried out in plants are given in chronological order. The size of the blue globes is proportional to the number of ubiquitinated proteins reported in the study. A legend is given in the bottom left. The number of detected sites is given above (when available) relative to the 10,000 site bench mark in the mammalian field in the pie charts above. When no sites are shown, it indicates that there was no site specific information reported in the concerned study.

For both studies, the false discovery rates were calculated. All methods available to profile the ubiquitinome are subject to false positive identifications. As mentioned before, purification techniques can also enrich for promiscuous proteins, interaction partners and others. Even the antibodies potentially enrich for proteins modified by other PTMs, such as neddylation, which in plants is thought to have a broader action than what has been described in mammals (Mergner et al. 2015). However, to our knowledge, despite this fact, none of the studies that aim to profile ubiquitinated proteins in plants report an FDR ((Maor et al., 2007; Manzano et al., 2008; Saracco et al., 2009; Kim et al., 2013; Li et al. 2015; Xie et al. 2015). To evaluate the number of identified false positives, we ran a blank ubiquitin COFRADIC experiment in which the USP2 step was omitted, on a comparable sample as the actual experiment. This allowed us to assess the acetylation efficiency, which is in our methodology the most likely source of possible false positives. While in the original protocol performed in Jurkat cells an FDR of around 0.06 was obtained, it fell below 0.01 in Arabidopsis. This is probably a fortunate side effect of the precipitation based protocol we implemented to improve protein yield from Arabidopsis cell cultures. Indeed, the early precipitation of proteins causes the endogenous deubiquitinases to be put rapidly and definitively out of action. Ineffective inactivation of deubiquitinases can give rise to the identification of false positives, through the removal of ubiquitin moieties before the acetylation "blocking" step in our protocol. Through this extra effort, we hope to have encouraged future authors to associate an estimated FDR to their studies, thereby setting a new

quality standard in the plant ubiquitin field and increasing the reliability of the data available to the science community. Finally, to bring this dataset to the plant scientists, we created a website, The UbiquitinationSite that harbors a searchable database of all identified sites. This allows users to test if their protein of interest is found to be ubiquitinated in our profiling studies and to obtain specific information concerning the exact site localization.

Building on the promising results from the ubiquitin COFRADIC in Arabidopsis, the technique was used to study changes in the ubiquitinome after application of GR24 (**Chapter 7**). Using this treatment as a proof of concept, peptides derived from SMXL proteins would be expected to present after treatment with GR24 (Soundappan et al. 2015; Wang et al. 2015). Indeed, via comparison of the ubiquitinomes extracted from cells that had been treated with 1 μM GR24 or the acetone carrier (mock control), SMXL6 was retrieved within the proteins detected to be ubiquitinated only upon GR24 treatment. It is not entirely clear why other members of this family were not found, however this result corresponds with the finding that *BRC1* gene responds to GR24 in cell cultures as both *BRC1* and SMXL6 are known to be involved in giving rise to the same GR24-dependent phenotype, shoot branching (Braun et al. 2012; Soundappan et al. 2015; Wang et al. 2015). This might be due to the fact that this is the only member of the *SMXL* family expressed in cell cultures.

Despite the fact that we are not the first to describe the ubiquitination of SMXL6 upon GR24 treatment, the COFRADIC technology not only provides information on the ubiquitination status of the protein, but also on the exact site of ubiquitination. We were therefore able to identify Lys750 as the probable site of ubiquitination on this MAX2 target. A recent study has proposed a model in which the degron, which is the part of a protein that allows it to be recognized for ubiquitin-mediated proteasomal degradation is made up of three parts: a primary degron which is composed of a sequence of amino acids recognized by the E3-ligase, a secondary degron which is a receiving lysine and finally a disordered segment which allows the initiation of the protein's processing by the 26S proteasome (Guharoy et al., 2016). Previously, it was shown that the deletion of a small linear sequence on the SMXL6 and SMXL7 proteins rendered these gene products resistant to degradation (Wang et al. 2015). Therefore, we hypothesize that this first linear sequence possibly corresponds to the primary degron, whereas the site identified by our study is likely to be the secondary degron. This hypothesis is reinforced by the fact that upon alignment, this lysine is conserved in SXML6, 7 and 8, which are known to be targeted by the SCF^{MAX2} complex in collaboration with D14, but not in SMAX1, which is targeted rather by the SCF^{MAX2} complex in collaboration with KAI2. The next step in this project will be to generate the lysine to arginine substitution through site directed mutagenesis. Interestingly, this is the substitution that can be observed in the SMAX1 protein compared to SMXL6, 7 and 8.

In order to use this technique in a differential setup, the size of the overlap between the ubiquitination sites identified in separate samples needs to be improved. Indeed, in our initial study in

Arabidopsis cell cultures, we observed a 13% difference when comparing the ubiquitinated proteins identified in 2 samples grown and harvested simultaneously in the same conditions. This difference likely arises from the fact that the ubiquitin COFRADIC only provides a snapshot of the ubiquitinome at the time of the harvesting of the cell cultures. As the cells are not synchronized, differences can arise due to the fact that in one sample a protein happens to be ubiquitinated whereas its counterpart in the other sample by chance is not be subject to this PTM at the time of sampling. When seeking to profile the ubiquitinome in general, as in **Chapter 5 and 6**, these difference do not represent a real problem, however, in a differential setup they become problematic. As seen in **Chapter 7**, although we do identify SMXL6 as being ubiquitinated in the GR24 treated sample and not in the mock control sample, there are more than 1000 other sites that also appear to behave the same way. Seeing as the members of the SMXL family have been argued to be the only direct targets of MAX2 upon GR24 detection (Soundappan et al. 2015), this result is not biologically relevant. In sum, in order to be used in a discovery phase of a project aiming to identify specific targets of a given E3-ligase, the size of the list of sites that the COFRADIC setup indicates as being differentially ubiquitinated needed to be reduced. Several modifications to the current protocol could provide solutions to this problem. First, adopting an experimental design including biological repeats should give rise to a more refined selection of proteins, which are ubiquitinated only under one or several of the conditions tested. Another factor that could help would be to carry out a differential ubiquitin COFRADIC study in a quantitative manner. A quantitative approach would allow for the identification of proteins that are significantly 'more' ubiquitinated based on their relative abundance over a number of samples. This would help discriminate these noisy sites from sites with regulatory significance with respect to the conditions tested. This can be accomplished in two ways. A first possibility would be to introduce a stable isotope labeling step directly in the ubiquitin COFRADIC protocol. This step could for example be executed by replacing the glycine in the Gly-BOC label used to mark the site of ubiquitination with a larger amino acid in which more heavy C atoms could be incorporated to provide a more subsequent shift. Stable isotope variants (^{13}C) of this amino acid could be used to specifically mark peptides from a given sample. Samples can next be mixed and these labels would allow for relative quantification of the ubiquitinated peptides. Combining the samples would also reduce the number of LC-MS runs necessary and would reduce experimentally induced variability between samples. Alternatively, label free quantification could be put to use. However, the 60 fractions per sample in the current setup would compromise the quality of a Label Free Quantification (LFQ) analysis. Ideally, miniaturization (i.e. reduction of the number of LC-MS runs per sample) of the ubiquitin COFRADIC would solve this problem. In sum, we have produced a new tool which, upon minor adjustments, has the potential to be of great use in differential ubiquitination studies in plants.

Summary

Over the past decade strigolactone signaling has been rapidly unraveled and early steps in the signaling are now reasonably well known, with the recent key roles of the KAI2 and D14 stereospecific recognition of GR24 molecules and the subsequent targeted degradation of either SMAX1 or SMXL6,7 and 8 respectively. However, information is still lacking concerning how the degradation of these proteins leads to the well described strigolactone phenotypes. With this work we have made use of various new tools in plant research, based on mass spectrometry-driven proteomics, in order to dissect both the early and the late signaling steps in this hormonal pathway, with a special focus on the roots. We have uncovered a new strigolactone induced root readout, consisting in a sharp measurable increase in flavonol production. This new readout, along with various other root phenotypes has allowed us to implicate both the transcription factor HY5 and MYB12 that coordinate an intricate transcriptional response to GR24 in the root of Arabidopsis. It will now be necessary to bridge the gap between the GR24 dependent action of these transcription factors and the degradation of SMXL proteins to fully understand how SL signaling occurs.

In our attempt to identify ubiquitination sites on the targets of the MAX2 F-box protein, which belongs to an SCF complex involved in SMAX1 and SMXL ubiquitination, we have developed a new COFRADIC based tool to allow for the profiling of ubiquitination events on the site level in Arabidopsis. We have provided an online database where all sites identified have been deposited and are accessible to plant scientist working on ubiquitination. This technique also allowed us in a differential experiment to identify an ubiquitination event on Lys750 of SMXL6 that only occurred in the presence of GR24. To continue this work we will use site directed mutagenesis to test whether the substitution of the lysine for and arginine can render this protein resistant to degradation.

Taken together, we have provided new insight into strigolactone signaling events. This work is also proof of the deep insight that newly implemented mass spectrometry based proteomics techniques can provide in plant research and we have even contributed to expanding this tool kit with the development of the Ubiquitin COFRADIC technology.

Nederlandse Samenvatting

Strigolactonen zijn belangrijke rhizosfeersignalen en plantenhormonen. Ze controleren de interacties van planten met arbusculaire mycorrhizae en plantenparasieten die behoren tot de familie van de Orobanchaceae. In hun functie als plantenhormoon controleren ze de kieming, de scheutarchitectuur maar ook de wortelarchitectuur van de plant. In het afgelopen decennium werd strigolactonsignalisatie in detail onderzocht. Deze signalisatie blijkt te starten met de stereospecifieke herkenning van strigolactonen door de KAI2 en D14 eiwitten, en de daaropvolgende gerichte afbraak van hun negatieve regulatoren, respectievelijk SMAX1 of SMXL6, 7 en 8 door het SCFMAX2 complex. Er ontbreekt echter nog informatie over hoe de afbraak van deze eiwitten leidt tot de goed beschreven strigolactonfenotypes.

In dit werk hebben we gebruik gemaakt van massaspectrometrie-gedreven proteoomanalyses om zowel de vroege als de late signalisatiestappen te ontleden, met een speciale focus op de strigolactoneffecten in de wortels van Arabidopsis thaliana. We ontdekten een nieuw strigolacton geïnduceerde worteleffect bestaande uit een duidelijk meetbare toename van de flavonolproductie. Dit nieuw fenotype, samen met diverse andere wortelfenotypes liet ons verder toe om zowel de transcriptiefactor HY5 als de transcriptiefactor MYB12 in de transcriptiecascade te plaatsen die door strigolactonen in de wortel van Arabidopsis geactiveerd wordt.

In een poging om meer inzichten te verwerven in de manier waarop SMXL eiwitten door het SCFMAX2 complex geubiquitineerd worden, werd een COFRADIC gebaseerde techniek ontwikkeld voor de profilering van ubiquitineringsplaatsen op eiwitten. Deze techniek leidde tot de identificatie van duizenden Arabidopsis geubiquitineerde sites die in een online database kunnen worden geraadpleegd. Dezelfde techniek, nu in een differentiële benadering, leidde tot de identificatie van de ubiquitinering van een specifiek lysine in SMXL6 en dit enkel in de aanwezigheid van strigolactones. De relevantie van deze site zal in de toekomst geanalyseerd worden.

Samenvattend hebben we nieuwe inzichten verworven in strigolactonsignalisatie, en dit vooral in de Arabidopsis wortel. Dit werk is ook een bewijs voor het effectief gebruik van nieuwe massaspectrometrie-gebaseerde proteoomanalytische technieken in het plantenonderzoek waarbij we zelf bijgedragen hebben door de ontwikkeling van de ubiquitine COFRADIC technologie.

CV

Alan WALTON
14 Heerweg zuid – 9052 Zwijnaarde
Tel. 0032493521027 – alwal@psb.vib-ugent.be
28 ans

Agricultural Engineer / PhD Biotechnology

PROFESSIONAL EXPERIENCE

Since 2014 — Research scientist: Plant Systems Biology (PSB)
Ghent (Belgium)
Improvement of root architecture
- Setting up bioassay pipelines
- Data analysis
- Presenting and communicating results
- Initiating and coordinating collaborations
- Project supervision

2012 (2 yr) — Research scientist: Medical Biotechnology Center (MBC)
Zwijnaarde (Belgique)
Designing biochemical tools to study plant proteins
- Development of new technologies (Ubiquitin COFRADIC, qTAP)
- Competitive intelligence, technological foresight

2011 (6 m) — Internship - Engineer: LRSV - CNRS
Toulouse
Improving the potential of Eucalyptus as a source of biofuel
- Yeast 2 hybrid
- Expression analysis and cloning of key genes

2010 (9 m) — Intership - Engineer: AgroCampus Ouest / INRA
Rennes
Inventory of biodiversity indicator insects by DNA barcoding (PCR-based).

EDUCATION

2016 — PhD in biotechnology/biochemistry
Crop improvement
Ghent University/ Flemish Insititute for biotechnology (VIB)

2012 — Speciialized Masters degree in plant biotech
Institut National Polytechnique – Toulouse

2011 — Engineer (Agronomy)
Ecole Nationale Supérieure Agronomique de Toulouse (ENSAT)

INTERESTS

- Sport: Squash, Football, Marathon
- Music: Trumpet, guitar
- Travel

KEY SKILLS

Team work ●●●●●	●●●●● Initiative
Communication ●●●●○	●●●●● Leadership
Analytical thinking ●●●●○	●●●●○ Perseverance
Adaptability ●●●●○	●●●○○ Patience
Project management ●●●●●	●●●○○ Receptiveness

RELATED KNOWLEDGE

- ❑ Communication
  - International seminars, Scienitific publications
- ❑ Data Analysis (Pack Office, R, SAS, Knime…)
- ❑ Languages/ International mobility

- English	Mother Tongue
- French	Bilingual (Lived 8 years in France)
- Portugeuse	Good Level (Erasmus Brazil – 6 months)
- Dutch	Good Level (Lived 4 years in Flanders)

3 QUALITES & 3 WEAKNESSESS

Hardworking
I devote myself to the projects I carry.

Impatient
I don't like it when things aren't progressing

Resourceful
I always come up with a solution

Competitive
I like having good results, sometimes a bit too much

Leadership
I'm good at motivating people to work towards a common goal

Convinvced
I'm learning to consider the ideas of others as much as I promote my own

RECOMMENDATIONS

Prof. Kris Gevaert
Vice-Directer of MBC
Tel: +32-92649274
kris.gevaert@vib-ugent.be

Prof. Sofie Goormachtig
Group leader PSB
Tel:+32 (0)9 331 39 10
sogoo@psb.vib-ugent.be

Dr. Elisabeth Stes
Science Communication
Tel: +32 9 244 66 11
elisabeth.stes@vib.be

➢ Scientific publications (A1 – published in journals listed in the ISI Web of Knowledge)

	IF	Ranking		Titre
1	3.807	17/79	(Q1)	**Walton A**, Stes E, De Smet I, Goormachtig S, Gevaert K (2015), 'Plant hormone signalling through the eye of the mass spectrometer', Proteomics 15, 11113-1126.
2	9.338	4/204	(Q1)	**Walton A**, Stes E, Cybulski N, Van Bel M, Inigo S, Nagels Durand A, Timmerman E, Heyman J, Pauwels L, De Veylder L, Goossens A, De Smet I, Coppens F, Goormachtig S, Gevaert K, 'It's time for some "site"-seeing: novel tools to monitor the ubiquitin landscape in Arabidopsis thaliana', Plant Cell, in press.
3	2.747	35/73	(Q2)	**Walton A**, Tsiatsiani L, Jacques S, Stes E, Messens J, Van Breusegem F, Goormachtig S, Gevaert K, 'Diagonal chromatography to study plant protein modifications', Biochim. Biophys. Acta, 2016.
4	3.263	33/204	(Q1)	Matthys, C., **Walton, A**., Struk, S., Stes, E., Boyer, F. D., Gevaert, K., & Goormachtig, S. (2016). The Whats, the Wheres and the Hows of strigolactone action in the roots. Planta, 1-11.
5	6.494	11/145	(Q1)	Derocles, S. A., Le Ralec, A., Besson, M. M., Maret, M., **Walton, A**., Evans, D. M., & Plantegenest, M. (2014). Molecular analysis reveals high compartmentalization in aphid–primary parasitoid networks and low parasitoid sharing between crop and noncrop habitats. Molecular ecology, 23(15), 3900-3911.
6	4.245	14/79	(Q1)	Stes E, Laga M, **Walton A**, Samyn N, Timmerman E, De Smet I, Goormachtig S, Gevaert K (2014), 'A COFRADIC protocol to study protein ubiquitination', J. Proteome Res. 13, 3107-3113.
7	9.338	4/204	(Q1)	Nelissen H, Eeckhout D, Demuynck K, Persiau G, **Walton A**, van Bel M, Vervoort M, Candaele J, De Block J, Aesaert S, Van Lijsebettens M, Goormachtig S, Vandepoele K, Van Leene J, Muszynski M, Gevaert K, Inzé D, De Jaeger G (2015), 'Dynamic Changes in ANGUSTIFOLIA3 Complex Composition Reveal a Growth Regulatory Mechanism in the Maize Leaf', Plant Cell 27, 1605-1619.

Supplementary data

Note: All data is available on the google drive.

Chapter 3

Supplemental Table 1: Overview of median log2 ratio values and p-vlaues for all proteins for which at least one of the terms tested was significant.

Supplemental Table 2: Overview of all log2 ratio values for all proteins indeitified and quantified during the shotgun experiement.

Chapter 5

Supplemental Table 1: Summary of N-terminal ubiquitination sites detected in the CoFraDic expereiment.

Supplemental Table 2: Summary of all ubiquitination sites found in Jurkat cells using the CoFraDic technology.

Chapter 6

Supplemental Table 1: Summary of all ubiquitination sites found in Arabidopsis cell cultures using the CoFraDic technology.

Supplemental Table 2: All proteins detected in the affinity enrichment protocol using HextaHis:UBQ10 lines

Chapter 7

Supplemental Table 1: summary of all ubiquitination sites found in mock and GR24 treated cell cultures from Arabidopsis.

References

Abe, S., Sado, A., Tanaka, K., Kisugi, T., Asami, K., Ota, S., Kim, H.I., Yoneyama, K., Xie, X., Ohnishi, T., Seto, Y., Yamaguchi, S., Akiyama, K., Yoneyama, K., and Nomura, T. (2014). Carlactone is converted to carlactonoic acid by MAX1 in *Arabidopsis* and its methyl ester can directly interact with AtD14 in vitro. *Proc. Natl. Acad. Sci. USA* 111, 18084-18089.

Akiyama, K., Matsuzaki, K.-i., and Hayashi, H. (2005). Plant sesquiterpenes induce hyphal branching in arbuscular mycorrhizal fungi. *Nature* 435, 824-827.

Al-Babili, S., and Bouwmeester, H.J. (2015). Strigolactones, a novel carotenoid-derived plant hormone. *Annu. Rev. Plant Biol*. 66, 161-186.

Alder, A., Holdermann ,I., Beyer, P., and Al-Babili, S. (2008). Carotenoid oxygenases involved in plant branching catalyse a highly specific conserved apocarotenoid cleavage reaction. *Biochem. J*. 416, 289-296.

Alder, A., Jamil, M., Marzorati, M., Bruno, M., Vermathen, M., Bigler, P., Ghisla, S., Bouwmeester, H., Beyer, P., and Al-Babili, S. (2012). The path from β-carotene to carlactone, a strigolactone-like plant hormone. *Science* 335, 1348-1351.

Alvarez, S., Hicks, L.M., and Pandey, S. (2011). ABA-dependent and -independent G-protein signaling in *Arabidopsis* roots revealed through an iTRAQ proteomics approach. *J. Proteome Res*. 10, 3107-3122.

Alvarez, S., Roy Choudhury, S., Hicks, L.M., and Pandey, S. (2013). Quantitative proteomics-based analysis supports a significant role of GTG proteins in regulation of ABA response in *Arabidopsis* roots. *J. Proteome Res*. 12, 1487-1501.

Arite, T., Kameoka, H., and Kyozuka, J. (2012). Strigolactone positively controls crown root elongation in rice. *J. Plant Growth Regul*. 31, 165-172.

Bainbridge, K., Sorefan, K., Ward, S., and Leyser, O. (2005). Hormonally controlled expression of the Arabidopsis *MAX4* shoot branching regulatory gene. *Plant J*. 44, 569-580.

Banfield, M.J. (2015). Perturbation of host ubiquitin systems by plant pathogen/pest effector proteins. *Cell. Microbiol*. 17, 18-25.

Bantscheff, M., Lemeer, S., Savitski, M.M., and Kuster, B. (2012). Quantitative mass spectrometry in proteomics: critical review update from 2007 to the present. *Anal. Bioanal. Chem*. 404, 939-965.

Barneche, F., Malapeira, J., and Mas, P. (2014). The impact of chromatin dynamics on plant light responses and circadian clock function. *J. Exp. Bot*. 65, 2895-2913.

Bennett, T., and Leyser, O. (2014). Strigolactone signalling: standing on the shoulders of DWARFs. *Curr. Opin. Plant Biol*. 22, 7-13.

Bennett, T., Sieberer, T., Willett, B., Booker, J., Luschnig, C., and Leyser, O. (2006). The *Arabidopsis MAX* pathway controls shoot branching by regulating auxin transport. *Curr. Biol*. 16, 553-563.

Beveridge, C.A., Dun, E.A., and Rameau, C. (2009). Pea has its tendrils in branching discoveries spanning a century from auxin to stringolactones. *Plant Physiol*. 151, 985-990.

Bindschedler, L.V., Palmblad, M., and Cramer, R. (2008). Hydroponic isotope labelling of entire plants (HILEP) for quantitative plant proteomics; an oxidative stress case study. *Phytochemistry* 69, 1962-1972.

Bish, R.A., and Myers, M.P. (2007). Werner helicase-interacting protein 1 binds polyubiquitin via its

zinc finger domain. *J. Biol. Chem*. 282, 23184-23193.

Bloom, J., Amador, V., Bartolini, F., DeMartino, G., and Pagano, M. (2003). Proteasome-mediated degradation of p21 via N-terminal ubiquitinylation. *Cell* 115, 71-82.

Booker, J., Auldridge, M., Wills, S., McCarty, D., Klee, H., and Leyser, O. (2004). MAX3/CCD7 is a carotenoid cleavage dioxygenase required for the synthesis of a novel plant signaling molecule. *Curr. Biol*. 14, 1232-1238.

Booker, J., Sieberer, T., Wright, W., Williamson, L., Willett, B., Stirnberg, P., Turnbull, C., Srinivasan, M., Goddard, P., and Leyser, O. (2005). *MAX1* encodes a cytochrome P450 family member that acts downstream of *MAX3/4* to produce a carotenoid-derived branch-inhibiting hormone. *Dev. Cell* 8, 443-449.

Bratzel, F., López-Torrejón, G., Koch, M., Del Pozo, J.C., and Calonje, M. (2010). Keeping cell identity in *Arabidopsis* requires PRC1 RING-finger homologs that catalyze H2A monoubiquitination. *Curr. Biol*. 20, 1853-1859.

Braun, N., de Saint Germain, A., Pillot, J.-P., Boutet-Mercey, S., Dalmais, M., Antoniadi, I., Li, X., Maia-Grondard, A., Le Signor, C., Bouteiller, N., Luo, D., Bendahmane, A., Turnbull, C., and Rameau, C. (2012). The pea TCP transcription factor PsBRC1 acts downstream of strigolactones to control shoot branching. *Plant Physiol*. 158, 225-238.

Braun, P., Aubourg, S., Van Leene, J., De Jaeger, G., and Lurin, C. (2013). Plant protein interactomes. *Annu. Rev. Plant Biol*. 64, 161-187.

Cadwell, K., and Coscoy, L. (2005). Ubiquitination on nonlysine residues by a viral E3 ubiquitin ligase. *Science* 309, 127-130 [Erratum *Science* 311, 177].

Calderon-Villalobos, L.I., Tan, X., Zheng, N., and Estelle, M. (2010). Auxin perception--structural insights. *Cold Spring Harb. Perspect. Biol*. 2, a005546.

Carrano, A.C., and Bennett, E.J. (2013). Using the ubiquitin-modified proteome to monitor protein homeostasis function. *Mol. Cell. Proteomics* 12, 3521-3531.

Chandrudu, S., Simerska, P., and Toth, I. (2013). Chemical methods for peptide and protein production. *Molecules* 18, 4373-4388.

Chapman, E.J., and Estelle, M. (2009). Mechanism of auxin-regulated gene expression in plants. *Annu. Rev. Genet*. 43, 265-285.

Chen, L., and Hellmann, H. (2013). Plant E3 ligases: flexible enzymes in a sessile world. *Mol. Plant* 6, 1388-1404.

Chen, Y., Hoehenwarter, W., and Weckwerth, W. (2010). Comparative analysis of phytohormone-responsive phosphoproteins in *Arabidopsis thaliana* using TiO_2-phosphopeptide enrichment and mass accuracy precursor alignment. *Plant J*. 63, 1-17.

Cheng, N.-H., Liu, J.-Z., Liu, X., Wu, Q., Thompson, S.M., Lin, J., Chang, J., Whitham, S.A., Park, S., Cohen, J.D., and Hirschi, K.D. (2011). *Arabidopsis* monothiol glutaredoxin, AtGRXS17, is critical for temperature-dependent postembryonic growth and development via modulating auxin response. *J. Biol. Chem*. 286, 20398-20406.

Chevalier, F, Nieminen, K, Sánchez‐Ferrero, J.C., Rodríguez, M.L., Chagoyen, M., Hardtke, C.S., and Cubas, P. (2014). Strigolactone promotes degradation of DWARF14, an α/β hydrolase essential for strigolactone signaling in *Arabidopsis*. *Plant Cell* 26, 1134-1150.

Cho, H., Ryu, H., Rho, S., Hill, K., Smith, S., Audenaert, D., Park, J., Han, S., Beeckman, T., Bennett, M.J., Hwang, D., De Smet, I., and Hwang, I. (2014). A secreted peptide acts on BIN2-mediated phosphorylation of ARFs to potentiate auxin response during lateral root development. *Nat. Cell Biol*. 16, 66-76.

Ciechanover, A., and Ben-Saadon, R. (2004). N-terminal ubiquitination: more protein substrates join in. *Trends Cell Biol*. 14, 103-106.

Clague, M.J., and Urbé, S. (2010). Ubiquitin: same molecule, different degradation pathways. *Cell* 143, 682-685.

Cluis, C.P., Mouchel, C.F., and Hardtke, C.S. (2004). The *Arabidopsis* transcription factor HY5 integrates light and hormone signaling pathways. *Plant J.* 38, 332-347.

Colaert, N., Helsens, K., Martens, L., Vandekerckhove, J., and Gevaert, K. (2009). Improved visualization of protein consensus sequences by iceLogo. *Nat. Methods* 6, 786-787.

Conn, C.E., Bythell-Douglas, R., Neumann, D., Yoshida, S., Whittington, B., Westwood, J.H., Shirasu, K., Bond, C.S., Dyer, K.A., and Nelson, D.C. (2015). Convergent evolution of strigolactone perception enabled host detection in parasitic plants. *Science* 349, 540-543.

Cook, C.E., Whichard, L.P., Wall, M.E., Egley, G.H., Coggon, P., Luhan, P.A., and McPhail, A.T. (1972). Germination stimulants. II. The structure of strigol--a potent seed germination stimulant for witchweed (*Striga lutea* Lour.). *J. Am. Chem. Soc*. 94, 6198-6199.

Cox, J., and Mann, M. (2008). MaxQuant enables high peptide identification rates, individualized p.p.b.-range mass accuracies and proteome-wide protein quantification. *Nat. Biotechnol*. 26, 1367-1372.

Cox, J., Neuhauser, N., Michalski, A., Scheltema, R.A., Olsen, J.V., and Mann, M. (2011). Andromeda: a peptide search engine integrated into the MaxQuant environment. *J. Proteome Res*. 10, 1794-1805.

Crawford, S., Shinohara, N., Sieberer, T., Williamson, L., George, G., Hepworth, J., Müller, D., Domagalska, M.A., and Leyser, O. (2010). Strigolactones enhance competition between shoot branches by dampening auxin transport. *Development* 137, 2905-2913.

Cuéllar Pérez, A., and Goossens, A. (2013). Jasmonate signalling: a copycat of auxin signalling? *Plant Cell Environ*. 36, 2071-2084.

Cui, F., Liu, L., Zhao, Q., Zhang, Z., Li, Q., Lin, B., Wu, Y., Tang, S., and Xie, Q. (2012). *Arabidopsis* ubiquitin conjugase UBC32 is an ERAD component that functions in brassinosteroid-mediated salt stress tolerance. *Plant Cell* 24, 233-244.

Danielsen, J.M.R., Sylvestersen, K.B., Bekker-Jensen, S., Szklarczyk, D., Poulsen, J.W., Horn, H., Jensen, L.J., Mailand, N., and Nielsen, M.L. (2011). Mass spectrometric analysis of lysine ubiquitylation reveals promiscuity at site level. *Mol. Cell. Proteomics* 10, M110.003590.

Davière, J.-M., and Achard, P. (2013). Gibberellin signaling in plants. *Development* 140, 1147-1151.

De Cuyper, C., Fromentin, J., Yocgo, R.E., De Keyser, A., Guillotin, B., Kunert, K., Boyer, F.-D., and Goormachtig, S. (2015). From lateral root density to nodule number, the strigolactone analogue GR24 shapes the root architecture of *Medicago truncatula*. *J. Exp. Bot.* 66, 137-146. [Corrigendum *J. Exp. Bot.* 66, 4091]

del Pozo, J.C., Dharmasiri, S., Hellmann, H., Walker, L., Gray, W.M., and Estelle, M. (2002). AXR1-ECR1-dependent conjugation of RUB1 to the Arabidopsis cullin AtCUL1 is required for auxin response. *Plant Cell* 14, 421-433.

Deng, Z., Oses-Prieto, J.A., Kutschera, U., Tseng, T.-S., Hao, L., Burlingame, A.L., Wang, Z.-Y., and Briggs, W.R. (2014). Blue light-induced proteomic changes in etiolated *Arabidopsis* seedlings. *J. Proteome Res*. 13, 2524-2533.

Deng, Z., Zhang, X., Tang, W., Oses-Prieto, J.A., Suzuki, N., Gendron, J.M., Chen, H., Guan, S., Chalkley, R.J., Peterman, T.K., Burlingame, A.L., and Wang, Z.-Y. (2007). A proteomics study of brassinosteroid response in *Arabidopsis*. *Mol. Cell. Proteomics* 6, 2058-2071.

Deruyffelaere, C., Bouchez, I., Morin, H., Guillot, A., Miquel, M., Froissard, M., Chardot, T., and D'Andrea, S. (2015). Ubiquitin-mediated proteasomal degradation of oleosins is involved in oil body mobilization during post-germinative seedling growth in Arabidopsis. *Plant Cell Physiol*. 56, 1374-1387.

Devoto, A., Muskett, P.R., and Shirasu, K. (2003). Role of ubiquitination in the regulation of plant defence against pathogens. *Curr. Opin. Plant Biol*. 6, 307-311.

Dharmasiri, N., Dharmasiri, S., and Estelle, M. (2005). The F-box protein TIR1 is an auxin receptor. *Nature* 435, 441-445.

Dharmasiri, S., Dharmasiri, N., Hellmann, H., and Estelle, M. (2003). The RUB/Nedd8 conjugation pathway is required for early development in *Arabidopsis*. *EMBO J*. 22, 1762-1770.

Dhonukshe, P., Huang, F., Galvan-Ampudia, C.S., Mähönen, A.P., Kleine-Vehn, J., Xu, J., Quint, A., Prasad, K., Friml, J., Scheres, B., and Offringa, R. (2010). Plasma membrane-bound AGC3 kinases phosphorylate PIN auxin carriers at TPRXS(N/S) motifs to direct apical PIN recycling. *Development* 137, 3245-3255.

Dill, A., Thomas, S.G., Hu, J., Steber, C.M., and Sun, T.-p. (2004). The Arabidopsis F-box protein SLEEPY1 targets gibberellin signaling repressors for gibberellin-induced degradation. *Plant Cell* 16, 1392-1405.

Domagalska, M.A., and Leyser, O. (2011). Signal integration in the control of shoot branching. *Nat. Rev. Mol. Cell Biol*. 12, 211-221.

Dreher, K., and Callis, J. (2007). Ubiquitin, hormones and biotic stress in plants. *Ann. Bot.* 99, 787-822.

Drummond, R.S.M., Martínez-Sánchez, N.M., Janssen, B.J., Templeton, K.R., Simons, J.L., Quinn, B.D., Karunairetnam, S., and Snowden, K.C. (2009). *Petunia hybrida CAROTENOID CLEAVAGE DIOXYGENASE7* is involved in the production of negative and positive branching signals in petunia. *Plant Physiol*. 151, 1867-1877.

El-Showk, S., Ruonala, R., and Helariutta, Y. (2013). Crossing paths: cytokinin signalling and crosstalk. *Development* 140, 1373-1383.

Engelsberger, W.R., and Schulze, W.X. (2012). Nitrate and ammonium lead to distinct global dynamic phosphorylation patterns when resupplied to nitrogen-starved Arabidopsis seedlings. *Plant J*. 69, 978-995.

Foo, E., Bullier, E., Goussot, M., Foucher, F., Rameau, C., and Beveridge, C.A. (2005). The branching gene *RAMOSUS1* mediates interactions among two novel signals and auxin in pea. *Plant Cell* 17, 464-474.

Furniss, J.J., and Spoel, S.H. (2015). Cullin-RING ubiquitin ligases in salicylic acid-mediated plant immune signaling. *Front. Plant Sci*. 6, 154.

Gagne, J.M., Smalle, J., Gingerich, D.J., Walker, J.M., Yoo, S.-D., Yanagisawa, S., and Vierstra, R.D. (2004). *Arabidopsis* EIN3-binding F-box 1 and 2 form ubiquitin-protein ligases that repress ethylene action and promote growth by directing EIN3 degradation. *Proc. Natl. Acad. Sci. USA* 101, 6803-6808.

Gampala, S.S., Kim, T.-W., He, J.-X., Tang, W., Deng, Z., Bai, M.-Y., Guan, S., Lalonde, S., Sun, Y., Gendron, J.M., Chen, H., Shibagaki, N., Ferl, R.J., Ehrhardt, D., Chong, K., Burlingame, A.L., and Wang, Z.-Y. (2007). An essential role for 14-3-3 proteins in brassinosteroid signal transduction in *Arabidopsis*. *Dev. Cell* 13, 177-189.

Gevaert, K., Impens, F., Van Damme, P., Ghesquière, B., Hanoulle, X., and Vandekerckhove, J. (2007). Applications of diagonal chromatography for proteome-wide characterization of protein modifications and activity-based analyses. *FEBS J*. 274, 6277-6289.

Gevaert, K., Van Damme, J., Goethals, M., Thomas, G.R., Hoorelbeke, B., Demol, H., Martens, L., Puype, M., Staes, A., and Vandekerckhove, J. (2002). Chromatographic isolation of methionine-containing peptides for gel-free proteome analysis: identification of more than 800 *Escherichia coli* proteins. *Mol. Cell. Proteomics* 1, 896-903.

Ghelis, T. (2011). Signal processing by protein tyrosine phosphorylation in plants. *Plant Signal. Behav*. 6, 942-951.

Ghesquière, B., Colaert, N., Helsens, K., Dejager, L., Vanhaute, C., Verleysen, K., Kas, K., Timmerman, E., Goethals, M., Libert, C., Vandekerckhove, J., and Gevaert, K. (2009). *In vitro* and *in vivo* protein-bound tyrosine nitration characterized by diagonal chromatography. *Mol. Cell. Proteomics* 8, 2642-2652.

Gilroy, S., and Jones, D.L. (2000). Through form to function: root hair development and nutrient uptake. *Trends Plant Sci*. 5, 56-60.

Gomez-Roldan, V., Fermas, S., Brewer, P.B., Puech-Pagès, V., Dun, E.A., Pillot, J.-P., Letisse, F., Matusova, R., Danoun, S., Portais, J.-C., Bouwmeester, H., Bécard, G., Beveridge, C.A., Rameau, C., and Rochange, S.F. (2008). Strigolactone inhibition of shoot branching. *Nature* 455, 189-194.

Gray, W.M., Kepinski, S., Rouse, D., Leyser, O., and Estelle, M. (2001). Auxin regulates SCF^{TIR1}-dependent degradation of AUX/IAA proteins. *Nature* 414, 271-276.

Gu, C., Kolodziejek, I., Misas-Villamil, J., Shindo, T., Colby, T., Verdoes, M., Richau, K.H., Schmidt, J., Overkleeft, H.S., and van der Hoorn, R.A.L. (2010). Proteasome activity profiling: a simple, robust and versatile method revealing subunit-selective inhibitors and cytoplasmic, defense-induced proteasome activities. *Plant J*. 62, 160-170.

Guharoy, M., Bhowmick, P., Sallam, M., and Tompa, P. (2016). Tripartite degrons confer diversity and specificity on regulated protein degradation in the ubiquitin-proteasome system. *Nat. Commun*. 7, 10239.

Guilfoyle, T.J., and Hagen, G. (2007). Auxin response factors. *Curr. Opin. Plant Biol*. 10, 453-460.

Guo, H., Li, L., Aluru, M., Aluru, S., and Yin, Y. (2013). Mechanisms and networks for brassinosteroid regulated gene expression. *Curr. Opin. Plant Biol*. 16, 545-553.

Guo, Y., Zheng, Z., La Clair, J.J., Chory, J., and Noel, J.P. (2013). Smoke-derived karrikin perception by the α/β-hydrolase KAI2 from *Arabidopsis*. *Proc. Natl. Acad. Sci. USA* 110, 8284-8289.

Guseman, J.M., Hellmuth, A., Lanctot, A., Feldman, T.P., Moss, B.L., Klavins, E., Calderón Villalobos, L.I.A., and Nemhauser, J.L. (2015). Auxin-induced degradation dynamics set the pace for lateral root development. *Development* 142, 905-909.

Ha, C.V., Leyva-González, M.A., Osakabe, Y., Tran, U.T., Nishimaya, R., Watanabe, Y., Tanaka, M., Seki, M., Yamaguchi, S., Dong, N.V., Yamaguchi-Shinozaki, K., Shinozaki, K., Herrera-Estrella, L., and Tran, L.-S.P. (2014). Positive regulatory role of strigolactone in plant responses to drought and salt stress. *Proc. Natl. Acad. Sci. USA* 111, 851-856.

Hakenjos, J.P., Richter, R., Dohmann, E.M.N., Katsiarimpa, A., Isono, E., and Schwechheimer, C. (2011). MLN4924 Is an efficient inhibitor of NEDD8 conjugation in plants. *Plant Physiol*. 156, 527-536.

Hale, J.E., Butler, J.P., Knierman, M.D., and Becker, G.W. (2000). Increased sensitivity of tryptic peptide detection by MALDI-TOF mass spectrometry is achieved by conversion of lysine to homoarginine. *Anal. Biochem*. 287, 110-117.

Hamiaux, C., Drummond, R.S.M., Janssen, B.J., Ledger, S.E., Cooney, J.M., Newcomb, R.D., and Snowden, K.C. (2012). DAD2 is an α/β hydrolase likely to be involved in the perception of the plant branching hormone, strigolactone. *Curr. Biol*. 22, 2032-2036.

Hardtke, C.S., Gohda, K., Osterlund, M.T., Oyama, T., Okada, K., and Deng, X.W. (2000). HY5 stability and activity in *Arabidopsis* is regulated by phosphorylation in its COP1 binding domain. *EMBO J*. 19, 4997-5006.

Hayward, A., Stirnberg, P., Beveridge, C., and Leyser, O. (2009). Interactions between auxin and strigolactone in shoot branching control. *Plant Physiol*. 151, 400-412.

He, J.-X., Gendron, J.M., Yang, Y., Li, J., and Wang, Z.-Y. (2002). The GSK3-like kinase BIN2 phosphorylates and destabilizes BZR1, a positive regulator of the brassinosteroid signaling pathway in *Arabidopsis*. *Proc. Natl. Acad. Sci. USA* 99, 10185–10190.

Hendriks, I.A., D'Souza, R.C., Chang, J.-G., Mann, M., and Vertegaal, A.C.O. (2015). System-wide identification of wild-type SUMO-2 conjugation sites. *Nat. Commun.* 6, 7289.

Heride, C., Urbé, S., and Clague, M.J. (2014). Ubiquitin code assembly and disassembly. *Curr. Biol.* 24, R215-R220.

Hjerpe, R., and Rodríguez, M.S. (2008). Efficient approaches for characterizing ubiquitinated proteins. *Biochem. Soc. Trans*. 36, 823-827.

Hotton, S.K., and Callis, J. (2008). Regulation of cullin RING ligases. *Annu. Rev. Plant Biol*. 59, 467-489.

Hua, Z., and Vierstra, R.D. (2011). The cullin-RING ubiquitin-protein ligases. *Annu. Rev. Plant Biol*. 62, 299-334.

Hua, Z., Zou, C., Shiu, S.-H., and Vierstra, R.D. (2011). Phylogenetic comparison of *F-Box* (*FBX*) gene superfamily within the plant kingdom reveals divergent evolutionary histories indicative of genomic drift. *PLoS ONE* 6, e16219.

Hwang, I., Sheen, J., and Müller, B. (2012). Cytokinin signaling networks. *Annu. Rev. Plant Biol*. 63, 353-380.

Igawa, T., Fujiwara, M., Takahashi, H., Sawasaki, T., Endo, Y., Seki, M., Shinozaki, K., Fukao, Y., and Yanagawa, Y. (2009). Isolation and identification of ubiquitin-related proteins from *Arabidopsis* seedlings. *J. Exp. Bot*. 60, 3067-3073.

Ippel, J.H., Pouvreau, L., Kroef, T., Gruppen, H., Versteeg, G., van den Putten, P., Struik, P.C., and van Mierlo, C.P.M. (2004). *In vivo* uniform ^{15}N-isotope labelling of plants: using the greenhouse for structural proteomics. *Proteomics* 4, 226-234.

Ishikawa, S., Maekawa, M., Arite, T., Onishi, K., Takamure, I., and Kyozuka, J. (2005). Suppression of tiller bud activity in tillering dwarf mutants of rice. *Plant Cell Physiol*. 46, 79-86.

Jiang, L., Liu, X., Xiong, G., Liu, H., Chen, F., Wang, L., Meng, X., Liu, G., Yu, H., Yuan, Y., Yi, W., Zhao, L., Ma, H., He, Y., Wu, Z., Melcher, K., Qian, Q., Xu, H.E., Wang, Y., and Li, J.(2013). DWARF 53 acts as a repressor of strigolactone signalling in rice. *Nature* 504, 401-405.

Jiang, L., Matthys, C., Marquez-Garcia, B., De Cuyper, C., Smet, L., De Keyser, A., Boyer, F.-D., Beeckman, T., Depuydt, S., and Goormachtig, S. (2016). Strigolactones spatially influence lateral root development through the cytokinin signaling network. *J. Exp. Bot.* 67, 379-389.

Jurado, S., Abraham, Z., Manzano, C., López-Torrejón, G., Pacios, L.F., and Del Pozo, J.C. (2010). The *Arabidopsis* cell cycle F-box protein SKP2A binds to auxin. *Plant Cell* 22, 3891-3904.

Kapulnik, Y., and Koltai, H. (2014). Strigolactone involvement in root development, response to abiotic stress, and interactions with the biotic soil environment. *Plant Physiol*. 166, 560-569.

Kapulnik, Y., Delaux, P.-M., Resnick, N., Mayzlish-Gati, E., Wininger, S., Bhattacharya, C., Séjalon-Delmas, N., Combier, J.-P., Bécard, G., Belausov, E., Beeckman, T., Dor, E., Hershenhorn, J., and Koltai, H. (2011). Strigolactones affect lateral root formation and root-hair elongation in *Arabidopsis*. *Planta* 233, 209-216.

Kapulnik, Y., Resnick, N., Mayzlish-Gati, E., Kaplan, Y., Wininger, S., Hershenhorn, J., and Koltai, H. (2011). Strigolactones interact with ethylene and auxin in regulating root-hair elongation in *Arabidopsis*. *J. Exp. Bot*. 62, 2915-2924.

Karlova, R., Boeren, S., Russinova, E., Aker, J., Vervoort, J., and de Vries, S. (2006). The *Arabidopsis* SOMATIC EMBRYOGENESIS RECEPTOR-LIKE KINASE1 protein complex includes BRASSINOSTEROID-INSENSITIVE1. *Plant Cell* 18, 626-638.

Kasai, K., Takano, J., and Fujiwara, T. (2014). Analysis of endocytosis and ubiquitination of the BOR1 transporter. In *Plant Endosomes: Methods and Protocols* (Methods in Molecular Biology Series, Vol. 1209), M.S. Otegui (Ed.). New York, Humana Press, pp. 203-217 [ISBN 978-1-4939-1419-7].

Kelley, D.R., and Estelle, M. (2012). Ubiquitin-mediated control of plant hormone signaling. *Plant Physiol*. 160, 47-55.

Kepinski, S., and Leyser, O. (2005). The *Arabidopsis* F-box protein TIR1 is an auxin receptor. *Nature* 435, 446-451.

Kerkeb, L., Mukherjee, I., Chatterjee, I., Lahner, B., Salt, D.E., and Connolly, E.L. (2008). Iron-induced turnover of the Arabidopsis IRON-REGULATED TRANSPORTER1 metal transporter requires lysine residues. *Plant Physiol*. 146, 1964-1973.

Kierszniowska, S., Walther, D., and Schulze, W.X. (2009b). Ratio-dependent significance thresholds in reciprocal ^{15}N-labeling experiments as a robust tool in detection of candidate proteins responding to biological treatment. *Proteomics* 9, 1916-1924.

Kim, D.-Y., Scalf, M., Smith, L.M., and Vierstra, R.D. (2013). Advanced proteomic analyses yield a deep catalog of ubiquitylation targets in *Arabidopsis*. *Plant Cell* 25, 1523-1540.

Kim, W., Bennett, E.J., Huttlin, E.L., Guo, A., Li, J., Possemato, A., Sowa, M.E., Rad, R., Rush, J., Comb, M.J., Harper, J.W., and Gygi, S.P. (2011). Systematic and quantitative assessment of the ubiquitin-modified proteome. *Mol. Cell* 44, 325-340.

King, B., Trimarchi, T., Reavie, L., Xu, L., Mullenders, J., Ntziachristos, P., Aranda-Orgilles, B., Perez-Garcia, A., Shi, J., Vakoc, C., Sandy, P., Shen, S.S., Ferrando, A., and Alfantis, I. (2013). The ubiquitin ligase FBXW7 modulates leukemia-initiating cell activity by regulating MYC stability. *Cell* 153, 1552-1566.

Kinoshita, A., ten Hove, C.A., Tabata, R., Yamada, M., Shimizu, N., Ishida, T., Yamaguchi, K., Shigenobu, S., Takebayashi, Y., Iuchi, S., Kobayashi, M., Kurata, T., Wada, T., Seo, M., Hasebe, M., Blilou, I., Fukuda, H., Scheres, B., Heidstra, R., Kamiya, Y., and Sawa, S. (2015). A plant U-box protein, PUB4, regulates asymmetric cell division and cell proliferation in the root meristem. *Development* 142, 444-453.

Kleine-Vehn, J., Huang, F., Naramoto, S., Zhang, J., Michniewicz, M., Offringa, M., and Friml, J. (2009). PIN auxin efflux carrier polarity is regulated by PINOID kinase-mediated recruitment into GNOM-independent trafficking in *Arabidopsis*. *Plant Cell* 21, 3839-3849.

Kline, K.G., Barrett-Wilt, G.A., and Sussman, M.R. (2010). *In planta* changes in protein phosphorylation induced by the plant hormone abscisic acid. *Proc. Natl. Acad. Sci. USA* 107, 15986-15991.

Kohlen, W., Charnikhova, T., Liu, Q., Bours, R., Domagalska, M.A., Beguerie, S., Verstappen, F., Leyser, O., Bouwmeester, H., and Ruyter-Spira, C. (2011). Strigolactones are transported through the xylem and play a key role in shoot architectural response to phosphate deficiency in nonarbuscular mycorrhizal host Arabidopsis. *Plant Physiol*. 155, 974-987.

Koltai, H. (2011). Strigolactones are regulators of root development. *New Phytol*. 190, 545-549.

Koltai, H., Dor, E., Hershenhorn, J., Joel, D.M., Weininger, S., Lekalla, S., Shealtiel, H., Bhattacharya, C., Eliahu, E., Resnick, N., Barg, R., and Kapulnik, Y. (2010). Strigolactones' effect on root growth and root-hair elongation may be mediated by auxin-efflux carriers. *J. Plant Growth Regul*. 29, 129-136.

Komander, D., and Rape, M. (2012). The ubiquitin code. *Annu. Rev. Biochem*. 81, 203-229.

Kong, X., Zhang, M., and Ding, Z. (2014). D53: the missing link in strigolactone signaling. *Mol. Plant* 7, 761-763.

Koornneef, M., Rolff, E., and Spruit, C.J.P. (1980). Genetic control of light-inhibited hypocotyl elongation in *Arabidopsis thaliana* (L.) Heynh. *Z. Pflanzenphysiol*. 100, 147-160.

Koren, D., Resnick, N., Mayzlish Gati, E., Belausov, E., Weininger, S., Kapulnik, Y., and Koltai, H. (2013). Strigolactone signaling in the endodermis is sufficient to restore root responses and involves SHORT HYPOCOTYL 2 (SHY2) activity. *New Phytol*. 198, 866-874.

Kravtsova-Ivantsiv, Y., and Ciechanover, A. (2012). Non-canonical ubiquitin-based signals for proteasomal degradation. *J. Cell Sci*. 125, 539-548.

Kretzschmar, T., Kohlen, W., Sasse, J., Borghi, L., Schlegel, M., Bachelier, J.B., Reinhardt, D., Bours, R., Bouwmeester, H.J., and Martinoia, E. (2012). A petunia ABC protein controls strigolactone-dependent symbiotic signalling and branching. *Nature* 483, 341-344.

Lassmann, T., and Sonnhammer, E.L.L. (2005). Kalign – an accurate and fast multiple sequence alignment algorithm. *BMC Bioinformatics* 6, 298.

Lazar, G., and Goodman, H.M. (2006). *MAX1*, a regulator of the flavonoid pathway, controls vegetative axillary bud outgrowth in *Arabidopsis*. *Proc. Natl. Acad. Sci. USA* 103, 472-476.

Lee, J., He, K., Stolc, V., Lee, H., Figueroa, P., Gao, Y., Tongprasit, W., Zhao, H., Lee, I., and Deng, X.W. (2007). Analysis of transcription factor HY5 genomic binding sites revealed its hierarchical role in light regulation of development. *Plant Cell* 19, 731-749.

Leitner, J., Petrášek, J., Tomanov, K., Retzer, K., Pa_ezová, M., Korbei, B., Bachmair, A., Za_ímalová, E., and Luschnig, C. (2012). Lysine^{63}-linked ubiquitylation of PIN2 auxin carrier protein governs hormonally controlled adaptation of *Arabidopsis* root growth. *Proc. Natl. Acad. Sci. USA* 109, 8322-8327.

Lewandowska, D., ten Have, S., Hodge, K., Tillemans, V., Lamond, A.I., and Brown, J.W.S. (2013). Plant SILAC: stable-isotope labelling with amino acids of *Arabidopsis* seedlings for quantitative proteomics. *PLoS ONE* 8, e72207.

Leyser, O. (2006). Dynamic integration of auxin transport and signalling. *Curr. Biol*. 16, R424-R433.

Li, J., Wen, J., Lease, K.A., Doke, J.T., Tax, F.E., and Walker, J.C. (2002). BAK1, an *Arabidopsis* LRR receptor-like protein kinase, interacts with BRI1 and modulates brassinosteroid signaling. *Cell* 110, 213-222.

Li, L., Nelson, C.J., Solheim, C., Whelan, J., and Millar, A.H. (2012). Determining degradation and synthesis rates of *Arabidopsis* proteins using the kinetics of progressive ^{15}N labeling of two-dimensional gel-separated protein spots. *Mol. Cell. Proteomics* 11, M111.010025.

Li, X.-M., Chao, D.-Y., Wu, Y., Huang, X., Chen, K., Cui, L.-G., Su, L., Ye, W.-W., Chen, H., Chen, H.-C., Dong, N.-Q., Guo, T., Shi, M., Feng, Q., Zhang, P., Han, B., Shan, J.-X., Gao, J.-P., and Lin, H.-X. (2015). Natural alleles of a proteasome α2 subunit gene contribute to thermotolerance and adaptation of African rice. *Nat. Genet*. 47, 827-833.

Li, Z., Czarnecki, O., Chourey, K., Yang, J., Tuskan, G.A., Hurst, G.B., Pan, C., and Chen, J.-G. (2014). Strigolactone-regulated proteins revealed by iTRAQ-based quantitative proteomics in *Arabidopsis*. *J. Proteome Res*. 13, 1359-1372.

Lian, H.-L., He, S.-B., Zhang, Y.-C., Zhu, D.-M., Zhang, J.-Y., Jia, K.-P., Sun, S.-X., Li, L., and Yang, H.-Q. (2011). Blue-light-dependent interaction of cryptochrome 1 with SPA1 defines a dynamic signaling mechanism. *Genes Dev*. 25, 1023-1028.

Lin, H., Wang, R., Qian, Q., Yan, M., Meng, X., Fu, Z., Yan, C., Jiang, B., Su, Z., Li, J., and Wang, Y. (2009). DWARF27, an iron-containing protein required for the biosynthesis of strigolactones, regulates rice tiller bud outgrowth. *Plant Cell* 21, 1512-1525.

Lin, W., Li, B., Lu, D., Chen, S., Zhu, N., He, P., and Shan, L. (2014). Tyrosine phosphorylation of

protein kinase complex BAK1/BIK1 mediates *Arabidopsis* innate immunity. *Proc. Natl. Acad. Sci. USA* 111, 3632-3637.

Lin, Z., Zhong, S., and Grierson, D. (2009). Recent advances in ethylene research. *J. Exp. Bot*. 60, 3311-3336.

Liu, B., Zuo, Z., Liu, H., Liu, X., and Lin, C. (2011). *Arabidopsis* cryptochrome 1 interacts with SPA1 to suppress COP1 activity in response to blue light. *Genes Dev*. 25, 1029-1034.

Liu, H., and Stone, S.L. (2011). E3 ubiquitin ligases and abscisic acid signaling. *Plant Signal. Behav*. 6, 344-348.

Liu, H., and Stone, S.L. (2013). Cytoplasmic degradation of the *Arabidopsis* transcription factor ABSCISIC ACID INSENSITIVE 5 is mediated by the RING-type E3 ligase KEEP ON GOING. *J. Biol. Chem*. 288, 20267-20279.

Liu, H., Sadygov, R.G., Yates, J.R., III (2004). A model for random sampling and estimation of relative protein abundance in shotgun proteomics. *Anal. Chem*. 76, 4193-4201.

Liu, J., Novero, M., Charnikhova, T., Ferrandino, A., Schubert, A., Ruyter-Spira, C., Bonfante, P., Lovisolo, C., Bouwmeester, H.J., and Cardinale, F. (2013). *CAROTENOID CLEAVAGE DIOXYGENASE 7* modulates plant growth, reproduction, senescence, and determinate nodulation in the model legume *Lotus japonicus*. *J. Exp. Bot*. 64, 1967-1981.

Livak, K.J., and Schmittgen, T.D. (2001). Analysis of relative gene expression data using real-time quantitative PCR and the $2^{-\Delta\Delta C_T}$ method. *Methods* 25, 402-408.

López-Bucio, J., Cruz-Ramírez, A., and Herrera-Estrella, L. (2003). The role of nutrient availability in regulating root architecture. *Curr. Opin. Plant Biol*. 6, 280-287.

López-Ráez, J.A., and Bouwmeester, H. (2008). Fine-tuning regulation of strigolactone biosynthesis under phosphate starvation. *Plant Signal. Behav*. 3, 963-965.

Maloney, G.S., DiNapoli, K.T., and Muday, G.K. (2014). The *anthocyanin reduced* tomato mutant demonstrates the role of flavonols in tomato lateral root and root hair development. *Plant Physiol*. 166, 614-631.

Mann, M. (2006). Functional and quantitative proteomics using SILAC. *Nat. Rev. Mol. Cell Biol*. 7, 952-958.

Manzanillo, P.S., Ayres, J.S., Watson, R.O., Collins, A.C., Souza, G., Rae, C.S., Schneider, D.S., Nakamura, K., Shiloh, M.U., and Cox, J.S. (2013). The ubiquitin ligase parkin mediates resistance to intracellular pathogens. *Nature* 501, 512-516.

Manzano, C., Abraham, Z., López-Torrejón, G., and Del Pozo, J.C. (2008). Identification of ubiquitinated proteins in Arabidopsis. *Plant Mol. Biol*. 68, 145-158.

Maor, R., Jones, A., Nühse, T.S., Studholme, D.J., Peck, S.C., and Shirasu, K. (2007). Multidimensional protein identification technology (MudPIT) analysis of ubiquitinated proteins in plants. *Mol. Cell. Proteomics* 6, 601-610.

Marino, D., Peeters, N., and Rivas, S. (2012). Ubiquitination during plant immune signaling. *Plant Physiol*. 160, 15-27.

Martins, S., Dohmann, E.M.N., Cayrel, A., Johnson, A., Fischer, W., Pojer, F., Satiat-Jeunemaître, B., Jaillais, Y., Chory, J., Geldner, N., and Vert, G. (2015). Internalization and vacuolar targeting of the brassinosteroid hormone receptor BRI1 are regulated by ubiquitination. *Nat. Commun*. 6, 6151.

Martín-Trillo, M., and Cubas, P. (2010). TCP genes: a family snapshot ten years later. *Trends Plant Sci*. 15, 31-39 (2010).

Mashiguchi, K., Sasaki, E., Shimada, Y., Nagae, M., Ueno, K., Nakano, T., Yoneyama, K., Suzuki, Y., and Asami, T. (2009). Feedback-regulation of strigolactone biosynthetic genes and strigolactone-regulated genes in Arabidopsis. *Biosci. Biotechnol. Biochem*. 73, 2460-2465.

Mayzlish-Gati, E., De-Cuyper, C., Goormachtig, S., Beeckman, T., Vuylsteke, M., Brewer, P.B., Beveridge, C.A., Yermiyahu, U., Kaplan, Y., Enzer, Y., Wininger, S., Resnick, N., Cohen, M., Kapulnik, Y., and Koltai, H. (2012). Strigolactones are involved in root response to low phosphate conditions in Arabidopsis. *Plant Physiol*. 160, 1329-1341.

Merchante, C., Alonso, J.M., and Stepanova, A.N. (2013). Ethylene signaling: simple ligand, complex regulation. *Curr. Opin. Plant Biol*. 16, 554-560.

Mergner, J., and Schwechheimer, C. (2014). The NEDD8 modification pathway in plants. *Front. Plant Sci*. 5, 103.

Mergner, J., Heinzlmeir, S., Kuster, B., and Schwechheimer, C. (2015). DENEDDYLASE1 deconjugates NEDD8 from non-cullin protein substrates in *Arabidopsis thaliana*. *Plant Cell* 27, 741-753.

Mertins, P., Qiao, J.W., Patel, J., Udeshi, N.D., Clauser, K.R., Mani, D.R., Burgess, M.W., Gillette, M.A., Jaffe, J.D., and Carr, S.A. (2013). Integrated proteomic analysis of post-translational modifications by serial enrichment. *Nat. Methods* 10, 634-637.

Mevissen, T.E.T., Hospenthal, M.K., Geurink, P.P., Elliott, P.R., Akutsu, M., Arnaudo, N., Ekkebus, R., Kulathu, Y., Wauer, T., El Oualid, F., Freund, S.M.V., Ovaa, H., and Komander, D. (2013). OTU deubiquitinases reveal mechanisms of linkage specificity and enable ubiquitin chain restriction analysis. *Cell* 154, 169-184.

Miura, K., and Hasegawa, P.M. (2010). Sumoylation and other ubiquitin-like post-translational modifications in plants. *Trends Cell Biol*. 20, 223-232.

Moon, J., Parry, G., and Estelle, M. (2004). The ubiquitin-proteasome pathway and plant development. *Plant Cell* 16, 3181-3195.

Muday, G.K., Rahman, A., and Binder, B.M. (2012). Auxin and ethylene: collaborators or competitors? *Trends Plant Sci*. 17, 181-195.

Murray, J.A.H., Jones, A., Godin, C., and Traas, J. (2012). Systems analysis of shoot apical meristem growth and development: integrating hormonal and mechanical signaling. *Plant Cell* 24, 3907-3919.

Nakashima, K., and Yamaguchi-Shinozaki, K. (2013). ABA signaling in stress-response and seed development. *Plant Cell Rep*. 32, 959-970.

Nam, K.H., and Li, J. (2002). BRI1/BAK1, a receptor kinase pair mediating brassinosteroid signaling. *Cell* 110, 203-212.

Nelson, C.J., Li, L., and Millar, A.H. (2014). Quantitative analysis of protein turnover in plants. *Proteomics* 14, 579-592.

Nelson, D.C., Flematti, G.R., Riseborough, J.-A., Ghisalberti, E.L., Dixon, K.W., and Smith, S.M. (2010). Karrikins enhance light responses during germination and seedling development in *Arabidopsis thaliana*. *Proc. Natl. Acad. Sci. USA* 107, 7095-7100.

Nelson, D.C., Scaffidi, A., Dun, E.A., Waters, M.T., Flematti, G.R., Dixon, K.W., Beveridge, C.A., Ghisalberti, E.L., and Smith, S.M. (2011). F-box protein MAX2 has dual roles in karrikin and strigolactone signaling in *Arabidopsis thaliana*. *Proc. Natl. Acad. Sci. USA* 108, 8897-8902.

Nguyen, H.N., Kim, J.H., Hyun, W.Y., Nguyen, N.T., Hong, S.-W., and Lee, H. (2013). TTG1-mediated flavonols biosynthesis alleviates root growth inhibition in response to ABA. *Plant Cell Rep*. 32, 503-514.

Nguyen, T.T., Volkening, J.D., Rose, C.M., Venkateshwaran, M., Westphall, M.S., Coon, J.J., Ané, J.-M., and Sussman, M.R. (2015). Potential regulatory phosphorylation sites in a *Medicago truncatula* plasma membrane proton pump implicated during early symbiotic signaling in roots. *FEBS Lett*. 589, 2186-2193.

Ni, W., Xu, S.-L., Tepperman, J.M., Stanley, D.J., Maltby, D.A., Gross, J.D., Burlingame, A.L., Wang, Z.-Y., and Quail, P.H. (2014). A mutually assured destruction mechanism attenuates light signaling in *Arabidopsis*. *Science* 344, 1160-1164.

Nijman, S.M.B., Luna-Vargas, M.P.A., Velds, A., Brummelkamp, T.R., Dirac, A.M.G., Sixma, T.K., and Bernards, R. (2005). A genomic and functional inventory of deubiquitinating enzymes. *Cell* 123, 773-786.

Olsen, J.V., and Mann, M. (2013). Status of large-scale analysis of post-translational modifications by mass spectrometry. *Mol. Cell. Proteomics* 12, 3444-3452.

Osterlund, M.T., Hardtke, C.S., Wei, N., and Deng, X.W. (2000a). Targeted destabilization of HY5 during light-regulated development of *Arabidopsis*. *Nature* 405, 462-466.

Osterlund, M.T., Wei, N., and Deng, X.W. (2000b). The roles of photoreceptor systems and the COP1-targeted destabilization of HY5 in light control of Arabidopsis seedling development. *Plant Physiol*. 124, 1520-1524.

Oyama, T., Shimura, Y., and Okada, K. (1997). The *Arabidopsis HY5* gene encodes a bZIP protein that regulates stimulus-induced development of root and hypocotyl. *Genes Dev*. 11, 2983-2995.

Pandya‐Kumar, N., Shema, R., Kumar, M., Mayzlish-Gati, E., Levy, D., Zemach, H., Belausov, E., Wininger, S., Abu-Abied, M., Kapulnik, Y., and Koltai, H. (2014). Strigolactone analog GR24 triggers changes in PIN2 polarity, vesicle trafficking and actin filament architecture. *New Phytol*. 202, 1184-1196.

Park, H.J., Kim, W.-Y., Park, H.C., Lee, S.Y., Bohnert, H.J., and Yun, D.-J. (2011). SUMO and SUMOylation in plants. *Mol Cells* 32, 305-316.

Park, J.-Y., Kim, H.-J., and Kim, J. (2002). Mutation in domain II of IAA1 confers diverse auxin-related phenotypes and represses auxin-activated expression of *Aux/IAA* genes in steroid regulator-inducible system. *Plant J*. 32, 669-683.

Patra, B., Pattanaik, S., and Yuan, L. (2013). Ubiquitin protein ligase 3 mediates the proteasomal degradation of GLABROUS 3 and ENHANCER OF GLABROUS 3, regulators of trichome development and flavonoid biosynthesis in Arabidopsis. *Plant J*. 74, 435-447.

Pauwels, L., Fernández Barbero, G., Geerinck, J., Tilleman, S., Grunewald, W., Cuéllar Pérez, A., Chico, J.M., Vanden Bossche, R., Sewell, J., Gil, E., García-Casado, G., Witters, E., Inzé, D., Long, J.A., De Jaeger, G., Solano, R., and Goossens, A. (2010). NINJA connects the co-repressor TOPLESS to jasmonate signalling. *Nature* 464, 788-791.

Pauwels, L., Ritter, A., Goossens, J., Nagels Durand, A., Liu, H., Gu, Y., Geerinck, J., Boter, M., Vanden Bossche, R., De Clercq, R., Van Leene, J., Gevaert, K., De Jaeger, G., Solano, R., Stone, S., Innes, R.W., Callis, J., and Goossens, A. (2015). The RING E3 ligase KEEP ON GOING modulates JASMONATE ZIM-DOMAIN12 stability. *Plant Physiol*. 169, 1405-1417.

Peer, W.A. (2013). From perception to attenuation: auxin signalling and responses. *Curr. Opin. Plant Biol*. 16, 561-568.

Peng, J., Schwartz, D., Elias, J.E., Thoreen, C.C., Cheng, D., Marsischky, G., Roelofs, J., Finley, D., and Gygi, S.P. (2003). A proteomics approach to understanding protein ubiquitination. *Nat. Biotechnol*. 21, 921-926.

Peralta, D.A., Araya, A., Nardi, C.F., Busi, M.V., and Gomez-Casati, D.F. (2013). Characterization of the *Arabidopsis thaliana* E3 ubiquitin-ligase AtSINAL7 and identification of the ubiquitination sites. *PLoS ONE* 8, e73104.

Péret, B., De Rybel, B., Casimiro, I., Benková, E., Swarup, R., Laplaze, L., Beeckman, T., and Bennett, M.J. (2009). *Arabidopsis* lateral root development: an emerging story. *Trends Plant Sci*. 14, 399-408.

Petricka, J.J., Schauer, M.A., Megraw, M., Breakfield, N.W., Thompson, J.W., Georgiev, S., Soderblom, E.J., Ohler, U., Moseley, M.A., Grossniklaus, U., and Benfey, P.N. (2012). The protein expression landscape of the *Arabidopsis* root. *Proc. Natl. Acad. Sci. USA* 109, 6811-6818.

Pickart, C.M., and Fushman, D. (2004). Polyubiquitin chains: polymeric protein signals. *Curr. Opin. Chem. Biol*. 8, 610-616.

Pollastri, S., and Tattini, M. (2011). Flavonols: old compounds for old roles. *Ann. Bot*. 108, 1225-1233.

Polyn, S., Willems, A., and De Veylder, L. (2015). Cell cycle entry, maintenance, and exit during plant development. *Curr. Opin. Plant Biol*. 23, 1-7.

Prayitno, J., Imin, N., Rolfe, B.G., and Mathesius, U. (2006). Identification of ethylene-mediated protein changes during nodulation in *Medicago truncatula* using proteome analysis. *J. Proteome Res*. 5, 3084-3095.

Rao, S.R., Ford, K.L., Cassin, A.M., Roessner, U., Patterson, J.H., and Bacic, A. (2010). Proteomic and metabolic profiling of rice suspension culture cells as a model to study abscisic acid signaling response pathways in plants. *J. Proteome Res*. 9, 6623-6634.

Rappsilber, J., Mann, M., and Ishihama, Y. (2007). Protocol for micro-purification, enrichment, pre-fractionation and storage of peptides for proteomics using StageTips. *Nat. Protoc*. 2, 1896-1906.

Rasmussen, A., Beveridge, C.A., and Geelen, D. (2012). Inhibition of strigolactones promotes adventitious root formation. *Plant Signal. Behav*. 7, 694-697.

Rasmussen, A., Heugebaert, T., Matthys, C., Van Deun, R., Boyer, F.-D., Goormachtig, S., Stevens, C., and Geelen, D. (2013). A fluorescent alternative to the synthetic strigolactone GR24. *Mol. Plant* 6, 100-112.

Rasmussen, A., Mason, M.G., De Cuyper, C., Brewer, P.B., Herold, S., Agusti, J., Geelen, D., Greb, T., Goormachtig, S., Beeckman, T., and Beveridge, C.A. (2012). Strigolactones suppress adventitious rooting in Arabidopsis and pea. *Plant Physiol*. 158, 1976-1987.

Renatus, M., Parrado, S.G., D'Arcy, A., Eidhoff, U., Gerhartz, B., Hassiepen, U., Pierrat, B., Riedl, R., Vinzenz, D., Worpenberg, S., and Kroemer, M. (2006). Structural basis of ubiquitin recognition by the deubiquitinating protease USP2. *Structure* 14, 1293-1302.

Rose, J.K.C., Bashir, S., Giovannoni, J.J., Jahn, M.M., and Saravanan, R.S. (2004). Tackling the plant proteome: practical approaches, hurdles and experimental tools. *Plant J*. 39, 715-733.

Roux, K.J., Kim, D.I., and Burke, B. (2013). BioID: a screen for protein-protein interactions. *Curr. Protoc. Protein Sci*. 74, 19.23.1-19.23.14.

Ruyter-Spira, C., Kohlen, W., Charnikhova, T., van Zeijl, A., van Bezouwen, L., de Ruijter, N., Cardoso, C., Lopez-Raez, J.A., Matusova, R., Bours, R., Verstappen, F., and Bouwmeester, H. (2011). Physiological effects of the synthetic strigolactone analog GR24 on root system architecture in Arabidopsis: another belowground role for strigolactones? *Plant Physiol*. 155, 721-734.

Ryu, K.-Y., Baker, R.T., and Kopito, R.R. (2006). Ubiquitin-specific protease 2 as a tool for quantification of total ubiquitin levels in biological specimens. *Anal. Biochem*. 353, 153-155.

Sadanandom, A., Bailey, M., Ewan, R., Lee, J., and Nelis, S. (2012). The ubiquitin--proteasome system: central modifier of plant signalling. *New Phytol*. 196, 13-28.

Santelia, D., Henrichs, S., Vincenzetti, V., Sauer, M., Bigler, L., Klein, M., Bailly, A., Lee, Y., Friml, J., Geisler, M., and Martinoia, E. (2008). Flavonoids redirect PIN-mediated polar auxin fluxes during root gravitropic responses. *J. Biol. Chem*. 283, 31218-31226.

Santino, A., Taurino, M., De Domenico, S., Bonsegna, S., Poltronieri, P., Pastor, V., and Flors, V. (2013). Jasmonate signaling in plant development and defense response to multiple (a)biotic stresses. *Plant Cell Rep*. 32, 1085-1098.

Santner, A., and Estelle, M. (2009). Recent advances and emerging trends in plant hormone

signalling. *Nature* 459, 1071-1078.

Santner, A., and Estelle, M. (2010). The ubiquitin-proteasome system regulates plant hormone signaling. *Plant J*. 61, 1029-1040.

Saracco, S.A., Hansson, M., Scalf, M., Walker, J.M., Smith, L.M., and Vierstra, R.D. (2009). Tandem affinity purification and mass spectrometric analysis of ubiquitylated proteins in Arabidopsis. *Plant J*. 59, 344-358.

Saracco, S.A., Hansson, M., Scalf, M., Walker, J.M., Smith, L.M., and Vierstra, R.D. (2009). Tandem affinity purification and mass spectrometric analysis of ubiquitylated proteins in Arabidopsis. *Plant J*. 59, 344-358.

Sarraf, S.A., Raman, M., Guarani-Pereira, V., Sowa, M.E., Huttlin, E.L., Gygi, S.P., and Harper, J.W. (2013). Landscape of the PARKIN-dependent ubiquitylome in response to mitochondrial depolarization. *Nature* 496, 372-376.

Sasse, J., Simon, S., Gübeli, C., Liu, G.-W., Cheng, X., Friml, J., Bouwmeester, H., Martinoia, E., and Borghi, L. (2015). Asymmetric localizations of the ABC transporter PaPDR1 trace paths of directional strigolactone transport. *Curr. Biol*. 25, 647-655.

Scaffidi, A., Waters, M.T., Ghisalberti, E.L., Dixon, K.W., Flematti, G.R., and Smith, S.M. (2013). Carlactone-independent seedling morphogenesis in Arabidopsis. *Plant J*. 76, 1-9.

Scaffidi, A., Waters, M.T., Sun, Y.K., Skelton, B.W., Dixon, K.W., Ghisalberti, E.L., Flematti, G.R., and Smith, S.M. (2014). Strigolactone hormones and their stereoisomers signal through two related receptor proteins to induce different physiological responses in Arabidopsis. *Plant Physiol*. 165, 1221-1232.

Scaglione, K.M., Basrur, V., Ashraf, N.S., Konen, J.R., Elenitoba-Johnson, K.S.J., Todi, S.V., and Paulson, H.L. (2013). The ubiquitin-conjugating enzyme (E2) Ube2w ubiquitinates the N terminus of substrates. *J. Biol. Chem*. 288, 18784-18788.

Seo, P.J., and Mas, P. (2014). Multiple layers of posttranslational regulation refine circadian clock activity in *Arabidopsis*. *Plant Cell* 26, 79-87.

Seto, Y., Sado, A., Asami, K., Hanada, A., Umehara, M., Akiyama, K., and Yamaguchi, S. (2014). Carlactone is an endogenous biosynthetic precursor for strigolactones *Proc. Natl. Acad. Sci. USA* 111 1640-1645.

Shahnawaz, M., Thapa, A., and Park, I.-S. (2007). Stable activity of a deubiquitylating enzyme (Usp2-cc) in the presence of high concentrations of urea and its application to purify aggregation-prone peptides. *Biochem. Biophys. Res. Commun*. 359, 801-805.

Sheard, L.B., Tan, X., Mao, H., Withers, J., Ben-Nissan, G., Hinds, T.R., Kobayashi, Y., Hsu, F.-F., Sharon, M., Browse, J., He, S.Y., Rizo, J., Howe, G.A., and Zheng, N. (2010). Jasmonate perception by inositol-phosphate-potentiated COI1—JAZ co-receptor. *Nature* 468, 400-405.

Shen, H., Luong, P., and Huq, E. (2007). The F-Box protein MAX2 functions as a positive regulator of photomorphogenesis in Arabidopsis. *Plant Physiol*. 145, 1471-1483.

Shi, F., Takasaki, H., and Komatsu, S. (2008). Quantitative analysis of auxin-regulated proteins from basal part of leaf sheaths in rice by two-dimensional difference gel electrophoresis. *Phytochemistry* 69, 637-646.

Shi, Y., Xu, P., and Qin, J. (2011). Ubiquitinated proteome: ready for global? *Mol. Cell. Proteomics* 10, R110.006882.

Shimizu, Y., Okuda-Shimizu, Y., and Hendershot, L.M. (2010). Ubiquitylation of an ERAD substrate occurs on multiple types of amino acids. *Mol. Cell* 40, 917-926.

Shin, E.J., Shin, H.M., Nam, E., Kim, W.S., Kim, J.-H., Oh, B.-H., and Yun, Y. (2012). DeSUMOylating isopeptidase: a second class of SUMO protease. *EMBO Rep.* 13, 339-346.

Shinohara, N., Taylor, C., and Leyser, O. (2013). Strigolactone can promote or inhibit shoot branching by triggering rapid depletion of the auxin efflux protein PIN1 from the plasma membrane. *PLoS Biol*. 11, e1001474.

Simicek, M., Lievens, S., Laga, M., Guzenko, D., Aushev, V.N., Kalev, P., Baietti, M.F., Strelkov, S.V., Gevaert, K., Tavernier, J., and Sablina, A.A. (2013). The deubiquitylase USP33 discriminates between RALB functions in autophagy and innate immune response. *Nat. Cell Biol*. 15, 1220-1230.

Slade, W.O., Ray, W.K., Williams, P.M., Winkel, B.S.J., and Helm, R.F. (2012). Effects of exogenous auxin and ethylene on the *Arabidopsis* root proteome. *Phytochemistry* 84, 18-23.

Snowden, K.C., Simkin, A.J., Janssen, B.J., Templeton, K.R., Loucas, H.M., Simons, J.L., Karunairetnam, S., Gleave, A.P., Clark, D.G., and Klee, H.J. (2005). The *Decreased apical dominance1/Petunia hybrida CAROTENOID CLEAVAGE DIOXYGENASE8* gene affects branch production and plays a role in leaf senescence, root growth, and flower development. *Plant Cell* 17, 746-759.

Soboleva, T.A., and Baker, R.T. (2004). Deubiquitinating enzymes: Their functions and substrate specificity. *Curr. Protein Pept. Sci*. 5, 191-200.

Song, Y.H., Estrada, D.A., Johnson, R.S., Kim, S.K., Lee, S.Y., MacCoss, M.J., and Imaizumi, T. (2014). Distinct roles of FKF1, GIGANTEA, and ZEITLUPE proteins in the regulation of CONSTANS stability in *Arabidopsis* photoperiodic flowering. *Proc. Natl. Acad. Sci. USA* 111, 17672-17677.

Sorefan, K., Booker, J., Haurogné, K., Goussot, M., Bainbridge, K., Foo, E., Chatfield, S., Ward, S., Beveridge, C., Rameau, C., and Leyser, O. (2003). *MAX4* and *RMS1* are orthologous dioxygenase-like genes that regulate shoot branching in *Arabidopsis* and pea. *Genes Dev*. 17, 1469-1474.

Soundappan, I., Bennett, T., Morffy, N., Liang, Y., Stanga, J.P., Abbas, A., Leyser, O., and Nelson, D.C. (2015). SMAX1-LIKE/D53 family members enable distinct MAX2-dependent responses to strigolactones and karrikins in Arabidopsis. *Plant Cell* 27, 3143-3159.

Sridhar, V.V., Kapoor, A., Zhang, K., Zhu, J., Zhou, T., Hasegawa, P.M., Bressan, R.A., and Zhu, J.-K. (2007). Control of DNA methylation and heterochromatic silencing by histone H2B deubiquitination. *Nature* 447, 735-738.

Staes, A., Impens, F., Van Damme, P., Ruttens, B., Goethals, M., Demol, H., Timmerman, E., Vandekerckhove, J., and Gevaert, K. (2011). Selecting protein N-terminal peptides by combined fractional diagonal chromatography. *Nat. Protoc*. 6, 1130-1141.

Staes, A., Van Damme, P., Helsens, K., Demol, H., Vandekerckhove, J., and Gevaert, K. (2008). Improved recovery of proteome-informative, protein N-terminal peptides by combined fractional diagonal chromatography (COFRADIC). *Proteomics* 8, 1362-1370.

Stanga, J.P., Smith, S.M., Briggs, W.R., and Nelson, D.C. (2013). *SUPPRESSOR OF MORE AXILLARY GROWTH2 1* controls seed germination and seedling development in Arabidopsis. *Plant Physiol*. 163, 318-330.

Stecker, K.E., Minkoff, B.B., and Sussman, M.R. (2014). Phosphoproteomic analyses reveal early signaling events in the osmotic stress response. *Plant Physiol*. 165, 1171-1187.

Stes, E., Laga, M., Walton, A., Samyn, N., Timmerman, E., De Smet, I., Goormachtig, S., and Gevaert, K. (2014). A COFRADIC protocol to study protein ubiquitination. *J. Proteome Res*. 13, 3107-3113.

Stieglitz, B., Morris-Davies, A.C., Koliopoulos, M.G., Christodoulou, E., and Rittinger, K. (2012). LUBAC synthesizes linear ubiquitin chains via a thioester intermediate. *EMBO Rep*. 13, 840-846.

Stirnberg, P., Furner, I.J., and Leyser, H.M.O. (2007). MAX2 participates in an SCF complex which acts locally at the node to suppress shoot branching. *Plant J*. 50, 80-94.

Stirnberg, P., van de Sande, K., and Leyser, H.M.O. (2002). *MAX1* and *MAX2* control shoot lateral branching in *Arabidopsis*. *Development* 129, 1131-1141.

Stone, S.L., Williams, L.A., Farmer, L.M., Vierstra, R.D., and Callis, J. (2006). KEEP ON GOING, a RING E3 ligase essential for *Arabidopsis* growth and development, is involved in abscisic acid signaling. *Plant Cell* 18, 3415-3428.

Stracke, R., Favory, J.-J., Gruber, H., Bartelniewoehner, L., Bartels, S., Binkert, M., Funk, M., Weisshaar, B., and Ulm, R. (2010). The *Arabidopsis* bZIP transcription factor HY5 regulates expression of the *PFG1/MYB12* gene in response to light and ultraviolet-B radiation. *Plant Cell Environ*. 33, 88-103.

Stracke, R., Jahns, O., Keck, M., Tohge, T., Niehaus, K., Fernie, A.R., and Weisshaar, B. (2010). Analysis of PRODUCTION OF FLAVONOL GLYCOSIDES-dependent flavonol glycoside accumulation in *Arabidopsis thaliana* plants reveals MYB11-, MYB12- and MYB111-independent flavonol glycoside accumulation. *New Phytol*. 188, 985-1000.

Strader, L.C., Chen, G.L., and Bartel, B. (2010). Ethylene directs auxin to control root cell expansion. *Plant J*. 64, 874-884.

Strzalka, W., Bartnicki, F., Pels, K., Jakubowska, A., Tsurimoto, T., and Tanaka, K. (2013). RAD5a ubiquitin ligase is involved in ubiquitination of *Arabidopsis thaliana* proliferating cell nuclear antigen. *J. Exp. Bot*. 64, 859-869.

Stuttmann, J., Lechner, E., Guérois, R., Parker, J.E., Nussaume, L., Genschik, P., and Noël, L.D. (2009). COP9 signalosome- and 26S proteasome-dependent regulation of SCF^{TIR1} accumulation in *Arabidopsis*. *J. Biol. Chem*. 284, 7920-7930.

Sullivan, J.A., Shirasu, K., and Deng, X.W. (2003). The diverse roles of ubiquitin and the 26S proteasome in the life of plants. *Nat. Rev. Genet*. 4, 948-958.

Sun, H., Tao, J., Hou, M., Huang, S., Chen, S., Liang, Z., Xie, T., Wei, Y., Xie, X., Yoneyama, K., Xu, G., and Zhang, Y. (2015). A strigolactone signal is required for adventitious root formation in rice. *Ann. Bot*. 115, 1155-1162.

Sun, H., Tao, J., Liu, S., Huang, S., Chen, S., Xie, X., Yoneyama, K., Zhang, Y., and Xu, G. (2014). Strigolactones are involved in phosphate- and nitrate-deficiency-induced root development and auxin transport in rice. *J. Exp. Bot*. 65, 6735-6746.

Svozil, J., Hirsch-Hoffmann, M., Dudler, R., Gruissem, W., and Baerenfaller, K. (2014). Protein abundance changes and ubiquitylation targets identified after inhibition of the proteasome with syringolin A. *Mol. Cell. Proteomics* 13, 1523-1536.

Sylvestersen, K.B., Young, C., and Nielsen, M.L. (2013). Advances in characterizing ubiquitylation sites by mass spectrometry. *Curr. Opin. Chem. Biol*. 17, 49-58.

Szemenyei, H., Hannon, M., and Long, J.A. (2008). TOPLESS mediates auxin-dependent transcriptional repression during *Arabidopsis* embryogenesis. *Science* 319, 1384-1386.

Takahashi, Y., Ebisu, Y., Kinoshita, T., Doi, M., Okuma, E., Murata, Y., and Shimazaki, K.-i. (2013). bHLH transcription factors that facilitate K^+ uptake during stomatal opening are repressed by abscisic acid through phosphorylation. *Sci. Signal*. 6, ra48.

Tan, C., Wang, H., Zhang, Y., Qi, B., Xu, G., and Zheng, H. (2011). A proteomic approach to analyzing responses of *Arabidopsis thaliana* root cells to different gravitational conditions using an agravitropic mutant, *pin2* and its wild type. *Proteome Sci*. 9, 72.

Tang, W., Deng, Z., Oses-Prieto, J.A., Suzuki, N., Zhu, S., Zhang, X., Burlingame, A.L., and Wang, Z.-Y. (2008a). Proteomics studies of brassinosteroid signal transduction using prefractionation and two-dimensional DIGE. *Mol. Cell. Proteomics* 7, 728-738.

Tang, W., Kim, T.-W., Oses-Prieto, J.A., Sun, Y., Deng, Z., Zhu, S., Wang, R., Burlingame, A.L., and Wang, Z.-Y. (2008b). BSKs mediate signal transduction from the receptor kinase BRI1 in *Arabidopsis*. *Science* 321, 557-560.

Tang, W., Yuan, M., Wang, R., Yang, Y., Wang, C., Oses-Prieto, J.A., Kim, T.-W., Zhou, H.-W., Deng, Z., Gampala, S.S., Gendron, J.M., Jonassen, E.M., Lillo, C., DeLong, A., Burlingame, A.L., Sun, Y., and Wang, Z.-Y. (2011). PP2A activates brassinosteroid-responsive gene expression and plant growth by dephosphorylating BZR1. *Nat. Cell Biol*. 13, 124-131.

Tatham, M.H., Plechanovová, A., Jaffray, E.G., Salmen, H., and Hay, R.T. (2013). Ube2W conjugates ubiquitin to α-amino groups of protein N-termini. *Biochem. J*. 453, 137-145.

Thieme, C.J., Rojas-Triana, M., Stecyk, E., Schudoma, C., Zhang, W., Yang, L., Miñambres, M., Walther, D., Schulze, W.X., Paz-Ares, J., Scheible, W.-R., and Kragler, F. (2015). Endogenous *Arabidopsis* messenger RNAs transported to distant tissues. *Nat. Plants* 1, 15025 [Erratum *Nat. Plants* 1, 15088].

Thines, B., Katsir, L., Melotto, M., Niu, Y., Mandaokar, A., Liu, G., Nomura, K., He, S.Y., Howe, G.A., and Browse, J. (2007). JAZ repressor proteins are targets of the SCF^{COI1} complex during jasmonate signalling. *Nature* 448, 661-665.

Toh, S., Holbrook-Smith, D., Stokes, M.E., Tsuchiya, Y., and McCourt, P. (2014). Detection of parasitic plant suicide germination compounds using a high-throughput *Arabidopsis* HTL/KAI2 strigolactone perception system. *Chem. Biol*. 21, 988-998.

Toh, S., Kamiya, Y., Kawakami, N., Nambara, E., McCourt, P., and Tsuchiya, Y. (2012). Thermoinhibition uncovers a role for strigolactones in Arabidopsis seed germination. *Plant Cell Physiol*. 53, 107-117.

Toh, S., McCourt, P., and Tsuchiya, Y. (2012). *HY5* is involved in strigolactone-dependent seed germination in Arabidopsis. *Plant Signal. Behav*. 7, 556-558.

Tsuchiya, Y., Vidaurre, D., Toh, S., Hanada, A., Nambara, E., Kamiya, Y., Yamaguchi, S., and McCourt, P. (2010). A small-molecule screen identifies new functions for the plant hormone strigolactone. *Nat. Chem. Biol*. 6, 741-749.

Tsuchiya, Y., Yoshimura, M., Sato, Y., Kuwata, K., Toh, S., Holbrook-Smith, D., Zhang, H., McCourt, P., Itami, K., Kinoshita, T., and Hagihara, S. (2015). Probing strigolactone receptors in *Striga hermonthica* with fluorescence. *Science* 349, 864-868.

Turnbull, C.G.N., Booker, J.P., and Leyser, H.M.O. (2002). Micrografting techniques for testing long-distance signalling in *Arabidopsis*. *Plant J*. 32, 255-262.

Udeshi, N.D., Mani, D.R., Eisenhaure, T., Mertins, P., Jaffe, J.D., Clauser, K.R., Hacohen, N., and Carr, S.A. (2012). Methods for quantification of *in vivo* changes in protein ubiquitination following proteasome and deubiquitinase inhibition. *Mol. Cell. Proteomics* 11, 148-159.

Udeshi, N.D., Mertins, P., Svinkina, T., and Carr, S.A. (2013a). Large-scale identification of ubiquitination sites by mass spectrometry. *Nat. Protoc*. 8, 1950-1960.

Udeshi, N.D., Svinkina, T., Mertins, P., Kuhn, E., Mani, D.R., Qiao, J.W., and Carr, S.A. (2013b). Refined preparation and use of anti-diglycine remnant (K-ε-GG) antibody enables routine quantification of 10,000s of ubiquitination sites in single proteomics experiments. *Mol. Cell. Proteomics* 12, 825-831.

Umehara, M., Hanada, A., Yoshida, S., Akiyama, K., Arite, T., Takeda-Kamiya, N., Magome, H., Kamiya, Y., Shirasu, K., Yoneyama, K., Kyozuka, J., and Yamaguchi, S. (2008). Inhibition of shoot branching by new terpenoid plant hormones. *Nature* 455, 195-200.

Umezawa, T., Sugiyama, N., Takahashi, F., Anderson, J.C., Ishihama, Y., Peck, S.C., and Shinozaki, K. (2013). Genetics and phosphoproteomics reveal a protein phosphorylation network

in the abscisic acid signaling pathway in *Arabidopsis thaliana*. *Sci. Signal*. 6, rs8.

Ünlü, M., Morgan, M. E., and Minden, J. S. (1997). Difference gel electrophoresis: a single gel method for detecting changes in protein extracts. *Electrophoresis* 18, 2071-2077.

Urquhart, S., Foo, E., and Reid, J.B. (2015). The role of strigolactones in photomorphogenesis of pea is limited to adventitious rooting. *Physiol. Plant*. 153, 392-402.

Van Leene, J., Eeckhout, D., Persiau, G., Van De Slijke, E., Geerinck, J., Van Isterdael, G., Witters, E., and De Jaeger, G. (2011). Isolation of transcription factor complexes form *Arabidopsis* cell suspension cultures by tandem affinity purification. In *Plant Transcription Factors: Methods and Protocols*, Methods in Molecular Biology, Vol. 754, L. Yuan, and S.E. Perry (Eds.). Totowa, NJ, Humana Press, pp. 195-218.

Van Leene, J., Hollunder, J., Eeckhout, D., Persiau, G., Van De Slijke, E., Stals, H., Van Isterdael, G., Verkest, A., Neirynck, S., Buffel, Y., De Bodt, S., Maere, S., Laukens, K., Pharazyn, A., Ferreira, P.C.G., Eloy, N., Renne, C., Meyer, C., Faure, J.-D., Steinbrenner, J., Beynon, J., Larkin, J.C., Van de Peer, Y., Hilson, P., Kuiper, M., De Veylder, L., Van Onckelen, H., Inzé, D., Witters, E., and De Jaeger, G. (2010). Targeted interactomics reveals a complex core cell cycle machinery in *Arabidopsis thaliana*. *Mol. Syst. Biol*. 6, 397.

Van Leene, J., Stals, H., Eeckhout, D., Persiau, G., Van De Slijke, E., Van Isterdael, G., De Clercq, A., Bonnet, E., Laukens, K., Remmerie, N., Henderickx, K., De Vijlder, T., Abdelkrim, A., Pharazyn, A., Van Onckelen, H., Inzé, D., Witters, E., and De Jaeger, G. (2007). A tandem affinity purification-based technology platform to study the cell cycle interactome in *Arabidopsis thaliana*. *Mol. Cell. Proteomics* 6, 1226-1238.

Van Leene, J., Witters, E., Inzé, D., and De Jaeger, G. (2008). Boosting tandem affinity purification of plant protein complexes. *Trends Plant Sci*. 13, 517-520.

Vandenbussche, F., Habricot, Y., Condiff, A.S., Maldiney, R., Van Der Straeten, D., and Ahmad, M. (2007). HY5 is a point of convergence between cryptochrome and cytokinin signalling pathways in *Arabidopsis thaliana*. *Plant J*. 49, 428-441.

Vanstraelen, M., and Benková, E. (2012). Hormonal interactions in the regulation of plant development. *Annu. Rev. Cell Dev. Biol*. 28, 463-487.

Vierstra, R.D. (2009). The ubiquitin–26S proteasome system at the nexus of plant biology. *Nat. Rev. Mol. Cell Biol*. 10, 385-397.

Vierstra, R.D. (2012). The expanding universe of ubiquitin and ubiquitin-like modifiers. *Plant Physiol*. 160, 2-14.

Viswanathan, S., Ünlü, M., and Minden, J.S. (2006). Two-dimensional difference gel electrophoresis. *Nat. Protoc*. 1, 1351-1358.

Vittal, V., Shi, L., Wenzel, D.M., Scaglione, K.M., Duncan, E.D., Basrur, V., Elenitoba-Johnson, K.S.J., Baker, D., Paulson, H.L., Brzovic, P.S., and Klevit, R.E. (2015). Intrinsic disorder drives N-terminal ubiquitination by Ube2w. *Nat. Chem. Biol*. 11, 83-89.

Vizcaíno, J.A., Côté, R., Reisinger, F., Foster, J.M., Mueller, M., Rameseder, J., Hermjakob, H., and Martens, L. (2009). A guide to the Proteomics Identifications Database proteomics data repository. *Proteomics* 9, 4276-4283.

Vogel, J.T., Walter, M.H., Giavalisco, P., Lytovchenko, A., Kohlen, W., Charnikhova, T., Simkin, A.J., Goulet, C., Strack, D., Bouwmeester, H.J., Fernie, A.R., and Klee, H.J. (2010). SlCCD7 controls strigolactone biosynthesis, shoot branching and mycorrhiza-induced apocarotenoid formation in tomato. *Plant J*. 61, 300-311.

Vriet, C., Russinova, E., and Reuzeau, C. (2013). From squalene to brassinolide: the steroid metabolic and signaling pathways across the plant kingdom. *Mol. Plant* 6, 1738-1757.

Wagner, S.A., Beli, P., Weinert, B.T., Nielsen, M.L., Cox, J., Mann, M., and Choudhary, C. (2011).

A proteome-wide, quantitative survey of in vivo ubiquitylation sites reveals widespread regulatory roles. *Mol. Cell. Proteomics* 10, 1-13.

Waldie, T., McCulloch, H., and Leyser, O. (2014). Strigolactones and the control of plant development: lessons from shoot branching. *Plant J*., in press (doi: 10.1111/tpj.12488).

Walton, A., Stes, E., Cybulski, N., Van Bel, M., Iñigo, S., Nagels Durand, A., Timmerman, E., Heyman, J., Pauwels, L., De Veylder, L., Goossens, A., De Smet, I., Coppens F., Goormachtig, S., and Gevaert, K. (2016). It's time for some "site"-seeing: novel tools to monitor the ubiquitin landscape in *Arabidopsis thaliana*. *Plant Cell* 28, 6-16.

Walton, A., Tsiatsiani, L., Jacques, S., Stes, E., Messens, J., Van Breusegem, F., Goormachtig, S., and Gevaert, K. (2016b). Diagonal chromatography to study plant protein modifications. *Biochim. Biophys. Acta*, in press (doi: 10.1016/j.bbapap.2016.01.001).

Walzthoeni, T., Leitner, A., Stengel, F., and Aebersold, R. (2013). Mass spectrometry supported determination of protein complex structure. *Curr. Opin. Struct. Biol*. 23, 252-260.

Wang, C., Shang, J.-X., Chen, Q.-X., Oses-Prieto, J.A., Bai, M.-Y., Yang, Y., Yuan, M., Zhang, Y.-L., Mu, C.-C., Deng, Z., Wei, C.-Q., Burlingame, A.L., Wang, Z.-Y., and Sun, Y. (2013). Identification of BZR1-interacting proteins as potential components of the brassinosteroid signaling pathway in *Arabidopsis* through tandem affinity purification. *Mol. Cell. Proteomics* 12, 3653-3665.

Wang, F., Bai, M.-Y., Deng, Z., Oses-Prieto, J.A., Burlingame, A.L., Lu, T., Chong, K., and Wang, Z.-Y. (2010). Proteomic study identifies proteins involved in brassinosteroid regulation of rice growth. *J. Integr. Plant Biol*. 52, 1075-1085.

Wang, L., Wang, B., Jiang, L., Liu, X., Li, X., Lu, Z., Meng, X., Wang, Y., Smith, S.M., and Li, J. (2015). Strigolactone signaling in Arabidopsis regulates shoot development by targeting D53-like SMXL repressor proteins for ubiquitination and degradation. *Plant Cell* 27, 3128-3142.

Wang, P., Xue, L., Batelli, G., Lee, S., Hou, Y.-J., Van Oosten, M.J., Zhang, H., Tao, W.A., and Zhu, J.-K. (2013). Quantitative phosphoproteomics identifies SnRK2 protein kinase substrates and reveals the effectors of abscisic acid action. *Proc. Natl. Acad. Sci. USA* 110, 11205-11210.

Wang, X., Kota, U., He, K., Blackburn, K., Li, J., Goshe, M.B., Huber, S.C., and Clouse, S.D. (2008). Sequential transphosphorylation of the BRI1/BAK1 receptor kinase complex impacts early events in brassinosteroid signaling. *Dev. Cell* 15, 220-235.

Wang, Y., Sun, S., Zhu, W., Jia, K., Yang, H., and Wang, X. (2013). Strigolactone/MAX2-induced degradation of brassinosteroid transcriptional effector BES1 regulates shoot branching. *Dev. Cell* 27, 681-688.

Wang, Z., Gerstein, M., and Snyder, M. (2009). RNA-Seq: a revolutionary tool for transcriptomics. *Nat. Rev. Genet*. 10, 57-63.

Wang, Z.-Y., Nakano, T., Gendron, J., He, J., Chen, M.., Vafeados, D., Yang, Y., Fujioka, S., Yoshida, S., Asami, T., and Chory, J. (2002). Nuclear-localized BZR1 mediates brassinosteroid-induced growth and feedback suppression of brassinosteroid biosynthesis. *Dev. Cell* 2, 505-513.

Wasternack, C., and Hause, B. (2013). Jasmonates: biosynthesis, perception, signal transduction and action in plant stress response, growth and development. An update to the 2007 review in *Annals of Botany*. *Ann. Bot*. 111, 1021-1058.

Waters, M.T., and Smith, S.M. (2013). KAI2- and MAX2-mediated responses to karrikins and strigolactones are largely independent of HY5 in *Arabidopsis* seedlings. *Mol. Plant* 6, 63-75.

Waters, M.T., Brewer, P.B., Bussell, J.D., Smith, S.M., and Beveridge, C.A. (2012). The Arabidopsis ortholog of rice DWARF27 acts upstream of MAX1 in the control of plant development by strigolactones. *Plant Physiol*. 159, 1073-1085.

Waters, M.T., Scaffidi, A., Flematti, G.R., and Smith, S.M. (2012). Karrikins force a rethink of strigolactone mode of action. *Plant Signal. Behav*. 7, 969-972.

Woo, H.R., Chung, K.M., Park, J.-H., Oh, S.A., Ahn, T., Hong, S.H., Jang, S.K., and Nam, H.G. (2001). ORE9, an F-box protein that regulates leaf senescence in Arabidopsis. *Plant Cell* 13, 1779-1790.

Wulfetange, K., Lomin, S.N., Romanov, G.A., Stolz, A., Heyl, A., and Schmülling, T. (2011). The cytokinin receptors of Arabidopsis are located mainly to the endoplasmic reticulum. *Plant Physiol*. 156, 1808-1818.

Xie, X., Kang, H., Liu, W., and Wang, G.-L. (2015). Comprehensive profiling of the rice ubiquitome reveals the significance of lysine ubiquitination in young leaves. *J. Proteome Res*. 14, 2017-2025.

Xing, M., and Xue, H. (2012). A proteomics study of auxin effects in *Arabidopsis thaliana*. *Acta Biochim. Biophys. Sin*. 44, 783-796.

Xu, G., Paige, J. S., and Jaffrey, S.R. (2010). Global analysis of lysine ubiquitination by ubiquitin remnant immunoaffinity profiling. *Nat. Biotechnol*. 28, 868-873.

Xu, T., Dai, N., Chen, J., Nagawa, S., Cao, M., Li, H., Zhou, Z., Chen X., De Rycke, R., Rakusová, H., Wang, W., Jones, A.M., Friml, J., Patterson, S.E., Bleecker, A.B., and Yang, Z. (2014). Cell surface ABP1-TMK auxin-sensing complex activates ROP GTPase signaling. *Science* 343, 1025-1028.

Xu, T., Wen, M., Nagawa, S., Fu, Y., Chen, J.-G., Wu, M.-J., Perrot-Rechenmann, C., Friml, J., Jones, A.M., and Yang, Z. (2010). Cell surface- and Rho GTPase-based auxin signaling controls cellular interdigitation in *Arabidopsis*. *Cell* 143, 99-110.

Yan, J., Li, H., Li, S., Yao, R., Deng, H., Xie, Q., and Xie, D. (2013). The *Arabidopsis* F-box protein CORONATINE INSENSITIVE1 is stabilized by SCF^{COI1} and degraded via the 26S proteasome pathway. *Plant Cell* 25, 486-498.

Yang, H.-Q., Tang, R.-H., and Cashmore, A.R. (2001). The signaling mechanism of Arabidopsis CRY1 involves direct interaction with COP1. *Plant Cell* 13, 2573-2587.

Yang, X., Lee, S., So, J.-h., Dharmasiri, S., Dharmasiri, N., Ge, L., Jensen, C., Hangarter, R., Hobbie, L., and Estelle, M. (2004). The IAA1 protein is encoded by *AXR5* and is a substrate of SCF^{TIR1}. *Plant J*. 40, 772-782.

Yu, Y., Wang, J., Zhang, Z., Quan, R., Zhang, H., Deng, X.W., Ma, L., and Huang, R. (2013). Ethylene promotes hypocotyl growth and HY5 degradation by enhancing the movement of COP1 to the nucleus in the light. *PLoS Genet*. 9, e1004025.

Zd'árská, M., Zatloukalová, P., Benítez, M., Šedo, O., Potěšil, D., Novák, O., Svačinová, J., Pešek, B., Malbeck, J., Vašíčková, J., Zdráhal, Z., and Hejátko, J. (2013). Proteome analysis in Arabidopsis reveals shoot- and root-specific targets of cytokinin action and differential regulation of hormonal homeostasis. *Plant Physiol*. 161, 918-930.

Zeng, L.-R., Vega-Sánchez, M.E., Zhu, T., and Wang, G.-L. (2006). Ubiquitination-mediated protein degradation and modification: an emerging theme in plant-microbe interactions. *Cell Res*. 16, 413-426.

Zhang, H., Zhou, H., Berke, L., Heck, A. J.R., Mohammed, S., Scheres, B., and Menke, F.L.H. (2013). Quantitative phosphoproteomics after auxin-stimulated lateral root induction identifies an SNX1 protein phosphorylation site required for growth. *Mol. Cell. Proteomics* 12, 1158-1169.

Zhang, K., Sridhar, V.V., Zhu, J., Kapoor, A., and Zhu, J.-K. (2007). Distinctive core histone post-translational modification patterns in *Arabidopsis thaliana*. *PLoS ONE* 2, e1210.

Zhang, X., Garreton, V., and Chua, N.-H. (2005). The AIP2 E3 ligase acts as a novel negative regulator of ABA signaling by promoting ABI3 degradation. *Genes Dev*. 19, 1532-1543.

Zhang, Y., Gao, P., and Yuan, J.S. (2010). Plant protein-protein interaction network and interactome. *Curr. Genomics* 11, 40-46.

Zhang, Y., Liu, S., Dai, S.Y., and Yuan, J.S. (2012). Integration of shot-gun proteomics and

bioinformatics analysis to explore plant hormone responses. *BMC Bioinformatics* 13, Suppl. 15, S8.

Zhao, Z., Stanley, B.A., Zhang, W., and Assmann, S.M. (2010). ABA-regulated G protein signaling in *Arabidopsis* guard cells: a proteomic perspective. *J. Proteome Res*. 9, 1637-1647.

Zhou, F., Lin, Q., Zhu, L., Ren, Y., Zhou, K., Shabek, N., Wu, F., Mao, H., Dong, W., Gan, L., Ma, W., Gao, H., Chen, J., Yang, C., Wang, D., Tan, J., Zhang, X., Guo, X., Wang, J., Jiang, L., Liu, X., Chen, W., Chu, J., Yan, C., Ueno, K., Ito, S., Asami, T., Cheng, Z., Wang, J., Lei, C., Zhai, H., Wu, C., Wang, H., Zheng, N., and Wan, J. (2013). D14--SCF^{D3}-dependent degradation of D53 regulates strigolactone signalling. *Nature* 504, 406-410.

Zhou, H., Ye, M., Dong, J., Corradini, E., Cristobal, A., Heck, A.J.R., Zou, H., and Mohammed, S. (2013). Robust phosphoproteome enrichment using monodisperse microsphere-based immobilized titanium (IV) ion affinity chromatography. *Nat. Protoc*. 8, 461-480.

Zou, J., Zhang, S., Zhang, W., Li, G., Chen, Z., Zhai, W., Zhao, X., Pan, X., Xie, Q., and Zhu, L (2006). The rice *HIGH-TILLERING DWARF1* encoding an ortholog of Arabidopsis MAX3 is required for negative regulation of the outgrowth of axillary buds. *Plant J*. 48, 687-696.

Zourelidou, M., Absmanner, B., Weller, B., Barbosa, I.C.R, Willige, B.C., Fastner, A., Streit, V., Port, S.A., Colcombet, J., de la Fuente van Bentem, S., Hirt, H., Kuster,B., Schulze, W.X., Hammes, U.Z., and Schwechheimer, C. (2014). Auxin efflux by PIN-FORMED proteins is activated by two different protein kinases, D6 PROTEIN KINASE and PINOID. *eLife* 3, e02860.

Zuo, Z.-C., Meng, Y.-Y., Yu, X.-H., Zhang, Z.-L., Feng, D.-S., Sun, S.-F., Liu, B., and Lin, C.-T. (2012). A study of the blue-light-dependent phosphorylation, degradation, and photobody formation of *Arabidopsis* CRY2. *Mol. Plant* 5, 726-733.